SEISMIC RETROFITTING
OF
STEEL AND COMPOSITE BUILDING STRUCTURES

L.DI SARNO AND A.S. ELNASHAI

Mid-America Earthquake Center
Civil and Environmental Engineering Department
University of Illinois at Urbana-Champaign

SEPTEMBER 2002

TABLE OF CONTENTS

ACKNOWLEDGEMENTS

The work in this report has been undertaken during the tenure of Dr.Luigi di Sarno (University of Napoli Federico II, Italy) as a post-doctoral researcher with the Mid-America Earthquake Center at the Civil and Environmental Engineering Department, University of Illinois at Urbana-Champaign. The work is part of MAE Center Project CM-4 'Structural Retrofit Strategies', PI: Professor Mary Beth Hueste, with the second author of this report as Co-PI. The MAE Center is a National Science Foundation Earthquake Engineering Research Center, grant reference EEC-9701785. The authors acknowledge the NSF support and the support of the MAE Center Director, Professor D.Abrams.

The report was expertly proof-read and reformatted by Helen Agans, Administrative Manager of the second author.

LIST OF FIGURES

LIST OF TABLES

LIST OF SYMBOLS

The symbols used frequently throughout the thesis are listed below and also given locally within the text. Symbols not contained in the list are only used locally and their definitions are given the first time they are encountered.

A	area
A_f	flange area
A_w	web area
B	width
b_f	flange width
d	depth
E	Young modulus
E_0	initial Young modulus
F	force
F_D	damping force
F_e	elastic force
f_y	yield strength
F_y	yield force
f_u	ultimate strength
F_u	ultimate force
g	acceleration of gravity
G	shear modulus
I	moment of inertia
k	stiffness
k_d	damper stiffness
k_{eff}	effective stiffness
k_s	story (shear) stiffness
l	length
m	mass
N	axial load
M	bending moment
M_y	yield moment
M_u	ultimate moment
r	radius of gyration
R	reduction force factor
t	thickness
t_f	flange thickness
t_w	web thickness
V	shear
V_B	base shear
V_y	yield shear
Z	plastic modulus

Δ	displacement
Δ_y	Yield displacement
e	strain
e_{el}	elastic strain
e_p	plastic strain
e_y	yield strain
e_u	ultimate strain
x_{eq}	equivalent damping ratio (as fraction of the critical)
m	ductility
J	rotation
J_p	plastic rotation
J_y	yield rotation
J_u	ultimate rotation
w	circular frequency

1. INTRODUCTION

1.1. SCOPE AND PURPOSE

This report provides criteria to evaluate the performance of existing buildings with steel and composite structures, either framed or braced. It also presents a comprehensive review of rehabilitation strategies to retrofit structural members and connections (*local intervention*) and/or frames (*global intervention*). The evaluation criteria and upgrade schemes have been derived from extensive experimental and numerical tests carried out in Europe, Japan and the US in the aftermath of recent earthquakes. They are intended to enhance the strength, stiffness and energy dissipation of existing framed buildings during future earthquakes. Indeed, it is expected that retrofitted buildings exhibit: (i) no damage during low-intensity earthquakes, (ii) some nonstructural damage during moderate earthquakes and (iii) structural and nonstructural damage during major events but the global collapse is prevented.

1.2. BACKGROUND

Steel structures have been extensively used in seismic areas worldwide because of their favorable mass-to-stiffness ratio, ductility and hence, enhanced energy absorption capacity. Indeed, the typical steel frame configurations, i.e., moment resisting frame (MRF), concentrically braced frame (CBF) and eccentrically braced frame (EBF), exhibit different behavior with regard to stiffness, strength and ductility. Indeed, MRFs provide a satisfactory strength and possess an excellent ductility but they suffer large story drifts due to low lateral stiffness. By contrast, CBFs are capable of ensuring both required strength and stiffness, but buckling failures limit the global ductility. EBFs combine the strength and the stiffness of the CBF with the ductility of MRF; therefore their intermediate behavior results in agreement with the stiffness, strength and ductility required in seismic design, thus limiting the structural damage during earthquake loading. On the other hand, MRFs exhibit damage generally limited to nonstructural components, while structural and nonstructural may be found in CBFs. Similarly, composite MRFs show damage concentrated in infills, claddings and other nonstructural components; while buckled and/or yielded braces characterize the seismic response of CBFs.

During recent earthquakes, e.g., Northridge (1994) and Kobe (1995), extensive and unexpected damage was observed in many framed steel and composite buildings (AIJ, 1995; Youssef *et al*., 1995). Indeed, several brittle fractures were detected in welded MRFs particularly at beam-to-column connections. The damage was found in a great population of buildings, with different heights (one story to about 25 stories) and ages (up to 30 years old), thus showing that steel structures are vulnerable to seismic loads. Typical damage consisted of fractures initiated at the weld between the beam bottom flange and column flanges. However, the crack patterns varied as a function of the joint details, e.g., through thickness welds, through the column flanges, extended into the column flange material behind the weld (*divot* or *nugget* failure) or into the column web. On the other hand, brittle behavior in CBFs was due to the fracture of connection elements or bracings. Net fracture at bolt holes, severe distortion of unstiffened beam in chevron braces, fracture of welded connections and web tear-out were common damage in braced frames.

Therefore, it is essential to provide rules and guidelines for seismic upgrading of existing steel and composite structures for different typologies of building structures. These issues have been discussed in the present report.

1.3. LIMITATIONS

Evaluation criteria to assess the seismic performance of existing steel and composite buildings have been provided in this report. Local and global retrofitting schemes have also been included. However, some aspects, e.g., advanced vibration control strategies (active, semi-active, hybrid), construction and quality assurance, have not been addressed in details. Yet, it is not the intent of the present work to provide quantitative comparisons in terms of cost-effectiveness for steel and composite constructions with other structural systems. Information provided hereafter has been derived in certain cases from research carried out in Japan and the US and/or post-earthquake data recorded worldwide. Thus, the data reflects different practices used in seismic design. To render uniform the large amount of information, it has been deemed necessary to adimensionalize the available data. As a result, general conclusions were attempted whenever possible.

Each building performance level (see examples in Section 1.5) consists of a structural level describing the limiting damage state of the structural systems and a nonstructural level describing the limiting damage state of the nonstructural components. However, in this report only the former are explicitly referred to.

1.4. SUMMARY

This report provides criteria to evaluate and retrofit existing steel and composite buildings damaged during past earthquakes. It consists of two chapters other than the present one. A brief description of the issues addressed in each section is given hereafter.

Chapter 1 provides the background of the research undertaken and defines the common terms used for seismic rehabilitation (because they are often open to misinterpretation). Limitations and assumptions have also been highlighted.

Chapter 2 summarizes the structural deficiencies that generally characterize steel and composite buildings. Thus, the damage observed in past earthquakes is discussed and a classification of such damage is attempted as a function of the structural components and the frame as a whole. On the other hand, the framework for seismic rehabilitation is dealt with. The rehabilitation objectives, expressed as the desired building performance at specified seismic hazard levels, are discussed. The performance evaluation processes, i.e., simplified and refined, are provided along with their limits of applicability. Moreover, the general and technical considerations that should be taken into account and the types of intervention are discussed. An overview of common upgrade strategies is first provided; special metal materials and nonconventional strategies, i.e., base isolation and supplemental damping, are then presented.

Finally, *Chapter 3* contains requirements and design rules to perform local or global rehabilitation interventions. Specifications for as-built and new materials are included. Requirements and adequate detailing for cross sections are provided to enhance flexural, shear and axial stiffness and strength other then improve the local ductility. Rules to design the seismic retrofitting of beams, beam-columns, braces and different types of connections are also included. Strategies to rehabilitate the framed structure as a whole have been then reviewed; such strategies refer to either traditional (bracing, encasement, dual systems) or nontraditional interventions (base isolation and damper devices).

1.5. DEFINITIONS

The terminology used in earthquake engineering for seismic rehabilitation of existing structures is open to misinterpretation. Therefore, common terms used in this report are italicized and defined as below.

Rehabilitation is an all-encompassing term that includes concepts of repair, retrofitting, strengthening and weakening that may minimize the vulnerability of building structures to earthquake loading. *Repair* is defined as the reinstatement of the original characteristics of a damaged section or member and is confined to dealing with the as-built system. The term *strengthening* is defined as the number of interventions that may improve one or more seismic response parameters (stiffness, strength and ductility) as a function of the desired structural performance level. Furthermore, strengthening includes the addition of structural elements or the change of the structural system. *Weakening* is an alternative scheme to upgrade existing structures; it consists of reducing the seismic demand in critical regions, e.g., beam-to-column connections.

Conventional intervention includes the established methods of repair, such as concrete encasement, use of bracings, strengthening or weakening of connections. By contrast *nonconventional intervention* refers to the use of novel metals, namely aluminum, stainless steel and shape memory alloys, and/or special devices, e.g., base isolation and dampers which significantly enhance the energy dissipation and hence reduce story drifts and shears.

Rehabilitation objective is the selection of desired damage levels or loss (*performance levels*) for a specific seismic demand (*hazard level*). Indeed, the performance levels define the expected behavior of the building in terms of allowable damage state to structural and nonstructural components for an identified earthquake ground motion.

Simplified rehabilitation methodology is an evaluation procedure applicable to small and regular buildings in low-to-moderate seismic zones. Moreover, such approach requires simplified analyses during the design of the rehabilitation intervention. By contrast, the *refined rehabilitation methodology* requires thorough assessment based on detailed as-built data and nonlinear static analyses either static (pushovers) or dynamic (time histories). Therefore, the refined approach is the more complete approach and can be applied to all structures.

In this report *steel buildings* are framed structures with bare steel beams, columns and/or braces. *Composite buildings* are framed structures with bare steel beams and composite columns, composite beams and bare steel columns or composite beams and columns. Similarly for the diagonal braces. The slabs can be either steel or composite steel and concrete.

2. POST-EARTHQUAKE INVESTIGATION AND EVALUATION

2.1. STRUCTURAL DEFICIENCIES

Recent earthquakes, e.g., Northridge (January 17, 1994, California, USA), Hyogoken-Nanbu (January 17, 1995, Japan) and Chi-Chi (September 21, 1999, Taiwan) provoked unexpected damage to steel and composite structures. Such damage was widespread, ranging from residential buildings to highways, bridges and lifelines. There were no casualties or complete collapse for building structures in the Northridge earthquake (Mahin, 1998); the damage occurred in new tall as well in small structures. However, the most severe effects were concentrated typically in low rise steel buildings (Miller, 1998). Such apartment buildings consisted of three stories with a ground level garage, second-story living quarters and third-story bedrooms. In Japan, extensive damage occurred in columns, braces, column bases and beam-to-column connections of old and new steel buildings (Watanabe *et al*., 1998). Unfortunately, 1,067 old buildings collapsed or were fatally damaged beyond repair (Nakashima *et al*., 1998). These buildings were constructed with bundled light-gauged sections for columns and trusses for beams. Moreover, about 100 new structures, consisting of two to five stories, collapsed, while 332 were rated as severe damaged. In Taichung, the largest city in the heavily shaken region in Taiwan, some high-rise dual systems and welded MRFs suffered localized yielding and damage to architectural features (FEMA 355E, 2000).

Generally, the deficiencies in steel and composite buildings are classified as structural and nonstructural. The former refers to: (i) sections, (ii) members, e.g., beam-columns and braces, (iii) connections, (iv) diaphragms, (v) foundation and (vi) systems. Nonstructural deficiencies comprise: (i) suspended ceilings, (ii) exterior ornamentation, (iii) mechanical and electrical utilities, (iv) poor construction quality, (v) deterioration and (vi) site characteristics.

Common structural deficiencies found in the aforementioned earthquakes may be summarized as follows (AIJ, 1995; Youssef *et al*., 1995):

- Poor quality of construction material.
- Slender sections.
- Inadequate lateral supports.
- Excessive component flexibility.
- Presence of brittle components.
- Inadequate steel reinforcement.
- Insufficient concrete cover.
- Poor quality and/or inadequate detailing.
- Excessive and/or unexpected beam over-strength.
- Excessive column panel flexibility.
- Inadequate column panel strength.
- Inadequate composite action.
- Excessive and/or unexpected brace over-strength.
- Inadequate bracing layouts.
- Lack and/or inadequate continuity between structural components.
- Incompatible deformations between joined parts.
- Inadequate diaphragm strength and/or rigidity.
- Poor connectivity of diaphragm to vertical elements of the lateral resisting systems.
- Lack of continuity of diaphragm.
- Incomplete and/or insufficient lateral force resisting system.
- Excessive lateral flexibility.

- Inadequate global strength and/or ductility.
- Inadequate foundation systems.
- Uplift forces and high overturning moments in foundation systems.

Figure 2.1 shows the main deficiencies as a function of the structural components and systems.

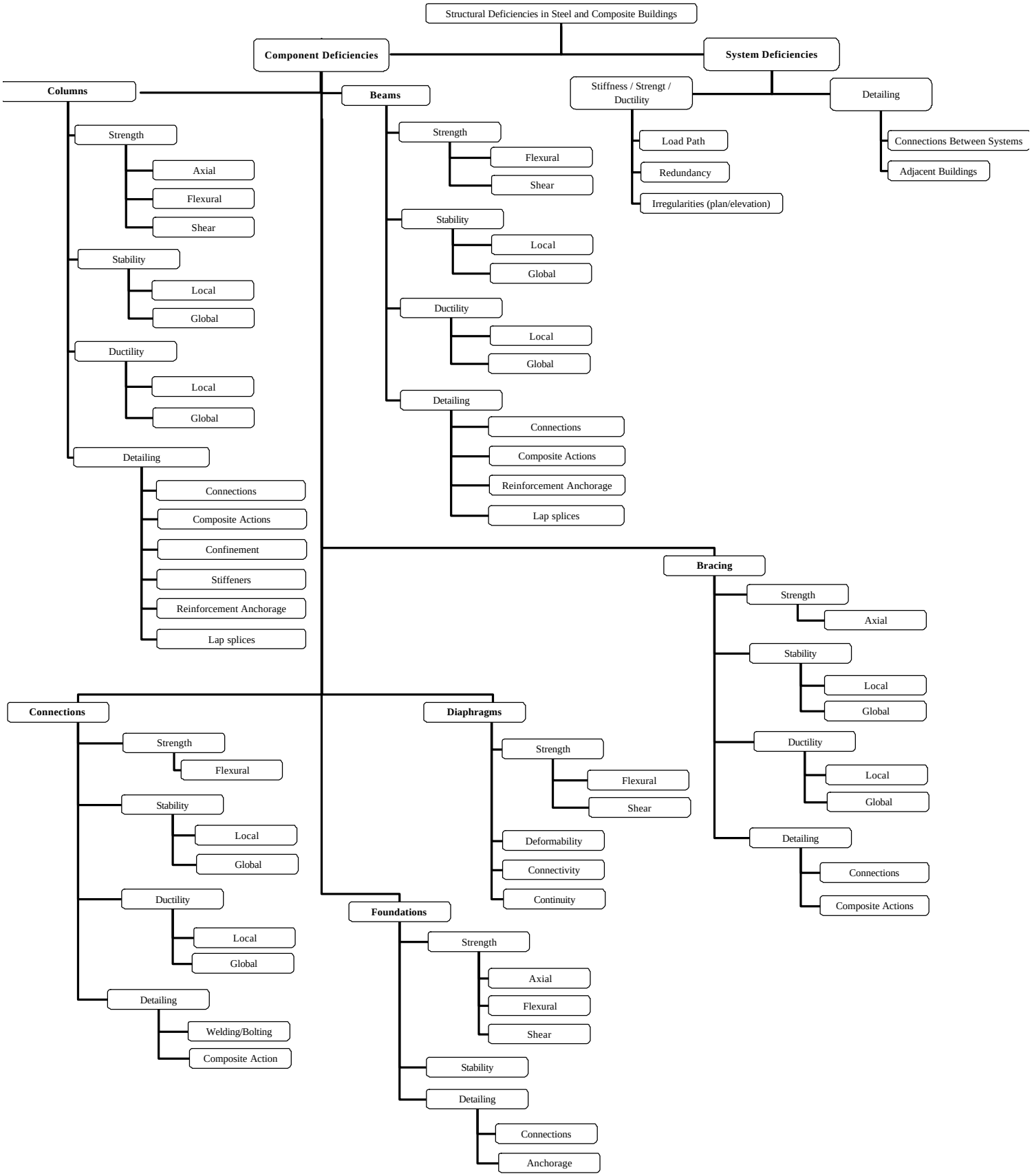

Figure 2.1. Common structural deficiencies for steel and composite buildings.

Inadequate component performance may be caused by insufficient strength, e.g., axial, flexural and/or shear for beam-columns, scarce stability (either local or global) and/or poor ductility, e.g., small connection rotations. Welded beam-to-column connections may suffer brittle fracture due to high inelastic demand at column face, inadequate material toughness or technological factors. Moreover, strong-column-weak-beam code requirements may not be sufficient to guarantee the formation of plastic hinges in beam elements. Weak connections are also common problems in existing braced frame systems as seismic codes have only recently required that braced frame connections be capacity designed. Furthermore, noncompact braces with high-to-intermediate slenderness may experience brittle fracture as a result of low-cycle fatigue, induced by large secondary stresses at buckled sections. In addition, beam and/or column failures may occur as a result of particular bracing layouts, e.g., beam failures may occur in chevron systems because of large unbalanced forces between the tensile brace and the buckled brace. However, it is worth noting that column failure in braced frame system can lead to a local collapse. Structural deficiencies in diaphragms and foundations may also undermine the building performance.

On the other hand, load paths, degree of redundancy and irregularities, in plan and/or elevation, are common global deficiencies affecting the performance of the steel and composite structures. Indeed, adequate lateral resisting force systems are required to transfer seismic forces from the slabs to the foundations. High redundancy is beneficial because it represents a further protection against the randomness of the ground motion and the uncertainties in the design. Moreover, structural regularity in plan and elevation prevents detrimental torsional effects and avoids high concentration of inelastic demands.

The damage in steel and composite buildings, due to the aforementioned structural deficiencies (Figure 2.1) that occurred in recent earthquakes, is discussed in the next section.

2.2. DAMAGE OBSERVED IN RECENT EARTHQUAKES

Steel structures have shown generally adequate seismic performance during several past earthquakes. In fact, due to their favorable mass-to-stiffness ratio, ductility and sustainable energy absorption capacity such structures can be designed to resist earthquakes very effectively. However, during recent earthquakes extensive brittle fracture was observed in framed structures (AIJ, 1995; Youssef *et al.*, 1995); this unexpected damage was localized particularly in braced bays of CBFs and beam-to-column connections of welded MRFs. The performance of steel and composite buildings during past earthquakes is outlined hereafter. It is aimed at identifying and classifying common damage experienced by such buildings.

In the US, steel frames were first shaken by intense earthquakes during the San Francisco earthquake of 1906. Several buildings which were designed for gravity loading only survived the major quake. Structures with steel interior frames and peripheral bearing walls suffered some damage but no collapse. By contrast, structures employing either rigid frames or X-bracing and generally with partitions from the first floor upwards, performed satisfactorily.

During the Mexico City earthquake of 1957, several high rise steel buildings (10 to 45 stories) were subjected to strong ground shaking. Their seismic behavior was observed to be very satisfactory, especially for the Latin American Tower which suffered no damage.

Severe local buckling was suffered by steel columns at the first and second floor of the Cordova building during the 1964 Alaska earthquake (Figure 2.2). This structure was a six-story office

building with a penthouse. The earthquake-resisting system consisted of a spatial MRF. Frames with full strength connections were used in the east-west direction, while partial moment-resisting connections were employed in the 20-cm RC wall service core (near the north facade) where the penthouse was standing. Such walls contributed significantly to the seismic response of the building. The main earthquake damage occurred in the first-story and at the penthouse, whose walls collapsed. The local buckling of the southeast corner column (Figure 2.2), which occurred just below the second floor level, was so severe that the flanges tore away from the web and the web crimped. As a result, the column shortened by about 3.8 cms. It is worth mentioning that the mid-story stair landing was connected to this corner column, making it shorter and therefore stiffer than the other columns.

Figure 2.2. Cordova building damaged during the 1964 Alaska earthquake: overall view (*left*), local buckling in columns with (*middle*) and without RC wall (*right*) (*after NISEE, 2000*).

The San Fernando earthquake of 1971 caused severe damage to reinforced concrete structures, such as the Olive View Hospital and the Joseph Jensen filtration plant, but no extensive damage was reported to steel buildings (Jennings, 1971). However, in some cases, as shown in Figure 2.3, steel diagonal braces were stretched beyond their elastic limit. The excessive deformations (buckling and yielding) of these braces resulted not only in the failure (rupture) of similar braces in the other north wall, but also in significant damage to the rest of the building.

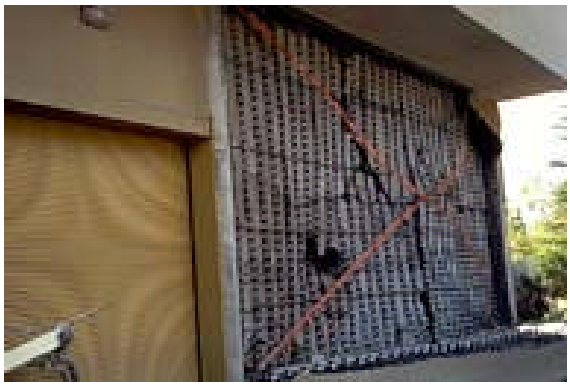

Figure 2.3. Yielding and buckling of diagonal braces in San Fernando earthquake (*after NISEE, 2000*).

The seven-story steel frame IBM building was shaken by the Managua, Nicaragua earthquake of 1972. The structure behaved well with no serious damage to structural members.

In Friuli, Italy, a small number of steel structures were subjected to a damaging earthquake in 1976. Whereas severe damage was sustained by reinforced concrete and traditional building, steel structures were not affected.

During the Romanian earthquake of 1977, local buckling was the most severe effect. Indeed, extensive buckling of long, open lattice, built-up steel columns was observed. Also, an eccentrically braced frame underwent large plastic deformations followed by fracture in the shear link panel zone, but no collapse occurred.

Structural steel is a very popular material in Japan. Several high-rise buildings employ steel frames and have survived a large number of past earthquakes without serious damage, e.g., the great Kanto earthquake in 1923 and Tokachi-Oki in 1968. However, during the Miyagiken-Oki earthquake in 1978 some damage was sustained by medium rise steel buildings, largely due to the fracture of bolted bracing connections. On the other hand, a seventeen-story government building amongst many other steel and composite structures survived with no reported structural damage.

In September 1985, Mexico City was severely shaken by the Michoacan Earthquake. A total of 12,700 structures were damaged; where 1,778 were severely damaged or collapsed and 4,826 experienced moderate damage (Tena-Corluga and Vergara, 1997). Medium-rise MRF buildings were among the most severely affected because the local soil conditions of the lake-bed region of Mexico City. As a consequence, the structural dynamics of these buildings led to resonant responses with the ground in many cases. Furthermore, severe localized damage was observed in high-rise structures. For example, the Pino Suarez Complex suffered local buckling and fracture (Figure 2.4) leading to global collapse. Nonetheless, many steel buildings, such as the 43-storey Latin American and the fifty-story PeMex Towers, survived the prolonged ground shaking with no damage to structural elements.

Figure 2.4. Local buckling in box column of Pino Suarez high rise buildings in Mexico City (*after* FEMA 355E, 2000).

The devastating June 21, 1990 earthquake of Northern Iran (M=7.7 and PGA=0.65g) was the worst seismic event of this century in densely populated areas. It killed more than 40,000 people, injured 100,000 and left more than half million homeless, causing the worst economic loss in the history of the nation (Nateghi, 1997). Medium rise steel frames for residential buildings were extensively damaged. These residential constructions were built in the 1980s; they were five-story MRFs with special semi-rigid beam-to-column connections (*Khorjinee*) and infill walls covering in between the framing. Khorjinee connections consist of continuous beams set on top of seat angles, which are welded to both sides of the columns (Figure 2.5).

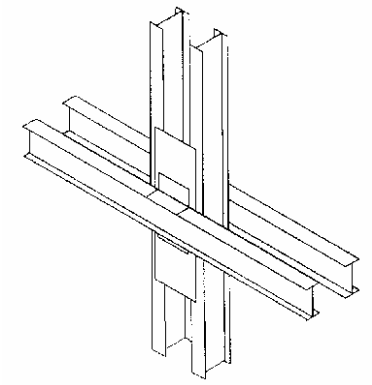

Figure 2.5. Typical Khorjinee beam-to-column connection used in Iran (*after* Nateghi, 1995).

The damage in more than 200 residential buildings was caused by excessive lateral deformability (Nateghi, 1995). Moreover slender braces buckled out-plane about weak axis thus causing extensive nonstructural damage. It is worth mentioning that these braces were designed for tension only using channel sections.

The 1994 Northridge Earthquake in California caused extensive structural damage to more than 100 modern steel welded frames. The systems employed in the majority of buildings were the special MRFs, which apparently met the stringent detailing requirements of the current building code. Such requirements were intended to ensure ductile performance during major earthquakes. However, although independent testing agencies had performed special inspections during construction, in some cases it was evident that the material properties, fabrication workmanship and inspection practices were partly to blame for the observed damage. Furthermore, in this event, the intensity of ground accelerations (both horizontal and vertical) was as much as twice that anticipated by the existing building codes, e.g., UBC 1991.

Reinforced concrete buildings were significantly damaged and some of them collapsed. By contrast, no structural collapses were observed for steel frame structures (Mahin, 1998); nevertheless, widespread brittle fracture was found in several steel-frame buildings (Youssef *et al*., 1995). Extensive damage occurred in new and old constructions (low-to-high rise) and it was localized primarily at beam-to-column connections. It is instructive to note that typical connection details utilized in the US practice consist of a shear tab shop-welded to the column, with the beam web bolted to the tab *in situ* for ease of assemblage. The top and bottom flanges are then field-welded. Predominant failures affected girder groove welds and column flanges. Such damage was typically localized in the lower flange-to-beam portion of the connection, while the top beam flange-to-column flange remained generally intact (Figure 2.6) (Miller, 1998).

The fractures initiated at the flange groove weld root, with the crack(s) propagating into the weld or column flange. In some cases the bolted shear tab experienced shared bolt tears through the tab between the bolt holes. Moreover, tears of the fillet welds from the column-face were also detected. However, this type of damage to the shear tab occurred only in the presence of damage to the bottom flange. However, failures occurred in connections with and without column-flange stiffeners as well as connections with and without return welds on the shear connection plates. Furthermore, both wide-flange columns and built-up box sections were affected by brittle fracture. Yet, it is worth mentioning that failures were observed in buildings with a relatively small number of frame bays in each direction as well as in buildings where nearly every girder line was part of a moment frame.

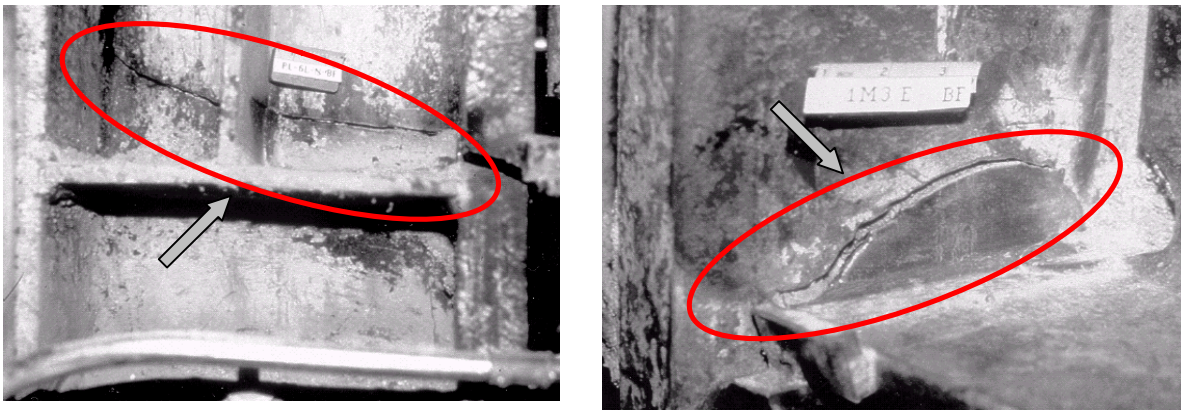

Figure 2.6. Brittle fracture of beam bottom flanges in welded MRF connection during Northridge earthquake: fracture propagating through column web and flange (*left*) and fracture causing a column divot fracture (*right*) (*after* Naeim, 2001).

Many similarities with the damage described above were found in the 1995 Hyogoken-Nanbu earthquake (M=7.2) which destroyed a large percentage of buildings in the Kobe area. Over 6,000 people died and 26,000 people reported injured; more than 108,000 residential and commercial structures were damaged beyond repair (Nakashima *et al*., 1998). Many steel and composite structures, either framed or braced, were seriously damaged by the quake (Watanabe *et al*., 1998). However, less than 10% of steel buildings collapsed (Figure 2.7); the vast majority were low-rise, i.e., lower than five stories.

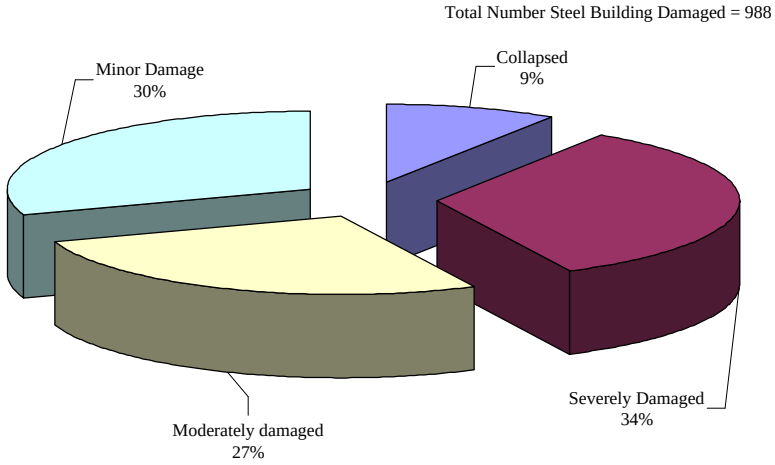

Figure 2.7. Type of damage observed in steel and composite buildings in Japan (*font* Nakashima *et al*., 1998).

It is instructive to note that the Kobe region contained several old steel buildings, constructed more than 30 years before the earthquake hit. These buildings employed bundled light-gauged sections (columns) and shallow trusses (beams). The trusses consisted of light-gauged rolled sections and round bars. Such structures were not properly designed to withstand seismic forces and their maintenance had been neglected. Indeed, corrosion and other material degradations were very common. As a result, they experienced extensive damage under the ground motion (Figure 2.8).

Figure 2.8. Damage to old steel buildings in the Kobe earthquake: collapse (*left*), construction with light gauged sections (*middle*) and corroded sections (*right*) (*after* FEMA 355E, 2000).

Steel, steel-encased and steel-infilled reinforced concrete buildings are very widely used in Japan. Of these, unbraced frames experienced the most severe damage; 432 buildings were completely unbraced, 134 were braced only in one direction and 34 braced in two orthogonal directions. Moreover, many of these buildings employed cold-formed hollow sections and shop-welded beam-to-column connections (Figure 2.9).

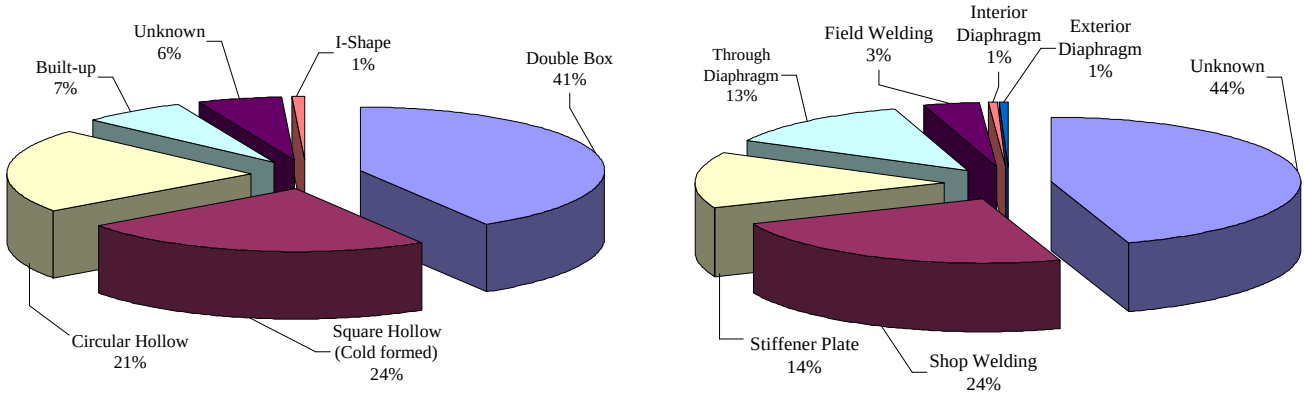

Figure 2.9. Type of columns (*left*) and beam-to-column connections (*right*) used in damaged steel and composite buildings in Japan (*font* Nakashima *et al*., 1998).

In addition, several modern high-rise steel buildings exhibited brittle fractures in columns and braces. They employed generally square tubes as columns; the depth varied between 500-550 mm, while the thickness was 50-55 mm. Many fractures occurred in base and parent metal in HAZ at beam-to-column connections (Figure 2.10). Brittle fracture was found either in shop fillet welds with small sizes or full penetration welds. However, plastifications and local buckling anticipated the rupture thus ensuring that the energy dissipation had taken place in the beams. Moreover, column-to-column splices also failed in a brittle manner. Plastification, excessive distortion and local buckling at the member ends were common in many columns of modern buildings.

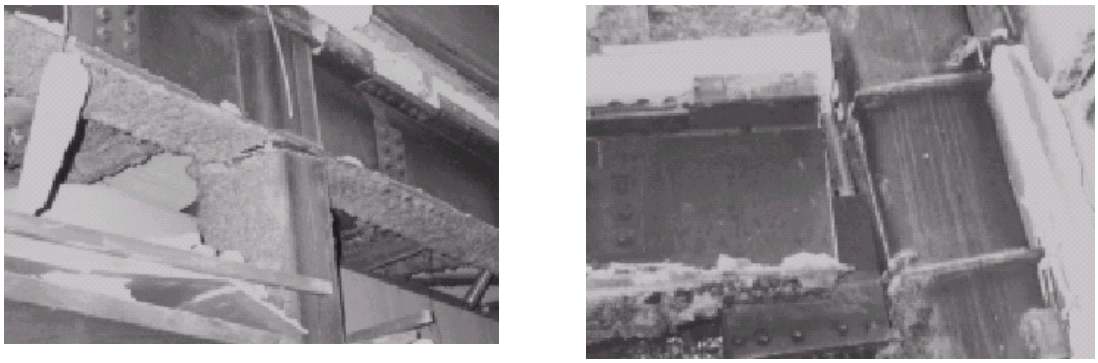

Figure 2.10. Damage at welded beam-to-column connections: fracture at column top (*left*) and beam end (*right*) in the Kobe earthquake (*after* FEMA 355E, 2000).

The limited ductility and corresponding brittle fractures in new CBFs manifested in the fracture of connection elements or bracing elements. For example, damage in braces consisted of: (i) net fracture at bolt holes, (ii) severe distortion of unstiffened beam in chevron braces (Figure 2.11), (iii) fracture of welded connections and (iv) web tear-out (Figure 2.12). Braces consisted mainly of rods, angles, flat plates and circular hollow sections. Smaller brace cross sections, e.g., rods, angles and flat plates, experience more severe brittle fractures. However, these types of braces were more common in older constructions.

Figure 2.11. Damage to nonductile braces in Kobe earthquake: net fracture at bolt holes (*left*) and severe distortion of unstiffened beam in chevron braces (*right*) (*after* Naeim, 2001).

Diagonal braces with larger cross-sections resulted in severe local buckling and brittle failures; these components failed mostly at the connection with beams and/or columns (Figure 2.13). Collapses have occurred as a consequence of such uncontrolled inelastic behavior.

Figure 2.12. Damage to nonductile braces in the Kobe earthquake: fracture of welded connections and web tear-out (*left*) and fracture of welded connections (*right*) (*after* Naeim, 2001).

Damage surveys detected many structural deficiencies also at the foundation levels (AIJ, 1995; Azizinamini and Ghosh, 1996). Indeed, three types of failure were observed in base column plate connections, namely: (i) damage to anchor bolts, (ii) failure of welds at base plates and (iii) excessive deformation of base plates. The causes of such damage may be attributed to the practice in Japan to design standard column base connections as pin-supported, i.e., no moment transfer at the column base.

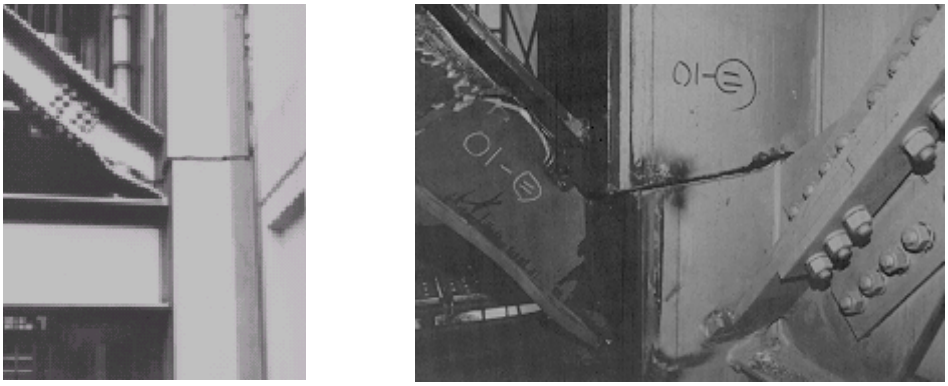

Figure 2.13. Fracture in brace connections: square tube jumbo column (*left*) and ordinary brace (*right*) in Kobe earthquake (*after* FEMA 355E, 2000).

The September 21, 1999 Chi-Chi earthquake in Taiwan caused serious damage and collapse to many building structures (Naeim *et al*., 2000). However, the adversely affected buildings were mostly RC (Figure 2.14) with the lateral resisting systems composed by MRFs.

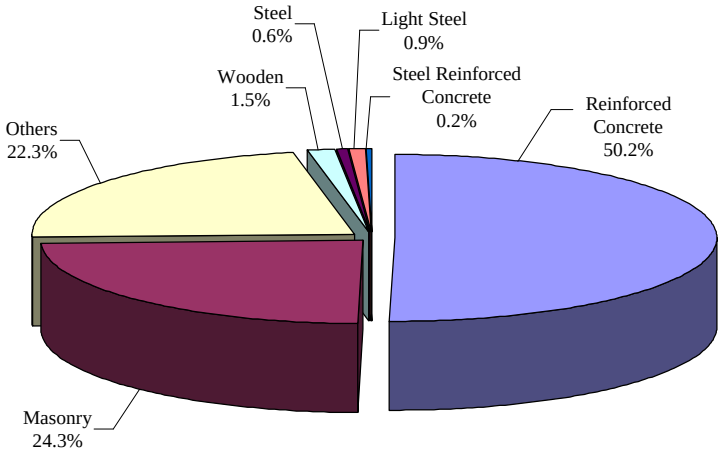

Figure 2.14. Damage observed in building structures in Taiwan (*font* FEMA 355E, 2000).

Several steel buildings with 20 to 50 stories were under construction at the time of the earthquake in Taipei and Taichung (the capital and the largest city in the shaken area, respectively). However, the only significant fracture-related damage was detected in two high-rise buildings located in Taichung. Surveys also found brittle fracture localized in braced connections (FEMA 355E, 2000). Moreover, low rise steel structures are generally used for either residential or commercial purposes in the shaken area. Such constructions employ welded and bolted end plate connections in light steel. Permanent lateral displacements with consequent nonstructural damage and yielding in bolted connections were observed (Figure 2.15). However, it is worth noting that these buildings, which are generally up to three stories, are not designed by qualified engineers but rather by fabricators and contractors.

Figure 2.15. Damage in Taiwan earthquake: permanent lateral displacement in small steel frame (*left*) and yielding in the connection of light steel frame (*right*) (*after* FEMA 355E, 2000).

Further data on the damage experienced by steel and composite buildings during past earthquakes may be found in Table 2.1.

Table 2.1. Damage to steel and composite buildings during past earthquakes.

Earthquake			
Location	Date	Magnitude	Damage to steel and composite buildings
San Francisco (California, USA)	1906	*n.a.*	• Partial infill and masonry piers in steel frames widely damaged by story racking. • Buckled column plates. • Yielded and buckled diagonal rod bracings. • Damage to riveted connections and some sheared rivets.
Kanto (Japan)	1923	*n.a.*	• Minor structural damage. • Significant damage to masonry infills and facades.
Kern County (California, USA)	1952	*n.a.*	• Minor structural damage. • Pounding.
Prince William Sound (Alaska, USA)	1964	7.5	• Beam-to-column weld failure. • Column base plates. • Buckled steel columns. • Damaged concrete core walls.
Venezuela	1967	6.5	• Low damage to multistory buildings.
San Fernando (California, USA)	1971	6.6	• Damage to steel diagonal braces. • Cracked welds in high-rise MRFs under construction.
Managua (Nicaragua)	1972	6.2	• Yielding in ground floor columns. • Extensive nonstructural damage.
Guatemala	1976	7.5	• Minor structural damage to MRFs.
Romania	1977	7.1	• Extensive local buckling.
Miyagiken-Oki (Japan)	1978	7.4	• Minor damage to shear walls in dual systems. • Buckling and fracture of steel braces.
Oaxaca-Guerrero (Mexico)	1978	7.7	• Pounding and nonstructural damage to high-rise buildings.
Coalinga (California, USA)	1983	6.7	• Minor structural damage.
Morgan Hill (California, USA)	1984	6.2	• Minor structural damage. • Nonstructural and contents damage.
Chile	1985	7.8	• Substantial non-structural damage to unbraced buildings.
Mexico	1985	8.1	• Collapse of old MRFs with infills, knee braces or riveted connections. • Collapse of braced frames. • Weld fracture. • Local buckling.
Whittier (California, USA)	1987	5.9	• Nonstructural damage.
Loma Prieta (California, USA)	1989	7.1	• Connection cracks. • Pounding damage at seismic joints.
Manjil-Roubar (Iran)	1990	7.7	• Brace buckling. • Nonstructural damage.

Landers and Big Bear (California, USA)	1992	7.0	• Beam-to-column connection cracks.
Hokkaido (Japan)	1993	7.1	• Buckling of braces.
Northridge (California)	1994	6.8	• Local buckling. • Column yielding. • Buckling and fracture of braces. • Brittle fracture in connections.
Kobe (Japan)	1995	7.2	• Local buckling. • Column yielding. • Damage at column base plates. • Buckling and fracture of braces. • Brittle fracture in connections.
Taiwan	1999	7.6	• Localized yielding. • Brittle fracture in connections.

Keys: *n.a.* = not available.

The above overview concerning the performance of steel and composite buildings during past earthquakes enables the classification of the damage as a function of the structural components, e.g., beams, columns, braces and connections, and the frame as a whole. Such classifications are provided in the next section.

2.3. DAMAGE CLASSIFICATION

Avoiding extensive damage of retrofitted structures in future earthquakes is the major task of adequate rehabilitation interventions. Therefore, it is useful to classify the common failures observed in the past events for steel and composite buildings (Section 2.2). Such classification may be expressed as a function of the member components, connections and frame as a whole (Azizinamini and Ghosh, 1996; Miller, 1998; Nakashima *et al*., 1998, FEMA 351, 2000).

The beam damage may be summarized:

- Buckled flange (top or bottom).
- Yielded flange (top and bottom).
- Flange fracture in HAZ (top and bottom).
- Flange fracture outside HAZ (top and bottom).
- Flange fracture top and bottom.
- Yielding or buckling of web.
- Fracture of web.
- Lateral torsional buckling of section.

Similarly, typical steel column failed due to the following:

- Incipient flange crack.
- Flange tear-out or divot.
- Full or partial flange crack outside HAZ.
- Full or partial flange crack in HAZ.
- Lamellar flange tearing.
- Buckled flange.
- Column splice failure.

The damage to brace members is:

- Local buckling and fracture as in beam-columns.
- Lateral torsional buckling of section.
- Member buckling.

Beam-to-column connection failures include (FEMA 355E, 2000):

- Cracks across the column-flange thickness.
- Weld metal fractures.
- Fractures at weld-metal/column-flange interfaces.
- Fractures or yielding of continuity plates.
- Cracks in doubler plate welds
- Cracks in continuity plate welds.
- Cracks in fillet welds at shear connection plates.
- Cracks in beam shear tab plates along the bolt line.
- Cracks in the shear tab in the plate at the end of the fillet welds.
- Excessive panel deformation.
- Panel shear yielding and/or buckling.

In addition, damage to other types of connections, e.g., for braces and base columns, may be summarized as:

- In brace connections: (i) breakage of bolts, (ii) weld metal fractures, (iii) net fracture at bolt holes, (iv) local yielding and (v) beam web buckling in brace connections.
- In column base plate connections: (i) damage to anchor bolts, (ii) failures of welds and (iii) excessive plate deformations.

Steel and composite MRFs exhibit generally:

- Excessive story drifts.
- Instability.
- Excessive story shears.
- Soft and/or weak stories.
- Column yielding and plastification.
- Failure of diaphragm shear connections.
- Concentrated yielding or fracture at the contact with infills.
- Uplifting and overturning.

Common failures in CBFs, either steel or composite, are given by:

- Fractures of braces and/or connection elements.
- Brace buckling.
- Failure of diaphragm shear connections.
- Concentrated yielding or fracture at the contact with infills.
- Uplift and overturning.

Finally, common damage in steel reinforced concrete frames is:

- Large tie spacing in columns.
- Base plate details.
- Vertical discontinuities in building stiffness.
- Foundation related failures.

2.4. PERFORMANCE EVALUATION

Consideration of non-linear response is of paramount importance for existing structures. Indeed, many steel and composite buildings may possess structural deficiencies that can be detected only via detailed nonlinear analyses, either static (pushovers) or dynamic (time histories). Moreover due to non-linear behavior, as well as the generally complex and indeterminate nature of lateral force

to non-linear behavior, as well as the generally complex and indeterminate nature of lateral force resisting systems, the retrofitting of such buildings is seldom a straightforward process, e.g., the demand is known and resisting elements are simply designed to suit. Typically, a wide variation in deformation capability among new and existing elements requires a verification analysis of the proposed retrofit to assure that all significant structural components fall within acceptable force and/or deformation limits.

The standard process to perform a complete rehabilitation analysis may be conveniently broken down into several steps (FEMA 356, 2000; Holmes, 2000). However, it is worth mentioning that an essential preliminary step is the review of the initial considerations. Issues, such as structural characteristics of the building, restrictions on the design of the rehabilitation measures, building use and occupancy, socio-economic considerations, seismic hazards and eventual geologic site hazards should be well-defined. A typical multi-step procedure is shown in Figure 2.16.

The first step of the process involves the collection of information relative to the as-built structure. Thus, the engineer should record: (i) the structural configuration, (ii) the material mechanical properties, (iii) the reinforcement detailing for the RC parts, (iv) the foundation system and (v) the level of damage. In addition, data of non-structural components influencing the seismic response of the structure, e.g., infills, claddings and roof panels, should be collected. Such data should be collected through compulsory visits to the site, constructional drawings (if available) and/or interviews with the owner/tenants or the original engineer/contractor. However, it is worth noting that the engineering judgement and experience play a significant role in the field investigations in order to collect the necessary data.

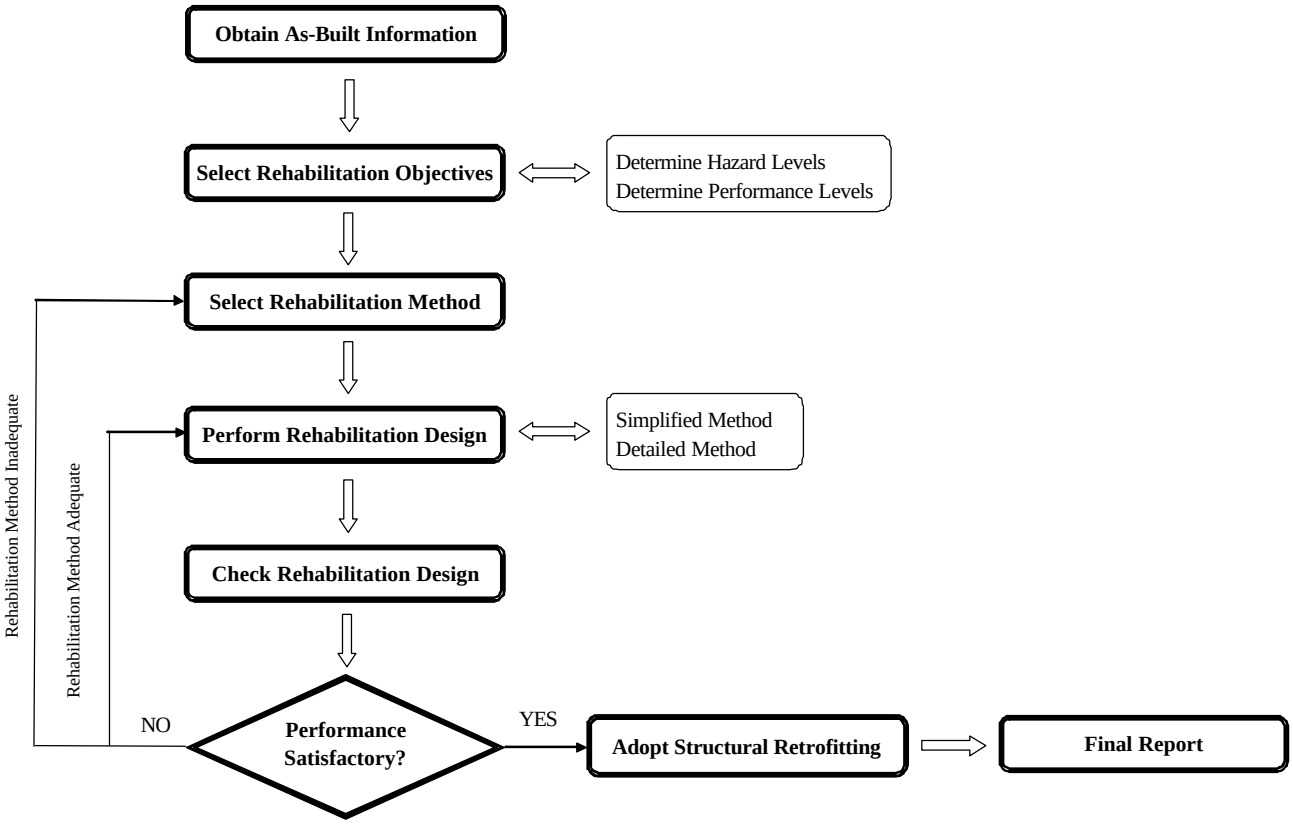

Figure 2.16. Standard process for the seismic rehabilitation.

The second step of the procedure is aimed at establishing the rehabilitation objectives. These objectives are selected from various combinations between performance targets (*damage state*) and earthquake hazard levels (*seismic hazard level*). The performance levels of the structure should be decided by the engineer with the owner. Furthermore, the performance target is set taking scope of an acceptable damage level. However, due to large uncertainties involved in the process, on the demand as well as on the capacity side, variations from the stated performance objectives should be expected. Variations in actual performance are mainly due to: (i) lack of knowledge in existing buildings, e.g., unknown geometry and member sizes, (ii) deterioration of materials, (iii) incomplete site data, (iv) variations of ground motions due to local effects and (v) incomplete knowledge and simplifications for structural modeling and analysis.

The selection of the rehabilitation method is performed in step 3. This part comprises the selection of the analysis procedure, the development of a preliminary rehabilitation scheme using one or more rehabilitation strategies, the analysis of the building (including rehabilitation measures) and the evaluation of the analysis results.

In the final steps, i.e., steps 4 and 5, the performance and verification of the rehabilitation design are conducted. Rehabilitation measures are designed using the applicable rehabilitation method. The rehabilitation design is verified to meet the requirements through an analysis of the building, including rehabilitation measures. A separate analytical evaluation is performed for each combination of building performance and seismic hazard specified in the selected rehabilitation objective.

It is instructive to note that if the rehabilitation design fails to comply with the acceptance criteria for the selected rehabilitation objective, then the rehabilitation measures should be redesigned. Alternatively, different rehabilitation strategies may be selected. This iterative process is repeated until the design complies with the target rehabilitation objectives. If the design meets such objectives then the decision is made to proceed with the rehabilitation.

The selection of the type of structural intervention adopted in the rehabilitation procedure is rather complex. There are many issues that need to be considered, classified as economical, social and technical. However, there are cases (e.g., the 1985 Mexico Earthquake) where aesthetical and psychological issues dictated the rehabilitation strategies. In Mexico City, external bracing was popular because it instilled a feeling of confidence in the occupants that significant and visible changes had been made to the structure to make it safer (Jirsa, 1994).

The criteria that influences the decision of the structural intervention type can be divided into two categories: criteria relative to social and economical issues (*general considerations*) and criteria referring to technical and structural issues (*technical considerations*). Such criteria are summarized hereafter.

i. General considerations:

- Cost versus importance of the structure.
- Available workmanship.
- Duration of works.
- Disruption to occupants.
- Fulfillment of the performance goals of the owner, i.e., life safety, essential facility, limited damage.
- Functionally and aesthetically compatible and complementary to the existing building.
- Reversibility of the intervention.
- Level of quality control.

- Political and/or historical significance.

ii. Technical considerations:

- Structural compatibility with the existing structural system.
- Irregularity of stiffness, strength and ductility.
- Adequacy of local stiffness, strength and ductility.
- Controlled damage to non-structural components.
- Sufficient capacity of foundation system.
- Repair materials and technology available.

The intervention program includes decisions on the level of intervention. These may be one of the following:

- Restriction or change of use of the building.
- Local or global modification (stiffness, strength, ductility) of elements and system.
- Addition of new lateral load resistance system.
- Partial demolition and/or mass reduction.
- Transformation of non-structural into structural components.
- Base isolation.
- Provision of supplementary damping via passive devices.

Intervention strategies, either traditional or nonconventional, are discussed in Section 2.5. However, it should be noted that in cases where seismic retrofit of buildings is quite expensive and disruptive, the alternatives of *no intervention* or *demolition* are more likely outcomes of the evaluation. Moreover, the aforementioned structural intervention measures may be combined in order to provide solutions. Therefore, generalization of rules for application in repair and strengthening is neither possible nor advisable. The flow chart for the investigation, evaluation and retrofitting of steel and composite buildings is provided in Figure 2.17.

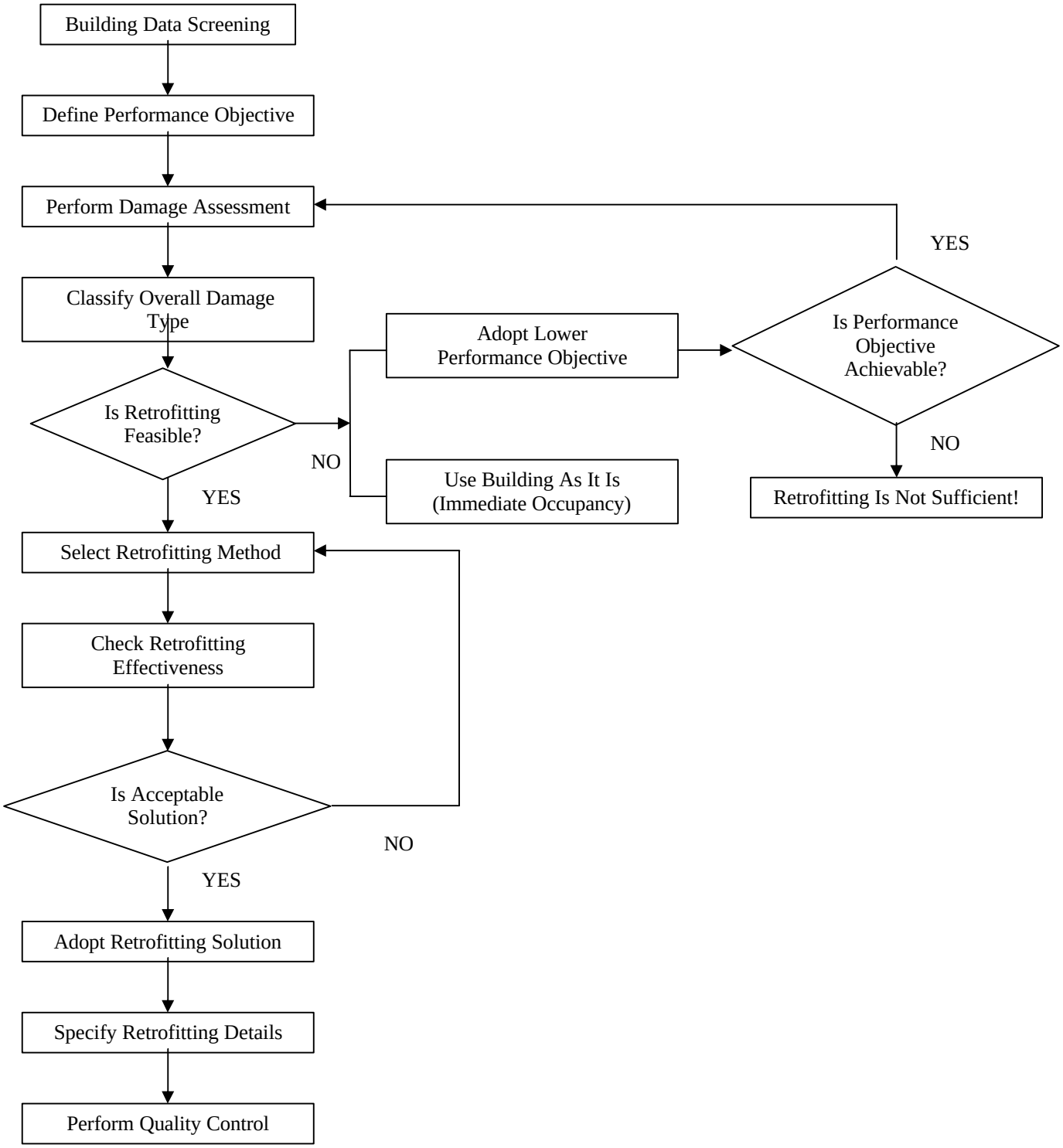

Figure 2.17. Flowchart for the investigation, evaluation and retrofitting of steel buildings.

The seismic performance of existing steel and composite buildings may be evaluated through either simplified or refined methodologies (FEMA 310, 1998; FEMA 356, 2000). However, the former is applicable only to regular buildings in low-to-moderate seismic zones, while the latter is a general procedure. The assumptions along with the steps of the evaluation process of such procedures along are provided hereafter.

2.4.1. SIMPLIFIED METHODOLOGY

This methodology is applicable to a selected group of buildings and should be used only to check the LS of near collapse, i.e., hazard level corresponding to earthquake probability of exceedance of 2% in 50 years (mean return period of 2,475 years). Similar recommendations may be found in the US guidelines (FEMA 310, 1998; FEMA 356, 2000) in which a set of five model structures is provided for steel and composite buildings (Table 2.2). These buildings are defined as regular and are generally low-rise; the maximum number of stories allowed for such an approach is provided as a function of the seismic hazard (Table 2.3). However, it is recommended that the simplified methodology should be used for limited rehabilitation objective, i.e., life safety performance level for an earthquake with 10% of probability in 50 years (return period of 475 years). Therefore, the US procedure is less stringent than that proposed above for retrofitting in Europe, life safety for 10% in 50 years *vs.* near collapse prevention for 2% in 50 years.

Table 2.2. Model steel and composite buildings (*adapted from* FEMA 310, 2000).

Building type	Description
MRFs	•Typical assembly of beam and columns with composite slabs. •Slabs can be either solid or with metal decks. Connections are rigid or semi-rigid. •Columns resist seismic forces with bending about major axis. •Walls may be panel curtains, glazing, brick masonry or pre-cast concrete panels. •Foundations are concrete spread footings or deep pile foundations. •Diaphragms may be either rigid or flexible.
Braced frames	•Include typical frames with braces, e.g., CBFs and EBFs. •Slabs can be either solid or with metal decks. •Connections are rigid or pinned. •Foundations are concrete spread footings or deep pile foundations. •Diaphragms may be either rigid or flexible.
Light frames	•Pre-engineered and prefabricated systems with steel frames. •Generally single-story. •Frames include tapered beams with roof and walls consisting of light weight metal, fiberglass or cementitious panels. •Connections are welded or bolted. •Lateral resisting force systems are rigid frames (transverse directions) and wall panel and rod bracings (longitudinal direction).
Frames with RC shear walls	•Steel frames with composite slabs (solid or metal decks). •Lateral forces resisted by shear walls and vertical loads carried by steel frames. •In dual systems frames and walls carry horizontal forces.
Frames with infill masonry shear walls	•Steel frames with composite slabs (solid or metal decks). •Masonry walls provide stiffness and resistance. •Diaphragms may be either rigid or flexible.

The simplified methodology should be used for buildings with characteristics similar to those described in Table 2.2 (*model buildings*); however, the structural regularity in plan and elevation should conform that of new buildings (EC8, 1998).

Table 2.3. Story number for simplified analysis of model building as a function of seismic hazard (*after* FEMA 356, 2000).

	Seismic hazard		
Building type	Low	Moderate	High
Moment resisting frame (stiff diaphragm)	6	4	3
Moment resisting frame (flexible diaphragm)	4	4	3
Braced frame (stiff diaphragm)	6	4	3
Braced frame (flexible diaphragm)	3	3	3
Light frame	2	2	2
Frame with concrete shear walls	6	4	3
Frames with infill masonry shear walls (stiff diaphragm)	3	3	*n.a.*
Frames with infill masonry shear walls (flexible diaphragm)	3	3	*n.a.*

Keys: *n.p.* = simplified analysis is not permitted.

The maximum height of the buildings is given in Table 2.4 for low-to-moderate seismic hazard; the simplified methodology is thus not recommended in zones with high seismicity. Furthermore, the structures with either supplemental damping devices or base isolation require detailed analyses; hence, they are not suitable for simplified approaches.

Table 2.4. Story number for simplified analysis of model building as a function of seismic hazard (*proposal for EC8*).

	Seismic hazard	
Building type	Low	Moderate
Moment resisting frame	4	4
Braced frame	3	3
Light frame	2	2
Frame with concrete shear walls	6	4
Frames with infill masonry shear walls	3	3

The steps of the simplified methodology may be summarized as follows (Figure 2.18):

1. Collect data of the building.
2. Classify the building using model buildings described in Table 2.2 as reference.
3. Identify potential structural deficiencies as described in Table 2.5. If the building does not require retrofitting then skip steps (4) through (7).
4. Rank structural deficiencies in priority order of correction.
5. Adopt ad hoc standard remedies to eliminate and/or mitigate structural deficiencies. Standard remedies should be chosen among those listed in Table 2.6.
6. Design the adopted rehabilitation.
7. Perform linear analyses, either static or dynamic, to check the fulfillment of performance objectives. Simplified mathematical models should be used for the analysis.
8. If the performance is not satisfactory, repeat steps (7) through (9) until the process converges. Alternatively, produce the final report.

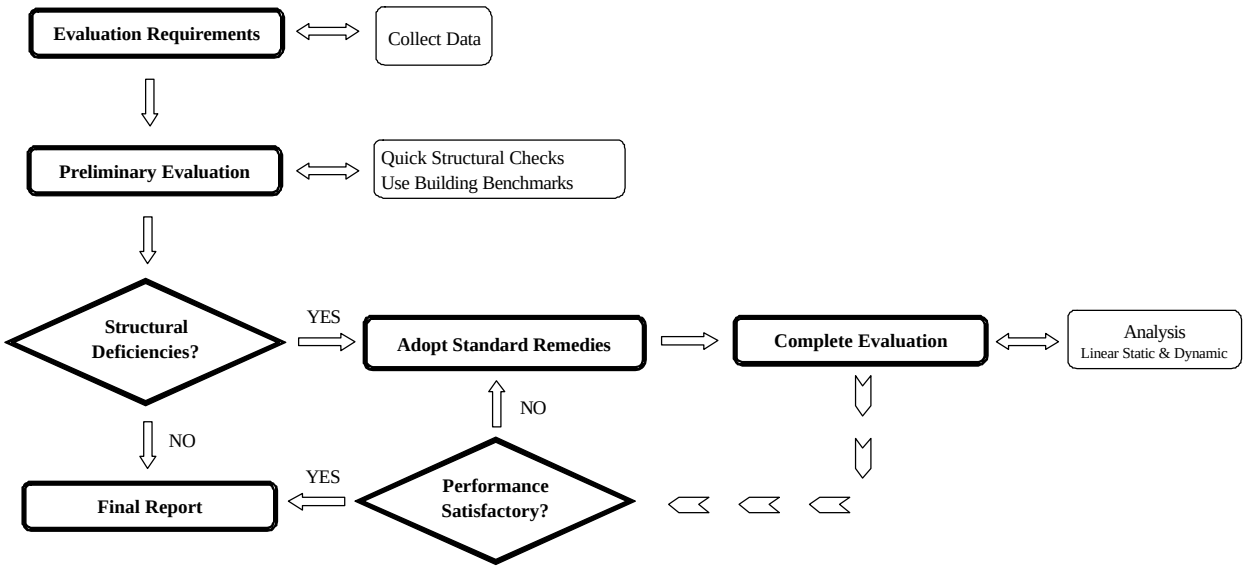

Figure 2.18. Evaluation process: simplified methodology.

Table 2.5. - Typical deficiencies for model steel and composite buildings (*adapted from* FEMA 356, 2000).

	MRFs	Braced frames	Frames with RC walls	Frames with masonry walls	Light frames
Structural deficiency	• Material (condition of steel). • Load path. • Redundancy. • Irregularities (plan and/or elevation). • Adjacent buildings. • Frame (drifts, frame concerns, strong-column-weak-beam, and connections). • Diaphragm (corners, openings, stiffness and/or strength, span-depth ratio, diaphragm/frame shear transfer, anchorage). • Foundations (anchorage, overturning, horizontal loads).	• Material (condition of steel). • Load path. • Redundancy. • Irregularities • (plan and/or elevation). • Bracings (strength and/or stiffness, chevron or K-bracings, connections). • Diaphragm (corners, openings, stiffness and/or strength, span-depth ratio, diaphragm/frame shear transfer, anchorage). • Foundations (anchorage, overturning, horizontal loads).	• Material (condition of steel and quality of concrete). • Load path. • Redundancy. • Irregularities (plan and/or elevation). • Concrete walls (shear stress, overturning, coupling beams, boundary component detailing, and reinforcement). • Diaphragm (corners, openings, stiffness and/or strength, span-depth ratio, diaphragm/wall shear transfer, anchorage). • Foundations (anchorage, overturning, horizontal loads).	• Material (condition of steel, quality of masonry). • Load path. • Redundancy. • Irregularities (plan and/or elevation). • Frame not effective for seismic forces. • Masonry walls (shear stress, reinforcing, proportions, solid walls, reinforcing at openings). • Unreinforced shear walls. • Infill walls. • Diaphragm (corners, openings, stiffness and/or strength, span-depth ratio, diaphragm/wall shear transfer, anchorage). • Foundations (anchorage, overturning, horizontal loads).	• Material (condition of steel, quality of concrete and masonry). • Load path. • Redundancy. • Irregularities (plan and/or elevation). • Frame (frame concerns). • Masonry shear walls (infill). • Braced frame (brace strength, connections). • Diaphragm (corners, openings, stiffness and/or strength, span-depth ratio, diaphragm/frame shear transfer, wall and roof panels, claddings). • Foundations (anchorage, overturning, horizontal loads).

Table 2.6. Standard remedies for structural deficiencies in model steel and composite buildings (*adapted from* FEMA 356, 2000).

Structural system	Structural deficiencies	Suggested remedies
General	Load path	• Add new well founded shear walls, frames to infill in existing shear walls or frames well connected to the foundations. • Improve connections between diaphragm and lateral resisting system.
	Redundancy	• Add new lateral force resisting system.
	Pan and vertical irregularities	• Add new braced frames or shear walls.
	Adjacent buildings	• Add new braced frames or shear walls (for connected structures). • Tie together existing structures to form single system (for separate structures). • Increase separation to eliminate pounding.
	Deflection compatibility	• Add new braced frames or shear walls.
MRFs	Frame concerns	• Add steel plates to beam-columns and braces. • Add lateral supports.
	Strong-column-weak-beam	• Add steel plates to columns. • Reduce beam sections.
	Connections	• Reinforce or weaken existing connections. • Use new connections. • Add continuity plates.
Braced frames	Braced frame concerns	• Add more braced bays. • Add shear walls.
	Diagonals	• Add shear walls.
	Chevron and/or K-bracings	• Add cover plates to the beams. • Add stiffeners to the beams. • Replace with different brace configuration.
	Connections	• Reduce connection eccentricities. • Add steel plates to beam-columns.
RC shear walls	Shear stress	• Add new shear walls. • Increase thickness existing walls.
	Overturning	• Lengthen existing walls. • Add new walls.
	Coupling beams	• Infill beams.
	Wall reinforcement	• Infill openings. • Increase thickness existing walls.
	Wall opening	• Infill openings.

Masonry shear walls	Reinforcement	• Add minimum reinforcement.
	Shear stress	• Add new walls. • Strengthen existing walls.
	Reinforcing at openings	• Add steel frames. • Add steel plates and/or profiles with bolts.
Unreinforced masonry walls	Solid walls	• Increase wall thickness. • Add new strong back-up systems. • Restraint out-of-plane movements.
	Infill walls	• Eliminate short column effects. • Add new back-up systems. • Restraint out-of-plane movements.
Diaphragms	Re-entrant corners	• Add new chords. • Add new shear connectors.
	Openings	• Add new drag struts. • Add new chords.
	Spans	• Add new vertical elements.
	Span-to-depth ratio	• Add new vertical elements.
	Continuity	• Add new vertical elements at the diaphragm offsets or expansion joints.
	Diaphragm-frame shear transfer	• Add collectors. • Add splice plates. • Add shear transfer devices.
	Diaphragm-wall shear transfer	• Add collectors and connect to the frame.
	Anchorage to normal forces	• Add new wall anchors.
Light frames	Girder-wall connections	• Improve existing connections. • Add new connections.
	Wall-panel and cladding connections	• Improve existing connections. • Add new connections.
	Light gage metal, plastic and cementitious roof panels	• Improve existing connections. • Add new diaphragms.
Foundation	Anchorage	• Improve existing column foot connections. • Add curbs or haunches.
	Overturning	• Spread footings. • Add new piles. • Add new lateral resisting systems.

The necessity of performing structural retrofitting and the acceptability of the standard remedies adopted may be judged on the basis of maximum interstory drift (d/h). Such a parameter is more suitable for steel buildings than the local (member) failure (Elnashai *et al*., 1998); values of d/h equal to 3% may be assumed as allowable drifts.

The evaluation of the seismic performance of buildings with irregularities in plan or elevations, or with energy dissipation devices, should be performed through detailed procedures, as outlined in the next section.

2.4.2. DETAILED METHODOLOGY

Steel and composite frames with structural characteristics different from those of model buildings in Table 2.2 and Table 2.4, or frames in zones of high seismicity, should be assessed through detailed methodologies. Indeed, the structural irregularities and number of stories greater than those listed in Table 2.4 may give rise to a peculiar structural response that simplified mathematical models and linear analyses are not able to predict. Moreover, seismic performance at different LSs may be quantified through detailed methodologies of structural assessment.

The detailed scheme for the evaluation process should conform to the flow chart in Figure 2.19. The evaluation requirements differ from the counterparts in the simplified methodology because of the

explicit determination of the rehabilitation objectives, i.e., cross relations between hazard levels and performance levels (Figure 2.20). Alternatively, the building performance can be described in terms of: (i) the safety afforded building occupants during and after the event, (ii) the cost and feasibility of restoring the building to pre-earthquake condition, (iii) the length of time the building is removed from service to effect repairs and (iv) economic, architectural or historic impacts on the larger community. However, the quantification of such aspects is generally not straightforward.

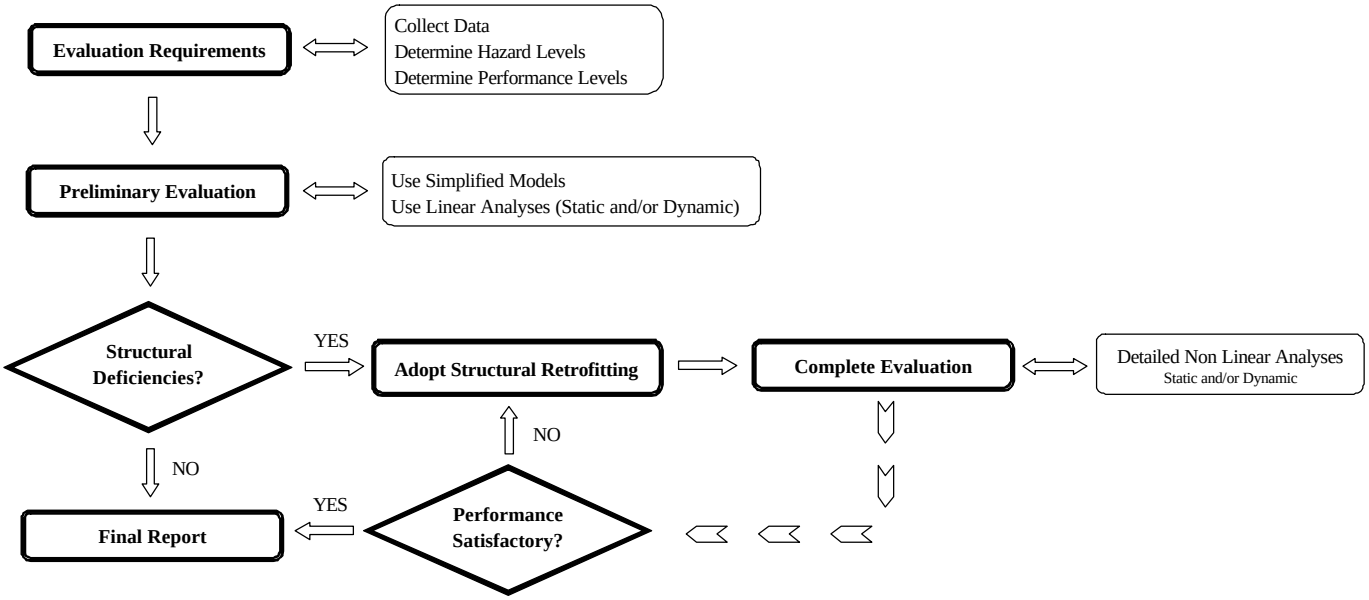

Figure 2.19. Evaluation process: detailed methodology.

Preliminary evaluations may be performed with reference to simplified building models using linear analyses: static or dynamic. By contrast, detailed evaluations of the seismic performance should be carried out through nonlinear analyses: static (pushovers) and/or dynamic (time histories). A set of representative ground motions should be used as input for the time histories analyses as for the design of new buildings (EC8, 1998); the performance parameters should be expressed as average values. Static pushovers should be carried out with two load/displacement patterns, i.e., inverted-triangular and uniform.

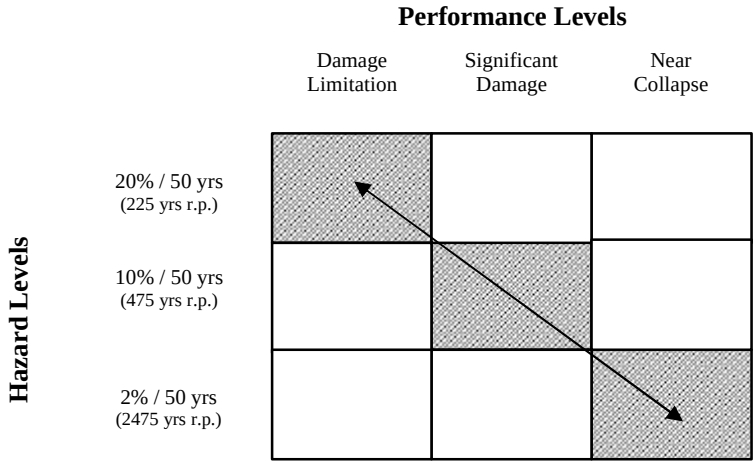

Figure 2.20. Performance objectives (*proposal for EC8*).

The structural response should be judged acceptable on the basis of the parameters provided in Table 2.7 as a function of the performance level. For example, a typical performance curve is given in Figure 2.21. Thus, it is evident that the stiffness, strength and ductility assume a paramount role in the behavior of structures as a whole. Indeed, to comply with the *damage limitation* performance target the structure needs enough stiffness to ensure that non-structural damage is minimized. Furthermore, sufficient strength to ensure elastic behavior and avoid extensive structural damage under medium events is also required to guarantee fulfillment of the *significant damage*. Moreover, in the case of a severe earthquake, the ductility of the structure plays a key role in the maintenance of its strength and reassures the fulfillment of *near collapse* prerequisites.

Table 2.7. Acceptance criteria at different levels of performance for steel and composite frames (*adapted from* FEMA 356, 2000).

		Performance Level		
	Element type	Damage Limitation	Significant Damage	Near Collapse
MRFs	Primary	• Minor local yielding at a few places. • No fractures. • Minor buckling or observable permanent distortion of members.	• Hinges form. • Local buckling of some beam elements. • Severe joint distortion. • Isolated moment connection fractures but shear connections remain intact. • A few elements may experience partial fracture.	• Extensive distortion of beams and column panels. • Many fractures at moment connections but shear connections remain intact.
	Secondary	• Same as primary	• Extensive distortion of beams and column panels. • Many fractures at moment connections but shear connections remain intact.	• Same as primary
	Drift	• 0.7% transient. • Negligible permanent.	• 2.5% transient. • 1.0% permanent.	• 5.0% transient. • 5.0% permanent.
Braced frames	Primary	• Minor yielding or buckling of braces.	• Many braces yield or buckle but do not totally fail. • Many connections may fail.	• Extensive yielding and buckling of braces. • Many braces and their connections may fail.
	Secondary	• Same as primary	• Same as primary	• Same as primary.
	Drift	• 0.7% transient. • Negligible permanent.	• 1.5% transient. • 0.5% permanent.	• 2.0% transient. • 2.0% permanent.

The multi-performance approach proposed above for the European Standards has already been adopted in other international guidelines either for retrofitting of existing structures (FEMA 356, 2000) or new buildings (SEAOC, 1995; FEMA 350, 2000). For example, four performance levels are used in Vision 2000 (SEAOC, 1995); such levels are summarized below in order of severity:

- *Fully operational* or *serviceable*: Facility continues in operation with negligible damage.
- *Operational* or *functional*: Facility continues in operation with minor damage and minor disruption in non-essential services.
- *Life safety*: Life safety is substantially protected and damage is moderate to extensive.
- *Near collapse* or *impeding collapse*: Life safety is at risk, damage is severe and structural collapse is prevented.

It is worth mentioning that each performance level is defined for the structural system (*structural performance level*), the non-structural system (*non-structural performance level*) and facility content (*content performance level*).

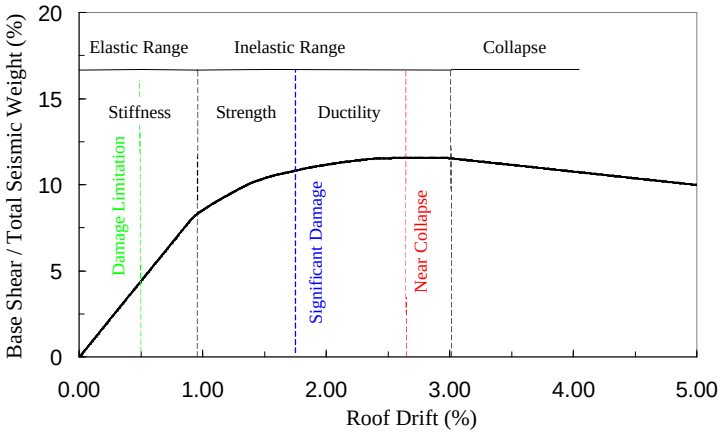

Figure 2.21. Typical performance curve (*capacity curve*) for framed structures.

On the other hand, recent guidelines for seismic rehabilitation (FEMA 273, 1997) and relative pre-standards (FEMA 356, 2000) provide a variety of performance objectives based upon cross relations between different performance objectives and associated probabilistic earthquake ground motion. Such rehabilitation objectives are generally expressed in matrix form as shown in Table 2.8.

Table 2.8. Rehabilitation objectives for building structures (*after* FEMA 356, 2000).

		Performance Levels			
		Operational (1-A)	Immediate Occupancy (1-B)	Life Safety (3-C)	Collapse Prevention (5-E)
Earthquake Hazard Level	50% / 50 year (Return Period 72 years)	*a*	*b*	*c*	*d*
	20% / 50 year (Return Period 225 years)	*e*	*f*	*g*	*h*
	10% / 50 year (Return Period 474 years)	*i*	*j*	*k*	*l*
	2% / 50 year (Return Period 2475 years)	*m*	*n*	*o*	*p*

Keys: *k* + *p* = Basic Safety Objective.
k + *p* + any of (*a*, *e*, *i*, *b*, *f*, *j*, *n*) = Enhanced Objectives.
o, *n*, *m* = Enhanced Objectives.
k, *p* = Limited Objectives.
c, g, d, h, l = Limited Objectives.

Each cell of the performance matrix represents a discrete rehabilitation objective which determines the cost and the feasibility of any rehabilitation project, as well as the benefit to be obtained in terms of improved safety, reduction in property damage and interruption in the use in the event of future earthquakes. Three types of rehabilitation objectives may be achieved by considering the cross relations in Table 2.8, i.e., *basic safety*, *enhanced* and *limited*, as described in the pre-standard document (FEMA 356, 2000).

It is instructive to note that three main differences arise when comparing the multi-performance approach proposed for the European Standards to the counterparts in the US practice. First, the seismic hazard levels are based on three types of earthquakes; ground motions with probability of exceedence 50%/50 years and return period of 72 years are not included in the proposal for Europe.

Second, the structural performance levels adopted in America are more detailed than those suggested for Eurocode 8, i.e., damage control. However, it is worth noting that the reduced number of structural performance levels proposed is adequate to describe the seismic performance of steel and composite buildings. Nevertheless, further studies should focus on the definition of similar damage states for the non-structural components.

2.5. UPGRADE STRATEGIES

Structural deficiencies in existing steel and composite buildings may be upgraded through several strategies, either traditional or nonconventional. Local and global interventions are effective methodologies to enhance the energy dissipation capacity of framed structures. However, novel materials (e.g., special metals) and technologies (e.g. base isolation and supplemental damping) are also available nowadays for structural retrofitting. The following section provides an outline of the traditional rehabilitation strategies for steel and composite frames. The main aspects of special metal materials and nonconventional strategies are reviewed critically.

2.5.1. OVERVIEW

Strategies for seismic retrofitting of steel and composite structures are generally based on strengthening or weakening of the existing structure or its components. Rehabilitation interventions are aimed at modifying structural strength, stiffness and damping to improve the seismic performance. However, two fundamental approaches may be followed in such interventions (FEMA 267, 1995; FEMA 351, 2000; FEMA 356, 2000): (i) local modification of structural components and connections and (ii) global modification of the structural system. Requirements for the fulfillment of these modifications are provided in the next chapter for each structural component and the frame system as a whole.

Effective local rehabilitation approaches consist of interventions (Figure 2.22) aimed at ensuring: (i) base and parent materials with adequate mechanical properties, (ii) sections and members with sufficient ductility and (iii) connections with adequate stiffness, strength and ductility. Furthermore, it is of paramount importance to avoid premature local and/or global (latero-torsional) buckling because it significantly reduces the energy dissipation capacity of steel structural members. However, based on the nature and extent of damage, several alternative local approaches to repair should be considered. Such approaches may be summarized as follows (FEMA 356, 2000):

- Replacement of damaged portions of base metal, e.g., beam-column sections.
- Replacement of damaged connection elements.
- Replacement of connection welds.
- Repairs to portions of any of the aforementioned components.

On the other hand, effective global rehabilitation approaches (Figure 2.22) are aimed at providing lateral force resisting systems with enhanced ductility. The improvement of the seismic performance may be achieved in different ways, depending on the structural deficiencies. For example, structures with irregularities in plan and/or elevations should be modified in order to regularize the system. Regular frames exhibit seismic performance superior to that of irregular counterparts. Moreover, mass reduction or lessening is benign because of the lower inertial forces attracted during earthquake loading.

Increasing the global stiffness, strength and damping is very effective to reduce story drifts and shears. Furthermore, higher global damping enhances the energy dissipation capacity of the structure. As a result, the structural damage is minimized and hence, the building may be safely

used in the aftermath of an earthquake. In several cases, e.g., office buildings, the business hosted in the structure is not interrupted; thus, reducing the economic losses due to the ground motion.

Enhanced global ductility may be achieved by forcing the inelasticity within dissipative zones and ensuring that the rest of the structure behaves linearly. Moreover, it is essential to guarantee:

- Regularity of mass.
- Regularity of stiffness distribution.
- Regularity of strength distribution.
- Continuity and redundancy between members.

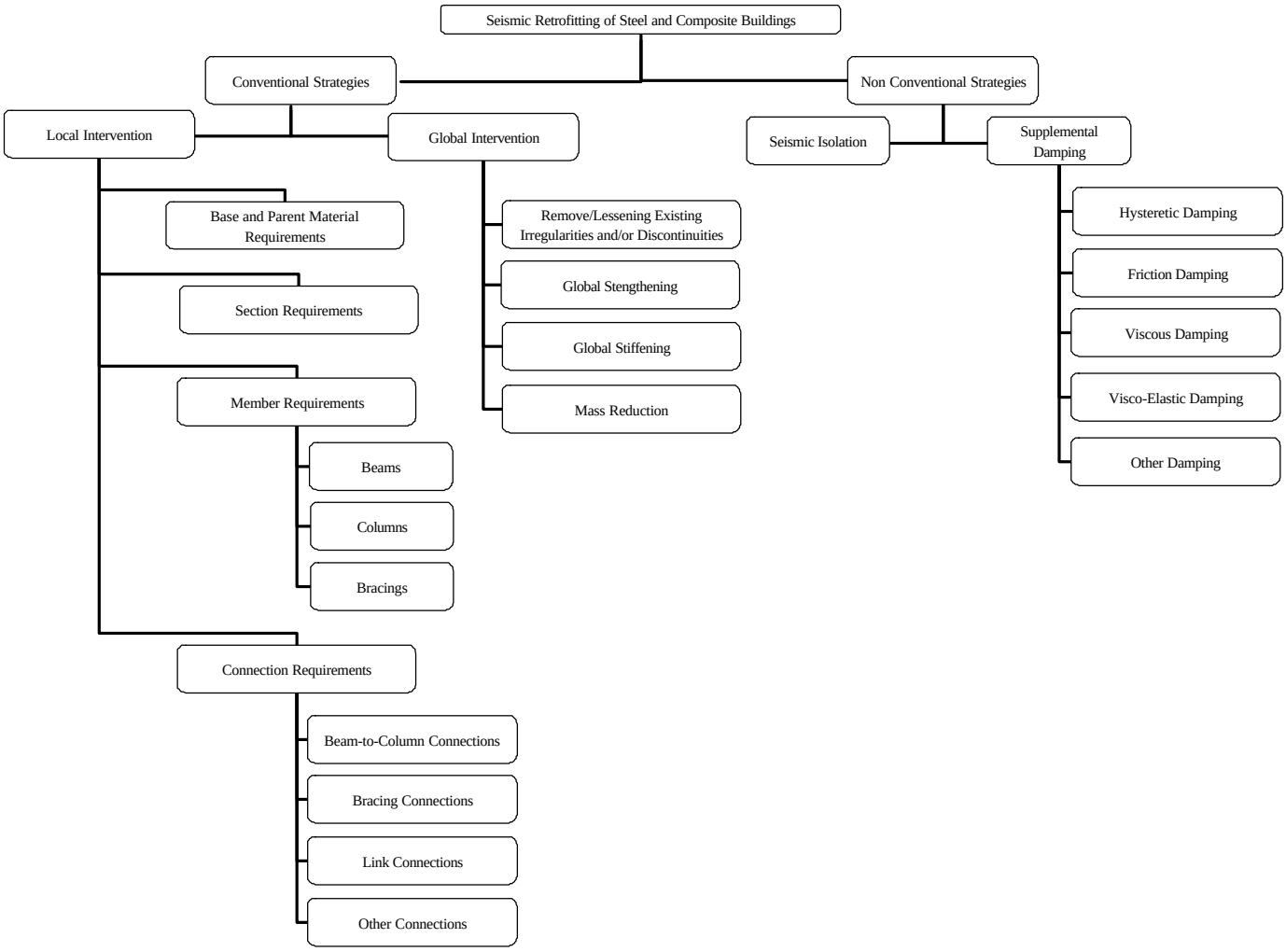

Figure 2.22. Retrofitting strategies for steel and composite buildings.

A detailed description of traditional local and global interventions is provided in the next chapter. The main aspects of special metals (aluminum, stainless steel and shape memory alloys) and nontraditional retrofitting strategies (seismic isolation and supplemental damping devices) are reviewed critically hereunder.

2.5.2. SPECIAL METAL MATERIALS

Innovative metal materials which can be used for retrofitting of steel and composite structures are:

- Aluminum alloys (AAs).
- Shape memory alloys (SMAs).
- Stainless steels (SSs).

These metals possess peculiar material characteristics that render them suitable in the field of seismic rehabilitation: (i) mechanical properties, (ii) corrosion resistance in harsh environments, (iii) heat resistance, (iv) weldability, (v) chemical-physical compatibility with other materials, (vi) life cycle cost and (vii) recyclability.

The mechanical properties of such novel metals are summarized in Table 2.9 (mild steel is also included and used as benchmark).

Table 2.9. Mechanical properties of steel and special metal alloys.

	Weight Volume (g/cm^3)	Young Modulus (GPa)	Yield Strength (MPa)	Ultimate Strength (MPa)	Elongation at Fracture (%)	Material Overstrength	Yield Strength-to-Weight Ratio ($x10^4$ cm)
Mild steels	7.9	205	215 ÷ 355	340 ÷ 510	10 ÷ 28	1.44 ÷ 1.58	27 ÷ 45
Aluminum alloys	2.7	65 ÷ 73	20 ÷ 360	50 ÷ 410	2 ÷ 30	1.14 ÷ 2.50	7 ÷ 133
SMAs (Ni-Ti)	6.5	28 ÷ 41 *m* 70 ÷ 83 *a*	70 ÷ 140 *m* 195 ÷ 690 *a*	1900 *w* 895 *f*	5 ÷ 10 *w* 25 ÷ 50 *f*	13.57 ÷ 27.14 *m* 1.30 ÷ 4.59 *a*	11 ÷ 22 *m* 30 ÷ 106 *a*
Stainless steels	8.0	193	180 ÷ 480	400 ÷ 660	35 ÷ 50	1.38 ÷ 2.22	23 ÷ 60

Keys: *a* = austenite; *m* = martensite; *f* = fully annealed; *w* = work hardened; material overstrength = ultimate/yield strength.

It is instructive to note that the density of all but SSs is generally lower than mild steels; AAs have a significantly reduced weight (one-third of mild steel). As a result, the latter is a viable solution when the minimization of added masses is of primary concern. However, this is not usually the case of normal buildings, but it can be crucial for other constructions (historical buildings, bridges, roofs). Moreover, AAs and SMAs are less rigid (about one-third the stiffness of steels). SSs have generally lower yield strengths than mild steels but higher strain hardening, see for example ductility ratios of 2.2 have been measured for the former, compared to 1.58 for the latter. AAs exhibit a wide range of variability for the yield strength (20 up to 360MPa). This is also the case of SMAs; however, the variability is less within a single phase, e.g., martensite (70 up to 140MPa) and austenite (195 up to 690MPa).

The values of ultimate elongation (*elongation at fracture*) show that SSs may undergo higher plastic deformations than mild steels (50 *vs.* 28). Material overstrength, that is a measure of the plastic redistribution, is high for AAa and SSs and exceptional for SMAs (up to 10 to 20).

Furthermore, they possess coefficient of thermal expansion similar to carbon steel: 17-19 x 10^{-6} $^oC^{-1}$ for SSs; 24-25 x 10^{-6} $^oC^{-1}$ for aluminum alloys; and 6.6-10 x 10^6 $^oC^{-1}$ for SMAs versus 12-15 x 10^{-6} $^oC^{-1}$ in mild steels. Strength-to-weight ratios show that special metal alloys, particularly SMAs and AAs, are extremely efficient. Therefore, they may be adequately exploited as suitable materials for retrofitting applications.

The choice of any such metal alloy for retrofitting should depend primarily upon: (i) mechanical properties (strength, stiffness and ductility), (ii) compatibility, (iii) corrosion and heat resistance and (iv) life cycle assessment. A comparison of the approximate cost of different materials is provided in Figure 2.23. It may be seen that AAs and SSs have similar costs for the raw materials; it is much higher (about four times) than MSs. However, as far as seismic retrofitting is concerned, the choice of design solutions should be performed on the basis of cost-benefit analysis accounting for life cycle costs; judgement of simple initial costs is, in fact, restrictive and unreliable.

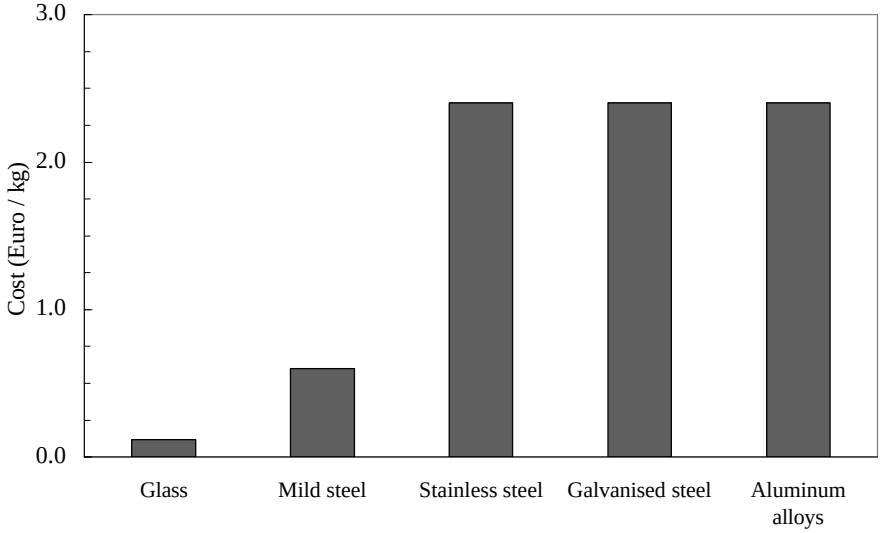

Figure 2.23. Approximate costs of some materials used in the construction industry.

An overview of the innovative metal alloys is provided herein; special emphasis is placed on their engineering properties that render them suitable for applications in seismic retrofitting of steel and composite structures. Issues concerning mechanical modeling are also briefly addressed.

2.5.2.1. ALUMINUM ALLOYS

New aluminum alloys based upon the relatively high strength, ductility, lightweight and good corrosion resistance are constantly being developed (Tryland *et al.*, 2001). The use of such metals for structural retrofitting has already been proved, especially to enhance the seismic resistance of shear links in braced frames (Rai and Wallace, 1998) or to rehabilitate historical and monumental structures (Mazzolani and Mandara, 2002). Therefore, they represent an attractive solution for steel and composite structures.

AAs are obtained by adding several chemical elements (e.g., copper, magnesium, manganese, silicon or zinc) to aluminum to increase its strength. Indeed, pure aluminum has good ductility properties but low strength. As a result, several alloys are available and their mechanical properties vary as a function of the chemical composition. For example, Al-Mg alloys (5000 series) exhibit high work-hardening along with good corrosion resistance. By contrast, series 6000 and 7000, i.e., Al-Si-Mg and Al-Zn-Cu alloys, have high strength and relatively reduced corrosion resistance and ductility (Mazzolani, 1995).

The stress-strain response for AAs is highly nonlinear and does not exhibit a well-defined yield point and generally (EC9, 1999) a *proof stress*, i.e., 0.20% offset permanent strain, is employed (Figure 2.24). The strain-hardening is also significant; material over-strength, i.e., ultimate-to-yield stress, may be as high as 2.50, thus giving rise to large plastic redistributions.

The increased strength-to-weight ratio (Table 2.9), low yield strength, strain-hardening, good ductility, ease of manufacture of components (either simple or with complex shapes) weldability, render aluminum an attractive metal for the improvement of existing structures. In fact, components in low yielding ductile AAs may function as fuse, limiting the maximum lateral force transmitted to primary structural members and provide significant energy dissipation. Unpinched and fully

hysteresis loops (*metallic hysteresis*) may be found either in normal or shear stresses (Rai and Wallace, 1998), provided that buckling phenomena are prevented.

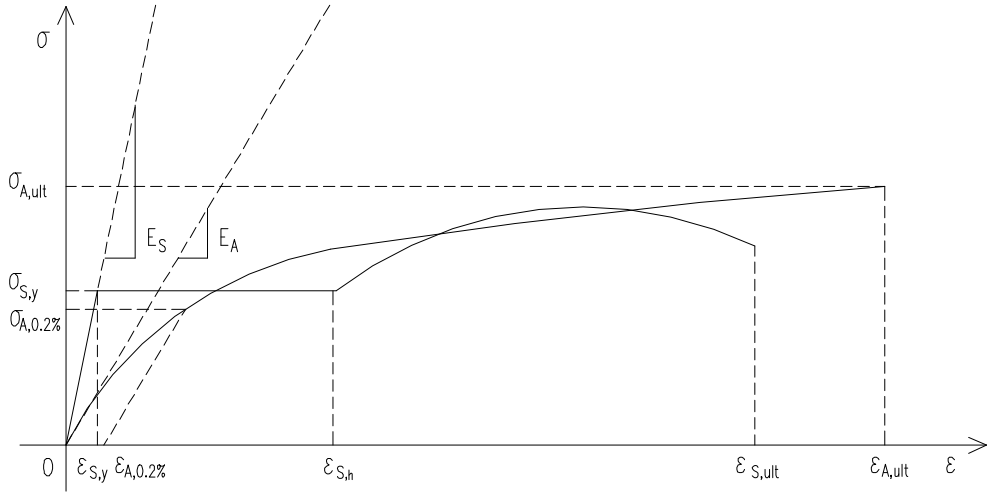

Figure 2.24 Stress-strain curves for aluminum (A) and steel (S).

Numerical analyses performed via finite element method (FEM) in inelastic regime, employ generally simplified mono-axial stress-strain formulations. The most common models comprise linear elastic perfectly plastic (LEPP), linear elastic strain hardening (LESH), linear elastic nonlinear hardening (LENLH) and Ramberg-Osgood model (ROM). The uniaxial stress-strain response for mild steel is usually modeled via LEPP, LESH or LENLH, while AAs aluminum may be reliably modeled via ROM, which is based on the following equation:

$$e = e_e + e_p = \frac{s}{E_0} + c \cdot \left[\frac{s}{s_y}\right]^n \tag{2.1}$$

where ε is the total strain, expressed as the sum of the elastic and plastic part, σ is the actual stress, E_0 the elastic (initial) modulus, σ_y is a proof stress; and c and n are model constants. The latter two parameters should be calibrated through tests on compression or tensile coupons, or more reliably from stub columns using curve fitting.

The Ramberg-Osgood curve is capable of closely approximating stress strain curves for a wide range of aluminum alloys. However, multi-axial models for metal plasticity are more reliable when cyclic loads are considered (Moen *et al*., 1999). The material can be modeled either as elasto-plastic with isotropic linear elasticity (von Mises yield criterion) and isotropic hardening or using more advanced formulations. For example, a multi-axial formulation with strain hardening, based on true stress-strain curve, has been proposed (Tryland *et al*., 2001); its expression is:

$$s_{eq} = Y_0 + Q \cdot \left(1 - e^{-C \cdot e_p}\right) \tag{2.2}$$

where σ_{eq} is the equivalent stress; ε_p the plastic strain; Y_0, Q and C are material properties; Y_0 is the proof stress; and Q and C determine the magnitude of the strain hardening and the shape of the curve, respectively. According to available experimental tests, suitable values for C are 10-20 (Moen *et al*., 1999; De Matteis *et al*., 2001; Tryland *et al*., 2001); whereas factor Q varies depending on the alloy, normally ranging between 80 MPa (*low hardening*) and 200 MPA (*high hardening*).

2.5.2.2. SHAPE MEMORY ALLOYS

Shape memory alloys (SMAs) have attracted extensive interest in seismic retrofitting in the past decade owing to their novel properties (Graesser and Cozzarelli, 1991; Housner *et al*., 1997; Dolce *et al*., 2000). SMAs are indeed metallic materials which may undergo large deformations (strains up to 10%) while recovering their initial configuration, without any residual deformation, at the end of cyclic loading. Thus, unlike common plastically deforming metals, nonlinear deformations are metallurgically reversible for such novel alloys. This is a result of martensitic phase-change which can be either temperature-induced or stress-induced. SMAs are two-phase metals that may exist either in austenitic or in martensitic form. The former has a stiffer metallographic structure that gives rise to high yield strength, while the latter exhibits lower yield and is less rigid. Thus, the material phase type and its transformation are of importance for mechanical properties of these alloys.

In thermal-induced transformations at constant stress, SMAs are characterized by four temperatures: M_s and M_f during cooling, A_s and A_f during heating (Figure 2.25). M_s and M_f correspond to the temperatures at which the transformation from the parent phase (austenite or beta-phase) into martensite starts and finishes, respectively. On the other hand, A_s and A_f are the temperatures at which the reverse transformation, i.e., martensite to beta-phase, starts and finishes. Martensite-to-austenite transformation occurs over a relatively narrow temperature range, lying between -100 and 100 ^oC, as a function of the alloy composition. However, the beginning and end of the transformation during heating or cooling extends over a much larger thermal range.

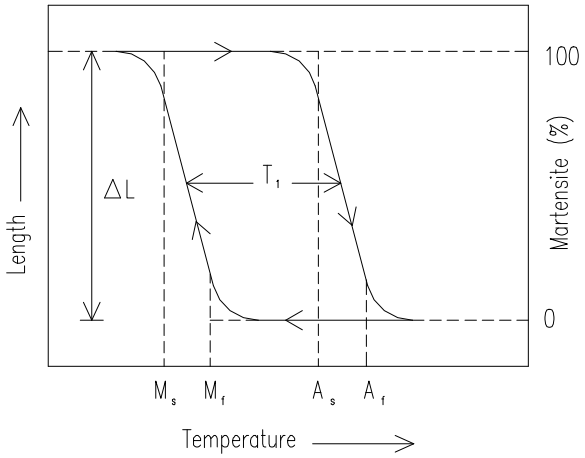

Figure 2.25. Typical transformation versus temperature curve for a SMA specimen (*constant stress*).

The overall metallurgical transformation describes a hysteresis loop (*thermal hysteresis*) of the order of 10 to 50^oC corresponding to T_1 in Figure 2.25; T_1 varies as a function of the alloying system (Van Humbeeck, 2001). It is worth mentioning that the thermal or transformation hysteresis is defined as the temperature difference between a phase transformation upon heating and cooling. In Ni-Ti alloys, for example, it is usually measured as the difference between A_p and M_p. A_p (M_p) is the temperature at which a shape memory alloy is about 50% transformed to austenite (martensite) upon heating (cooling).

In stress-induced isothermal transformations, austenite transforms to martensite at a critical stress, which varies as a function of the temperature. The higher the applied stress the higher the transition temperature is. Under uniaxial load, stress in austenite remains almost constant until the entire phase is fully transformed, although deformations increase. Further straining causes the elastic loading of martensite. By unloading, a reverse transformation occurs; unstressed martensite is, in

fact, unstable at such temperatures. The inverse transformation takes place at a lower stress level; hence, hysteresis occurs (*mechanical hysteresis*).

Depending on the material temperature (greater or lower than austenitic finish temperature A_f) SMAs exhibit two different mechanical properties (Figure 2.26). If the temperature is greater than A_f, strains attained on loading (even 8-10%) are completely and spontaneously recovered after unloading. This process leads to significant energy-absorbing capacity with zero residual strain (*superelasticity* or *pseudoelasticity*); this effect is defined *superelastic* because it is characterized by the impressive amount of possible elastic strain, which is more than 20 times higher compared to conventional materials. By contrast, if the material temperature is less than A_f, residual strains remain at the end of unloading but they may be recovered by heating above A_f (*shape memory effect*). It is worth noting that the residual strain is very large if the temperature is less than A_s, i.e., if the material phase is fully martensitic.

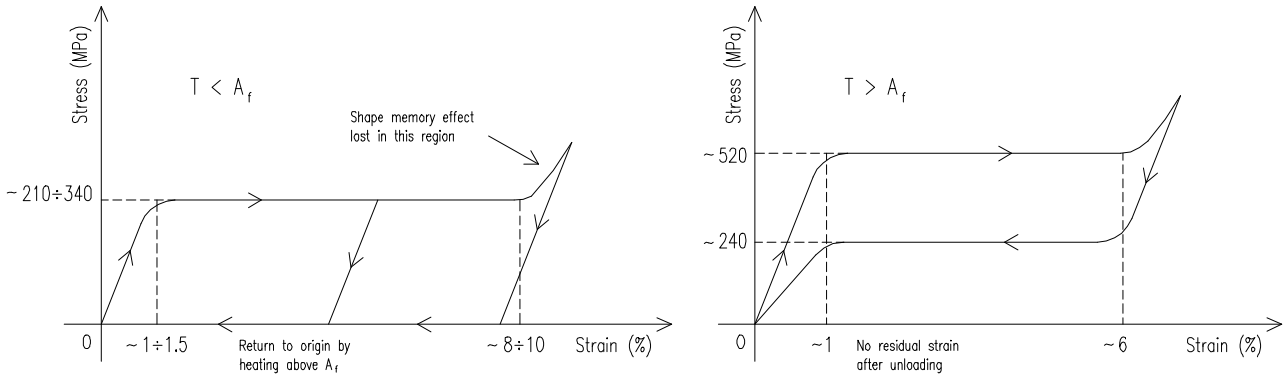

Figure 2.26. Stress-strain relationship showing shape memory effect (*left*) and super-elasticity (*right*).

During thermal and/or stress-induced phase transformations, the modulus of elasticity of SMAs varies significantly (*thermo-elasticity*); e.g. for Ni-Ti alloy it changes by a factor of 4. Similar changes may occur in yield strength. Yet, damping characteristics undergo significant changes with temperature. It is instructive to note that equivalent mechanical damping (ξ_{eq}) of these metal alloys, expressed as a percentage of the critical, is typically much higher than the steel counterpart, even when SMA material is near its activation temperature. Values of ξ_{eq} for these special metals are of the order of 15% to 20% *vs*. 0.1% to 0.2%, generally used for mild steel (Bachmann *et al*., 1995). The significant damping level is due to the large hysteresis loop involved in the loading and unloading process.

Five groups of SMAs are of interest for seismic rehabilitation: Ni-Ti, Fe-Mn-Si, two copper alloys (Cu-Zn-Al and Cu-Al-Ni) and some special stainless steel formulations (Dolce *et al*., 2000). Although Ni-Ti SMAs are more expensive and more difficult to machine than Cu-based SMAs, they are extensively used for structural applications. Such metals allow higher working stresses and strains and exhibit generally higher stability under cyclic loads. Other mechanical characteristics that render SMA, especially Ni-Ti alloys, desirable for seismic protection of structures, include (Duerig *et al*., 1990): (i) hysteretic damping, (ii) highly reliable energy dissipation based on a repeatable solid state phase transformation; (iii) self-centering capability, (iv) excellent low and cycle fatigue properties, and (v) excellent corrosion resistance and (vi) no degradation due to aging.

As far as the modeling is concerned, a thermodynamic formulation was proposed (Achenbach *et al*., 1986) for the constitutive law of SMAs: the model was derived in plane strain. However, the latter is complex and difficult to be implemented in FEM codes for structural analysis. As a result, simplified formulations have been adopted for engineering applications (Graesser and Cozzarelli,

1991; Wilde *et al.*, 2000). They are one-dimensional stress-strain relationships able to describe the behavior of superelastic alloys; the applicability of such mathematical models was verified via experimental tests (Graesser and Cozzarelli, 1991). These constitutive laws (σ-ε curves) have the following expression:

$$\dot{s} = E \cdot \left[\dot{e} - \left| \dot{e} \right| \cdot \left(\frac{s - b}{Y} \right)^n \right] \tag{2.3.1}$$

$$b = E \cdot a \cdot \left\{ e^{in} + f_t \cdot |e|^c \cdot erf\ (a \cdot e) \cdot \left[u\left(-\dot{e} \cdot e \right) \right] \right\} \tag{2.3.2}$$

where β is back-stress; Y is the SMA yield stress, i.e., the beginning of the stress-induced transition from austenite to martensite; n is the over-stress power; the constant α, given by $E_y/(E-E_y)$ controls the slope of the σ-ε curve; and the quantities E and E_y are the austenitic elastic modulus and the slope after yielding, respectively.

Moreover, inelastic strains (ε^{in}) are computed as follows:

$$e^{in} = e - \frac{s}{E} \tag{2.4}$$

while the error function *erf*(x) is given as:

$$erf\ (x) = \frac{2}{p} \cdot \int_0^x e^{-x^2} \cdot dx \tag{2.5}$$

and *u*(x) is the unit step function, whose expression is:

$$u(x) = \begin{cases} 0 & x < 0 \\ 1 & x \geq 0 \end{cases} \tag{2.6}$$

The constants f_t, c, and a are a function of the material; they control the recovery of the elastic strain during unloading.

Recently, the mathematical model expressed in Equations (2.3.1) and (2.3.2) was extended to represent the hardening of SMAs after the transition to the martensite is completed (Wilde *et al.*, 2000). Such a model allows describing of the material behavior over a wider range of strains; this is useful especially in the case of base isolation with SMA devices. The extended model replaces Equation (2.3.1) with the following:

$$\dot{s} = E \cdot \left[\dot{e} - \left| \dot{e} \right| \cdot \left(\frac{s - b}{Y} \right)^n \right] \cdot u_I(e) + E_m \cdot \dot{e} \cdot u_{II}(e) +$$

$$+ \left(3a_1 \cdot \dot{e}\, e^2 + 2 \cdot a_2 \cdot sign\ (e) \cdot \dot{e}\, e + a_3 \cdot \dot{e} \cdot u_{II}(e) \right) \tag{2.7}$$

with:

$$u_I(e) = \left(1 - u_{II}(e) - u_{III}(e)\right) \tag{2.8.1}$$

$$u_{II}(e) = \begin{cases} 0 & |e| < e_m \\ 1 & |e| \geq e_m \end{cases} \tag{2.8.2}$$

$$u_{III}(e) = \begin{cases} 1 & e \cdot \dot{e} > 0 \quad and \quad e_1 < |e| < e_m \\ 0 & otherwise \end{cases} \tag{2.8.3}$$

The elastic behavior of martensite depends upon the term $E_m \cdot \dot{e} \cdot u_{II}(\varepsilon)$; this response starts if strains are higher than e_m (Figure 2.27), which corresponds to the completion of the phase transformation from austenite to martensite. The transition from the stiffness E_y to E_m is smooth and is mathematically obtained by means of the last bracketed term in Equation (2.7); this term is computed only during loading and for strains $\varepsilon_1 < |e| < \varepsilon_m$. The curvature of the transition depends upon the constants a_1, a_2 and a_3, whose values are chosen in such a way the slope of the function in the last bracketed term in Equation (2.7), at ε_1 and ε_m, are consistent with: (i) the slope of SMA plastic behavior and (ii) elastic response of martensite. The slope evaluated in ε_2 controls the smoothness of the transition.

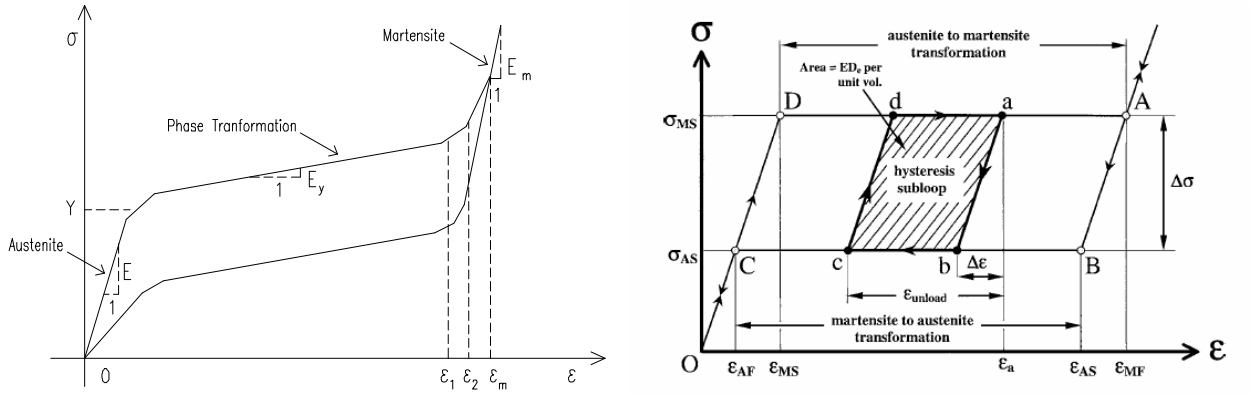

Figure 2.27. Cyclic stress-strain curves for SMAs: actual (*left*) and idealized (*right*).

For SMAs with perfect superelastic behavior the values of parameters controlling the shape of loops are: a=900, C=0.001, f_t=0.08, α=0.019 and n=1 (Wilde *et al*., 2000). The limit of the superelastic range is ε_m=0.08, while the points defining the transition from the slope E_y to E_m are ε_1=0.05 and ε_1=0.065; the latter is the mean of ε_1 and ε_m. Elastic modulus of martensite (E_m) is generally 30-35% lower than elastic modulus of SMA austenite state (E); they depend upon the alloy chemical composition; which is also the case of yield stress (Y).

2.5.2.3. STAINLESS STEELS

Stainless steels (SSs) are metal alloys which contain a high percentage of chromium (Cr); normal grades are obtained by adding at least 12% by weight to low-alloy carbon steel. The presence of Cr allows the formation of a protective oxide on the material surface (stainless metal). Furthermore, Cr is employed in the classification of SS groups (Figure 2.28), based on their micro-structure, as follows:

- Austenitic (ASS)
- Ferritic (FSS)

- Austenitic-ferritic (AFSS) or duplex
- Martensitic (MSS)
- Precipitation hardening (PHSS)

It should be pointed out that the choice of the most suitable type and grade of SS relies fundamentally upon the required corrosion resistance for the ambient conditions, namely the 'service environment' (Euro Inox, 1994). SS life expectancy cannot be separately treated from structural design as in mild steel, but it is strictly related to: (i) the initial selection of material grade, (ii) the design process, (iii) the fabrication route and (iv) the surface finishing and maintenance (EC3, 1996).

Therefore, among the aforementioned sub-groups, ASSs and AFSSs are usually employed for structural applications. So far, the former has been the most successfully used due to the wide range of available industrial products manufactured from it (structural profiled sections, bolts, nuts, etc.).

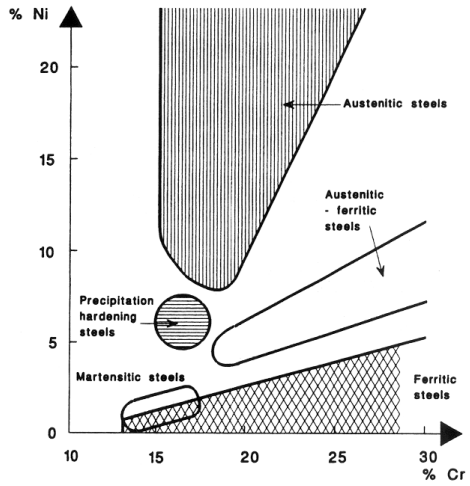

Figure 2.28. Schaeffler diagram for stainless steel (*after* EC3, 1992).

It is noteworthy that the application of SS in ordinary structural systems was prompted by recent analytical and experimental studies carried out world-wide (Aoki, 2000; Burgan *et al*., 2000; Johansson and Olsson, 2000; Di Sarno *et al*., 2002). Design procedures have been already implemented, although further developments as well as improvements are required to achieve the desired reliability and cost-effectiveness (Euro Inox, 1994; EC3, 1996).

The stress-strain response for SS shows a gradual transition for the elastic to the plastic branch; generally a 0.2% offset permanent strain is employed as yield strength. Moreover, its mechanical response is strongly dependent on the material composition. Figure 2.29 illustrates these properties by contrasting the stress-strain response of two types of SS, i.e., austenitic and austenitic-ferritic, to the mild steel.

SSs exhibit higher ultimate-to-yield stress (σ_u/σ_y) ratios than mild steels, thus leading to a larger spread of plasticity along the member length (Table 2.9). Furthermore, predefined material over-strength may be more easily achieved by manufacturers due to tighter quality controls. However, these improvements are achieved for higher material initial cost for SS (ranging between four and six times) compared to ordinary carbon steels.

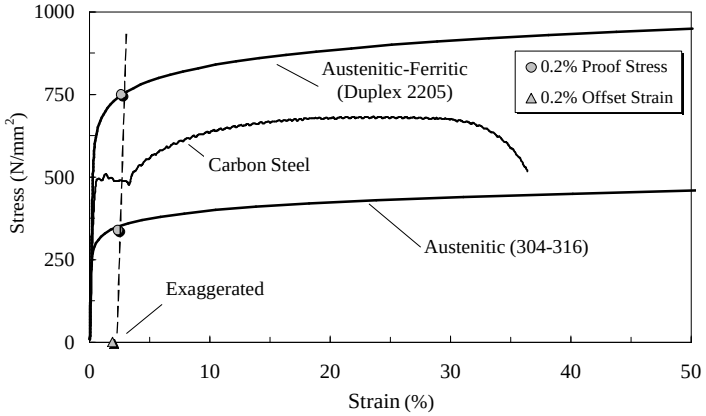

Figure 2.29. Typical stress-strain curve for stainless and mild steels.

SSs exhibit high values of elongation-to-fracture (ε_u) that increases with thickness. For ASS, i.e., S220 and S240 with thickness less than 3 mm the values vary between 35% (S240) and 37% (S220), while a value of 40% was found for greater thickness. However, these figures are lower bounds. Thus, this higher ultimate elongation has a beneficial influence for the application of SS in seismic design and/or retrofitting.

Experimental tests performed on SS beam-columns showed excellent energy absorption capacity (ductility); thus promoting the efficiency of SS in seismic applications (Aoki, 2000).

SS generally exhibits greater increases in strengths at fast rates of loading (Euro Inox, 1994). Annealed types of ASS exhibit a proof stress reduction of 15% and 30% for tests conducted with a strain rate from 10^{-3} to 10^{-5} and from 10^{-3} to 10^{-8} per second, respectively. More recently, dynamic tests on SS were performed over a range of strain rates from 1.4×10^{-4} to 8.0 sec^{-1} (Jones and Birch, 1998). It has been confirmed that the initial stress state of the material has an effect on the strain rate. Furthermore, the influence of the material strain rate sensitivity decreases with an increase in strain. As a result, the ultimate tensile strength for dynamic loading conditions is enhanced to a lesser extent than the yield stress for the same strain rate.

ASS and AFS possess greater toughness than mild steel and may be assumed not to be susceptible to brittle fracture for service temperatures down to -40^{o}C (EC3, 1996). Furthermore, recent fatigue tests (SCI, 2000), based upon constant amplitude axial tension loading, showed that longitudinal and transverse nonload carrying fillet welds for SS behave much better than equivalent welds in ordinary steels. Thus, reference S-N curves for mild steel underestimate the actual response of SS for the same fatigue classes. Nonetheless, it is thought that higher fatigue classes cannot be reliably used yet for designing construction in stainless steels, because of the limited experimental data. Therefore, further experimental work is required to validate the higher performance of SS. However, it has been observed, however, that there are no significant changes of fatigue strength with thickness (at least for thickness of between 8 and 12 mm) unlike mild steel for which the behavior generally deteriorates with increasing thickness.

The main reasons behind the use of SS for seismic rehabilitation are: (i) its manufacturing processes are amenable to tighter control of the variation of yield strength and hence of the stress ratio σ_u/σ_y and (ii) it exhibits greater ductility than ordinary steels.

However, material modeling for SSs is, however, cumbersome since it should be based upon multi-axial models for cyclic plasticity. Recently, a two-surface based formulation with distortional rules was proposed (Johansson and Olsson, 2000) for SS. This model (Figure 2.30) enables the plastic threshold for loading steps following to the initial one to be achieved by means of modifications

applied to the earlier material model (elastic [inner] and memory [outer] surfaces). Moreover, under stress reversals the stress vector is not cut off by the elastic limit surface. This specific feature does not apply for standard incremental plasticity-based models for continua. This two-surface model provides results in good agreement with experimental tests on SS both for uniaxial and biaxial stress states. Since the initial yielding criteria for the ASS grade are almost isotropic, the formulation (von Mises criterion) is well suited to define the mechanical response of the ASS rather than the AFSS grades.

Furthermore, the reduction of the yield strength in the direction opposite to the initial loading, i.e., Bauschinger effect, as well as the increased yield strength in the direction transverse to the initial loading, can be represented by Olsson's formulation (Johansson and Olsson, 2000). However, a reliable choice of the yield stress (proof stress) value is necessary. It is more advisable for numerical modeling of materials with no distinct yield point to employ the proportional limit ($\sigma_{0.01}$) rather than the 0.2% offset strain ($\sigma_{0.2}$) stress.

Generally, the uniaxial stress-strain response for SS is used for FEM calculations; in such cases the ROM is employed. However, the latter model is characterized by a progressive decrease of the plastic modulus and is unsuitable when employed for a limited strain range in the SS uniaxial response. Nonetheless, recent experimental investigations have shown that the Ramberg-Osgood curve perfectly matches the actual (experimental) stress strain relationship up to the equivalent yield point (Mirambell and Real, 2000). Beyond this stress value, the mismatch tends to diverge and hence an improvement of the original formula is required. Therefore, a composite Ramberg-Osgood formula may be used, as follows:

- for $s \leq s_y$:

$$e = \frac{s}{E_0} + e_{py} \cdot \left[\frac{s}{s_y}\right]^n \tag{2.9.1}$$

- for $s > s_y$:

$$e = \frac{s - s_y}{E_{0.2}} + e_{pu} \cdot \left[\frac{s - s_y}{s_u - s_y}\right]^{n'} + e_{ty} \tag{2.9.2}$$

where n and n' are parameters to be calibrated by fitting the experimental curves; ε_{py} and ε_{pu} are the plastic strains corresponding to the 0.2% proof stress (σ_y); and ultimate strength (σ_u), respectively; ε_{ty} is the total strain corresponding to σ_y; and E_0 and $E_{0.2}$ are the initial and the proof stress moduli. It is worth noting that the second branch of the curve has been derived by employing translation of the coordinate system from the origin to the 0.2% stress point and expressing the basic formula in the new reference system.

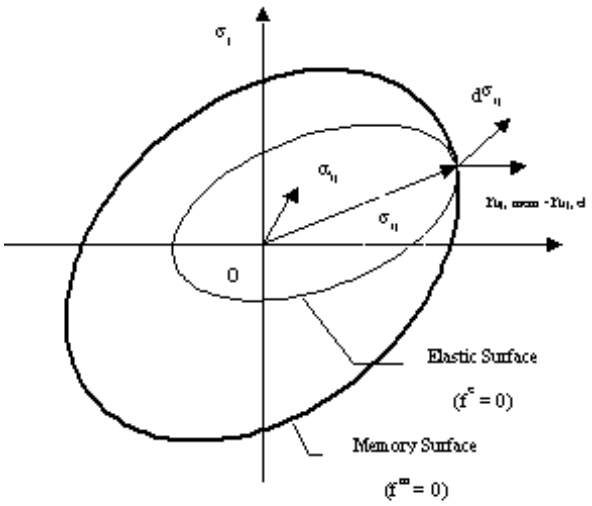

Figure 2.30. Translation elastic limit surface combined with expansion of memory surface.

It may be convenient and adequate to model the material response for AAs and SSs by means of uniaxial stress strain relationships of the Petersson and Popov multi-surface formulation (Petersson and Popov, 1977; Popov and Petersson, 1978). The latter employs a mixed isotropic and kinematic hardening rule and has been successfully adopted for several studies (Mizuno *et al*., 1987; Elnashai and Izzuddin, 1993). Its main advantage with respect to other simplified models, i.e., bilinear with/without hardening, was observed particularly in the large strain cyclic amplitudes (Elnashai and Izzuddin, 1993). Moreover, the multi-surface model gives a reliable estimate of the plastic hinge length as opposed to an overestimate of up to 50%, when employing simplified piecewise models, e.g., bilinear ones. Therefore, to obtain a realistic prediction of the system ductility as well as to achieve a rational representation of the structural (rather than numerical) collapse, the multi-surface model is a reliable formulation.

2.5.3. NONCONVENTIONAL STRATEGIES

Retrofitting of steel and composite structures may also be performed by modifying one of the mechanical parameters characterizing the dynamic response, namely: (i) mass distribution, (ii) stiffness distribution and (iii) structural damping. To do so, innovative seismic protection strategies, i.e., vibration control techniques, represent a viable solution (Soong and Spencer, 2002). These non-conventional techniques ensure vibration control and/or damage prevention by means of external dissipation devices; thus, primary structural components are protected for different seismic hazard levels.

The selection of a particular type of vibration control device is governed by a number of factors which include: (i) efficiency, (ii) compactness, (iii) weight, (iv) capital cost, (v) operating cost, (vi) maintenance requirements and (vii) safety. However, sound engineering practices enable, however, all but the capital and operating costs to be counteracted, which depend upon the required levels of reduced response and the complexity of the system to be dealt with.

2.5.3.1. REVIEW OF VIBRATION CONTROL DEVICES

The structural control of vibrations may be performed primarily by: (i) modifying masses, stiffness and damping and (ii) allowing passive or active counter forces to be generated. Despite its relatively recent development in civil engineering, these protection strategies have been growing very rapidly in Asia, Europe and the US, where several methodologies have been assessed, optimized and used successfully in practical applications (Nishitani and Inoue, 2001). A classification of the most common control systems is provided in Figure 2.31. Four groups are identified, i.e., (i) passive, (ii) active, (iii) hybrid and (iv) semi-active control systems, in compliance with the basic principles behind the control strategies (Housner *et al*., 1997). Relevant assumptions and peculiar mechanisms characterizing each category (Figure 2.32) are summarized hereafter.

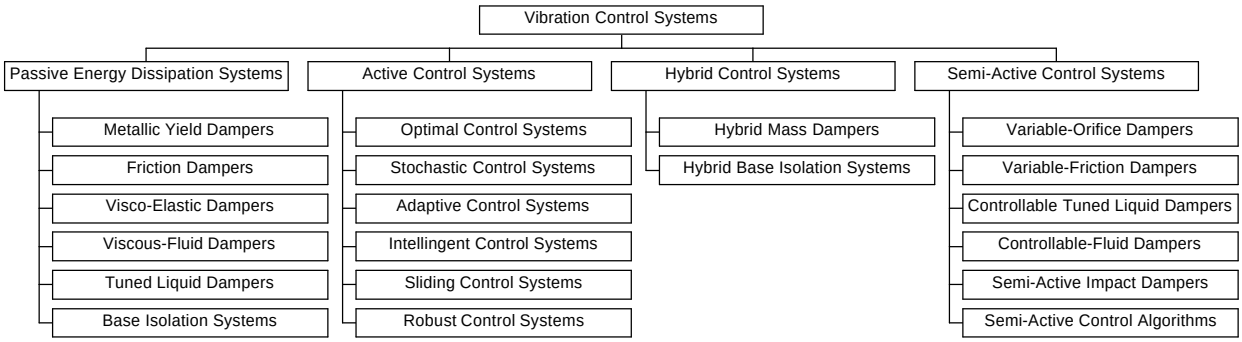

Figure 2.31. Common vibration control systems.

i. Active Control Systems

These systems possess external sources powering control actuator(s) that apply forces to the structure in a predefined manner. These forces can be used both to add and dissipate energy in the structure. In an active feedback control system, the signals sent to the control actuators depend upon the dynamic response of the system that is measured through physical sensors, i.e., optical, mechanical, electrical or chemical sensors.

ii. Passive Control Systems

Unlike active control systems, these devices do not require any external power source; they impart, in fact, forces due to the vibrations of the structure to protect. The energy in passively controlled structural systems, including the passive devices, cannot be increased by the passive control devices; by contrast, high damping levels may be beneficially achieved in the main structure.

iii. Hybrid Control Systems

These systems combine both active and passive control systems. To maximize the efficiency, it is common practice to employ active devices that may adequately improve drawbacks exhibited by certain passive dampers, or vice-versa.

iv. Semi-Active Control Systems

Similar in principle to active control systems, these systems require external energy sources which are of orders of magnitude smaller than ordinary active counterparts. Typically, they do not add mechanical energy to the structural system; therefore, bounded-input as well as bounded-output stability is guaranteed. Semi-active control devices are often viewed as controllable passive devices.

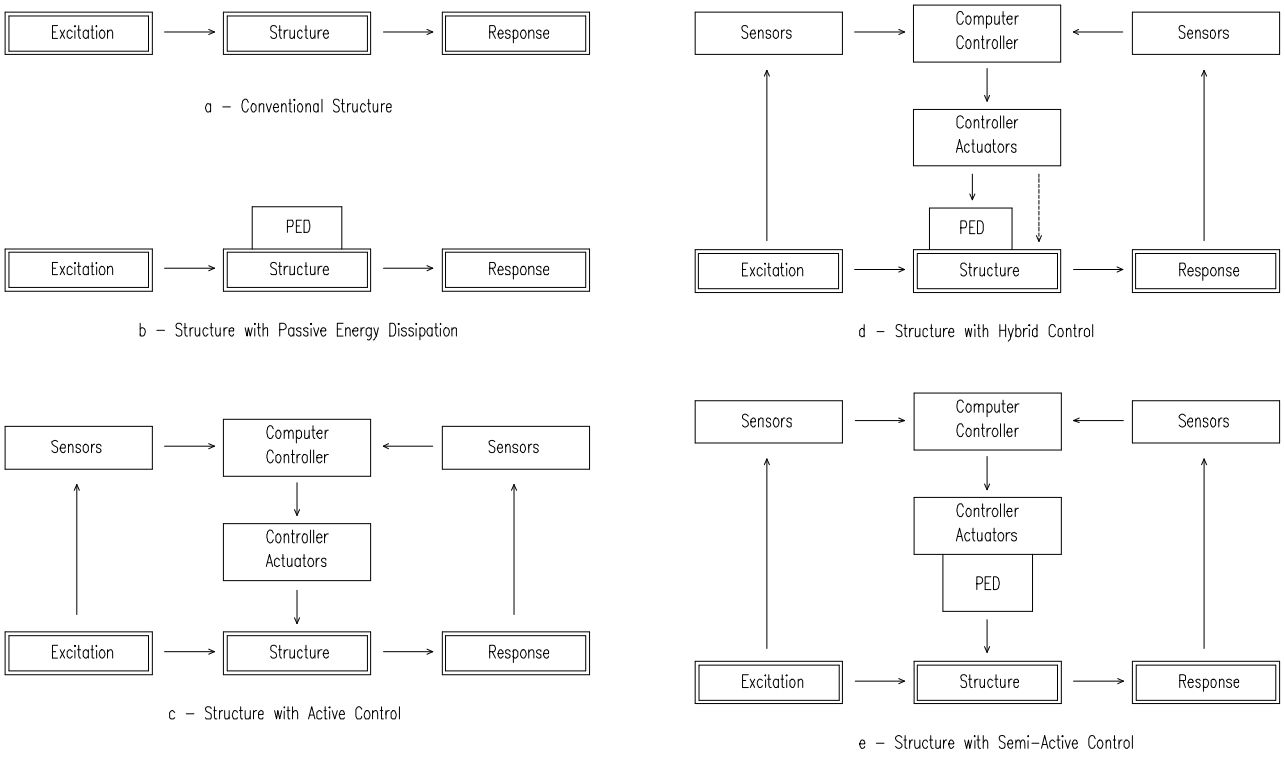

Figure 2.32. Structure with different control schemes (*after* Soong and Spencer, 2002).

Detailed descriptions and assessments of various vibration control devices may be found in literature (Housner *et al.*, 1997; Soong and Dargush, 1997; Naeim and Kelly, 1999; Soong and Spencer, 2002).

2.5.3.2. BASE ISOLATION AND SUPPLEMENTAL DAMPING

The efficiency of seismically isolated structures or structures with supplemental damping has been recently codified in international regulations and recommendations, especially in seismic design (FEMA 273, 1997; FEMA 356, 2000; FEMA 368, 2001). It is recognized that passive energy dissipation devices can absorb a portion of the earthquake-induced energy in the structure and reduce the energy demand on the primary structural members such as beams, columns, beam-column joints, and walls; thus, the structural safety may be adequately guaranteed. The conceptual design of seismic isolation and systems with energy dissipation is outlined in Figure 2.33; while their range of application and maturity is compared to other strategies of seismic control in Table 2.10.

Seismic isolation and supplemental damping systems are viable retrofitting strategies to enhance earthquake performances in building structures and/or whenever owners can afford the costs of design, fabrication, and installation of these special devices. However, these costs are offset by the reduced need for stiffening and strengthening otherwise required for rehabilitation objectives. The efficacy of such strategies is summarized in Table 2.11; US provisions (FEMA 274, 1997) are contrasted to a proposal for European standards, the latter are compliant with limit states adopted in EC8 draft for retrofitting (EC8, 1998).

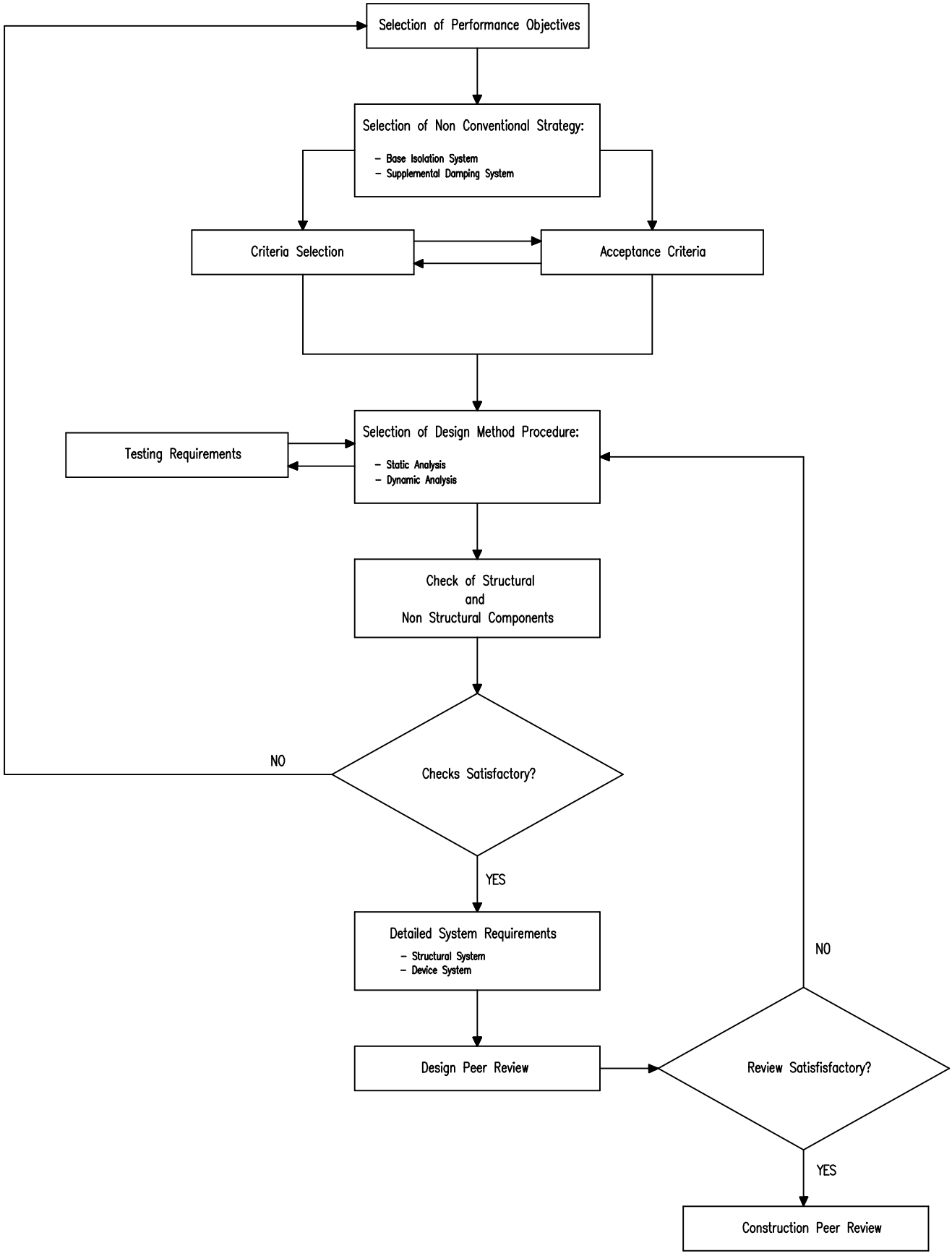

Figure 2.33. Conceptual design for base isolation and supplemental damping systems.

Table 2.10. Range of application and maturity of seismic control of structures.

Type of control	Range of application	Technical maturity
Seismic Isolation	• Low-to-medium rise buildings (either new or existing). • Bridges and subways. • Equipment or facilities.	• Mature technique. • Many theoretical and practical results. • Many applications world-wide.
Energy Dissipation	• Medium-to-high rise buildings (either new or existing). • Towers, stacks and chimneys. • Medium-to-long span bridges. • Lifelines.	• Mature technique. • Many theoretical and practical results. • Many applications world-wide.
Passive Control	• Medium-to-high rise buildings. • Towers, stacks and chimneys. • Medium-to-long span bridges. • Lifelines.	• Relatively mature technique. • Several theoretical and practical results. • Several applications world-wide.
Active, Semi-Active and Hybrid Control	• High rise buildings. • Towers, stacks and chimneys. • Medium-to-long span bridges.	• Ongoing research stage. • Several theoretical results. • Few applications world-wide.

Base isolation is a viable strategy for retrofitting steel and composite buildings due to several factors such as: (i) functionality, (ii) contents protection, (iii) investment protection and (iv) construction economy. Composite steel and concrete structures are used for buildings in commercial and financial areas. They contain sensitive and valuable equipment vital for business, commerce and emergency use; therefore, their disruption after an earthquake can have negative social-economic impacts. Fixed base buildings may, in fact, undergo large story drifts (flexible structures) or high floor accelerations (rigid structures) thus causing structural and/or nonstructural damage. In these cases, retrofitting via seismic isolation may result very efficient (Kelly, 1996); drifts and accelerations may, in fact, be reduced by a factor of two to six.

Table 2.11. Efficacy of isolation system and energy dissipation for retrofitting: (a) US guidelines and proposal for (b) EC8.

(a) *after* FEMA 274, 1997

Performance level	Isolation system	Energy dissipation
Operational	Very likely	Limited
Immediate occupancy	Likely	Likely
Life safety	Limited	Likely
Collapse prevention	Not practical	Limited

(b) *proposal for EC8*

Limit state	Isolation system	Energy dissipation
Damage limitation	Very likely	Limited
Significant damage	Likely	Likely
Collapse	Limited	Likely

A proposal for EC8 recommendations is provided in Table 2.12; alternative design approaches, i.e., base isolation or fixed base, are suggested as a function of earthquake ground motion levels (minor, moderate and major) and limit states (damage limitation, significant damage and collapse).

Table 2.12. Protection provided by isolation system for retrofitting (*proposal for EC8*).

	Earthquake ground motion level		
Limit state	Minor	Moderate	Major
Damage limitation	FBS / BIS	BIS	BIS
Significant damage	FBS / BIS	FBS / BIS	BIS
Collapse	FBS / BIS	FBS / BIS	FBS / BIS

Keys: BIS = base isolated system; FBS = fixed base system.

Buildings retrofitted with seismic isolation systems consist of three distinct parts: the structure above the isolation system, the isolation system itself and the foundation and other structural elements below the isolation system. Each of them should be properly assessed and detailed to achieve high effectiveness of this rehabilitation strategy. Moreover, transient design situations as lifting the superstructure, cutting structural elements, placing the isolators and giving back the load to the columns, should be adequately checked at the design stage. In fact, isolators are generally located in sub-basement, at top of basement columns, either at the bottom or top of first-story columns. Therefore, the working site is limited to garages or warehouses with no interruption for the activities within the building and no damage to the expensive finish and equipment.

The choice of bearing location within a building is not straightforward (Naeim, 2001); advantages and disadvantages of bearing locations mentioned above are provided in Table 2.13.

From a mechanical viewpoint, the use of isolation devices in seismic applications, particularly for retrofitting, relies upon three fundamental mechanical properties: (i) horizontal flexibility to increase structural period and reduce the transfer of seismic energy to the superstructure (except for very soft sites), (ii) energy dissipation (damping) to reduce displacements and (iii) sufficient stiffness at small displacements to provide adequate rigidity for service level environmental loads (Skinner *et al*., 1993). As a consequence, isolators should exhibit significant energy dissipation capacities and/or re-centering capabilities (Wilde *et al*., 2000). This target can be achieved either by choosing devices with intrinsic dissipative and re-centering capacities or by providing ad hoc additional elements.

Table 2.13. Advantages and disadvantages for different layout of base isolator locations (*after* Naeim, 2001).

Bearing Location	Advantages	Disadvantages
Sub-basement	• No special detailing required for separation of internal services, e.g., elevator and stairways. • No special cladding separation details. • Base of columns connected by diaphragm at isolation level. • Simple to incorporate back-up system of vertical loads.	• Added structural costs unless sub-basement required for other purposes. • Requires a separate (independent) retaining wall.
Top of basement columns	• No sub-basement requirement. • Minimal added structural costs. • Base of columns connected by diaphragm at isolation level. • Backup system for vertical loads provided by columns.	• May require cantilevered elevator shaft below first floor level. • Special treatment required for internal stairways below first floor level.
Bottom of first-story columns	• Minimal added structural costs. • Separation at level of base isolation is simple to incorporate. • Base of columns may be connected by diaphragm. • Easy to incorporate backup system for vertical loads.	• May require cantilever pit.
Top first-story columns	• Minimal added structural costs. • Economic if first level is for parking. • Backup system for vertical loads provided by columns.	• Special detail required for elevators and stairs. • Special cladding details required if first level is not open. • Special details required for vertical services.

Seismic isolators mainly include two groups, as a function of the technology used for energy dissipation mechanisms (Figure 2.34):

- *Elastomeric isolators*: They are usually made of layers of rubber separated by steel shims, which constrain lateral deformation of the rubber under vertical load. Elastomers

manufactured with special fillers provide generally elevated hysteretic energy dissipation. Elastomeric devices are high-damping rubber bearings (HDR), low-damping rubber bearings (RB) or low-damping rubber bearings with a lead core (LRB). These type of devices have been used extensively worldwide for new and existing structures because of its high efficiency (Soong and Constatinou, 1994).

- *Sliding isolators*: their main source of energy dissipation is friction. Two disadvantages have been found for such systems: (i) friction is usually difficult to quantify and (ii) permanent offset between the sliding parts may occur after an earthquake (*not re-centering systems*) (Naeim and Kelly, 1999). Sliding devices are usually flat assemblies, such as sliding poly-tetrafluoroethylene (PTFE), or have a curved surface, i.e., friction-pendulum system (FPS). It is worth mentioning that FPS overcomes both the above disadvantages by employing a curve rather flat surface upon which friction takes place. Further sliding isolators are *rolling isolators.* They consist of flat assemblies or have a curved or conical surface. A typical rolling system is the ball and a cone system (BNC).

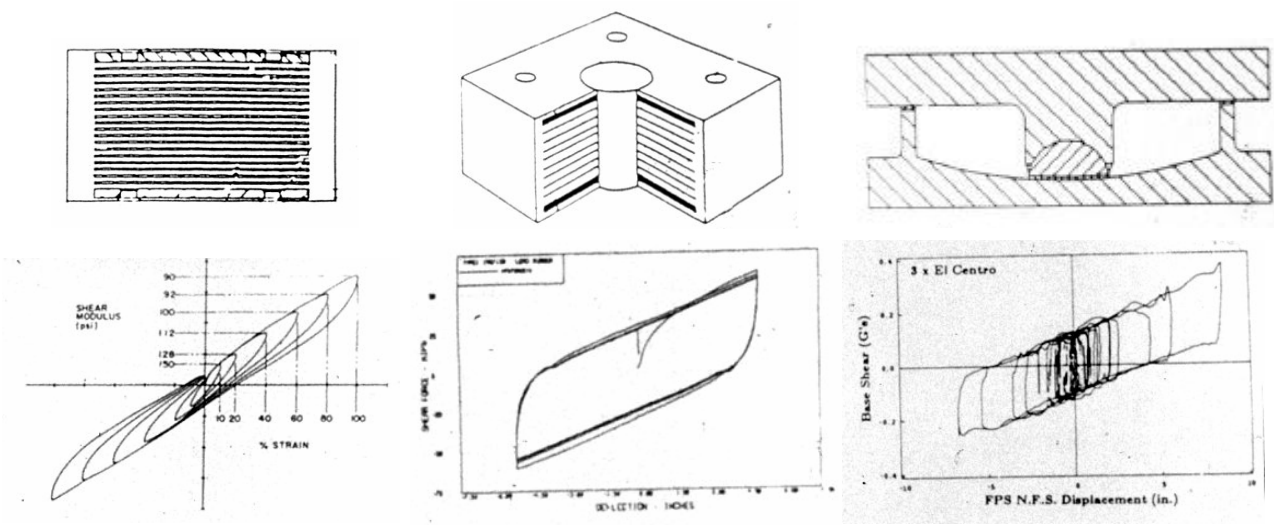

Figure 2.34. Common isolation devices and relative hysteretic loops: high damping rubber (*left*), lead rubber (*middle*) and friction pendulum (*right*) device.

The choice of an adequate isolator should comply with specific acceptance criteria. In particular, they should remain stable for the design displacements and provide increasing resistance with increasing displacement (no degradation) under repeated cyclic load. Advantages and disadvantages of common base isolators are provided in Table 2.14.

The mechanical response of isolation systems may be characterized via four types of relationships (as shown in Figure 2.35) in which the idealized curves are referred to the same design displacement (D_D):

- *Linear system*: The effective period does not change with the earthquake loading. Forces applied to the super-structure are proportional to the displacement across the isolation device. Some wind-restraining is required.

- *Hardening system*: the stiffness is initially lower (*long effective period*) and then it increases (*short effective period*) accordingly to the earthquake loading. The super-structure is subjected to higher forces than in a linear system; However, the displacements of the isolation system are smaller. A wind-restraining mechanism is required.

- *Softening system*: The stiffness is initially higher (*short effective period*) and then it decreases (*long effective period*) as the earthquake loading increases. The super-structure is subjected to lower forces than in a linear system; however, the displacements of the isolation system are higher.

- *Sliding system*: The effective period increases according to the earthquake loading. The superstructure is subjected to constant loads. Wind-restraining mechanisms are required for low values of friction.

Table 2.14. Advantages and disadvantages of common base isolator devices (*after* Kelly, 2001).

Isolator type	Advantages	Disadvantages
Elastomeric	• Low in-structure accelerations. • Low cost.	• High displacements. • Low damping. • No resistance to service load. • P-Δ moments top and bottom.
High Damping Rubber	• Moderate in-structure acceleration. • Resistance to service loads. • Moderate-to-high damping.	• Strain dependent stiffness and damping. • Complex analysis. • Limited choice of stiffness and damping. • Change in properties with scragging*. • P-Δ moments top and bottom.
Lead Rubber	• Moderate in-structure accelerations. • Wide choice of stiffness and damping.	• May require cantilever pit. • P-Δ moments top and bottom.
Flat Sliders	• Low profile. • Resistance to service loads. • High damping. • P-Δ moments can be top and bottom.	• High in-structure accelerations. • Properties depend on pressure and velocity. • Sticking. • No restoring forces.
Curved Sliders	• Low profile. • Resistance to service loads. • Moderate-to-high damping. • P-Δ moments can be top and bottom. • Reduced torsion response.	• High in-structure accelerations. • Properties depend on pressure and velocity. • Sticking.

* Scragging is the process of subjecting an elastomeric bearing to one or more cycle of large amplitude displacement. This process modifies the molecular structure of the elastomer and result in more stable hysteresis at strain level lower than that to which the elastomer was scragged.

Isolated buildings may be designed using either static analysis (*equivalent lateral force procedure*) or dynamic analysis (*dynamic lateral response procedures*); however, the latter is usually required because the simplified lateral force design has several limitations (FEMA 368, 2001). Such limitations depend upon the seismic input (site location with respect to active faults and local soil conditions) and the structural system (geometrical and mechanical properties of the building as well as the isolation system). Dynamic analyses are carried out via either response spectrum or time-history analysis. International standards and recommended provisions (IBC, 2000; FEMA 357; 2000; FEMA 368, 2001) and their commentaries (FEMA 369, 2001) may be used as reference for the formulation of the aforementioned methods of analysis. The use of UBC 1997 should be avoided because it is unnecessarily complicated and conservative (Naeim and Kelly, 1999).

Minimum design displacement and/or lateral forces on seismically isolated structures are based on the deformation characteristics of the isolation system, which can be represented either by an equivalent linearly elastic model or via nonlinear models (nonlinear time history analyses). The use of equivalent linear models is advised at this stage because they are more reliable than nonlinear ones.

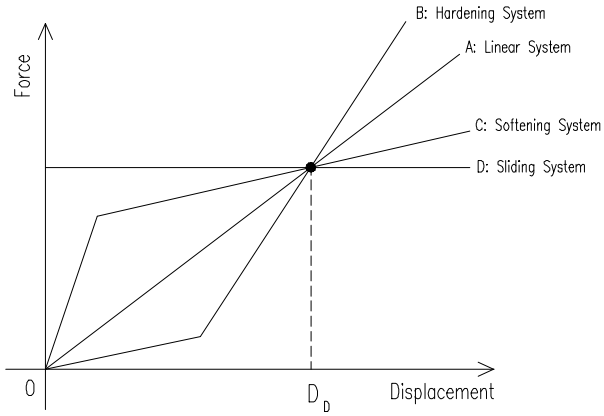

Figure 2.35. Idealized force-displacement relationships for isolation systems.

Design parameters of linearly elastic isolation systems include effective stiffness (k_{eff}) and damping (β_{eff}). These mechanical parameters may be determined via force-deflection curves obtained from hysteresis loops of device prototypes in cyclic load tests (Figure 2.36). The effective stiffness is as follows:

$$k_{eff} = \frac{\left|F^{+}\right| + \left|F^{-}\right|}{\left|\Delta^{+}\right| + \left|\Delta^{-}\right|} \tag{2.10}$$

where F^+ and F^- are the positive and negative forces at Δ^+ and Δ^-, respectively.

The effective damping is computed via the relationship:

$$b_{eff} = \frac{2}{p}\left[\frac{E_{loop}}{k'_{eff}\left(\left|\Delta^{+}_{p}\right| + \left|\Delta^{-}_{p}\right|\right)^{2}}\right] \tag{2.11}$$

where E_{loop} is the energy dissipated for cycle of loading; and $k`_{eff}$ is the effective stiffness based on peak negative and positive test displacements, Δ^{-}_{p} and Δ^{+}_{p} respectively.

It is worth mentioning that to determine design displacements, lowest effective stiffness and damping should be used. By contrast, design forces are due to the greatest stiffness values and lowest damping (FEMA 369, 2001).

Static analysis may be employed to establish a minimum level of design displacements and forces and for preliminary designs; therefore, an outline is provided hereafter.

Four distinct displacements should be computed according to the seismic hazard, i.e., 475 year return period earthquake (*LS of Significant Damage*) or 2,475 year return period earthquake (*LS of Collapse*).

These displacements are as follows:

- *Design displacement* (D_D): Displacement (in *mm*) at the center of rigidity of the isolation system at the LS of significant damage. It is computed as follows:

$$D_D = \left(\frac{g}{4 \cdot p^2} \right) \cdot \frac{S_D \cdot T_D}{B_D} \tag{2.12}$$

where g is acceleration of gravity (in mm/sec^2); S_D is design 5% damped spectral acceleration at T is 0.0 sec for 475 year return period earthquake; T_D is effective period of seismically isolated structure at the design displacement; and B_D is coefficient expressed as a function of the effective damping of the isolation system at the design displacement (β_D). It may be either expressed in tabular form (FEMA 368, 2001) or in a close-form (Naeim and Kelly, 1999); a graphical comparison is provided in Figure (2.37). The approximation is very close for the values of effective damping of interest for practical applications, i.e., less than 50%. The damping β_D in the system is as follows:

$$b_D = \frac{1}{2 \cdot p} \cdot \left(\frac{\sum E_D}{k_{D,\max} \cdot D_D^2} \right) \tag{2.13}$$

where $\sum E_D$ is the sum of the energy dissipated per cycle in all isolator units measured at D_D.

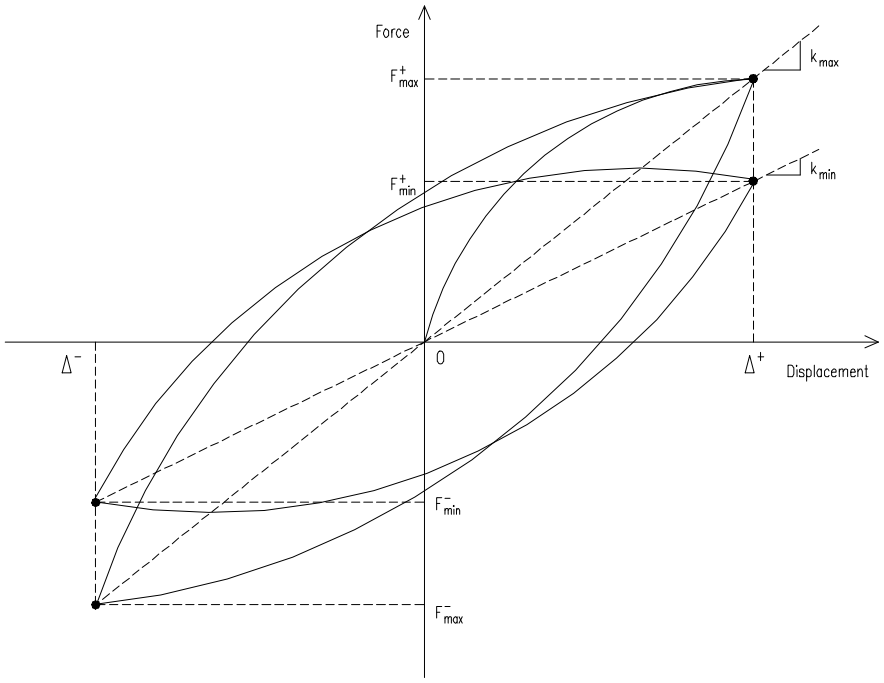

Figure 2.36. Design mechanical parameters for isolation systems.

- *Maximum Displacement* (D_M): displacement at the center of rigidity of the isolation system at the LS of collapse. Its expression is given by:

$$D_M = \left(\frac{g}{4 \cdot p^2} \right) \cdot \frac{S_M \cdot T_M}{B_M} \tag{2.14}$$

where S_M is the design 5% damped spectral acceleration at T = 0.0 sec for 2,475 year return period earthquake; T_M is the effective period of seismically isolated structure at the maximum displacement; and B_M is the coefficient expressed as a function of the effective damping of the isolation system at the maximum displacement (β_M).The damping β_M in the system is as follows:

$$b_M = \frac{1}{2 \cdot p} \cdot \left(\frac{\sum E_M}{k_{M,\max} \cdot D_M^2} \right) \tag{2.15}$$

where $\sum E_M$ is the sum of the energy dissipated per cycle in all isolator units measured at D_M.

The numerical value of B_M can be computed from Figure 2.37.

- *Total Design Displacement* (D_{TD}): Displacement of a bearing at a corner of the building, including the component of the torsional displacement in the direction of the design displacement. Therefore, it is computed at the LS of significant damage. Its expression is as follows:

$$D_{TD} = D_D \cdot \left[1 + y \cdot \left(\frac{12 \cdot e}{b^2 + d^2}\right)\right] \tag{2.16}$$

where y is the distance between the center of rigidity of the isolation system and the element of interest measured perpendicular to the direction of loading; e is the actual eccentricity between the center of mass of the super-structure and the center of rigidity of the isolation system plus accidental eccentricity equal to 5% of the longest plan dimension of the structure perpendicular to the direction of loading; b is the shortest plane dimension of the structure measured perpendicular to d; and d is the longest plan dimension of the structure. All distances are in *mm*.

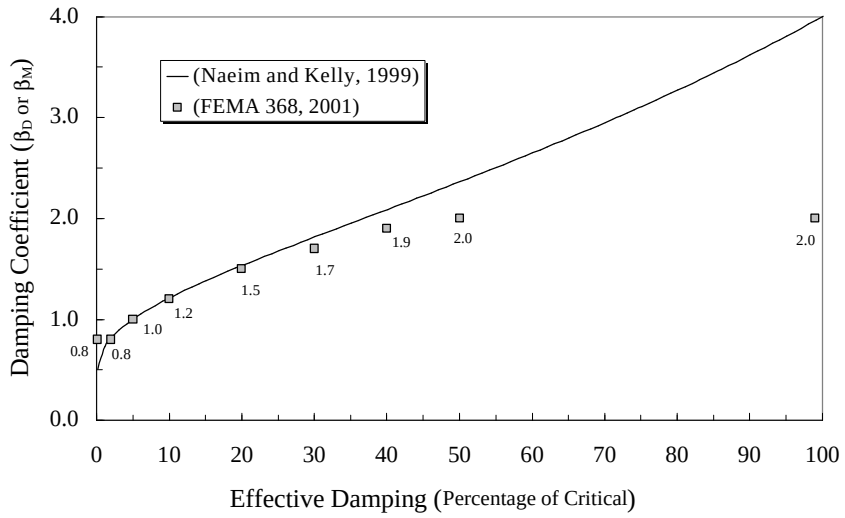

Figure 2.37. - Damping coefficients as a function of effective damping.

- *Total Maximum Displacement* (D_{TM}): Displacement of a bearing at a corner of the building, including the component of the torsional displacement in the direction of the maximum displacement. Therefore it is computed at the LS of Collapse. It may be evaluated through:

$$D_{TD} = D_M \cdot \left[1 + y \cdot \left(\frac{12 \cdot e}{b^2 + d^2}\right)\right] \tag{2.17}$$

The effective isolated periods at design displacement (T_D) and maximum displacement (T_M) are computed from:

$$T_D = 2 \cdot p \cdot \sqrt{\frac{W}{k_{D,\min} \cdot g}} \tag{2.18}$$

and

$$T_M = 2 \cdot p \cdot \sqrt{\frac{W}{k_{M,\min} \cdot g}} \tag{2.19}$$

where W is the weight of the building; g is the acceleration of gravity; $k_{D,min}$ is the minimum effective horizontal stiffness of the isolation system at the LS of significant damage; and $k_{M,min}$ is minimum effective horizontal stiffness of the isolation system at the LS of collapse.

Design forces are calculated at or below the isolation system (V_b) and for the superstructure (V_s); the relevant formulae are:

(*at or below isolation system*) $$V_b = k_{D,\max} \cdot D_D \quad (2.20.1)$$

(*regular superstructure*) $$V_s = \frac{k_{D,\max} \cdot D_D}{R'} \quad (2.20.2)$$

(*irregular superstructure*) $$V_s = k_{D,\max} \cdot D_D \cdot R' \quad (2.20.3)$$

in which R` is the force reduction factor for isolated structures, which is related to the counterpart for fixed base buildings via:

$$1.0 \le R' = \frac{3}{8} R \le 2.0 \quad (2.21)$$

The vertical distribution of design base shear along the super-structure is conservatively similar to that prescribed for fixed base buildings. The seismic isolation theory suggests a uniform distribution of forces over the height of the superstructure; however, to account for higher mode effects, the inverted triangular distribution is adopted (Kelly, 1996).

By performing dynamic analysis design displacements and forces less, the above may be used; a comparison of the design parameters used in static and dynamic analysis is provided in Table 2.15.

Table 2.15. Comparison between static and dynamic analysis limit.

		Dynamic Analysis	
Design Parameter	Static Analysis	Response Spectrum	Time History
Design Displacement (D_D)	$D_D = \frac{g}{4 \cdot p^2} \cdot \left(\frac{S_D \cdot T_D}{B_D} \right)$	*n.a.*	*n.a.*
Maximum Displacement (D_M)	$D_M = \frac{g}{4 \cdot p^2} \cdot \left(\frac{S_M \cdot T_M}{B_M} \right)$	*n.a.*	*n.a.*
Total Design Displacement (D_{TD})	$D_{TD} \ge 1.1 \cdot D_D$	$D_{TD} \ge 0.9 \cdot D_D$	$D_{TD} \ge 0.9 \cdot D_D$
Total Maximum Displacement (D_{TM})	$D_{TM} \ge 1.1 \cdot D_M$	$D_{TD} \ge 0.8 \cdot D_D$	$D_{TD} \ge 0.8 \cdot D_D$
Design Shear (V_b) (at or below isolation system)	$V_b = k_{D\,\max} \cdot D_D$	$\ge 0.9 \cdot V_b$	$\ge 0.9 \cdot V_b$
Design Shear (V_s) (Regular Super-structure)	$V_b = \frac{k_{D\,\max} \cdot D_D}{R'}$	$\ge 0.8 \cdot V_s$	$\ge 0.6 \cdot V_s$
Design Shear (V_s) (Irregular Super-structure)	$V_s = k_{D\,\max} \cdot D_D \cdot R'$	$\ge 1.0 \cdot V_s$	$\ge 0.8 \cdot V_s$
Story Drift (%)	1.5	1.5	2.0

Retrofitting of steel and composite buildings may also be performed by employing dampers. Recently, their use has been allowed by international standards (FEMA 356, 2000; FEMA 368, 2001) which also provided comprehensive design rules. These devices, like base isolation, reduce the demand on the structure by enhancing global damping; this limits the damage of structural and/or nonstructural components.

Dampers may be grouped as a function of their mechanical response as follows:

- *Displacement-dependent dampers*: force-displacement response characteristics depend primarily on the relative displacements. They include hysteretic (metallic), friction based, and SMA dampers.

- *Velocity-dependent dampers*: force-displacement response characteristics depend primarily on the relative velocity or the frequency of the motion. They include primarily viscous dampers. Visco-elastic devices are displacement and velocity dependent; they exhibit an elastic stiffness along with a viscous component.

All devices possess a similar feature, i.e., convert external kinetic energy into heat; however, the latter may be performed in different fashions. Common dampers are summarized in Table 2.16 together with relevant energy dissipation mechanisms.

Table 2.16. Common dampers and energy dissipation mechanisms.

Damper type	Response dependence	Energy Dissipation Mechanism
Metallic	Displacement	Inelastic deformation of metal plates
Friction	Displacement	Solid sliding friction
SMA	Displacement	Solid state phase transformation
Viscous	Velocity	Deformation of highly viscous fluid
Visco-Elastic	Displacement and velocity	Shear deformation of fluid

Moreover, dampers may assume different configurations with respect to the structural system that resists to lateral forces (FEMA 369, 2001) (Figure 2.38). They can be placed either externally or share common elements with the structural systems; intermediate layouts may also be effective.

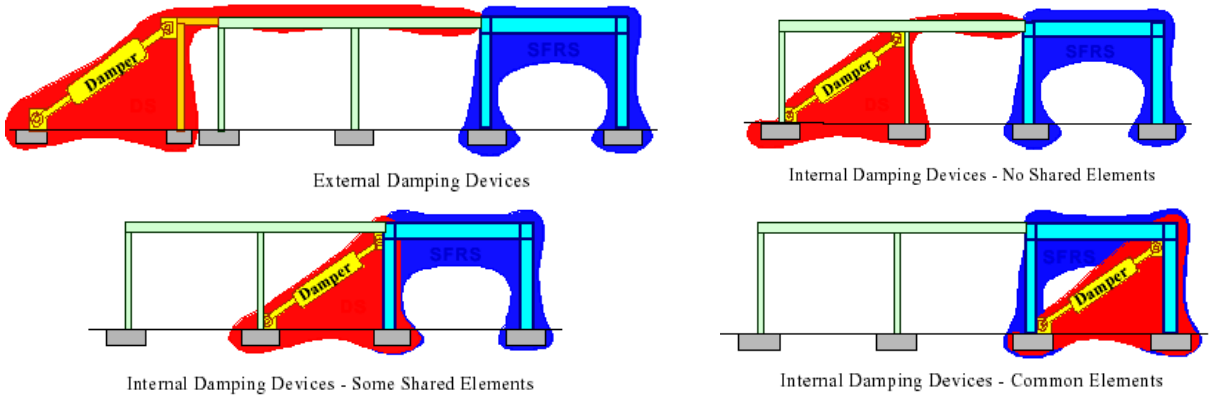

Figure 2.38. Different configuration of dampers and seismic force resisting system (SFRS) (*after* FEMA 369, 2001).

These layouts point to a fundamental difference between structures with dampers and base isolation (Table 2.17): the latter forms a series system (*structure and isolators*) while the former is a parallel system (*structure and dampers*). Therefore, isolators dissipate the input energy before it is transferred to the super-structure. By contrast, dampers receive and dissipate seismic energy in combination with the lateral force resisting structure. Such dissipation depends upon the dynamic characteristics of both components. As a result, the damping should be tuned for optimum performance of the overall system; this is usually a cumbersome iterative design procedure. Design issues of common dampers are addressed herein.

Table 2.17 Comparison between seismic isolation and damper devices.

System characteristics	Base isolation	Dampers
Location of devices	Concentrated at base	Distributed along height
Effect on mechanic response	Lengthening period (greater) and increasing damping (lesser)	Shortening period (lesser) and increasing damping (greater)
Structural benefits	Reduction of forces, displacements and accelerations (factors range 2 to 6)	Reduction of forces, displacements and accelerations (factor range: (1.5 to 2)
Mechanism of energy dissipation	Series system (structure and isolators)	Parallel system (structure and dampers)
Candidate buildings	Rigid buildings with stiff lateral load resisting structure (low-to-medium rise) Buildings on firm soil sites.	Flexible buildings with slender lateral load resisting structure (medium-to-high rise) Buildings on soft soil sites.
Device installation	Intrusive	Not intrusive
Cost	Expensive	Relatively cheap

2.5.3.3. HYSTERETIC DAMPERS

Hysteretic dampers are metal devices that can dissipate energy from an earthquake through inelastic deformations of metals. These dampers may in fact yield either in bending, torsion and/or axially (mild steel) or shear (mild steel or lead). Moreover, they usually have special shapes; e.g., triangular or X-shapes, so that yielding spreads uniformly throughout the material across the section (Soong and Constantinou, 1994). Typical added damping and added stiffness metallic dampers, triangular (TADAS) and X-shaped (ADAS) are provided in Figure 2.39 and Figure 2.40, respectively.

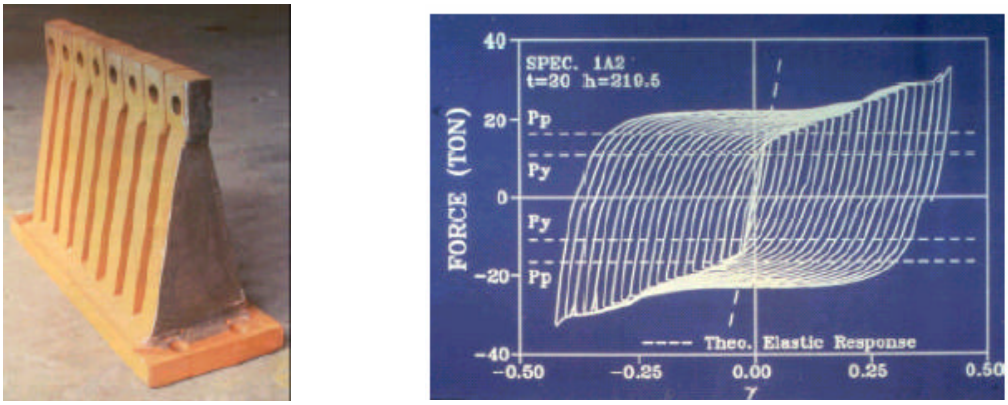

Figure 2.39. TADAS damper: geometry (*left*) and hysteresis loop (*right*).

Pioneering applications of ADAS are found in New Zealand and Japan; however, recently they have been used for seismic rehabilitation of steel and composite structures in the USA and Mexico (Aiken *et al*., 1993; Soong and Spencer, 2002). K-bracings are usually combined with ADAS devices (Figure 2.40); ADAS dampers, located between the end of cross braces and beam mid-span, are activated by story drifts. These dampers should be designed in such a way that at their yielding, axial loads in the braces are less than the buckling values. As a consequence, the design is uneconomical because the tensile plastic capacity of diagonals is not fully exploited. The performance of these dampers depends upon the elastic stiffness and yield force of the damper and the elastic stiffness of the structure to which it is applied. To achieve maximum effectiveness the device should have high stiffness and high yield strength (Whittaker *et al*., 1991; Xia and Hanson, 1992; Tsai *et al*., 1993). Moreover, in practical applications (damping of the device between 10% and 15%), it is difficult to separate the effects of added stiffness from the effects of added damping on response; both tend to reduce the displacement response. The higher the device-to-structure stiffness, the higher the damping. As a consequence, hysteretic dampers do not simply add damping but modify significantly the dynamic characteristics of the structure. Typically, they reduce the fundamental period thus increasing the base shear. However, these systems are particularly

attractive for retrofitting of steel buildings that are vulnerable to having resonant response with the ground (Tena-Colunga and Vergara, 1997).

By assuming that the response of hysteretic damper is elasto-perfectly plastic and provided that the structure behaves elastically, the equivalent viscous damping (Figure 2.41) is related to: (i) the ratio of the damper yield force (F_Y) to structure elastic force (F_E) and (ii) the ratio of damper elastic stiffness (k_D) to structure elastic stiffness (k_S) as follows:

$$b = \frac{2 \cdot \frac{F_Y}{F_E} \cdot \left(1 - \frac{F_Y}{F_E} \cdot \frac{k_D}{k_S} \right)}{p \cdot \left(1 + \frac{F_Y}{F_E} \right)} \tag{2.22}$$

The damping increases as a function of the damper relative stiffness. There is an optimum value of the brace strength to the elastic structure force; it varies with the stiffness ratio.

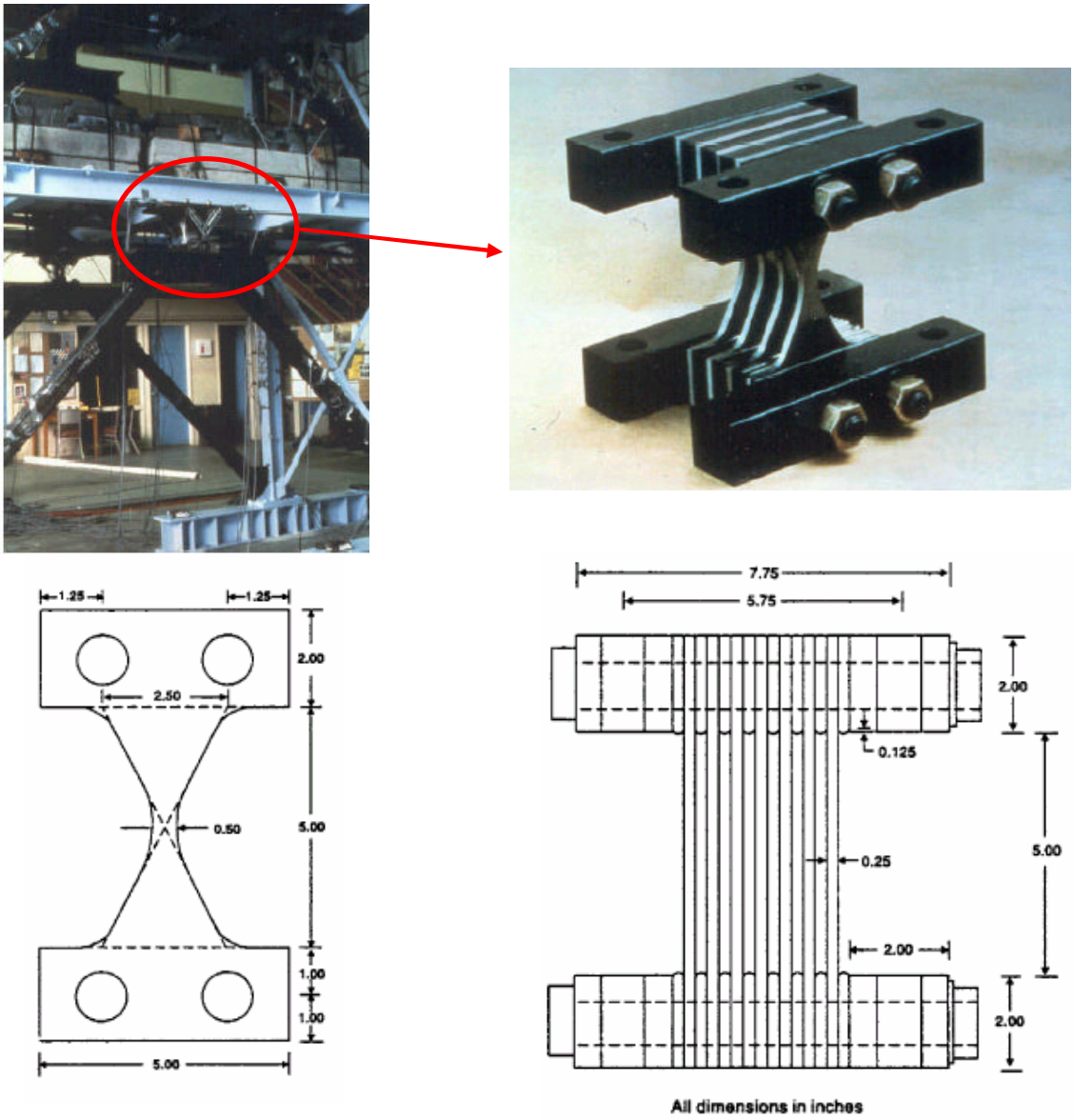

Figure 2.40. ADAS damper: location within a frame and close up (*top*) and typical geometry (*bottom*).

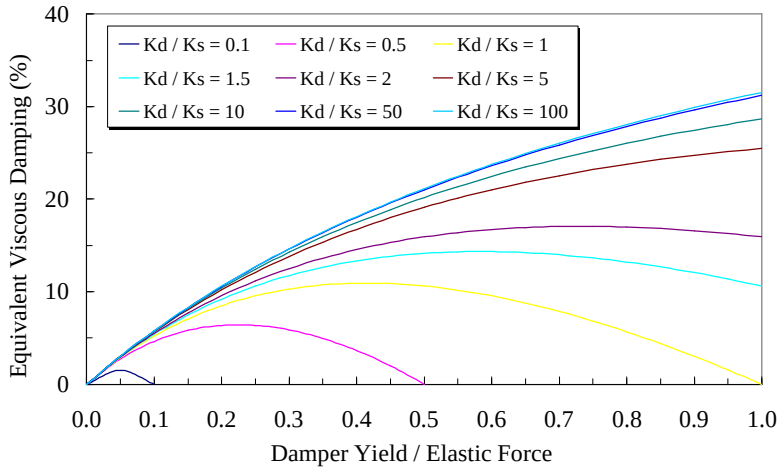

Figure 2.41. Equivalent viscous damping as a function of the brace properties.

The unbounded brace is based upon the same metallic yielding principle of ADAS, i.e., tension/compression yielding brace; this device is popular in Japan and the US (Housner *et al.*, 1997). It consists of a core steel plate (Figure 2.42) encased in a concrete filled steel tube. Yielding of the interior component under reversal axial loads provides stable energy dissipation; the exterior concrete filled steel tube prevents local and member buckling. A special coating is applied to reduce friction

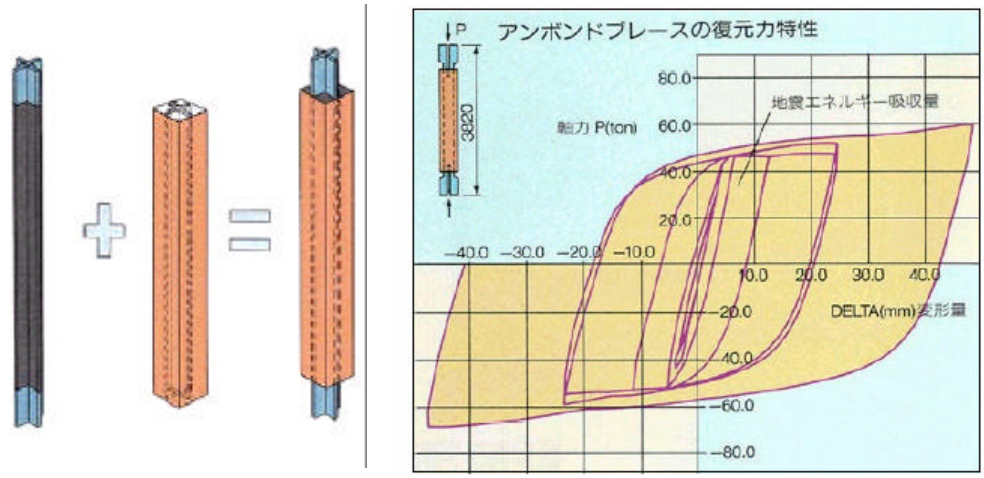

Figure 2.42. Unbounded brace: internal and external components (*left*) and hysteresis loop (*right*).

Experimental and analytical work on hysteretic dampers has been carried out in Europe during the last decade (Vulcano, 1991; Ciampi, 1993); several configurations and devices were proposed and compared with existing ones. For example, Figure 2.43 shows two braces connecting an outer rectangular to an inner smaller frame. This layout enhances the structural performance with respect to ordinary cross braces (Filiatrault and Cherry, 1987). In fact, the latter behave poorly under seismic loads because of buckling of compressed members; the proposed layout overcomes this drawback. In fact, it enables the brace to recover the deformation due to compression, either partially or entirely, thus improving the dissipative capacity of the system under earthquakes.

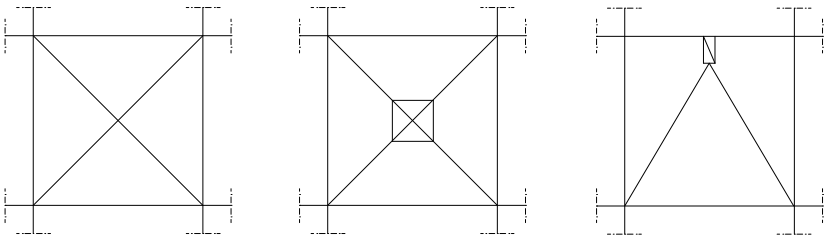

Figure 2.43. Bracing configurations: ordinary (*left*), with inner hysteretic damper (*middle*) and ADAS device (*left*).

Two devices were proposed for the inner frame (Figure 2.43); the tapered cross sections spread uniformly yielding of the material, thus achieving high dissipation. In the first device (Figures 2.44-a and 2.44-b), the geometric parameter (b) is perpendicular to the plane of the frame; in the second (Figures 2.44-c and 2.44-d) b is parallel to the frame plane. Therefore, the former is assembled via welding. Experimental tests have shown that welds fail with brittle fracture when they are close to inelastic deformation zones (Ciampi, 1993). By contrast, the second assembly (Figures 2.44-c and 2.44-d) is manufactured by a single plate; it exhibits enhanced inelastic performance.

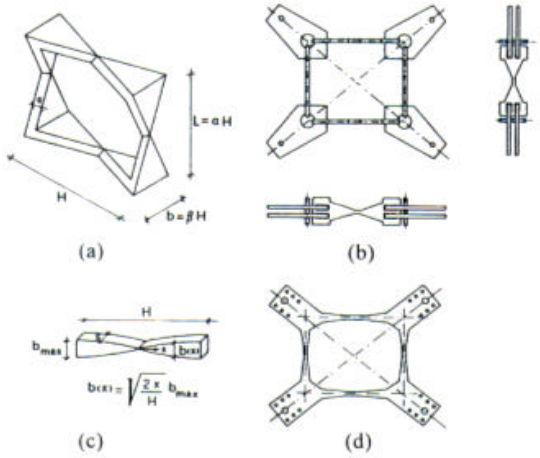

Figure 2.44. Hysteretic damper for braced system (*after* Ciampi, 1993).

To design these dampers, i.e., compute the forces relative the onset of their yielding, it suffices to define adequately their geometry. However, yielding of the devices should anticipate the yielding of cross braces. Such arrangements may, however, show out-plane vibrations at device locations. In fact, relatively small masses are placed at the center of bracings and can displace out sideways.

2.5.3.4. FRICTION DAMPERS

These dampers rely upon the mechanism of friction between two solid bodies sliding relative to one another. In fact, friction is an excellent mechanism of energy dissipation; it has been used extensively and successfully in automotive breaks to dissipate kinetic energy.

Various materials are used for the sliding surface such as brake pad material on steel, steel on steel, steel on brass in slip bolted connections, graphite impregnated bronze on stainless steel and other metal alloys. The choice of the base metal for friction dampers is crucial; poor corrosion resistance can often reduce the coefficient of friction assumed in the design for the intended life of the device. In fact, low carbon alloy steels corrode and their interface properties vary with time, while brass

and bronze promotes additional corrosion when in contact with low carbon. By contrast, stainless steels do not appear to suffer additional corrosion when in contact with brass or steel; therefore, they are suitable for such devices.

Generally, friction devices provide good performance and their response is independent from loading amplitude, frequency and number of cycles. Therefore, they combine high energy-dissipation potential and relatively low cost, they are easy to install and maintain. Other beneficial effects of such dampers were investigated during the last decades (Austin and Pister, 1985; Filiatrault and Cherry, 1987; Aiken and Kelly, 1990). It was found that in designing friction-based dampers it is essential to minimize stick-slip phenomena thus avoiding high-frequency excitation. Furthermore, the ratio of initial slip load to story yielding shear and ratio of bracing-to-story stiffness influence significantly the performance of the device.

Friction devices usually produce a stable rectangular hysteresis, although some are configured to produce self-centering force and provide nonrectangular hysteresis shapes with load proportional to displacement. A macroscopic hysteretic model for friction-based dampers is Coulomb with a constant coefficient of friction; a comparison of hysteretic loops for the assessed dampers is given in Figure 2.45.

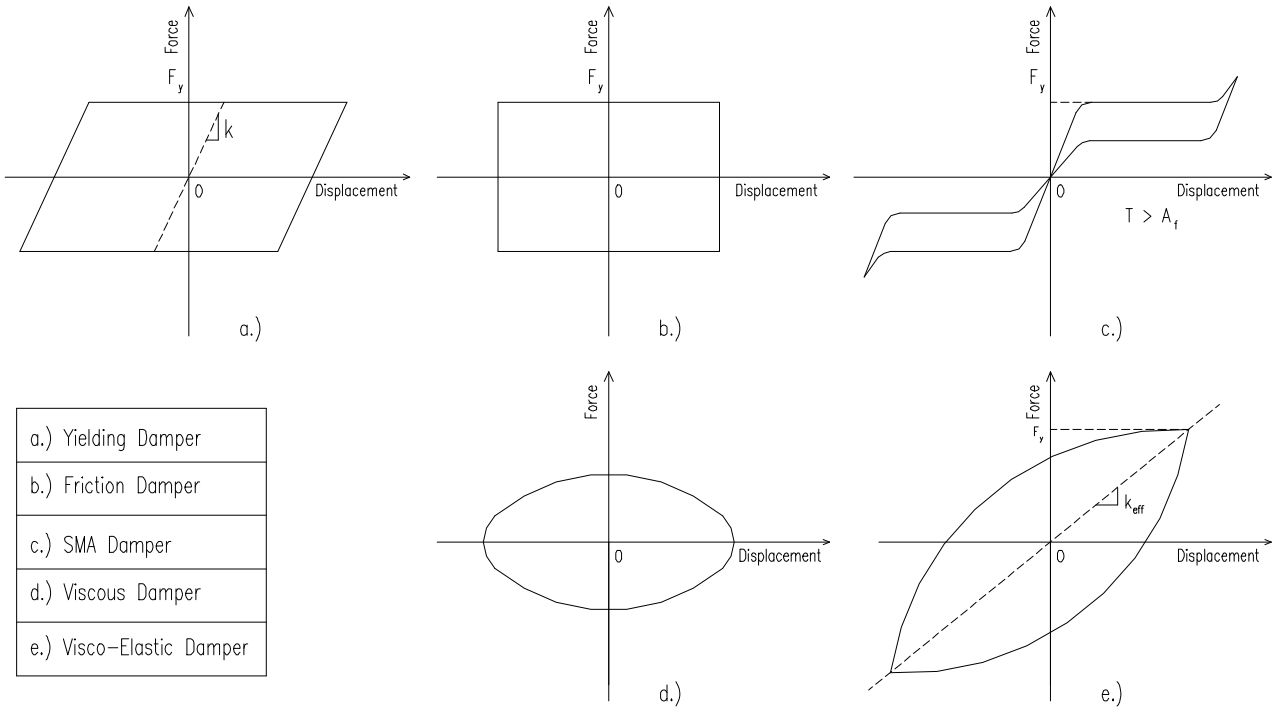

Figure 2.45. - Idealized force-displacement relationships for dampers.

The equivalent viscous damping of a friction damper may be computed as follows (Figure 2.46):

$$b = \frac{2 \cdot \frac{F_Y}{F_E}}{p \cdot \left(1 + \frac{F_Y}{F_E}\right)} \tag{2.23}$$

This formula may be derived from the counterpart in Equation (2.22) by setting the ratio of the damper stiffness (k_D) to structure stiffness (k_S) to 8 . It is instructive to note that when the force of

the friction device is greater than the structure force (Figure 2.46), the upper bound of the equivalent viscous damping of the damper is $2/\pi = 63.99\%$.

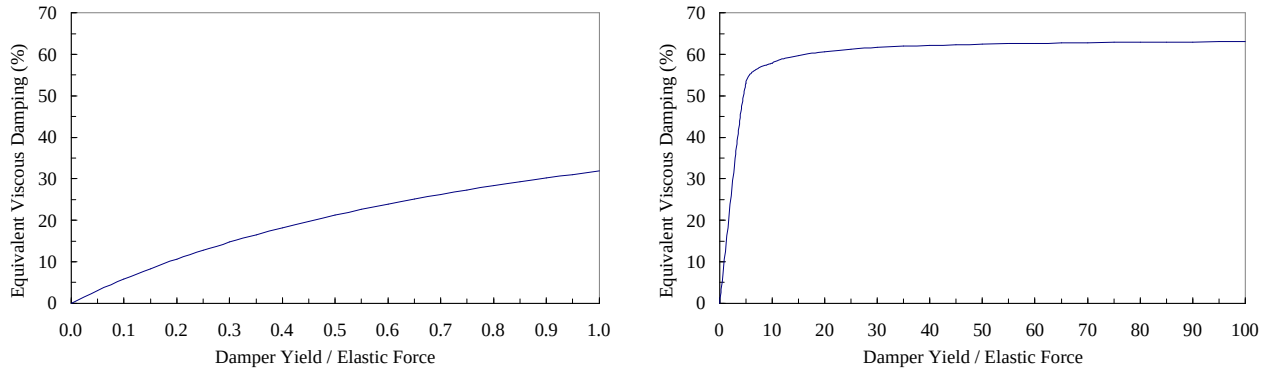

Figure 2.46. Equivalent viscous damping of friction device: force less (*left*) or greater (*right*) than structure.

Friction dampers have been most commonly placed within diagonal braces, as for yielding metal dampers, but can also be placed horizontally between the top of a wall and the beam above. These devices initially possess finite stiffness because they are mounted on braces; therefore, their behavior is similar to hysteretic damping.

A typical friction damper is shown in Figure 2.47 (Pall and Marsh, 1982): it can be installed at the crossing of two braces where tension in one brace forces the joint to slip, thus activating four links which in turn force the joint in the other brace to slip. This device is (Filiatrault and Cherry, 1990) fixed under wind and moderate earthquakes but slips under intense ground motions, thus protecting primary structural members from yielding.

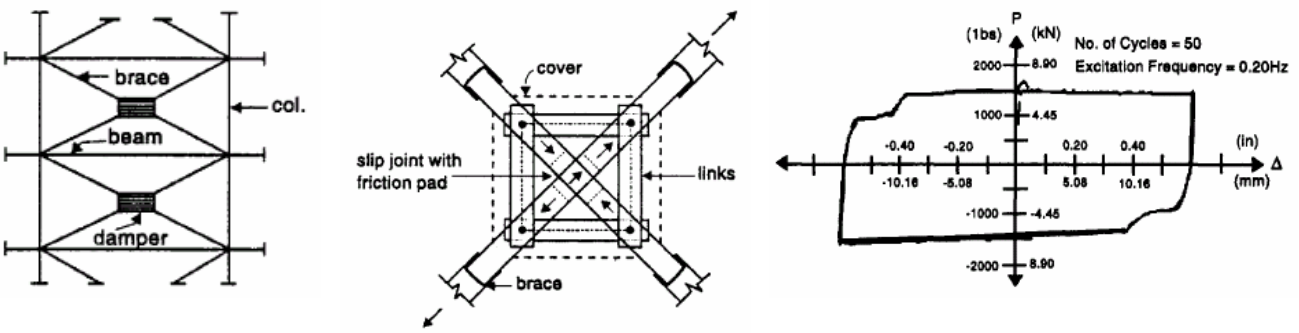

Figure 2.47. Pall friction device: frame location (*left*), device layout (*middle*) and hysteretic loop (*right*).

Sliding connections contribute to the elevated friction and hence, energy dissipation. Force acting within the joints can be easily controlled by satisfying the force equilibrium equation:

$$N_g = 2 \cdot N_1 - N_b \tag{2.24}$$

where N_g is the tensile force in the brace when slip starts and N_l is the correspondent force in the damper. By assuming slender diagonal braces, which can buckle elastically, the buckling load (N_b) is low and it may be neglected in Equation (2.24). Therefore:

$$N_g \approx 2 \cdot N_1 \tag{2.25}$$

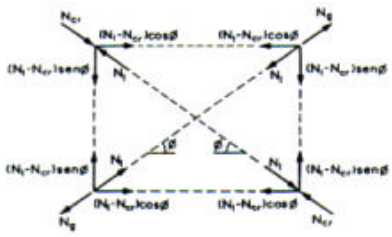

Figure 2.48. Pall friction device: load path.

The device can be calibrated via the tightening force applied to the bolts. Diagonal braces with Pall system possess enhanced dissipative capacity (the energy dissipation is about twice) with regard to ordinary cross bracings (Filiatrault and Cherry, 1989).

Recently, novel friction dampers have been tested experimentally and many of them have been installed in buildings, either new or existing ones, around the world (Aiken and Kelly, 1990; Grigorian *et al*., 1993; Balendra *et al*., 2001). Two examples of devices for braced connections are provided in Figure 2.48; they are slotted bolted connection energy dissipater (Balendra *et al*., 2001) and a novel device for inverted V-braced connections (Mualla and Belev, 2002), respectively.

Slotted bolted connections are becoming very popular for braced connections because they require a slight modification of standard construction practice, thus are easy to construct and implement (Levy *et al*., 2000). Moreover, they use materials widely available on the market. They are attractive for the use in retrofitting existing steel and composite framed buildings. These connections are designed to dissipate energy through friction between the steel surfaces along the brace in tension and compression loading cycles (Popov *et al.*, 1993); alternatively, brass in contact with steel may be used. Experimental tests have shown that the behavior of connections with brass on steel is more uniform (Grigorian *et al*., 1993); moreover, they are simpler to model analytically than the ones using steel on steel. Yet, their performance in braced systems is very satisfactory (Colajanni and Papia, 1997; Aiken *et al.*, 1993). The slotted connection in Figure 2.49 has shown excellent energy dissipation on knee-braced frames (Balendra *et al*., 2001). It has slotted holes in the main connection plate which are parallel to the line of loading. The main plate is sandwiched between two outer members. A friction lining pad is placed between each outer member and the main plate. The lining pad moves with the outer member. Two bolts are used to clamp together the plates and lining pads. Upon tightening the bolts, frictions develop between the contact surfaces of lining pads and slotted plate. When either tensile or compressive forces are applied to the connection and the friction is exceeded, the slotted plane slips relative to the lining pads and energy is dissipated.

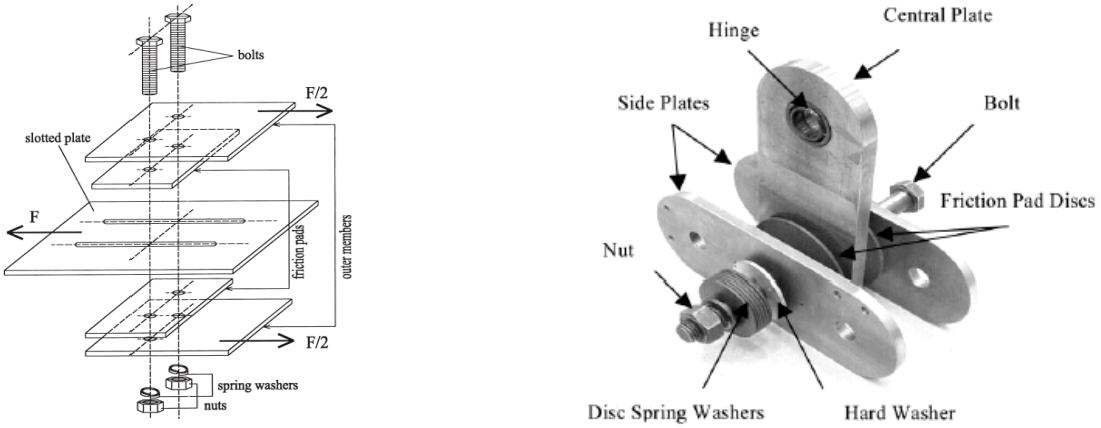

Figure 2.49. Novel friction dampers for braced connections: slotted bolted connection (*left*) and inverted V-braced connection (*right*).

The effectiveness of the novel damper for inverted V-braced connections (Figure 2.49) has been assessed experimentally and numerically (Mualla and Belev, 2002). The damper consists of three steel plates, i.e., one central (vertical), two on the side (horizontally) and two circular friction pad discs sandwiched between the steel plates. The central plate is used for the connection with the midspan of the floor beam in the frame. This connection is pinned, thus it increases the relative rotation between the central and the side plates; as a result, the energy dissipation is enhanced.

2.5.3.5. VISCOUS DAMPERS

Viscous dampers are similar to shock absorbers in a car. They consist of a piston within a damper chamber filled with a compound of siliconic oil (Makris *et al.*, 1993; Constantinou *et al*., 1993), eventually pressurized (Tsopelas and Constantinou, 1994; Pekcan *et al*., 1995). The piston rod is connected to a piston head with a number of small orifices. As the piston moves within the cylinder the oil is forced to flow through holes in the piston head thus causing friction. If the fluid is purely viscous (e.g., Newtonian) the output force of the damper is directly proportional to the velocity of the piston. The linear response characterizes a broad range of load frequencies and does not vary with the temperature. This is typical of dampers employing storage chamber and control valve (Figure 2.50); such devices are calibrated with threshold forces (cut-off frequencies) to enhance their dissipation capacity. Moreover, these viscous dampers exhibit stiffening characteristics at higher frequencies of deformation (Housner *et al*., 1997); thus, they are used to damp higher mode effects. Re-centering properties are typically found in dampers with pressurized fluids.

Damping walls (Figure 2.51), consisting of a rectangular steel plate immerged in a highly viscous fluid, showed high energy dissipation when installed in steel frames (Arima *et al*., 1988; Miyazaki and Mitsusaka, 1992). However, their damping characteristics vary significantly with load frequency and temperature.

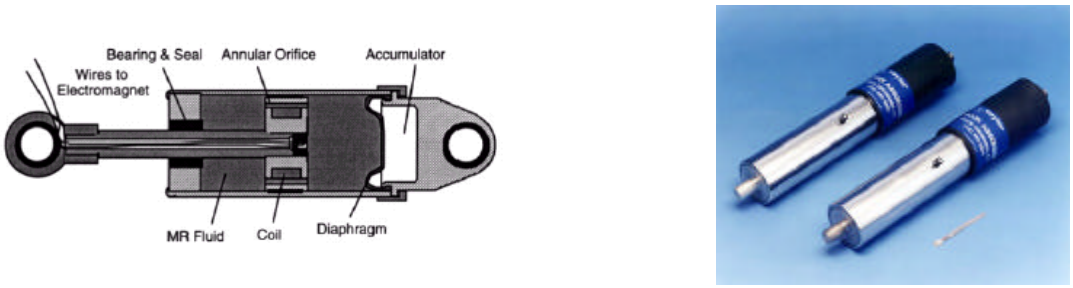

Figure 2.50. Typical viscous dampers: internal layout (*left*) and 225kN devices produced by Taylor (*right*).

Viscous dampers have low resistance to deformation when loads are applied slowly, but resistance increases as the applied deformation rate increases. When they are installed in buildings, usually in bracings, friction transforms input energy due to earthquake loading into heat. Viscous dampers have been used to control the vibrations of new buildings and to retrofit either RC or steel frames, especially in Japan and the US (Soong and Spencer, 2002).

Figure 2.51. Wall viscous dampers: dissipative mechanism (*left*) and lab test (*right*).

Fluid viscous dampers provide damping as a function of the velocity; the velocity is out of phase with the displacements. The relationship between the damper force (F_D) and the applied velocity ($\dot{u}$) is as follows:

$$F_D = C \cdot \left|\dot{u}\right|^{a} \operatorname{sgn}(\dot{u}) \tag{2.26}$$

in which α is the damper exponent and $\operatorname{sgn}(\dot{u})$ is the signum function defining the sign of the relative velocity. Therefore, the mechanical response of viscous dampers is governed by two parameters: the coefficient C and the power exponent α. For practical applications, the latter generally ranges between 0.3 and 1.0 (Housner *et al.*, 1997); α should be as high as possible, optimal value is 1.0 because it leads to a linearly elastic relationship between velocity and displacement. Lower limits of the exponent, say around 0.3, should be avoided; in these cases the damper forces are not out of phase with the displacements hence, they are additive to the structural ones. This coupling effect increases with the amount of damping provided; the more the damping provided, the smaller the benefit of having the damper force out of phase with the structure force.

The damper coefficient C can assume almost any value; in fact, C may be increased or decreased by simply installing more or less dampers in the structure. However, it is worth mentioning that certain

types of viscous dampers have a relief valve providing a limited velocity. It is useful in limiting forces but reduces out-phase between velocity and displacements. This effect may undermine the effectiveness of the damper on the global structural performance.

So far several methodologies have been provided to design viscous dampers (Soong and Costantinou, 1994). The determination of optimal locations to achieve maximum performance based on given constraints, such as the number of dampers and their capacity, is of paramount importance. Moreover, the interaction damper-structure should be explicitly accounted for because of the connection flexibility. Viscous dampers are usually mounted on steel braces and then installed in building frames (Figure 2.52). Therefore, the damper is linked in series with the brace and in parallel with the structure.

Figure 2.52. - Viscous dampers in steel framed building.

As a consequence, the brace reduces the deformation in the damper due to story drift. In fact, the former behaves like a spring while the damper is spring-dashpot system in series (Maxwell model); therefore the spring deformability reduces the relative displacement of the damper. However, this effect is a function of connection flexibility: the higher the connection flexibility the lower the damping force. The interaction damper-structure depends significantly on whether the structure undergoes inelastic deformations.

2.5.3.6. VISCO-ELASTIC DAMPERS

These devices are based on visco-elastic materials, such as copolymers or glassy substances, with high energy dissipation due to shear deformations. Visco-elastic materials have linear response over a wide range of strains provided the temperature is constant. At large strains, say 300% to 500%, the energy dissipation produces self-heating and the heat changes mechanical properties of the material, which becomes highly nonlinear.

Typical visco-elastic dampers, developed by 3M Company, are shown in Figure 2.53: they consist of visco-elastic layers bounded with steel plates. Mounted in the structure, shear deformations and hence, energy dissipation takes place when structural vibration induces relative motion between outer steel flanges and center plates.

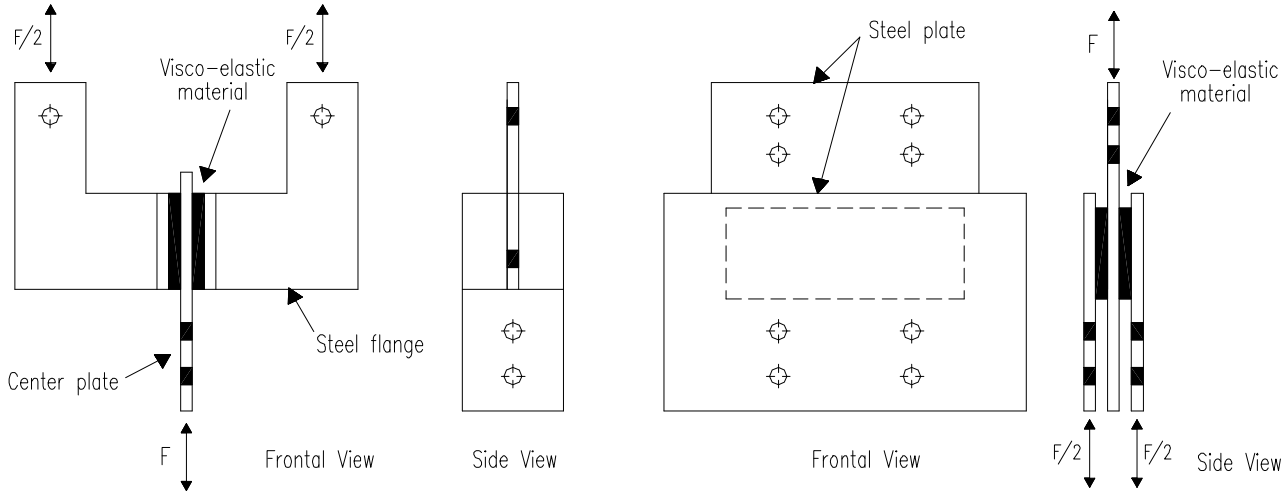

Figure 2.53. Typical visco-elastic dampers.

The damping force (F_D) is a function of the velocity ($\dot{u}$) and the displacement (u) and can be computed as:

$$F_D = k_{eff} \cdot u + C \cdot \dot{u} \tag{2.27}$$

where C is the damping coefficient and k_{eff} is the effective stiffness of the damper and is given as:

$$k_{eff} = \frac{G` \cdot A_b}{t} \tag{2.28}$$

in which G` is the shear storage modulus, A_b the bonded area of the device and t the total thickness of the visco-elastic material in the device (sum of the layers for the devices in Figure 2.53).

The damping coefficient C depends upon: (i) geometric properties of the device, (ii) mechanical properties of the material and (iii) frequency of the content of the applied load. It may be given as follows:

$$C = \frac{G`` \cdot A_b}{w \cdot t} \tag{2.29}$$

where G`` is the shear loss modulus; and ω is the frequency of the load.

The shear storage G` and shear loss G`` moduli are function of: (i) the material used, (ii) the strain, (iii) the frequency of the load and (iv) the service temperature (Chang *et al.*, 1992). The former influences the stiffness and hence the frequency of the damper, while the latter relates to the energy dissipated in each cycle. Their ratio (*loss factor*) varies usually between 0.8 and 1.40; for practical applications it does not depend upon strain and temperature.

Several analytical expressions are provided in literature for G` and G`` (Shen and Soong, 1995); there are four parameter formulations either based upon experimental tests or Boltzmann's superposition principle.

Recent experimental and numerical tests have demonstrated the effectiveness of these dampers for retrofitting of either steel or RC structures (Foutch *et al.*, 1993; Chang *et al.*, 1995; Shen *et al.*, 1995; Soong and Spencer, 2002). However, the design of visco-elastic dampers is generally complex and cumbersome and is based upon iterative procedures. The proposed methodologies, common to the design of viscous dampers, may be categorized in two groups based on the behavior of framed structures, i.e., elastic (Chang *et al.*, 1993; Chang *et al.*, 1996; Kasai *et al.*, 1998; Fu and Kasai, 1998) and inelastic with plastic deformations (Abbas and Kelly, 1993; Ciampi *et al.*, 1997). The design steps for the design of these dampers for seismic retrofitting are as follows:

1. Establish the number and location of dampers. Generally the location depends upon the story displacements. The optimum location is where the drifts cause maximum relative displacement of the brace with dampers. It is important to account for the increment of axial load in the columns due to the bracings. This issue is less important for viscous dampers because of the out-of-phase between damper and structural forces. Other criteria for the optimal location of dampers may be found in literature (Zhang and Soong, 1992; Shukla and Datta, 1999).
2. Define through experimental tests or design spectra the design parameters of dampers, i.e., G` and G` for visco-elastic and C and α for viscous (Abbas and Kelly, 1993; Ciampi *et al.*, 1997; Kasai *et al.*, 1998; Fu and Kasai, 1998).
3. Evaluate the stiffness of dissipative braces, assuming elastic response for braces and avoiding buckling. For visco-elastic dampers, the area of the cross section of visco-elastic material may be computed by using Equation (2.28). The stiffness of the dissipative brace is computed through the following relationships (Fu and Kasai, 1998):

$$x_{eq}^{i} = \frac{1}{2}\overline{\overline{k}}^{i} \cdot \left[1 - \left(\frac{w_{s}^{i}}{w_{s,b}^{i}}\right)^{2}\right] \tag{2.29.1}$$

$$\overline{\overline{k}}^{i} = \left(\frac{\overline{k'_{eff}}}{k_{eff}}\right)_{i} \tag{2.29.2}$$

$$\left(\overline{k_{eff}}\right)_{i} = \left[\frac{\left(k_b + k_{eff}\right)\cdot k_b \cdot k_{eff} + k_b \cdot k'^{\,2}_{eff}}{\left(k_b + k_{eff}\right)^2 + k'^{\,2}_{eff}}\right]_{i} \tag{2.29.3}$$

$$\left(\overline{k'_{eff}}\right)_{i} = \left[\frac{k_b^{\,2} \cdot k'^{\,2}_{eff}}{\left(k_b + k_{eff}\right)^2 + k'^{\,2}_{eff}}\right]_{i} \tag{2.29.4}$$

where w_{s}^{i} and $w_{s,b}^{i}$ are the *i-th* frequencies of the structure without and with dampers; the *i-th* frequency is the frequency of the mode to mitigate (usually it is the first mode); k_b is the stiffness of the brace with the damper; k_{eff} is given in Equation (2.28); and $k`_{eff}$ has the same expression as k_{eff} but with G`` replacing G`.
4. The thickness should comply with the maximum shear deformations, e.g., 150% (LS of significant damage) and 250% (LS of collapse).
5. Perform dynamic analysis of structure with dampers to check that the target equivalent viscous damping is achieved. Iterative procedure is required to adjust the damper characteristics in order to achieve the target.

2.5.3.7. SMA DAMPERS

Shape memory alloys (SMAs) are special metal alloys with superelastic properties, i.e., they can undergo large strains (up to 10%) with no residual deformation after unloading. This mechanism is based upon reversible solid-to-solid phase transformation (austenite to martensite), which can be either thermal or stress induced. The mechanical properties of these novel alloys were discussed in Section 2.5.2.

Under uniaxial load, SMA response is characterized by *critical stress* corresponding to the completion of the austenite to martensite transformation. This stress is a function of the temperature (Duerig *et al.*, 1990). The austenite to martensite transformation increases deformations for constant stress. Dissipative capacity of SMAs depends upon the hysteretic loop generated upon unloading; it is due to the chemical instability of the martensite which switches to austenite at low stresses.

SMAs possess enhanced re-centering properties along with high low-cyclic fatigue resistance and low life cycle cost; therefore, they have all the attributes for seismic retrofitting applications. Moreover, experimental tests showed that Ni-Ti alloys perform better than other alloys (Cu-Al-Zn, Cu-Al-Ni, Fe-Mn e Mn-Cu) (Grasser and Cozzarelli, 1991; Dolce *et al*., 2000; Des Roches and Delemont, 2002); they have superior superelastic properties, low sensitivity to temperature, significant fatigue and corrosion resistance. They are implemented in dissipative devices for seismic engineering (Wilde *et al*., 2000).

SMA devices consist of bars and wires which differ for diameter, stress state during service life and phase. Wires are generally manufactured up to 2 mm primarily as austenite phase; by contrast, bars may have diameters up to 8 mm and can be either austenite or martensite; special bars are manufactured to 50 mm. Generally, wires are used for pure axial loads, while bars are suitable for bending and/or shear and/or torsion.

Martensite bars, under cyclic bending and torsion, dissipate large amounts of energy (equivalent viscous damping up to 15%-20%), have high fatigue resistance, and mechanical behavior that is independent of temperature and load frequency. However, they exhibit residual deformations upon unloading. By contrast, austenite bars possess lower energy dissipation (equivalent viscous damping is 5%-10%) with no residual deformations (superelasticity).

SMA dampers may be used for seismic applications, especially for retrofitting of steel, composite and RC frames structures (Housner *et al*., 1997; Dolce *et al*., 2000; Soong and Spencer, 2002). Braces with martensite bars under bending are very effective to mitigate seismic vibrations; pre-tensioned austenite wires are usually combined with martensite bars to enhance mechanical performance of the dampers. The manufacturing of bending bars is usually easier than torsion counterparts; moreover, they are compact and easy to install into the device. Therefore, bending bars are more common for practical applications.

SMA dampers are based upon re-centering and high energy dissipation of Ni-Ti alloys. However, the higher the re-centering, the lower the dissipation.

Ni-Ti alloys are still expensive, thus the use is optimized by loading them mainly in tension. To do so, wires are initially pre-tensioned by imposing strains (ε_{pret}), which are half of strains (ε_m) relative to austenite-martensite transformation, i.e., ε_{pret} is 1/2 ε_m. Pretension may also prevent buckling of wires under compression.

SMA dampers may be arranged as in Figure (2.54); they consist of two co-axial pipes with two groups of bolts: 3+3 are placed laterally (*dissipative group*) and 2 are on top (*re-centering group*). The dissipative group has two bolts connected with the internal pipe while the third bolt is connected to the external pipe. The re-centering group has bolts connected to the inner and outer pipe, respectively.

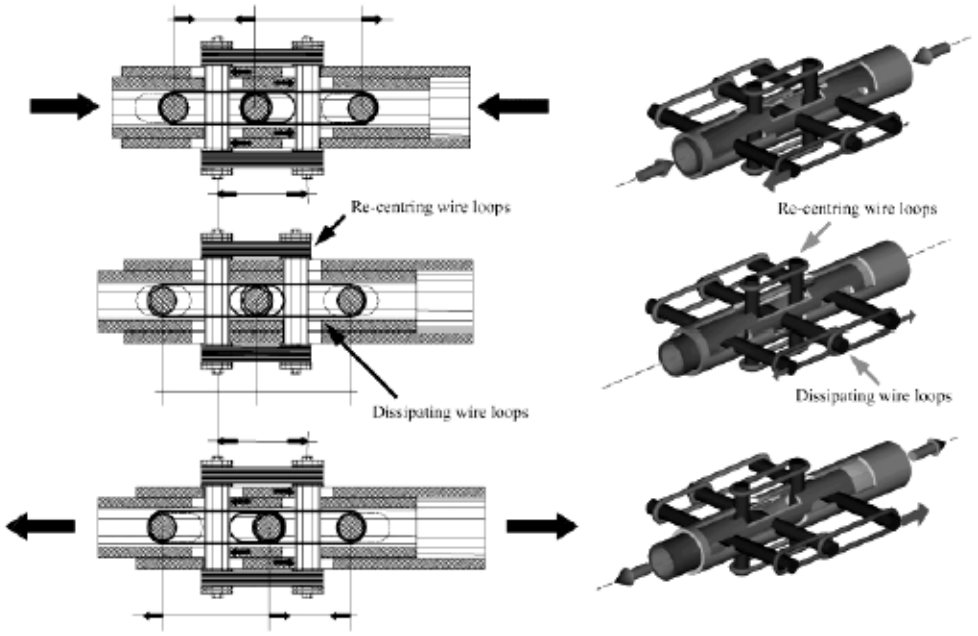

Figure 2.54. SMA damper (working mechanism) (*after* Dolce *et al*., 2000).

Thus, the re-centering group forms a parallel system with the dissipative group. The former exhibits rigid-hardening behavior while the latter behaves like a Coulomb-friction system. As a consequence, by combining re-centering and dissipative groups (Figure 2.55), flag-shaped symmetric hysteretic loops are obtained.

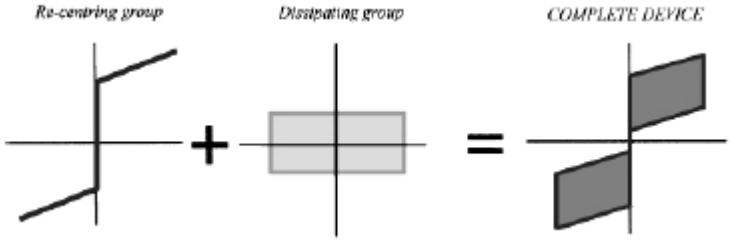

Figure 2.55. Idealized behavior of SMA device.

Thus, three types of SMA devices may be implemented as shown in Figure (2.56), where the relevant hysteretic force-displacement loops are also included:

- Re-centering devices (SRCDs)
- Dissipative devices (NRCDs)
- Re-centering and dissipative devices (RCDs)

Optimal devices for seismic applications are RCDs; they do not exhibit negligible residual deformations and significant dissipative capacity. Moreover, the equivalent viscous damping (ξ_{eq}) of RCDs with austenite wires (re-centering group) and martensite bars (dissipative group) ranges between 4% and 12%. Using austenite wires for re-centering and austenite groups, ξ_{eq} increases to 12-18%. SRCDs have relatively small ξ_{eq}; it varies between 2% and 8%. By contrast, ordinary equivalent damping for NRCDs are in the order of 40% when pre-tensioned austenite wires are used.

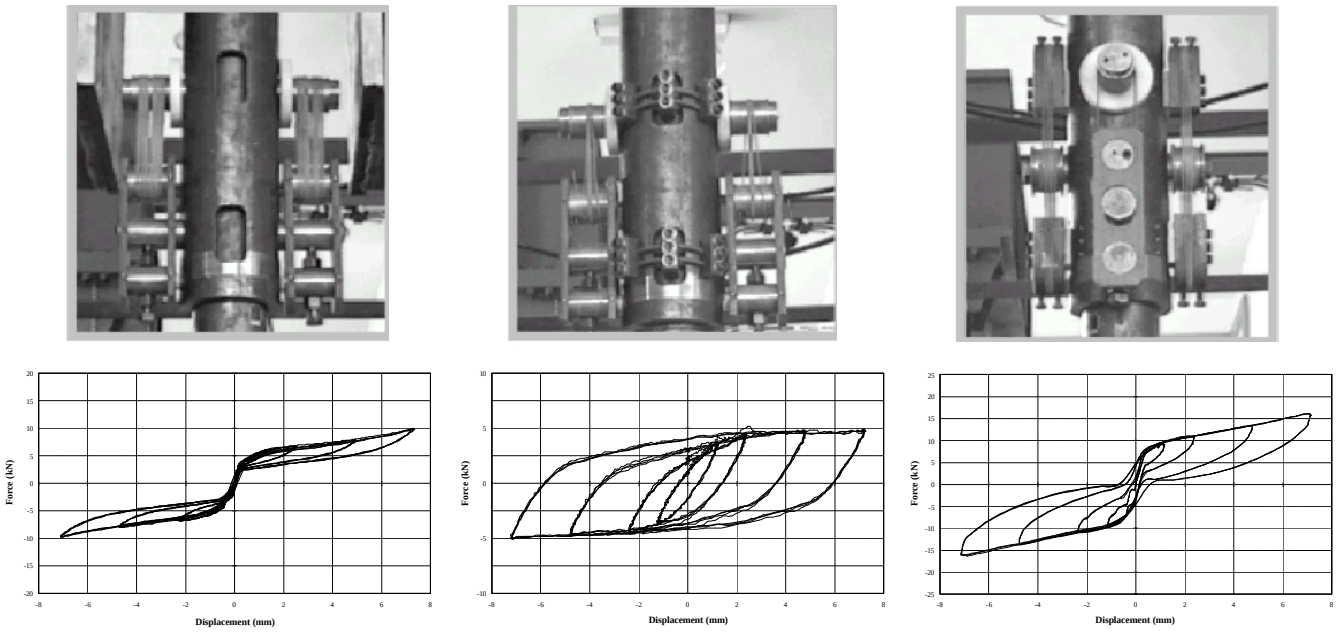

Figure 2.56. SMA damper for steel brace: re-centering (SCRD) (*left*), dissipative (NRCD) (*middle*) and re-centering-dissipative (RCD) (*right*) (*after* Dolce *et al*., 2000).

Therefore, to design SMA dampers, it is essential to choose an adequate number and type of wires and bars, and calibrate the pretension. The design should be targeted to achieve high re-centering capacity, high stiffness for small displacements and elevated energy dissipation.

3. RETROFITTING OF STEEL AND COMPOSITE BUILDINGS

3.1. MATERIAL SPECIFICATIONS

3.1.1. GENERAL

Material properties significantly influence local ductility of steel structures (Figure 3.1), which is an important index of the ability to withstand inelastic deformations without fracture (FEMA 355A, 2000). Therefore, yield and tensile strengths, ultimate elongation, hysteretic behavior, low cycle fatigue and fracture (notch) toughness should be adequately evaluated to perform reliable assessment of local dissipation capacities and hence, global performance under seismic loading. Moreover, strain rate effects and loading amplitudes should also be accounted for because they can detrimentally influence the inelastic response of existing steel and composite buildings.

However, as far seismic retrofitting is concerned, the extent of definition and quantification of steel properties depends on the level of knowledge of structural data (limited, normal or full knowledge), type of evaluation to be performed (linear and/or dynamic analysis) and level of certainty with the regard to the conclusions of the evaluation (FEMA, 273, 1997; SAC 1999).

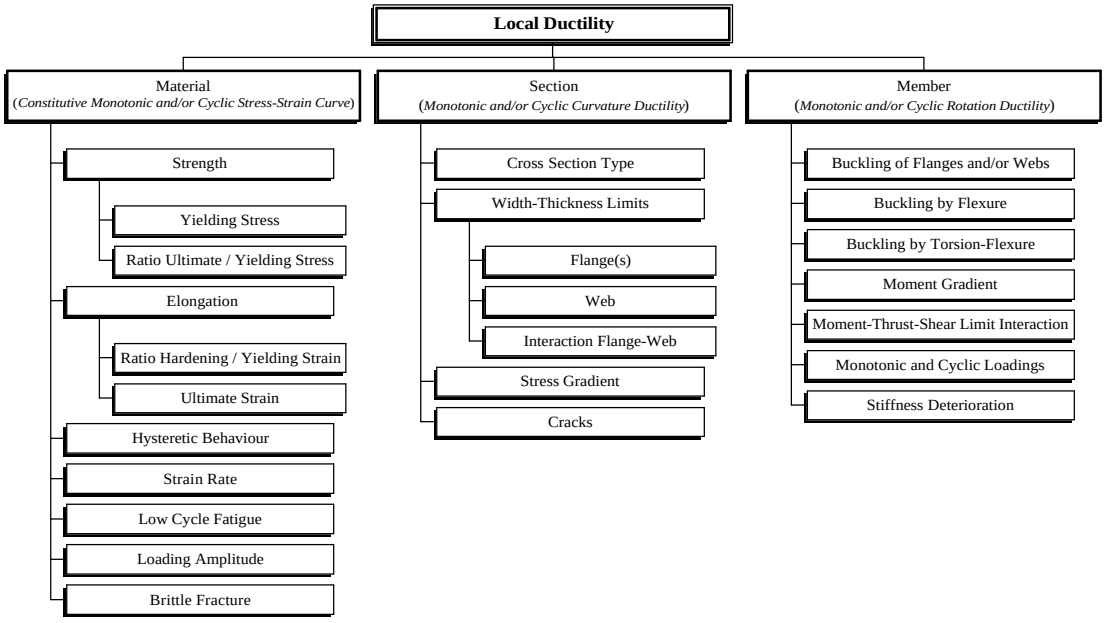

Figure 3.1. Factors influencing local ductility of steel members.

Structural steel for seismic retrofitting should generally possess: (i) consistent strength, (ii) high yield-to-tensile strength ratio (f_u/f_y) of 1.25, (iii) large inelastic strains (e.g., elongation at fracture not less than 20%) (iv) free from lamination, (v) notch-ductile as established via Charpy test and (vi) good weldability. Similar requirements are provided in the US standards for seismic design of new buildings (AISC, 1997). However, the latter require that the f_u/f_y ratio should be at least 1.18 (f_y/f_u=0.85) but do not propose an upper bound. This is a drawback which does not limit the over-strength randomness and may affect the structural reliability of failure mode control (Elnashai and Chryssanthopoulos, 1991; Fukumoto, 2000). Statistical distributions of f_y/f_u from mill production of structural steels in the US are provided in Figure 3.2; it is shown that generally f_y/f_u values are less than 0.80. Nevertheless, some North American structural shape producers are starting to manufacture grade 50 steels with specified yield strength of 345 N/mm^2, upper limit of 448 N/mm^2 on yield strength and specified maximum yield-to-tensile ratio of 0.85 (f_u/f_y=1.8) (Plumier, 2000).

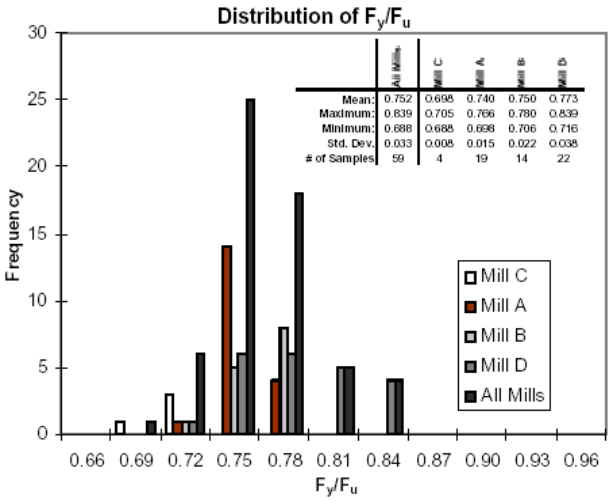

Figure 3.2. Distribution of yield- to-tensile strength ratio (*after* FEMA 355A, 2000).

With regards to composite structures the requirements for mechanical properties of materials should comply with relevant parts in codes dealing with RC, steel and composite structures (EC2, 1992; EC3, 1992; EC4, 1994; EC8, 1998). However, concrete classes for seismic rehabilitation should range between C20/25 and C40/50, either for dissipative or nondissipative zones. In fact, robustness of elastic members or connections is useful for abnormal loadings other than earthquakes. Cracking of concrete should be adequately considered because it significantly influences the computation of the deformations in composite structures. Moreover, reinforcement steels, should fulfill material requirements, as specified above, for structural steels. Bars, stirrups and welded meshes should be ribbed and adequately anchored; simple overlaps should be preferred to bar welds, thus reducing the risk of embrittlement.

Some additional remarks on mechanical properties of structural steels to be employed in seismic rehabilitation are provided below.

3.1.2. STRENGTH AND OVERSTRENGTH

Overstrength is a key parameter in capacity design when a member or connecting members (*nondissipative components*) must have design strength not less than the strength of other members or connecting elements (*dissipative components*). In such cases, yield and tensile strengths to evaluate force demand on nondissipative components should be based upon expected ($f_{y,e}$ and $f_{u,e}$, respectively) rather than nominal ($f_{y,nom}$ and $f_{u,nom}$) values. By contrast, specified minimum yield strengths should be used to design dissipative components that are expected to yield during design earthquake.

Expected strengths may be evaluated as follows:

$$f_{y,e} = R \cdot f_{y,nom} \tag{3.1.1}$$

$$f_{u,e} = R \cdot f_{u,nom} \tag{3.1.2}$$

where the factor R should be assumed equal to 1.4 for rolled sections and bars independently of steel grade, i.e., S235, S275, and S355. This value of R is similar to those provided in the US standards (AISC, 1997). The latter require for W-shapes and bars in grade A36 R-factors equal to 1.5 and 1.3 for A572 grade 40. For rolled shapes and bars of other grades and for plates, R is 1.1. It is worth mentioning that requirements in EC8 (EC8, 1998) for reinforcing steel in critical regions of

RC structures specify that the ratio of measured-to-nominal yield strengths should be not greater than 1.25 (*medium ductility*) or 1.20 (*high ductility*). Moreover, reduced values of R may be established upon either testing or other supporting data, say, e.g., from literature (Galambos and Ravindra, 1978). Thus, it is generally recognized that steels produced several years ago should have lower R.

R-values provided in the US provisions were evaluated through an extensive survey supported by the Structural Shape Producer Council (SSPC, 1994) and SAC Steel Project (FEMA 355A, 2000). The value of R proposed for seismic retrofitting of steel and composite structures in Europe is derived as a mean of US values for grade A36 and A572 grade 40. It accounts for two design issues typical of European practice. In fact, smaller members are generally used for seismic design in Europe, especially beams, with depth between 300 and 450 mm (Mele, 2002). Smaller members have higher measured strengths than deeper American W-sections; this feature increases R. However, negligible variations of measured yield and tensile strengths from nominal values are found in European steel manufacturing; the latter lowers R-values.

Recent surveys carried out in Europe on steel manufacturers have shown small variations of measured yield strengths from nominal values (Manzocchi *et al*., 1992; Byfield and Nethercot, 1997; Cecconi *et al*., 1997). Values lower than 10% are found for laminated plates; the range is between 3.8% (S355 plates with thickness $3 \leq t < 5$ mm) and 7.1% (S235 plates and thickness $8 \leq t < 25$ mm). For hot rolled profiles, correlation functions showed that grade S355 exhibits lower coefficients of variation (COVs) than S275 (Figure 3.3). Variations for grade S355 are lower than 5%; 3.9% for $0 < t < 10$ mm; and 4.2% for $10 \leq t < 20$ mm. COVs for S275 decrease when the thickness increases; variations are still negligible (values range between 4.2% and 4.9%). Mean yield strengths for S275 are generally (Figure 3.3) two standard deviations above nominal values as specified in the standards where characteristic values are used (EN 10025, 1990). Variations are less than 10% with average values of 20 N/mm^2.

Moreover, scatter of ultimate strengths is smaller than yield counterparts: COVs equal to 3% to 4% were found for grade S275 (Manzocchi *et al*., 1992). However, yield and ultimate strengths are strongly correlated and can be assessed by means of correlation matrices (Table 3.1). The correlation increases (Cecconi *et al*., 1997) as a function of the steel grade. Recently, closed form expressions have been proposed to correlate yield and ultimate strengths (Fukumoto, 1996); they are based upon regression analysis of 1612 test coupon tests. These relationships may be used to evaluate the ultimate strength from yield strength or vice-versa, depending on the known resistance; therefore, they are useful to design seismic retrofitting of steel and composite structures. The proposed formula is as follows:

$$f_u = 0.83 \cdot \left(f_y + 245.6 \right) \tag{3.2}$$

with the stresses in (N/mm^2). The predictions provide close approximations (within 10%) of European standardized grades (EN 10025, 1990).

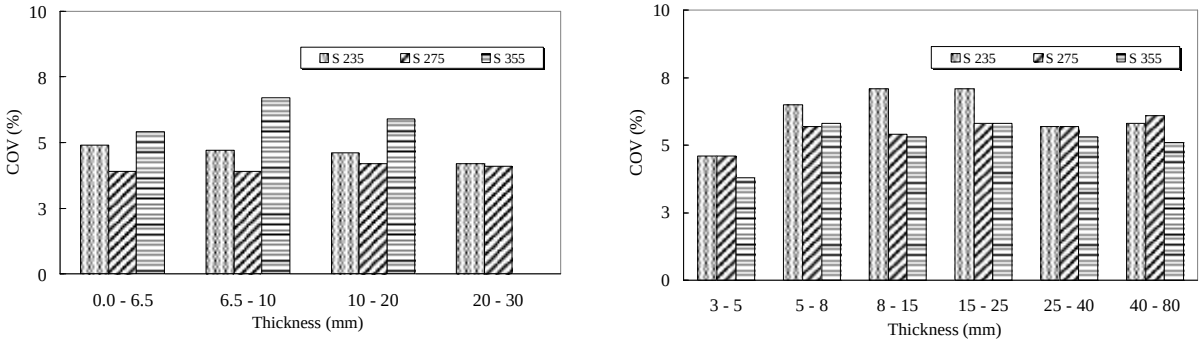

Figure 3.3. COVs of measured mean yield strengths: hot rolled sections (l*eft*) and laminated plates (*right*).

The above findings show that the quality of European steels (EN 10025, 1990; EC3, 1992) is close to AISC-LRFD specifications (AISC, 1993). Their mean yield strengths exceed minimum required values by less than 10%; 5% for flange; and 10% for web plates with COVs equal to 10% and 11%, respectively. It is instructive to note that in the Japanese seismic code design, yield strength of steel is 1.10 times the nominal yield values with COVs on average of 10% (Kuwamura and Kato, 1989).

Significant correlation exists between high ductile behavior and stress ratio, (f_u/f_y) (Kuwamura, 1988, Fukumoto, 1996, El-Tawil *et al*., 2000). The higher f_u/f_y, the higher the ductility and hence, the higher is the energy absorption (Kuwamura and Kato, 1989). However, lower and upper bounds of f_u/f_y are essential for seismic retrofitting. Moreover, values of ultimate and yield strengths are correlated (Table 3.1); a closed form expression to evaluate f_u/f_y ratios is as follows (Fukumoto, 1996):

$$\frac{f_u}{f_y} = 0.83 + \frac{203.8}{f_y} \tag{3.3}$$

with the stresses in (N/mm^2). Predictions from Equation (3.3) may be used in retrofitting whenever material data records are not complete.

Table 3.1. Coefficients of correlation: grade 43A (non*bracketed*) and 50A (*bracketed*).

	Yield Strength	Ultimate Strength	Ultimate Elongation	Yield Ratio
Yield Strength	1.000	0.800 (0.700)	-0.461 (-0.314)	0.905 (0.861)
Ultimate Strength	-	1.000	-0.480 (-0.473)	0.471 (0.240)
Ultimate Elongation	-	-	1.000	-0.337 (-0.086)
Yield Ratio	-	-	-	1.000

Recent studies show that the minimum f_u/f_y ratio (Table 3.2) for standardized European steels (EC3, 1992) is 1.44 (grade S355); maximum f_u/f_y for profiles with thickness less than 40 mm is 1.56 (grade S275) (Di Sarno, 2000). Overstrength ratios for S275 are greater than S235 counterparts; independently of material thickness.

As a consequence, to account for steel strain hardening, capacity checks should be performed with a factor of about 1.4 in place of 1.20 (EC8, 1998). Lower values of overstrength ratio are allowed but should be based on material testing. Strain hardening is also accounted for in recent US design recommendations (FEMA 355A, 2000); a multiplier factor, ranging between 1.10 and 1.20 as a function of the grade, is used to compute plastic section capacities. Therefore, the worst design scenario in the US practice is obtained by combining the scatter in yield stress for low grade ASTM 36 steel, which leads to expected yield strengths equal to 1.5 times nominal values and

strain hardening factors of 1.2. Thus the increase of yield strength is 1.8 (1.2x1.5) times the nominal values. Performing similar calculations for European design, the yield strength should be increased up to about 2.0 (=1.4 x 1.4).

Table 3.2. Standard yield and ultimate strengths for European steels (Stress is in N/mm^2).

Steel Grade		f_y	f_u	f_u / f_y	f_y	f_u	f_u / f_y
EN 10025	(EC3, 1996)	$t \le 40mm$			$40mm \le t \le 100mm$		
Fe 360	S235	235	360	1.53	215	340	1.58
Fe 430	S275	275	430	1.56	255	410	1.61
Fe 510	S355	355	510	1.44	335	490	1.46

It is worth mentioning that mean values of yield and tensile strengths in European steel profiles have different values for flanges and webs (Figure 3.4) (Byfield, 1996). However, the difference of yield strength between flange and webs is generally low (less than 10%). Due to metallurgical features, such as grain size and concentration of carbon content in central regions, yield stress is higher in webs (smaller grain size) than in flanges.

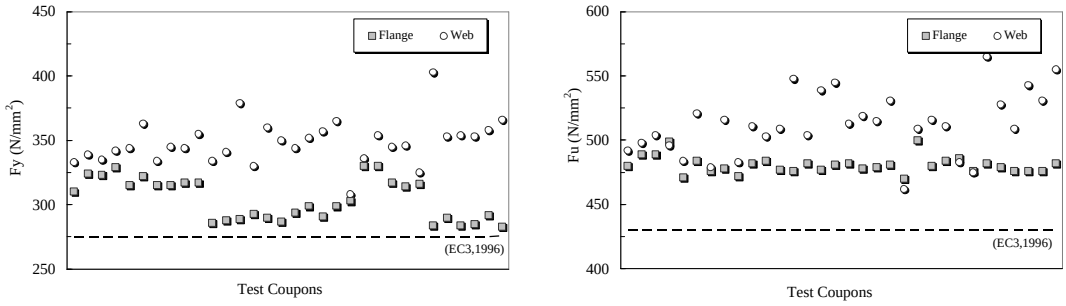

Figure 3.4. Strength properties for hot rolled sections grade S275: yield (l*eft*) and ultimate strength (*right*).

Therefore, if the factor *R* is determined by testing, strength properties should be referred to the web of rolled profiles (Plumier, 2000). For nondissipative members, yield and tensile strengths should be based on specimen cut from beam or column flanges (EC3, 1996). Steels produced before the 1970s are susceptible to lamellar tearing for through-thickness loading (Dexter and Melendrex, 2000). Therefore the through-thickness resistance in column flanges should be based upon the reduced strength as follows:

$$f_u = 0.90 \cdot f_y \tag{3.4}$$

This requirement is aimed at limiting the through-thickness resistance, because brittle fracture can occur in connections, either beam-to-column or brace-to-column, as a result of lamellar tearing due to stress concentrations (Barsom and Korvink, 1998; FEMA 355A, 2000). However, through-thickness failures are caused by several factors: metallurgy of steel (particularly its lamellar tearing) effects of axial loads, loading rate, triaxial restraint, local hardening and embrittlement in the heat affected zones in welds, stress concentration, defects at the root of the beam to column flange welds and effects of deformations caused by connection components (Plumier, 2000). The proposed reduced strength in Equation (3.4) was chosen in compliance with American provisions (AISC, 1997).

3.1.3. ELONGATION AND DUCTILITY

The values of elongation-to-fracture (ε_u) observed in tests performed on European structural steels are, on average, larger than the minimum required in the codes (Manzocchi *et al.*, 1992; Byfield and Nethercot, 1997; Cecconi *et al.*, 1997). Ultimate strain values are greater than 20% for common hot rolled profiles, the highest values generally being for flange material in standard column sections and for the web material in universal beams. Therefore, steel possesses adequate ε_u for the design of retrofitting of existing steel and composite structures. However, in specific circumstances, it may be required to ascertain the ultimate elongation of in-place material. American provisions suggest in such cases to express ε_u as a function of the true strain at fracture as follows (FEMA 355A, 2000):

$$e_u = \ln\left(\frac{l_f}{l_0}\right) = \ln\left(\frac{A_f}{A_0}\right) \tag{3.5}$$

in which l_0 and l_f are respectively the gage initial length and the length after fracture of the specimen. Similarly, A_0 and A_f are the original cross-sectional area and after fracture.

Alternatively, correlations between ultimate strains and yield strengths and/or f_u/f_y ratios may be used (Fukumoto, 1996); they are as follows:

$$0.83 \cdot f_y + 203.8 = \frac{f_y}{\exp\left\{-\ln(1+e_u)\cdot\left[\ln(\ln(1+e_u)+4.3\right]\right\}} \tag{3.6.1}$$

or the simplified expression:

$$e_u = 0.60 \cdot \left(1 - \frac{f_y}{f_u}\right) \tag{3.6.2}$$

These relationships are useful in designing the retrofit of steel and composite structures when the knowledge of steel material data is not complete.

3.1.4. STRAIN RATE

Material properties of structural steel are generally influenced by strain rate (Soroushian and Choi, 1987; Elnashai and Izzudin, 1993). Yield (f_y) and tensile (f_u) strengths increase at higher strain rates, but f_y increases more then f_u. The overstrength ratio (f_u/f_y) is thus reduced and the spreading of plasticity limited. This effect influences the response of stiff structures, e.g., braced frames and, within such structures, the behavior of the high frequency structural components. It was found that the strain rate effect reduces the ratio f_u/f_y in braced frames by up to a half for a variation of strain rate from 10^6 to 10^{-3} seconds (Lee *et al.*, 1992). This loading rate dependence is due to the higher steel strain rates in buckled braces and the uniform stress state in brace members (Elnashai and Izzudin, 1993). Therefore, strain-rate sensitivity should be adequately quantified via testing for steel, to be used for retrofitting of braced systems. Alternatively, the increased yield strength can be predicted via analytical relationships expressed as a function of yield stress (f_y) and strain rate (ε`) (Wakabayashi *et al.*, 1978; Jones and Birch, 1998).

3.1.5. TOUGHNESS

Fracture toughness values at high loading rates, e.g., at 10^{-1}/second, are lower than those measured at slower loading rate, say at 10^{-4}/sec; these values vary with the temperature. The higher the temperature, the higher is the fracture toughness (Figure 3.5). Moreover, tests conducted on fracture mechanics show a decrease of measured toughness values at the onset of rapid crack propagation (*trans-granular cleavage*) for dynamic loading, compared to quasi-static loading (Matos and Dodds, 2002). At a fixed temperature in the ductile-to-brittle region (Figure 3.5), dynamic loading lowers the cleavage toughness. However, the toughness reduction due to dynamic loads depends upon: (i) strain rates ahead of the crack front, (ii) the sensitivity of the material flow properties to strain rate and (iii) temperature. Therefore, adequate toughness should be checked and/or guaranteed for new structural steel used for retrofitting. Brittle fracture at the lowest service temperature expected during the design life should be avoided; while welded components should possess sufficient fatigue strength (Barsom and Rolfe, 1999).

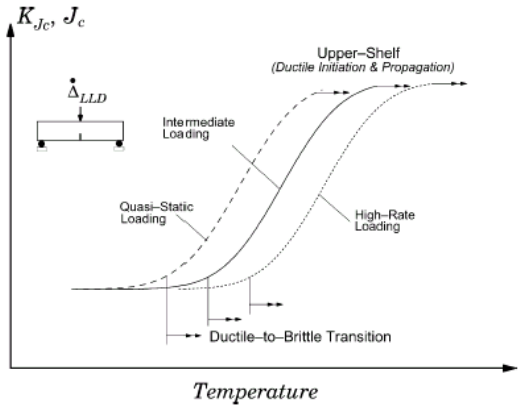

Figure 3.5. Schematic representation of combined temperature and loading rate effects on fracture toughness (*after* Matos and Dodds, 2002).

Charpy V-Notch (CVN) test, which characterizes the energy absorption capability of the material realized in the specimen by spreading of plasticity in dynamic conditions, is adequate to perform toughness tests on steel for seismic applications. Coupons should be cut from intersection zones between flange and web. In fact, this is an area (*k-area*) of potentially reduced notch toughness because of the slow cooling process during fabrication (Tide, 2000). Structural profiled sections with plates thicker than 38 mm should possess a minimum toughness of 27J measured at 20^{o}C. A similar requirement is provided in the US practice (AISC, 1997; FEMA, 355A, 2000). Sections with plate thickness less than 38 mm generally possess adequate toughness (Plumier, 2000).

For welded components and/or connections toughness should be assessed on the weld itself as released in a test coupon representative of the real weld. The toughness of parent material should be greater than the base material counterpart.

3.1.6. DATA COLLECTION

In-place properties of steels, i.e., yield and tensile strengths, ultimate elongation, Charpy (notch) toughness and weldability, if required, should be evaluated as follows:

- *Data collection from original records of the structure:* Either executive structural drawings or records of laboratory testing on the materials at the time of construction, if any, are a primary source for gathering information. If material data records exist and show that the structure was code-compliant, then default properties (as in the code at time of construction) can be used as basis for the design of retrofitting. This procedure is straightforward but usually not applicable because records are not available. Default material properties can be used merely to perform linear analyses, either static or dynamic. For nonlinear analyses, static (pushovers) or time-histories, testing is compulsory.

- *Sampling of coupons for laboratory testing:* At least three samples should be taken randomly from each representative structural component, namely beam-columns, braces and connections. Alternatively, the number of specimen increases; at least two from each representative components, every flour floors. Areas of reduced stress, such as flange tips at beam-column ends and external plate edges, should be selected as far as possible. However, to evaluate expected strengths, samples should be removed from web plates of hot rolled profiles for components designed as dissipative. Flange plate specimens should be used to characterize the material properties of nondissipative members and/or connections. If values from tests for expected strengths are lower than default values in the code at time of construction, more detailed assessment is required. It is worth noting that the extent of sampling on representative structural components for laboratory testing varies with the type of structural system, desired accuracy, in-place quality of materials and ease of accessibility. For encased members, such as in composite buildings, it is required to remove preliminary encasement at critical locations, hence, cut material samples.

- *Other destructive and/or nondestructive in situ testing methods available* (FEMA 355A, 2000) *and cost-effective should be used to quantify the mechanical properties of structural steel*. Moreover, these methods are suitable when accessibility is limited or for composite components. Gamma radiography, ultrasonic testing through the architectural fabric or boroscopic review through drilled access holes, are then viable solutions.

More extensive sampling and laboratory testing are required to qualify material properties for structural connections, either welded or bolted. Soundness of base and filler materials should be proved on the basis of chemical and metallurgical data. CVN toughness tests should prove that heat affected zones, if any, and surrounding material have adequate resistance for brittle fracture. Similarly, bolts and/or rivets used for connections should possess adequate resistance for the intended use. Recent experimental tests performed on bolted connections, using 10.9 bolts code-compliant designed, showed that strain rate does not detrimentally affect the connection performance; the tests were carried quasi statically and dynamically (Plumier, 2000). In all the performed tests the bolts were pre-stressed at the standard value of $0.7 \cdot f_{uB} A_s$.

The performance of steel and/or composite buildings may also be affected by physical properties of base materials as well as their possible state of degradation. For example, for structural steels, state of corrosion, damage from either chemical attacks or fire, damage due to previous earthquake loading or fatigue, micro-cracks should be adequately ascertained. To do so, visual inspection is a rapid and economic method, though is limited to superficial screening. Destructive (sampling) and/or nondestructive testing (liquid penetrant, magnetic particle, acoustic emission), ultrasonic or tomographic methods can be used for thorough checks.

3.2. SECTION REQUIREMENTS

3.2.1. GENERAL

Existing buildings suffered significant overstress and local failures when subjected to moderate or strong intensity earthquakes (Mahin, 1998; Nakashima *et al.*, 1998). The failure of plastic sections, properly supported in the lateral direction, may be caused by local buckling of compression flanges (Figure 3.6). The onset of local buckling is dependent on the section width to thickness ratio; hence, strict limitations are necessary to ensure the development of the full plastic moment capacity over the required number of load cycles experienced by a structure during severe ground motion. Load reversals imposed by earthquakes are a demanding loading condition (Vann *et al.*, 1973) since the rotation ductility demand should be sustained for a number of cycles, as high as 40 (Bertero, 1988). Therefore, it is imperative for seismic retrofitting of steel structures to apply strict limitations to section dimensions.

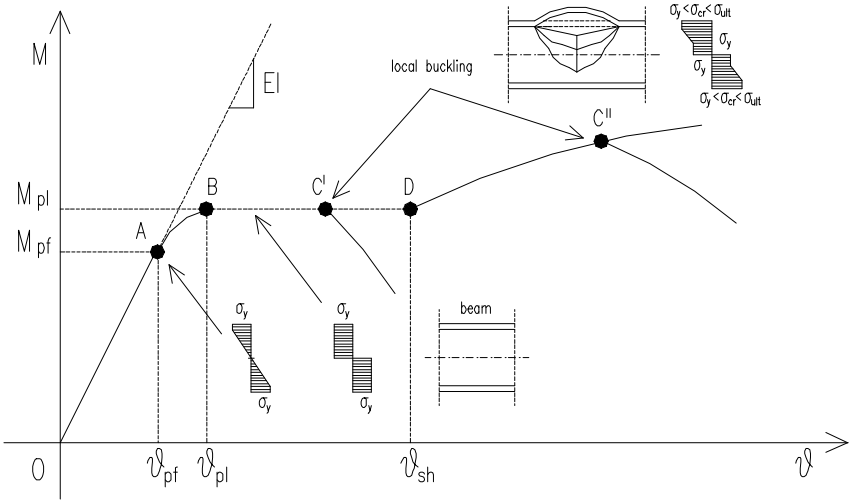

Figure 3.6. Typical moment-rotation curves for steel slender cross sections.

3.2.2. STABILITY AND STRENGTH

Traditionally, slenderness limitations have been provided for webs and flanges separately. However, a great deal of experimental and numerical research has been recently dedicated to investigate coupled buckling of flange and web plates (Kato, 1989; Schneider *et al.*, 1993). As a result, interaction formulae were proposed and included in the Japanese code for seismic design (Kato, 1994). Such relationships were recommended for the seismic design of new buildings in European standards; they should also be extended to seismic retrofitting (Elnashai, 2000).

Limitations for coupled buckling are given (Kato, 1989) as a function of either ductility class or rotation ductility $R_\theta = \theta_{pl}/\theta_y$; where θ_{pl} and θ_y are the plastic and yielding rotations, respectively. For seismic rehabilitation the most restrictive limitations should be used to achieve high R_θ values (Class 1 sections), e.g., 5 or 10; therefore, the width-thickness ratios should comply with the following:

$$\frac{\left(\frac{b}{t_f}\right)^2}{\left(\frac{K_1}{\sqrt{f_y}}\right)^2} + \frac{\left(\frac{d_e}{t_w}\right)^2}{\left(\frac{K_2}{\sqrt{f_y}}\right)^2} \le 1 \tag{3.7}$$

where b and t_f are the flange outstand and thickness; t_w is the web thickness; and f_y is the yield strength which should be conservatively assumed to be equal to the web yield strength (Section 3.1). Equation (3.7) holds for H-sections, either welded or rolled; however, analogous expressions are available in literature for hollow sections or cold formed (Kato, 1989).

The web height (d) in Equation (3.7) is replaced by the effective section height (d_e) to account for the web stress gradient. Indeed, Equation (3.7) was derived from tests on stub columns and hence, the webs are subjected to uniform compression. Therefore, d_e may be assumed as follows:

$$d_e = \frac{1}{2}\left[1 + \frac{A}{A_w} \cdot s\right] \cdot d \tag{3.8}$$

in which A_w and A are the web and total area of profiled sections. The validity of Equation (3.8) and similar expression for d_e proposed in literature has been checked by comparing predicted values with experimental tests (Daali and Korol, 1995).

The normalized critical stress ($s = f_{cr}/f_y$) was computed via regression analysis and is given by:

$$\frac{1}{s} = 0.689 + 0.651 \frac{1}{\alpha_f} + 0.0553 \frac{1}{\alpha_w} \pm 0.0303 \tag{3.9}$$

with flange (α_f) and web (α_w) slenderness parameters expressed as:

$$\alpha_f = \frac{E}{f_{fy}} \cdot \left(\frac{t_f}{b}\right)^2 \tag{3.10.1}$$

$$\alpha_w = \frac{E}{f_{wy}} \cdot \left(\frac{t_w}{d_e}\right)^2 \tag{3.10.2}$$

and setting conservatively $f_{fy} = f_{wy} = f_y$ in Equations (3.10.1) and (3.10.2).

The coefficients K_1 and K_2 depend upon the rotation ductility ratio R_θ and the level of axial load (ρ), if any. Values for beams and beam-columns are provided in Table 3.3 for low-to-high rotational ductilities, i.e., 2 to 10; however, high R_θ (e.g., between 5 and 10) are recommended. The limiting ratios in Equation (3.7) are significantly influenced by the level of axial stress present; thus, the higher the axial stress, the more critical local buckling is expected to be.

Table 3.3. K_1 and K_2 for beams and columns.

	BEAMS (ρ=0)			COLUMNS (ρ=0.30*)		
	R_θ			R_θ		
	2	4	10	2	4	10
K_1	200	181	139	208	192	150
K_2	1289	1170	893	869	710	557

Keys: * allowable axial ratio for composite columns in Eurocode 8.

It is worth mentioning that the Equation (3.7) and hence, K_1 and K_2 coefficients are based upon the following assumptions:

(i) The yield strength for flanges and web is equal, i.e., $f_{yf} = f_{wy}$.
(ii) The initial-to-hardening modulus ratio is $E/E_{st} = 70$.
(iii) The hardening-to-yield strain ratio is $\varepsilon_{st}/\varepsilon_y = 10$.
(iv) The total-to-web area ratio is $A/A_w = 2.5$.
(v) The depth-to-width ratio is $h/(b/2) = 4$.

Assumptions: (i), (ii) and (iii) are conservative, while ratios in (iv) and (v) refer to average values for hot rolled sections (Table 3.4). Moreover, K_1 and K_2 coefficients for beam-columns are provided in Table 3.3 for ρ=0.3, i.e., axial load equal to 30% of the squash load. Values of K_1 and K_2 for other level of axial loads and/or different R_θ should be computed through the following procedure:

1. Define the geometry of the section.
2. Define the mechanical properties of the steel in web and flange plates; conservatively use the higher value for strengths and lower values for stiffness in the calculations.
3. Define the level of axial load expected in beam-columns.
4. Define the target rotation ductility ratio R_θ; however, values should not be less than 5.

Table 3.4. Properties of some European rolled sections for beams (IPE) and columns (HE).

Sections (type)	h (mm)	b (mm)	A_w (mm^2)	A (mm^2)	h / (b/2)	A / A_w
IPE 100	100	55	363	1030	3.6	2.8
IPE 200	200	100	1025	2850	4.0	2.8
IPE 300	300	150	1978	5380	4.0	2.7
IPE 400	400	180	3208	8450	4.4	2.6
IPE 500	500	200	4774	11600	5.0	2.4
IPE 600	600	220	6744	15600	5.4	2.3
HE 100B	100	100	480	2600	2.0	5.4
HE 200B	200	200	1530	7810	2.0	5.1
HE 300B	300	300	2882	14900	2.0	5.2
HE 400B	400	300	4752	19800	2.7	4.2
HE 500B	500	300	6438	23900	3.3	3.7
HE 600B	600	300	8370	27000	4.0	3.2

5. Using the following relationships, as appropriate, solve for the critical stress ratio s:
   - *Beams* (ρ=0.0):

$$R_q = \frac{1}{s}\cdot\left\{\left(\frac{E\cdot I}{E_{st}\cdot I_e}\right)\cdot(s-1)^2 + \left(\frac{e_{st}\cdot h}{e_y\cdot h_e}\right)\cdot(s-1)\right\} \qquad (3.11.1)$$

   - *Beam-Columns*:

for $0 < r < \frac{s-1}{2}$:

$$R_q = \frac{s-1}{(1-r)\cdot(s-r)}\cdot\left\{\frac{E\cdot I}{E_{st}\cdot I_e}\cdot\left[\left(s-2r-1^2\right)+2r^2\right]+\left(\frac{e_{st}\cdot h}{e_y\cdot h_e}\right)\cdot(s-1)\right\} \qquad (3.11.2)$$

for $r > \frac{s-1}{2}$:

$$R_q = \frac{s-1}{2\cdot(1-r)\cdot(s-r)}\cdot\left\{\left(\frac{E\cdot I}{E_{st}\cdot I_e}\right)\cdot(s-1)+2\cdot\left(\frac{e_{st}\cdot h}{e_y\cdot h_e}\right)\right\} \qquad (3.11.3)$$

where h_e and I_e are the distance between the geometrical centers of flanges and the moment of inertia of the equivalent section, respectively. It is instructive to note that for values of axial load $0<\rho<(s-1)/2$, the tension flange is within the elastic range when the compressed flange buckles. By contrast, for higher axial loads (i.e., $\rho>(s-1)/2$) the tension flange yields before failure; however, the latter failure mode is recommended. Moreover, for typical H-sections, the ratios between actual and equivalent properties are given below:

$$\frac{h}{h_e} = \frac{2 + 0.30 \cdot h/b}{2 + 0.15 \cdot h/b} \tag{3.11.4}$$

$$\frac{I}{I_e} = \frac{(2 + 0.30 \cdot h/b)\cdot(2 + 0.10 \cdot h/b)}{(2 + 0.15 \cdot h/b)^2} \tag{3.11.5}$$

6. Equate the value of s derived above to the value given by the regression expression in Equation (3.9).
7. Limitations on width-to-thickness ratios for web and flanges and hence, K_1 and K_2 coefficients for Equation (3.9) are then obtained in terms of: (i) initial-to-strain hardening moduli, (ii) yield-to-strain hardening strains, (iii) properties of original and equivalent sections and (iv) applied-to-yield axial stress.

However, for welded or rolled H-sections of beams and beam-columns with low axial loads, the following relationship may be used:

$$\frac{\left(\frac{b}{t_f}\right)^2}{\left(\frac{E}{1.6 \cdot f_{fy}}\right)\cdot\left(\frac{1}{s} - 0.6003\right)} + \frac{\left(\frac{d_e}{t_w}\right)^2}{\left(\frac{E}{0.1535 \cdot f_{wy}}\right)\cdot\left(\frac{1}{s} - 0.6003\right)} \le 1 \tag{3.12}$$

which is derived by combining Equation (3.9) for the critical stress ratio (s) with Equation (3.11.1) for the rotation capacity (R_θ).

It is worthwhile to note that limiting width thickness ratios provided in European standards (EC3, 1992; EC8, 1998) for Class 1 sections should be further reduced in seismic retrofitting of steel structures. In the US seismic provisions (e.g., AISC [AISC, 1997]), limitations for local buckling are more restrictive than for nonseismic design (Galambos, 1998; AISC, 1993); a reduction of about 25% characterizes flanges of I-shaped beams and channels in flexure, e.g., $138/\sqrt{f_y}$ *vs.* $172/\sqrt{f_y}$ (Table 3.5). More strict limitations (up to 72%) are required for hollow structural sections. Such reductions ensure structural members can withstand not less than 10 to 15 inelastic deformations without local buckling (Astaneh, 1995). Similar reductions are not used for seismic design in Europe.

Table 3.5. Width-to-thickness limits for compressed flanges of Class 1 sections.

	EC 3, 1992	UBC, 1997	AISC LRFD, 1993	AISC, 1997
Limits	$10\cdot\sqrt{235/f_y}$	$0.31\cdot\sqrt{E/f_y}$	$172/\sqrt{f_y}$	$138/\sqrt{f_y}$
S 235*	10.0	9.3**	11.2	9.0
S 275*	9.2	8.6**	10.4	8.3
S 355*	8.1	7.5**	9.1	7.3
Variation (%)	0***	- 7.5	+ 12.0	- 11.1

Keys: * Steel grades as in EC3; ** E = 210000 N/mm^2; *** Benchmark value.

Moreover, recent studies on the variability of steel properties showed consistent deteriorations of local ductility ($\mu=\varepsilon_u/\varepsilon_y$) for compressed flange plates (Fukumoto, 2000). Three cases of actual-to-

nominal yield strength ratios were considered, i.e., 1.00, 1.15 and 1.45. It was found that the higher the variability of yield stress the lower is μ. As a result, it was suggested that the limiting width-to-thickness ratio (b/t) should be multiplied by the factor $k = \sqrt{f_{y,act} / f_{y,nom}}$ to account for the yield strength variability. This effect, which may erode the local ductility of steel sections, is not considered in the Eurocode 3 (EC3, 1992).

Therefore, the extremely simplified formulation for cross sections in European standards has many shortcomings and does not account for fundamental aspects influencing the local ductility (Gioncu and Mazzolani, 1994; Broderick and Elnashai, 1996). To avoid inadequate evaluations of the rotation capacity for beams and beam-columns, which may lead to unreliable structural performance assessments, interaction formulae discussed above are recommended for seismic rehabilitation.

On the other hand, if the local buckling does not occur then the failure due to the onset of the ultimate moment. It is determined by reaching the ultimate tensile stresses in the extreme fibers (Figure 3.7) and some cracks may appear in the tensile zones.

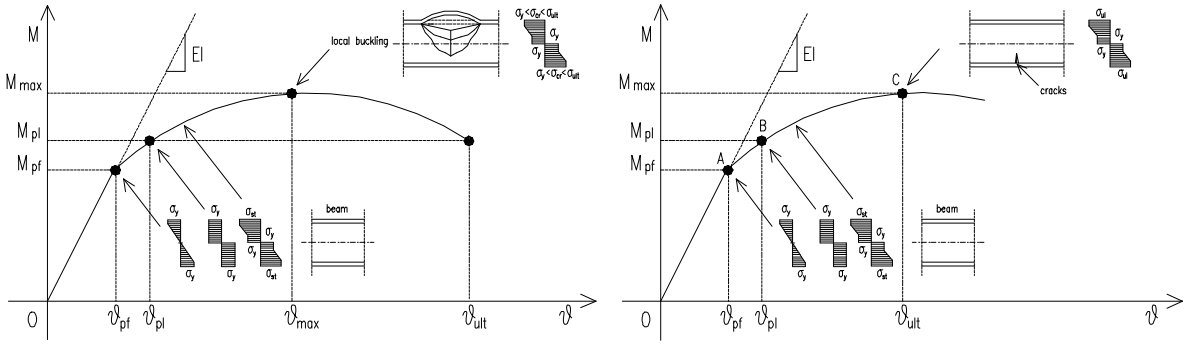

Figure 3.7. Typical moment-rotation curves for steel cross sections: slender (*left*) and stocky (*right*) sections.

The evaluation of ultimate moments (M_u) may be used in the design of nondissipative members. Several formulations have been proposed for M_u as a function of the overstrength (f_u/f_y) and the plastic moment (M_p); some of them are summarized in Table 3.6 (Lay and Galambos, 1965; Gioncu and Petcu, 1997; Galambos, 1998).

Table 3.6. Ultimate moments for steel sections.

	after Lay and Galambos, 1965	*after* Gioncu and Petcu, 1997	*after* Galambos, 1998
M_u	$\left(1/2\right)\cdot\left[1+\left(f_u/f_y\right)\right]\cdot M_p$	$\left(1/4\right)\cdot\left[1+3\cdot\left(f_u/f_y\right)\right]\cdot M_p$	$\left(f_u/f_y\right)\cdot M_p$
Range of M_u	1.22 to 1.27 M_p	1.33 to 1.40 M_p	1.40 to 1.55 M_p

Keys: M_p = plastic bending moment; M_u = ultimate bending moment.

It is suggested to compute ultimate moments without reducing ultimate tensile strengths because the values are higher than those obtained by reduced strengths, i.e., either $(f_y+f_u)/2$ or $(f_y+3\cdot f_u)/4$; M_u ranges between 1.40 and 1.55 M_p.

The ultimate rotation θ_u corresponding to the M_u (Figure 3.7) may be derived from the ultimate strain as follows (Galambos, 1998):

$$J_u = 2 \cdot e_u \tag{3.13}$$

which ranges between 0.40 and 0.50; at this stage cracks may be found in the beams.

3.2.3. COMPOSITE SECTIONS

In composite members, large rotation ductilities, which should be accommodated within plastic hinges, require that the component structural materials, i.e., structural steel and RC, should be capable to undergo large strains without significant loss of stiffness and resistance (Elnashai and Broderick, 1994). Requirements of structural steels were addressed above. For RC, crushing and spalling of concrete due to excessive compressive strains should be avoided. These requirements can be achieved by either providing adequate transverse reinforcement in compliance with RC design rules for medium ductility (EC8, 1998) or by placing restrictions on the plastic neutral axis (PNA) depth of the section (Broderick and Elnashai, 1996). In fact, the latter is important in avoiding reinforcement fracture for high rotational ductility demand. To achieve ductility in plastic hinges, the distance from the concrete compression fiber to the plastic neutral axis should not be more than 15% of the overall depth of the composite cross section; this limit is the one used in nonseismic design (EC4, 1994). However, other PNA requirements may be found in literature (Plumier, 2000; Kemp and Nethercot, 2001); they are generally less stringent. e.g., several recent experimental and analytical tests showed that PNA for composite beams should be located between the mid-depth and a level 15% above the bottom flange of the steel section (Kemp and Nethercot, 2001). This recommendation is similar to US counterparts (AISC, 1997); the latter require that for composite beams the distance from the maximum concrete compression fiber to PNA should be less than the following value:

$$PNA \le \frac{25.4 \cdot (d_b + d_c)}{1 + 1700 \cdot \left(\frac{f_y}{E} \right)} \tag{3.14}$$

with d_b the depth of the beam and d_c the concrete cover thickness, if any; both lengths are in mm. Equation (3.14) ensures that the strain in the steel at the extreme fiber is about five times the tensile yield strain prior to concrete crushing (strain equal to $3^{\circ}/_{\infty}$). The recommended PNA is contrasted to US requirements in Figure 3.8; the concrete cover is assumed equal to 55mm.

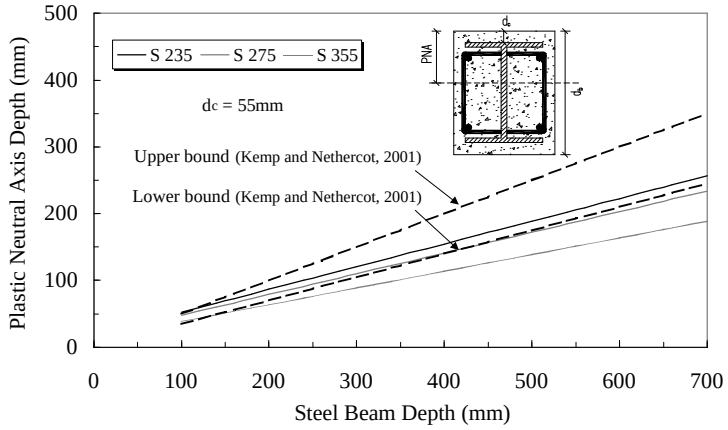

Figure 3.8. Allowable plastic neutral axis depth for composite beams.

It is worth mentioning that composite beams exhibit high shape factors, generally between 1.25 and 1.35, while those relative to steel H-sections are generally less than 1.20. As a consequence, higher demands are imposed on the ultimate elongation (ε_u) of the steel reinforcement (Nethercot *et al.*, 1995). Recent studies showed that the ε_u of reinforcing bars is the most important mechanical parameter controlling the collapse of composite beams (Fabbrocino *et al.*, 2001). This result characterizes the collapse either under negative or positive bending; however, it is as a function of shear connector interactions. Failure of beams with full shear connection is controlled solely by the

fracture of reinforcing bars. For partial connections, the main contribution to rotation capacity is the slip at the slab-profile interface; rotations depend on the slip capacity of shear connectors. Moreover, European composite constructions in seismic employ generally full interaction. As a result, reinforcement steels used for retrofitting should possess enhanced ductility (class H is advised). Such a requirement should be applied for either dissipative or nondissipative zones to provide structural robustness for abnormal loading other than earthquakes, i.e., blasts, impacts and fire.

Greater rotation capacities may also be achieved through the use of composite steel columns. Composite columns comprise sections with an area of structural steel of at least 4% (AISC, 1997) of the total composite section. Alternatively, the columns should conform to design rules for RC. In fact, mutual benefits provided by the steel and concrete components ensure that local buckling occurs only at high strains (Elnashai and Broderick, 1996). Thus, the limits for width-to-thickness ratios given above for bare steel members, e.g., Equation (3.6), should be reduced; threshold values may be assumed 15% to 20% lower in the interaction formula to benefit of composite action.

Therefore, by employing partially-encased composite beam-column sections (Figure 3.9), traditional benefits offered by composite columns, i.e., global stability and fire protection, are retained, while at the same time achieving increased rotation capacities, without resorting to uneconomical section details. Furthermore, the inclusion of additional reinforcement, such as the transverse links (Figure 3.9), ensures higher rotation capacities even with slender flanges and webs. Such transverse bars are welded between the flanges; they can be spaced as transverse stirrups for encasing RC.

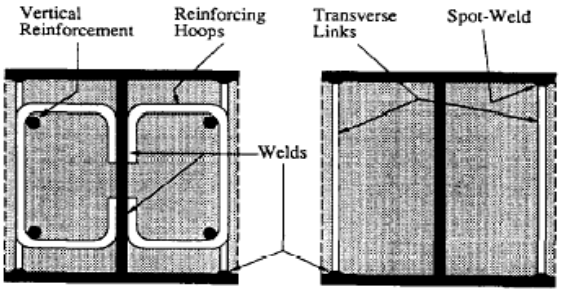

Figure 3.9. Partially encased beam-column sections: stirrups and flange buckling inhibitors (*left*) and flange buckling inhibitors (*right*).

Encased beam-columns are thus a viable solution in seismic retrofitting to enhance local ductility of bare steel members. In such cases, the detailing of these members should be carried out in compliance with the requirements of RC high ductility class and composite members (EC8, 1998). Reinforced concrete covers of at least 55 mm (AISC, 1997) should be used for compressed beam flanges; alternatively, local buckling requirements, as specified above, apply. Ductile ribbed bars with adequate anchorage and splices are advised for steel reinforcements. Welds should be performed in such a way to reduce risks of brittle fractures for HAZs or surrounding areas.

3.3. MEMBER RETROFITTING

3.3.1. GENERAL

The mechanical response of structural members and connections in steel and composite frames depends upon: (i) cross section areas, (ii) width-to-thickness slenderness ratios, (iii) lateral torsional

buckling resistance and (iv) connection details. Therefore, to design adequate seismic retrofitting of damaged components in such structures, it is first necessary to acquire information relative to physical and mechanical properties of in-place components. Then ad hoc repairing strategies selected on the basis of the reliability and economy can be implemented.

Primary sources for the properties of structural components are the original drawings, if available. Alternatively, thorough inspections on site will help to identify the necessary design data; some of these are summarized below:

- Original cross-sectional shape and physical dimensions.
- Size and thickness of additional connected materials (including cover plates, bracings and stiffeners).
- Existing cross-sectional area, section moduli, moments of inertia and torsional properties at critical sections.
- Component orientation and geometrical and/or mechanical imperfections.
- As-built configuration of intermediate, splice and end connections.
- Current physical condition of base metal and connector materials, including presence of deformation.

Once the necessary data have been acquired, the next step is to select the repairing solution for each damaged structural component. The requisite strategies for beams, columns, braces and connections are detailed hereunder. These strategies are aimed at enhancing either the member and connection strength or stiffness; however almost all of them increase both stiffness and strength. Therefore, it is strongly advised to account for both effects when assessing the frame performance and failure modes.

3.3.2. BEAMS

Common damage observed in steel beams in recent earthquakes consists of buckling and/or fracture of flange plates (Mahin, 1998; Nakashima *et al*., 1998). In such cases damaged plates should either be strengthened or replaced with new ones; however, other strategies are available but usually require skilled workmanship. For example, three viable solutions exist to repair buckled bottom and/or top flanges:: (i) full height web stiffeners, (ii) heat straightening and (iii) cutting of the buckled flange and replacement with a similar plate. In such a case, it is required to provide special shoring of the replaced flange plate. Generally, beam flanges buckle on both sides of the webs; hence, two plates should be attached onto the web, for each of the beam side. It is recommended to locate (Figure 3.10) the two stiffeners at the edge and centre of the buckled flange, respectively; the stiffener thickness should be equal to the beam web. Replacement with new plates is also effective to repair fractured flanges. In some cases the added plate can be welded in the same location as the original flange, i.e., welding the plate directly to the beam web. Instead, more often the new plate is welded onto the existing flange (Figure 3.10). However, in both cases it is required to orientate new plates with the rolling direction in the proper direction and take care of the welding details.

On the other hand, limitations of width-to-thickness ratios for flanges and webs (as given in Section 3.2) should be fulfilled. Local buckling of beam flanges affect in fact the frame strength degradation through the increase of story drifts and hence, second order effects (P-Δ effects). Furthermore, flange buckling gives rise to large strains, which reduce the low-cycle fatigue resistance by tearing the beam flange. To prevent these effects, the flanges should be stiffened either by welding new plates or by encasing the beam in RC (composite action); the encasement can be either partial or full. Stiffening bars welded transversally between flanges are efficient to avoid local buckling.

However, the design of a full encased beam is not included in the European standards for composite buildings (EC4, 1994; EC8, 1998); however, rules for columns may be conservatively used. This is the approach of other International codes of practice (AIJ, 1995; AISC, 1997). Moreover, fully encased beams have higher fire-resistance than partially encased. Further details of this solution are given in Section 3.2. However, it is worth mentioning that beams with very thick flanges are not recommended (FEMA 352, 2000). In fact, such beams should be avoided especially for seismic retrofitting of welded structures because they require joints with thick welds. These details give rise to high residual stresses and are difficult to control. Therefore, RC encasement should be preferred to plates welded onto the flanges, particularly in welded frames.

Generally web buckling is not critical for hot rolled sections; by contrast it can control the design of built-up beams or certain types of new beam shapes, as discussed later. Webs with low slenderness are recommended; welded plates may be added to stiffen beam webs either longitudinally or transversally. The thickness of the welded plates should be not less than that of the original web.

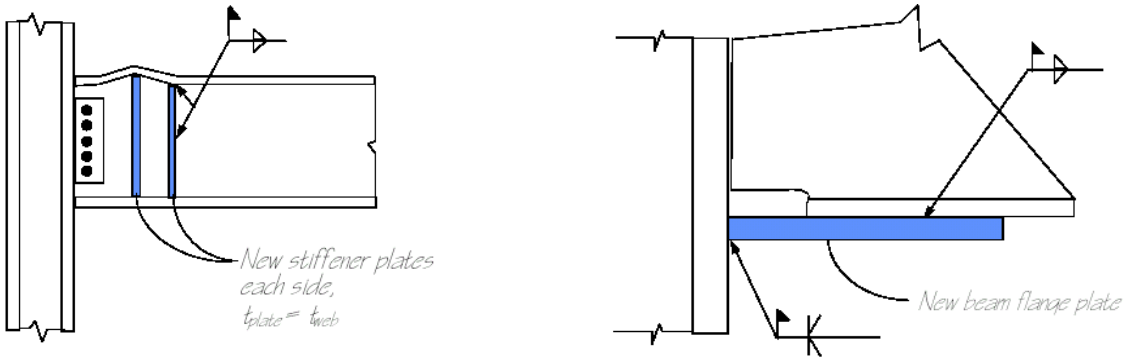

Figure 3.10. Typical repairs for buckled (*left*) and fractured (*right*) flanges of steel beams (*after* FEMA 351, 2000).

Moreover, lateral torsional buckling (LTB) resistance should be checked for retrofitting of existing steel and composite buildings; ratios of unsupported length (L_b) to minimum cross section radius (r_y) should range between 60 and 70 to achieve adequate rotation ductility, e.g., about 8 (Figure 3.11). Earthquake ground motion is between monotonic and cyclic regimes. The recommended unbraced length between lateral supports complies with the US provisions (AISC, 1997). This stipulates for special moment resisting frames (SMRFs), i.e., frames with significant inelastic deformations capacity that:

$$\frac{L_b}{r_y} \leq \frac{17500}{f_y} \tag{3.15}$$

This maximum distance was derived by plastic analysis, assuming that beams are generally under double curvature in framed structures and accounting for the uncertainty of the location of plastic hinges due to earthquake loading.

Following the SAC Interim Guidelines (SAC, 1997), lateral support capable of resisting a minimum of 2% of the unreduced flange force (Figure 3.12) should be provided such that the unbraced length as in Equation (3.15) is satisfied.

Equation (3.15) is as a function of the yield strength (f_y); it provides values of slenderness less than 80 for European grades of structural steels (EN 10025, 1990), namely 74 (S235), 64 (S275) and 49 (S355).

These values have been included in Figure 3.11 for comparative purposes; the limitation used in the Japanese code of practice, i.e., $L_b/r_y \leq 130$, has also been considered. Suggested values for European

standards are close to the US limits, which are, however, considered too stringent (Uang and Fan, 1999; FEMA 355D, 2000). In fact, past earthquakes have shown (AIJ, 1995) that LTB is unlikely even tough for beams designed according to the Japanese practice, i.e., with high slendernesses.

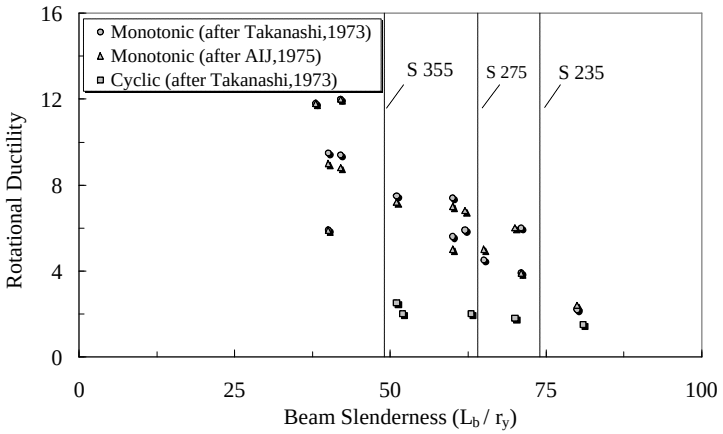

Figure 3.11. Beam rotation ductility as a function of the member slenderness (simple supported beam with mid-span point load).

LTB of unsupported beams is generally influenced by the composite action resulting from solid concrete or composite slabs attached via shear studs to the top flanges of the beam (Figure 3.12). Indeed, the slab restraints compressed beam top flanges under sagging moments. However, composite slabs shift the PNA toward the concrete slab (Figure 3.13), thus increasing the strains in the bottom flange and reducing the ductility of sections (Leon *et al*., 1998). Moreover, the composite action also increases the effective strength of the girder significantly, particularly at sections where top flanges are compressed (Plumier, 2000) and for shallower beams with full interaction (Leon *et al*., 1998). At a given curvature deep beams or beams with effective composite action experience larger strains than shallower beams (Figure 3.13). These aspects are particularly important for European design practice where deep beams and partial interactions are not very common (Mele, 2002). Therefore, these effects should be accounted for in the structural assessment for seismic retrofitting because they may lower the local and/or global ductility. For example, it is required to ascertain that maximum tensile strains do not provoke flange tearing or unintentional weak-column strong-beams effects.

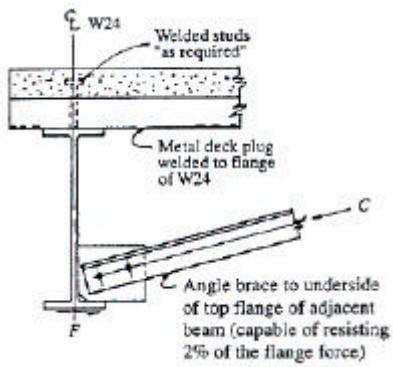

Figure 3.12. Lateral support for steel beam with composite slab (*after* Naeim, 2001).

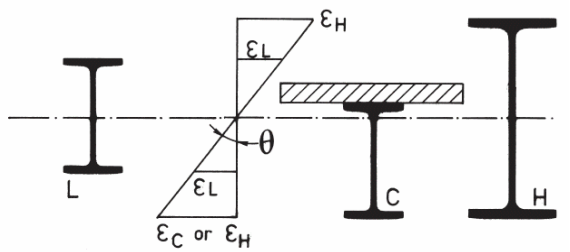

Figure 3.13. Strain increase as a function of the section depth and shape.

However, it is required that welded shear studs connecting steel beams and composite slabs should not be used within plastic zones; shear connector welds may introduce (FEMA 355D, 2000) flaws and reduced toughness thus leading to early fracture of the beam. The *hinging zone*, which is related to the yielding length (Figure 3.14), can be defined as (FEMA 350, 2000) the part of the beam between the edge section and one-half the beam depth beyond the location of the hinge point. For ductile connectors (EC4, 1994), partial shear connection may be adopted (Richard-Yen *et al*., 1997; Bursi and Zandonini, 1998). A minimum connection degree of 0.80 should though be used. Full shear connection is required when nonductile connectors are used. The design resistance of connectors in dissipative zones should be obtained from the design resistance provided for nonseismic design (EC4, 1994), applying a reduction factor equal to 0.75 (Bursi and Gramola, 1999). Studs should be attached to flanges arc-spot welds, but without full penetration of the flange. Either shot or screwed attachments should be avoided.

Furthermore, beams with low span-to-depth ratios, e.g., less than five or six, exhibit sharp bending moment variations along the span. As a result, the length of the beam participating to the energy absorption, i.e., plastic hinges, is reduced while inelastic strains are increased. It is recommended to use beam with span-to-depth ratios lying between seven and ten.

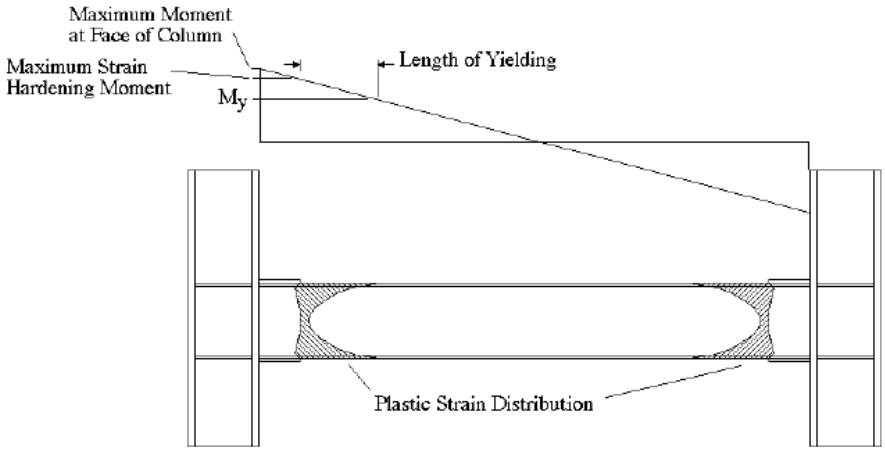

Figure 3.14. Typical yielding length for beams within MRFs (*after* FEMA 350, 2000).

Other deficiencies observed for steel beams are provided in Table 3.7 along with the suggested retrofitting strategies; however, such remedies are primarily aimed at increasing the resistance. The design of the added plates or details for RC encasement should be carried out in compliance with codes of practice for new buildings for permanent (EC2, 1992; EC3, 1992; EC4, 1994) and seismic (EC8, 1998) loads.

Table 3.7. Retrofitting strategies for steel beams in framed structures.

	Deficiency		
	Flexural Capacity	Shear Capacity	Stability
Retrofitting Strategy	• Add steel plates to bottom flange only (slab composite action is reliable). • Add steel plates to top and bottom flanges (slab composite action is not reliable). • Encase bare steel beam in RC with adequate longitudinal reinforcement bars. • Augment composite slab participation.	• Add steel plates parallel to the web. • Encase bare steel beam in RC. • Provide additional transverse reinforcement of RC encasement.	• Reduce flange and/or web slenderness ratios adding steel plates. • Reduce flange and/or web slenderness ratios via RC encasement with welded transverse stiffening bars between flanges. • Provide lateral support for bottom flange only (slab composite action effect is reliable). • Provide lateral support for top and bottom flanges (slab composite action effect is not reliable). • Augment composite slab participation.

It is worth noting that all member-strengthening strategies also increase the stiffness of each component. The enhancement of rigidity varies with the adopted remedy. For instance, either added steel plates or augmentation of composite action give rise to moderate stiffening effects. On the other hand, concrete encasement is the most viable way to substantially increase the stiffness. As a result, the effects of enhanced stiffness on frame strength and failure modes should be properly accounted for in the performance assessment.

The capacity design of framed structures requires that plastic hinges should form at beam ends. However, this requirement has lead to large through-thickness inelastic strain demand on the column flange of beam-to-column connections (Mahin, 1998; Nakashima *et al*., 1998), particularly within the HAZ, if any, and/or surrounding material where brittle failures were observed (Miller, 1998; Watanabe *et al*., 1998). Therefore, to improve the local ductility, the weakening of beam sections at desired locations for plastic hinge formation (Figure 3.15), i.e., shifted from column flanges, has been recommended either in the US (AISC, 1997; SAC, 1997; FEMA 352, 2000) or in Europe for existing and new steel and composite buildings (Plumier, 2000).

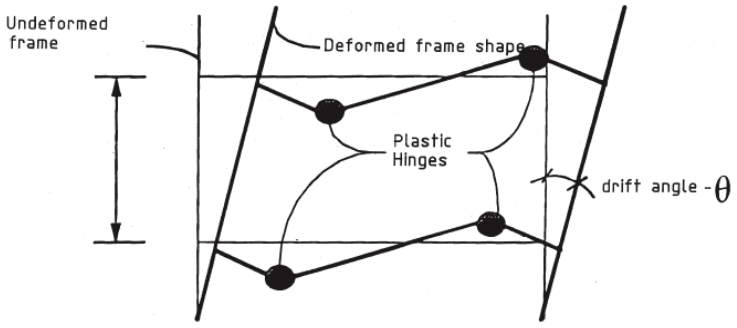

Figure 3.15. Desired location for plastic hinges formations in beams.

Reduced beam sections (RBSs) or dog-bones behave like a fuse, thus protecting beam-to-column connections against early fracture. The beam section is adequately reduced at a distance from the connection (Figure 3.16) so that yielding is concentrated within the weakened section. As a result,

bending moments at the column face are lower than those corresponding to the full inelastic demand of the connection.

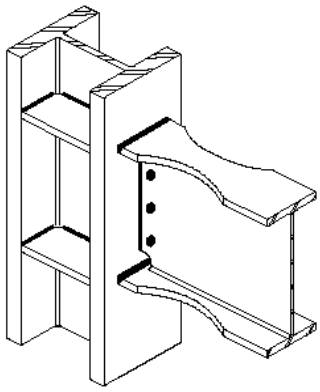

Figure 3.16. Typical RBS beam-to-column connection.

RBS solution was introduced in the 1990s and later studied and developed worldwide (Plumier, 1990). For example, in the US several configurations of RBS have been studied as an alternative repairing strategy (*weakening*) for beam-to-column connections since the Northridge earthquake (Chen, 1996; Iwankiw and Carter, 1996; Engelhardt *et al.*, 1998). The assessed RBS types include constant tapered or curved sections and drilled holes patterns, either constant or tapered. However, it has been found that some configurations perform better than others (FEMA 355D, 2000). In fact, sections with drilled holes may suffer tensile failure across the reduced net section of the flange, thus exhibiting lower ductility. On the other hand, RBSs failed within the reduced sections at plastic rotations below 0.02 radians for straight cuts and generally between 0.03 and 0.05 radians for tapered and radius cuts, thus exhibiting adequate plastic rotations of the latter design details. Failures occurred at locations with a change in direction of cuts in the beam flange, resulting in a notch effect; this effect is significant for RBS with straight cuts and to a lesser extent for tapered beam sections, provided 'radiused' returns are employed (Figure 3.17). The former fractured after initial yielding because of large strains concentrated at the corner cuts; the latter fractured at the return from the tapered section to the full beam flange width. As a consequence, it is of paramount importance to enhance the inelastic performance of RBSs. This indicates that the pattern of any flange cuts should be proportioned and shaped to avoid sharp corners. All corners should be rounded to minimize notch effects. Grinding parallel to the flange prevents grind marks perpendicular to the loading direction, which may behave as stress raisers. Finished cuts should have a final surface roughness of about 13 μm; any discontinuities, particularly nicks and gouges, should be avoided.

Tapered cuts allow uniform spreading of plasticity because they match the gradient of bending moments; nevertheless, the performance is sensitive to fabrication details. By contrast, radius cuts lead to yielding with variable pattern within the reduced section, but their dissipation capacity is more stable; therefore, they have been widely used for seismic retrofitting of steel beams.

Moreover, the reduction of beam flange (*flange removal* given as $(2 \cdot c/b_f) \cdot 100$) should be of 35 to 45%; moments at the face of the column and hence, stresses on welds, if any, should be 80-100% of the expected bending capacity of framing beams. It is worth mentioning that both welded and bolted webs provided satisfactory seismic performance; therefore, the design solution depends solely upon the economy (Plumier, 2000).

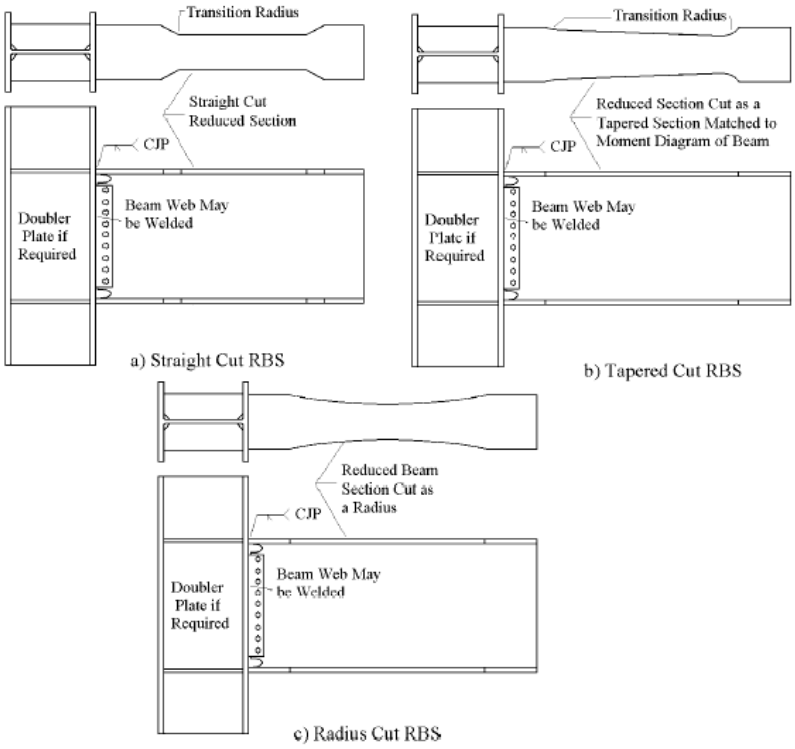

Figure 3.17. Common RBS configurations: straight cut (*a*), tapered cut (*b*) and radius cut (*c*) RBSs (*after* FEMA 355D, 2000).

RBSs used for beam-to-column connections lead to yield mechanisms and failure modes as shown in Figure 3.18. Significant flexural yielding affects the beam reduced section and the panel zone, thus leading to high plastic rotations. By contrast, limited yielding occurs in the beam outside the reduced zone; the contribution to the rotation is negligible. Failure modes provided in Figure 3.18 show that hinging at reduced sections may be prone to flange buckling. However, straight, tapered or radius cuts have very compact flanges in the weakened zone; hence, they do not suffer flange buckling. Nevertheless, numerical studies carried out in the US showed that web slenderness is a critical parameter in designing RBSs because it erodes the rotational capacity of the beam (FEMA 355D, 2000). As a result, a more stringent limit to control web buckling was recommended for beams with reduced sections; the reduction is about 25%, $1106/\sqrt{f_y}$ *vs.* $1376/\sqrt{f_y}$, with f_y in MPa.

The interaction formula given in Section 3.2 (Equation (3.7)) should account for this reduction of the web slenderness; shorter flanges restraint less the local buckling of the web. The recommended interaction formula for RBSs is provided herein in the section dealing with the design procedure.

On the other hand, the sensitivity to LTB is significantly increased for RBSs, thus lateral bracing of beam flanges should be required near the reduced section. It is worth mentioning that lateral support is generally required for both flanges of beams at any plastic hinge location (AISC, 1997). If the plastic hinge is located at the column face the support is provided by the column flange and/or connection. However, in RBSs the plastic hinge is shifted away from the column face hence, the LTB restraint is not guaranteed. As a consequence, US recommendations require that both flanges of beam should be laterally supported directly or indirectly and the allowable unsupported length is as in Equation (3.15). Any lateral support adjacent to RBSs should possess design strength ($F_{d,ls}$) similar to lateral support of links in eccentric brace frames given as follows:

$$F_{d,ls} = 0.06 \cdot R \cdot f_y \cdot b_f \cdot t_f \tag{3.16}$$

where R is the actual-to-nominal yield strength, defined in Section 3.1. Therefore, end supports should have 6% of the expected nominal strength of the reduced flange of the beam.

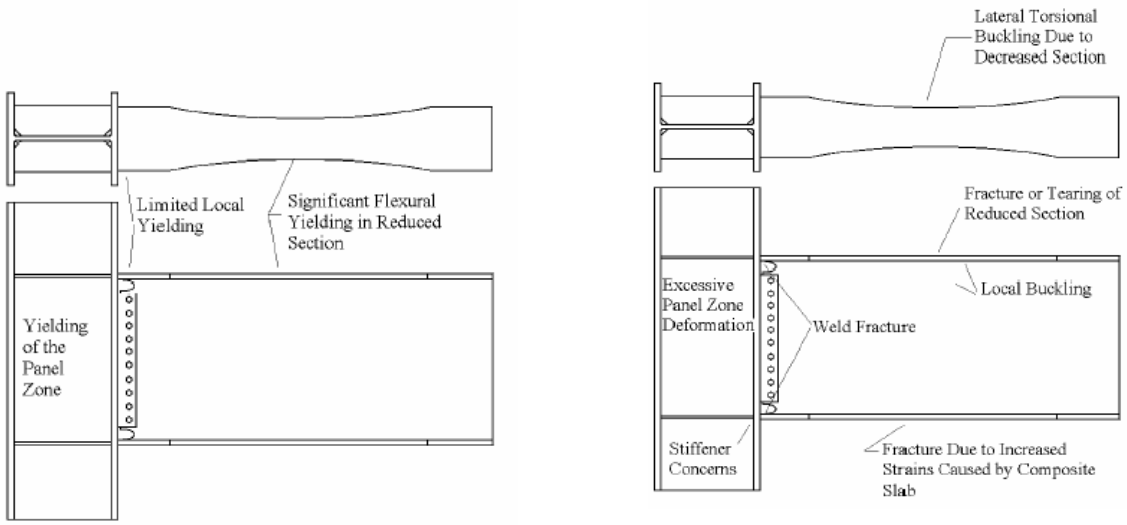

Figure 3.18. Radius cut RBSs: yield mechanism (*left*) and failure modes (*right*) (*after* FEMA 355D, 2000).

Nevertheless, lateral supports are usually expensive and research has recently shown that attachment to yielding flanges may cause local fracture. Moreover, experimental tests performed at University of San Diego in California within the SAC Steel Project showed that lateral bracings lower the rate of deterioration of the resistance at increased plastic rotations (FEMA 355D, 2000). Further analytical studies aimed at investigating the local buckling, LTB and the axial restraint in RBSs found that the inelastic behavior is marginally influenced by the unsupported length and the axial restraint mitigates the post-buckling inelastic degradation. However, either composite metal deck and concrete or solid concrete slabs are used in real framed structures; hence, they provide adequate axial restraints to the beam. Consequently, composite slabs reduce the sensitivity to LTB in RBSs, especially within the range of drifts considered for common LSs, e.g., 1.5% and 3.0%. Therefore, the lateral support at the reduced sections is not necessarily required to assure adequate performance in retrofitting of steel and/or composite buildings.

Moreover, the presence of composite slabs may reduce the effectiveness of RBSs, particularly when the top flange is compressed. Experimental tests showed that to minimize such effects, shear studs should not be included in the region of reduced flange (Plumier, 2000). For RBS beam-to-column connections, welded studs should not be placed in the area of the beam flange between the column and 150 mm beyond the extreme end of the RBS. Moreover gaps of about 30 mm between the slab and the column are recommended to minimize the influence of the slab at the column face.

The strength of RBSs should be designed with respect to the reduced or complete section as appropriate. However, plastic resistance of the reduced section should not be less than 70% of the capacity of a full section. The flange cuts reduce also the section stiffness; this effect marginally influences the lateral stiffness of framed buildings. Analytical tests showed that drifts increase less than 5% to 7% when RBSs are employed (FEMA 355D, 2000); thus, there is no need to increase the beam depth to control the frame lateral deformability.

The design of RBS beams can be carried out through the procedure outlined hereafter:

1. Compute the length and position of the flange reduction by defining *a* and *b* (Figure 3.19) as follows:

$$a = 0.60 \cdot b_f \tag{3.17.1}$$

$$b = 0.75 \cdot d_b \tag{3.17.2}$$

where b_f and d_b are the flange width and beam depth, respectively. The recommended value of a ensures that stresses spread uniformly throughout the flange in the reduced section of the beam before reaching the column flange. On the other hand, *b* is large enough to avoid excessive inelastic strains within the reduced section.

2. Compute the distance of the plastic hinge formation (s) from the beam edge given by:

$$s = a + \frac{b}{2} \tag{3.18}$$

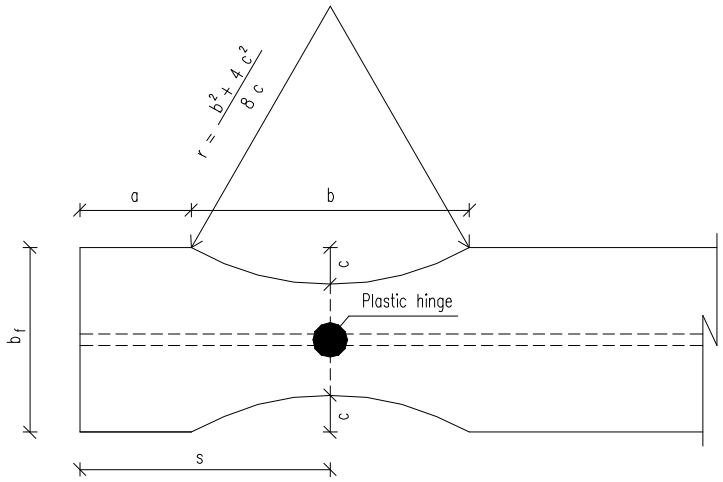

Figure 3.19. Geometry of radius cut for RBS.

3. Compute the depth of the flange cut (c). The c-value controls the maximum moment developed within the RBS and hence, influences the maximum moment and shear at the column flange. It should be not greater than $0.25 \cdot b_f$. However, as a first trial, assume that:

$$c = 0.20 \cdot b_f \tag{3.19}$$

This value corresponds to 40% flange removal; hence, it is in agreement with results of experimental work (Englehardt, *et al.*, 1998; Plumier, 2000).

4. Compute the plastic module (Z_{RBS}) and hence, the plastic module ($M_{pl,RBS}$) of the RBS:

$$M_{pl,RBS} = Z_{RBS} \cdot f_y \tag{3.20}$$

The plastic module of the RBS is $Z_{RBS} = Z_b - 2 \cdot c \cdot t_f \cdot (d_b - t_f)$; where Z_b is the plastic module of the beam.

5. Compute the plastic shear (V_{pl}) in the section of plastic hinge formation via the free body equilibrium of the beam part (L`) between hinges (Figure 3.20):

$$V_{pl} = \frac{2 \cdot M_{pl,RBS}}{L'} + \frac{w \cdot L'}{2} \tag{3.21}$$

where *w* is the uniform beam gravity loads. Additional point loads along the beam span, if any, should be however accounted for.

6. Compute the beam expected plastic moment ($M_{pl,be}$) as follows:

$$M_{pl,be} = \left(\frac{f_{te} + f_{ye}}{2 \cdot f_{ye}} \right) \cdot Z_b \cdot f_{ye} \tag{3.22}$$

where f_{te} and f_{ye} are the tensile and yield expected strengths, respectively.

7. Check that the bending moment M_f is less than $M_{pl,be}$; otherwise, increase the cut-depth *c* and repeat steps (4) to (6). In fact, c should be chosen such that the maximum moment at the column flange is about 85% to 100% of the beam expected plastic moment.

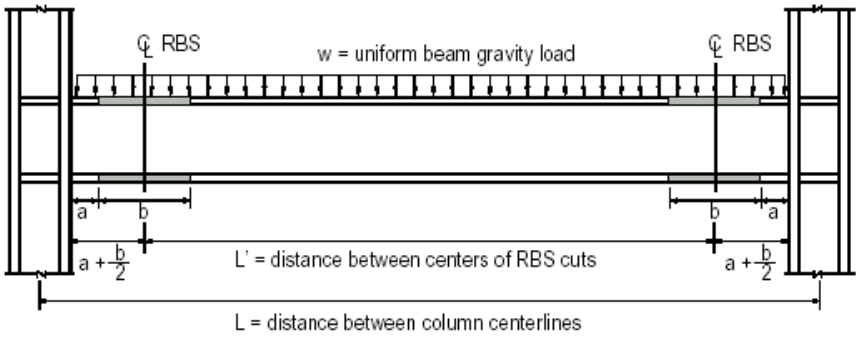

Figure 3.20. - Typical sub-frame assembly with RBS.

8. Check width-to-thickness ratios to prevent local buckling. The interaction formula given in Section 3.2 (Equation (3.7)) can be used; however, it should account for the likelihood of web buckling in RBS. A decrease of about 25% is deemed necessary for the web slenderness; therefore, the following should be employed:

$$\frac{\left(\frac{b}{t_f}\right)^2}{\left(\frac{E}{1.6 \cdot f_{fy}}\right) \cdot \left(\frac{1}{s} - 0.6003\right)} + \frac{1.25 \cdot \left(\frac{d_e}{t_w}\right)^2}{\left(\frac{E}{0.1535 \cdot f_{wy}}\right) \cdot \left(\frac{1}{s} - 0.6003\right)} \leq 1 \tag{3.23}$$

The flange width should be measured at the ends of the centre of two-thirds of the reduced section of the beam, unless gravity loads are large enough to shift the hinge point significantly from the centre point of the reduced section.

9. Compute the radius (r) of cuts in both top and bottom flanges over the length *b* of the beam:

$$r = \frac{b^2 + 4 \cdot c^2}{8 \cdot c} \tag{3.24}$$

10. Check that the fabrication process ensures adequate surface roughness, i.e., 13 μm; for the finished cuts and grind marks are not present.

Plastic rotations of RBSs designed according to the above procedure are satisfactory for seismic design and retrofitting. Regression analyses of experimental tests carried out at the University of Texas A&M show that mean plastic rotations of beam-to-column sub-assemblages with RBS beams are as follows:

$$q_{pl,b,e} = 0.05 - 0.0076 \cdot d_b \tag{3.25}$$

with the rotations in radians and the beam depth (d_b) in mm. The values derived from Equation (3.25) are much higher than the recommended rotation for steel framed structures, i.e., 0.03 radians (FEMA 352, 2000). It is worthwhile noting that the beam depth marginally influences the plastic rotations of RBSs.

3.3.3. COLUMNS

The retrofitting of steel columns should avoid axial and/or flexural yielding and buckling, either local or global, i.e., LTB. These failure detrimentally affect the global performance of framed building structures. Buckling of columns should be avoided because of their primary importance in load-bearing capacity. High axial loads are induced in columns under large lateral displacements, hence, adequate member slenderness should be employed. LTB of columns should be prevented, particularly in braced frames where bracings transmit high axial force to beam-columns. However, columns adequately designed significantly enhance the global ductility. Analytical studies showed that columns carry as much as 40% of the story shear in concentric braced frames after buckling and yielding of braces, provided their design prevent buckling (Galambos, 1998).

Rectangular or square hollow sections (RHSs or SHSs) may be a viable solution to prevent LTB; they also provide high strength and ductility. Concrete-filled steel tubular structures are very common in Japan where hollow sections are used for their high bending resistance (Morino, 1998). RHSs and SHSs are also generally used as formwork for concrete filled columns to lower the construction costs. Nevertheless, more stringent width-to-thickness slenderness ratios for the wall thickness are required (AISC, 1997). Reductions between 60% and 70% with respect to nonseismic design are recommended for round hollow sections ($9100/f_y$ *vs.* $14490/f_y$ with f_y in N/mm^2) and RHSs ($291/\sqrt{f_y}$ *vs.* $503/\sqrt{f_y}$ with f_y in N/mm^2) in axial compression or flexure (AISC, 1993). Such reductions are due to the lack of information available on the inelastic seismic performance of columns with hollow sections, either bare steel or composite. They do not apply, though, to circular pipes (Boyd *et al*., 1995; Schneider, 1998). A reduction of 20% of slenderness ratios derived from the interaction formula for hollow sections is recommended (Kato, 1989). This guideline accounts for the performance of several concrete filled buildings in Japan during the 1995 Hyogoken-Nanbu earthquake (Nakashima *et al*., 1998). RHSs and SHSs with width of 400-900 mm and width-to-thickness ratios of 10-54 are common in Japan for buildings for regular layout, while circular tubes (diameter of 450-1000 mm and diameter-to-thickness ratios of 17-65) are generally used for irregular buildings. Moreover, steel tubes may be assumed to act both as load-carrying element and a confining element for concrete. This rule is based on the Japanese design practice (Morino, 1998); in the US, hollow sections are generally used only as a confining element (Roeder, 1998).

It is worth noting that column LTB at the location of the beam top flange is generally prevented by the composite slab. On the other hand, perpendicular beams and/or ad hoc stiffeners at beam bottom flanges may be assumed to provide lateral support. This solution is efficient for shallow columns with wide flanges (FEMA 350, 2000). However, deeper columns are more prone to LTB and hence, require adequate support. The following limitation may be used to establish whether or not lateral bracing of column flange is required at beam-to-column connections (FEMA 350, 2000):

$$\frac{\sum \overline{M_i^c}}{M_c} \geq 2.0 \tag{3.26}$$

where $\sum \overline{M_i^c}$ is the sum of the moment capacities of columns above and below the joint, at the intersection of the beam and column centerlines. These moments are evaluated by referring to nominal flexural strength $f_{yc,nom}$ and accounting for a reduction for the axial load in the column; thus they should be computed as follows:

$$\sum \overline{M_i^c} = \sum \left[Z_c \cdot \left(f_{yc,nom} - \frac{P_c}{A_c} \right) \right]_i \tag{3.27}$$

where Z_c is the plastic modulus of the column section, evaluated on the basis of actual geometrical properties, if available, rather than from standard tables. The plastic modulus should account for haunches, if any. P_c and A_c are the axial load and the area of the column section, respectively.

On the other hand, M_c is the bending moment in the critical section at column centerline:

$$M_c = M_{pr} + V_p \cdot \left(x + \frac{d_c}{2} \right) \tag{3.28}$$

where M_{pr} and V_p are the beam plastic moment and the shear at the plastic hinge, respectively (Figure 3.21); and *x* is the distance between the plastic hinge and the column face.

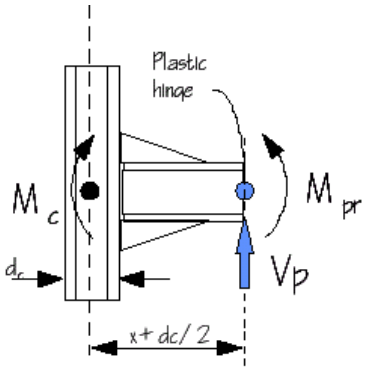

Figure 3.21. Moment in the critical section at column centerline.

Therefore, the assumed position of plastic hinges influences column LTB; examples of hinge locations in typical reinforced beam-to-column connections are provided (FEMA 355D, 2000) in Figure 3.22.

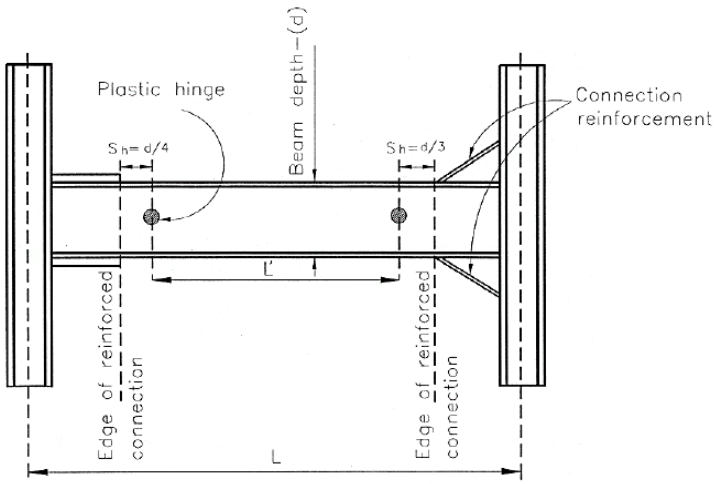

Figure 3.22. Typical plastic hinge locations for reinforced connections.

However, the use of deep columns, i.e., beam-type, should be avoided for retrofitting of existing buildings. Indeed, recent studies showed that deeper column sections, i.e., W24 vs. W14, behave poorly and may fail through the development of fracture between the column web and flange, i.e.,

k-area (FEMA 350, 2000). Columns in European practice may consist of built-up members (Mele, 2002). It is recommended to check the load transfer mechanism between each plate by welding, bolting or riveting; it significantly influences both strength and stiffness.

To splice columns, groove welds (GWs) should be used; in fact, it was found that partial penetration groove welds in column splices fail in a brittle manner (Bruneau and Mahin, 1990). By contrast, the US guidelines allow the use of either fillet welds or partial-joint-penetration grove welds (PJPGWs) (AISC, 1997). Though, to reduce the effect of flexure it is required that they shall not be placed within 1.20m (4.0ft) or one-half the column clear height of beam-to-column connections, whichever is greater. Moreover, PJPGWs should be designed to resist 200% of the strength by elastic analysis using code-compliant forces (*capacity design*). Therefore, it is considered safer, economical and simpler to recommend GWs rather than PJPGWs. Moreover, net tension forces should be avoided in the welds because they may cause brittle fracture. To minimize the effects of flexure in ordinary steel buildings, it is advised to locate splices in the middle third of the column clear height. Such splices should be designed to develop nominal strength not less than expected shear strength of the smaller connected member and 50% of the expected flexural strength of the smaller connected section. These recommendations comply with the US requirements for special concentric braced frames which are more stringent than those for special moment resisting frames with regard to columns (AISC, 1997). It is instructive to note that nominal strengths are computed on the basis of steel nominal yield strengths as provided in the code of practice, e.g., 235, 275 or 355 N/mm^2, while expected values should employ the over-strength factor *R*, as given in Section 3.1 (EC3, 1992). Thus, e.g., each flange of welded column splices should satisfy the following:

$$A_{pl} \cdot f_{y,pl} \geq 0.50 \cdot R \cdot f_{y,fl} \cdot A_{fl} \tag{3.29}$$

where A_{pl} and $f_{y,\,pl}$ are the area and the nominal yield strength of each flange; and the second member of Equation (3.29) represents the expected yield strength of the column material. A_{fl} is the flange area of the smaller column connected.

On the other hand, moment resisting frames designed according to capacity design should exhibit strong column weak beam (SCWB) response. This requirement is provided in European standards for either steel or composite framed buildings (EC8, 1998); for beam-to-column connections the minimum column-beam moment ratio (CBMR) is given as follows:

$$CBMR = \frac{\sum M_i^c}{\sum M_j^b} \geq 1.20 \tag{3.30}$$

where $\sum M_i^c$ is the sum of the moment capacities of columns above and below the joint; and $\sum M_j^b$ is the sum of the moment capacities of the beams framing in the columns.

It is recommended to replace the expression of CBMRs given in Equation (3.30) with the following:

$$CBMR = \frac{\sum \overline{M_i^c}}{\sum \overline{M_j^b}} \geq 1.50 \tag{3.31}$$

where $\sum \overline{M_i^c}$ is defined in Equation (3.27), while $\sum \overline{M_i^b}$ is the sum of expected flexural strengths at plastic hinge locations to the column centerline. It can be approximated as follows:

$$\sum \overline{M_i^b} = \sum \left[Z_b \cdot f_{yb,e} + M_v \right]_i \tag{3.32}$$

in which Z_b is the plastic modulus of the beam section at the potential plastic hinge location; it should be computed on the basis of the actual geometry. For beam-to-column connections with RBSs, the minimum plastic section modulus Z can be used in Equation (3.32). $f_{yb,e}$ is the expected yield strength of the beams; it is conservative to use values of yielding referred to flanges rather than webs. The quantity M_v accounts for the additional moment at the column centerline due to the eccentricity of shear at the plastic hinge within the beam. The formulation in Equation (3.30) is more general and complete than the European counterpart (EC8, 1998); it accounts for beam-to-column connections in which plastic hinges are shifted away from the column face into the beam. The detrimental effect of axial loads within columns is also included. Moreover, the allowable value assumed in Equation (18) for CBMRs has been chosen on the basis of the results of recent studies, which showed that plastic hinges in columns cannot be prevented by simply satisfying the requirement CBMR≥1.20 (Nakashima and Sawaizumi, 2000); but minimum CBMR values depend significantly upon: (i) specific ground motion and (ii) importance of higher vibration modes of vibrations exhibited by the structure. As rule of thumb, CBMRs ranging from 1.5 to 2.0 are required to ensure elastic response of column members; however, 1.5 was assumed in Equation (3.31).

Moreover, slender column panel zones are prone to buckle. Web buckling is significantly influenced by continuity plates generally placed at the same distance of beam flanges (Stojadinovic *et al.*, 2000). Their use is strongly recommended within beam-to-column connections of existing (FEMA 350, 2000) and new (FEMA 352, 2000) buildings because they act as a boundary to the panel zone where high stresses are concentrated. They consist of steel plates welded, preferably via full penetration welds to column webs; symmetric arrangements, i.e., on both side of the web, are advised. The thickness of continuity plates should be equal to that of beam flanges; the use of very thick continuity plates may give rise to large residual stresses, thus compromising the performance of the column panel zone. However, provided continuity plates exist, the thickness (t) of the column web should comply with the following empirical equation to prevent premature local buckling under large inelastic shear deformations:

$$t \le \frac{d_z + w_z}{90} \tag{3.33}$$

where d_z and w_z are the panel-zone depth between continuity plates and panel-zone width between column flanges, respectively. Whenever the above limit is not fulfilled, panel-zone doubler plates welded to column flanges (Figure 3.23) may be used. Such plates may be either placed against the column web or placed away from it; in the latter case, symmetrical pairs arrangement of plates are recommended by the US provisions (AISC, 1997). The welds should be either complete penetration groove or fillet, depending on the detail used for the doubler plate (Figure 3.23). As a result, the thickness t to use in Equation (3.33) may be assumed as the sum of the column web thickness and the doubler plate thickness. However, plug welds between web and added plate are required. If pair of equal thickness web doubler plates are employed, then Equation (3.33) should be satisfied independently by the column web and doubler plate.

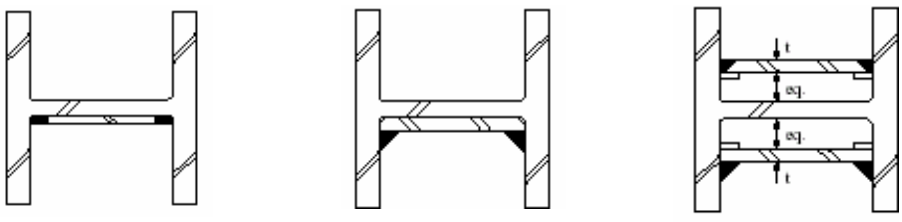

Figure 3.23. Typical web doubler plates: single plate with groove (*left*) or fillet (*middle*) welds and pair of equal thickness plates with groove or fillet welds (*right*).

Surveys carried out in the aftermath of recent earthquakes showed that old partially and/or fully restrained frames may exhibit low lateral stiffness (AIJ, 1995; Youssef *et al*., 1995). Hence, to limit structural and non-structural damage, story drifts may be reduced by encasing columns in concrete. Full encasement is recommended, thus fire-protection is guaranteed. The solution will also increase the global stability of the frame, thus reducing sensitivity to P-Δ effects. Details should conform to the design of columns in new composite steel and concrete buildings (EC8, 1998). However, two transverse ties welded to the flanges may be used to prevent the onset of local buckling (see Section 3.2); their spacing should conform to the rules for transverse steel reinforcement. Maximum hoop spacing of about $7.0 \cdot d_{bl}$ (d_b is the minimum diameter of longitudinal reinforcement bars) may be assumed. Experimental tests carried out on a series of eight, two-thirds scale tests showed that such spacing allows rotation ductility not less than 6.0 (Ricles and Paboojian, 1994). Examples of close hoops for encased columns are provided in Figure 3.24. To achieve effective composite action, shear stresses should be transferred between the encased steel and reinforced concrete; hence, shear connectors may be placed along the column (Figure 3.24). Generally they are placed arbitrarily along the column. However, shear connectors are expensive and they may jeopardize the encasement of structural profile with concrete. Moreover, experimental tests showed that shear connectors are not necessarily needed for good column performance (Roeder, 1998). Therefore, the use of shear studs is not compulsory.

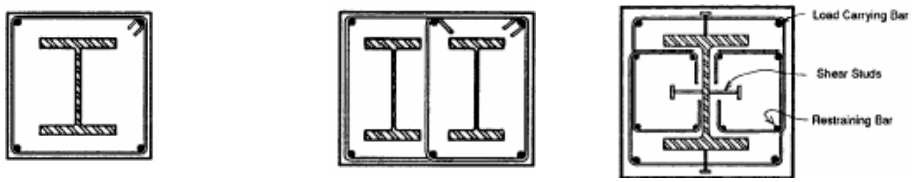

Figure 3.24. Typical close hoop details for encased composite columns: single (*left*) or double (*middle*) structural steel components and with shear studs (*right*).

The shear strength of composite columns should avoid shear bond failure, which results (Figure 3.25) in cracks along the interface of steel flanges and concrete. Bond failure is critical when the steel flange width is large and approaching the overall width of the composite section. Alternatively, the other shear failure mode is the diagonal shear failure, which is similar to the shear failure of ordinary RC members. Recent experimental and numerical tests showed to prevent shear bond failure, the steel flange ratio (b_f/B) should be less than that *critical steel flange ratio* defined as follows (Weng *et al*., 2001):

$$\left(\frac{b_f}{B}\right)_{cr} = 1 - 0.35 \cdot \left[0.17 \cdot \left(1 + 0.073 \cdot \frac{N_d}{A_g}\right) \cdot \sqrt{f_c} + 0.20 \cdot r_w \cdot f_{yh}\right] \qquad (3.34)$$

where N_d is the design axial; A_g the gross area of the section; f_c is the concrete compressive strength; ρ_w and f_{yh} are the ratio and yield strength of transverse reinforcement, respectively; B is the width of the composite section; and b_f is the flange width.

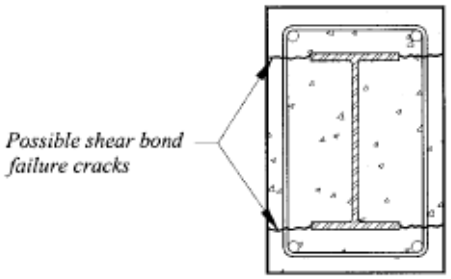

Figure 3.25. Shear bond failure for composite columns.

Common structural deficiencies of beam-columns are provided in Table 3.8 along with the suggested retrofitting strategies. The design of the added plates or details for RC encasement should be carried out in compliance with codes of practice for new buildings for permanent (EC2, 1992; EC3, 1992; EC4, 1994) and seismic (EC8, 1998) loads. Remedies for combined deficiencies, e.g., axial and flexural capacity or flexural and shear capacity, may employ a combination of the strategies outlined in Table 3.8. However, such retrofitting strategies are aimed at enhancing the strength of columns. Notwithstanding, they are also effective as rehabilitation measures for deformation deficiencies, i.e., to increase column stiffness; though, the effectiveness is dependant on the intervention used. For example, minor stiffening is achieved by means of additional welding, replacement of rivets/bolts and addition of continuity plates. By contrast, composite action is the most effective to increase the lateral stiffness of steel columns and reduce the axial deformations (Roeder, 1998). Nevertheless, in some cases RC encasement may cause potential undesirable failure modes; thus, its removal or modification of details should be considered. In addition, abrupt changes in stiffness and strength should be avoided in the composite-to-RC transition zones. In fact, extensive damage was, in fact, observed in Japan at the connection of encased columns and concrete columns and/or concrete foundations (Azizinamini and Ghosh, 1996).

Table 3.8. Retrofitting strategies for steel beam-columns in framed structures.

	Deficiency			
	Axial Capacity	Flexural Capacity	Shear Capacity	Stability
Retrofitting Strategy	• Add steel plates parallel to flanges or the web. • Add steel plates parallel to the wall thickness. • Encase bare steel column in RC and use welded transverse stiffening bars between flanges. • Reduce the level of axial load to one-third of the squash load.	• Add steel plates to the flanges or the wall thickness. • Encase bare steel column in RC with adequate longitudinal reinforcement bars.	• Add steel plates parallel to the web. • Encase bare steel column in RC. • Provide additional transverse reinforcement of RC encasement.	• Reduce flange and/or web slenderness ratios adding steel plates. • Reduce wall slenderness by adding external plates. • Reduce flange and/or web slenderness ratios via RC encasement with welded transverse stiffening bars between flanges. • Provide lateral support for both flanges.

Finally, ad hoc repairing strategies should used for localized damage of columns, namely buckled flanges, flange fractures and splice fractures. Two strategies are available to repair buckled flanges: removal and replacement of the buckled plate (Figure 3.26) or flame straightening. The latter is

generally more effective, but requires skilled workmanship and hence, may be uneconomical (Avent *et al*., 2001). By contrast, the removal and replacement of buckled plates with steel grades of similar mechanical properties is simpler to perform, even though shoring is necessary.

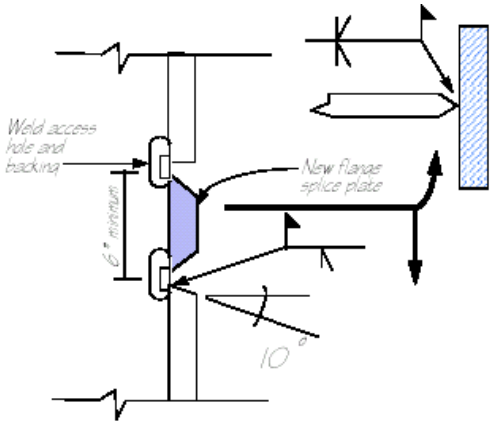

Figure 3.26. Column flange repair.

On the other hand, splice fractures may be repaired either with the addition of external plates on the column flanges or by removing and replacing the damaged part with sound material. CJPGWs should be used to connect the added plates because their performance is superior to partial joint penetration groove welds (FEMA 350, 2000). Alternatively, if the column section may withstand the loads without the damaged flange, the latter should be removed and replaced; shoring is though required. The thickness of added plates should be equal to the existing ones and the replacement material should be aligned with the rolling direction matching that of the column. Repairing of column fractures is generally more complex due to the necessity of having temporary shoring and removal of existing beam sections for access. Moreover, thermal treatments should be carried out with thorough inspection because cracks propagate faster as the temperature rises. However, drilling small holes at the edge of the crack may prevent the propagation. Magnetic particle or liquid dye penetrant tests should be used to ascertain that within a circular neighbor of the cracks, with a radius of about 150 mm, that there are no defects and/or discontinuities.

3.3.4. BRACES

Steel and/or composite braces are effective structural elements to resist lateral forces induced by either wind or earthquake loadings (Bruneau *et al*., 1997). However, during severe ground motions, bracings experience large cyclic excursions in tension and compression. Diagonal braces may sustain plastic deformations and dissipate energy through successive cycles of yielding and buckling. Energy absorption by tension yielding of braces though, is more reliable than buckling. Such response allows the structure to survive strong earthquakes without losing gravity loads (Tremblay *et al*., 1995); in fact, the failure of braces (*dissipative zones*) prevents the yielding of beams, columns and connections (non*dissipative zones*). However, the energy absorption capability of compressed braces depends on their slenderness ratios, i.e., (L/r), and the resistance to local buckling during repeated cycles of inelastic deformations (Tremblay *et al*., 1996). It is instructive to note that L is the member unsupported length and r is the radius of inertia. Clearly, to maximize the slenderness ratio one should refer to the minimum radius of inertia. The unsupported length is expressed as KL in the US design practice. For example, Figure 3.27 shows the cyclic behavior of typical braces as a function of the member slenderness. The higher the slenderness, generally the lower is the energy dissipation. Nevertheless, analytical and experimental work

showed that the post-buckling cyclic fracture life of braces decreases with an increase in slenderness ratio (Tang and Goel, 1989). As a result, the seismic retrofitting of steel and/or composite braces should employ adimensionalized slendernesses $\overline{l}$ higher than the value (1.5) provided for new buildings (EC8, 1998). An upper bound though, is deemed necessary to avoid excessive L/r. Therefore, it is recommended that slenderness ratios should comply with the limitation $1.5 \leq \overline{l} \leq 1.8$.

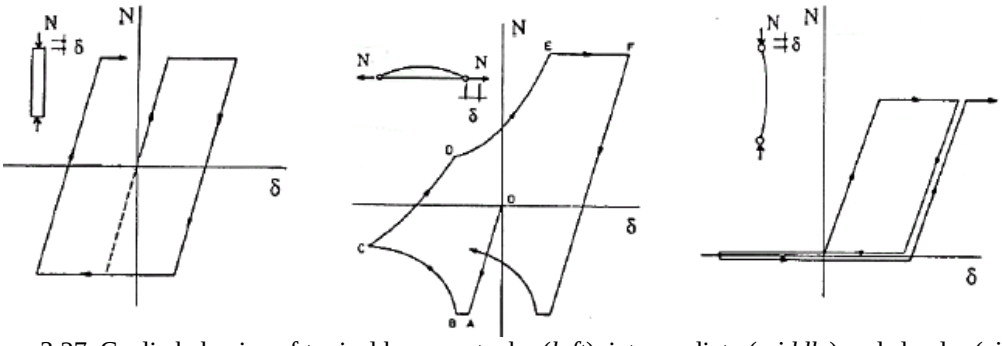

Figure 3.27. Cyclic behavior of typical braces: stocky (*left*), intermediate (*middle*) and slender (*right*).

It is worth noting that the US guidelines for seismic design recognize that the slenderness (KL/r) has a major effect on the ability of a brace to dissipate hysteretic energy (AISC, 1997). Indeed, for special concentric braced frames (SCBFs), i.e., structural systems with significant inelastic deformation capacity, threshold values for KL/r are less stringent than those for ordinary concentric braced frames (OCBFs), i.e., frames with limited inelastic deformations. In such a case, a relaxation of about 40% is allowed for KL/r, $K \cdot L/r \leq 2646/\sqrt{f_y}$ (OCBFs) *vs.* $K \cdot L/r \leq 1905/\sqrt{f_y}$ (SCBFs). Unsupported lengths computed on the basis of American guidelines are provided in Figure 3.28 for typical European structural steel grades, namely S235, S275 and S355; the L/r for unbraced columns in special moment resisting frames is also included for comparisons. It may be noted that slendernesses higher than 150 are allowed for S235 and S275; these steel grades are more suitable than S355 for braces due to lower yield strength.

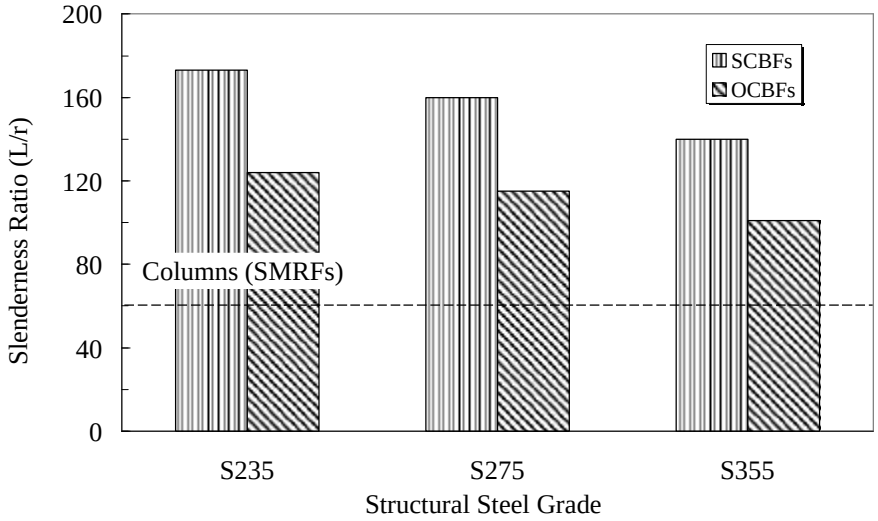

Figure 3.28. Slenderness ratios for braces in ordinary and special braced frames (OCBFs and SCBFs).

On the other hand, extensive analytical and experimental work showed that to improve the seismic performance of braces, particularly for CBFs, it is of paramount importance to limit width-thickness ratios, thus minimizing local buckling (Aslani and Goel, 1991; Goel, 1992a). Consequently, the

limitations provided in Section 3.2.2 for compressed members should be checked; this requirement also applies to the unstiffened walls of hollow sections (HSs). An effective rehabilitation measure for HSs is to fill the bare steel brace with reinforced concrete. Such repairing strategy will enhance both the strength and the stiffness, local and global, of the brace. However, it may be not straightforward to cast concrete within the HS and hence, it may be required to dismount the brace from the frame. This operation may be time-consuming and in certain circumstances, e.g., in braces with welded connections, either complex or prohibitive. Partial or full RC encasements of steel braces are viable solutions for I and H-sections; transverse stiffeners welded between flanges, as for columns (Section 3.3.3) should be placed to restraint their buckling. Moreover, transverse confinement of RC should be spread uniformly along the brace because high rotations are expected at the edges and in the middle. Detailing for stirrups should comply with relevant standards (EC2, 1992; EC4, 1994, EC8, 1998); details for medium ductility should be fulfilled in order to limit excessive over-strength of the brace. The capacity design checks for CBFs or EBFs should be based on expected rather than nominal resistances and should adequately account the overstrength of the brace due to the material and/or composite action, if any (EC8, 1998). Similarly, the real resistance of beams, columns and connections should be thoroughly assessed in order to control the failure modes. It is advised that composite braces in tension should be designed on the basis of the steel section alone.

Stringent compactness criteria may also enhance the post-buckling response and hence, energy dissipation of double-angle and double-channel braces. Toe-to-toe configurations of double angles should be preferred because they generally minimize bending strains and local buckling. Furthermore, it was found that close spacing of stitches is effective to improve the post-buckling response of braces, particularly for double-angle and double-channel braces (Aslani and Goel, 1991). The buckling of such members imposes large shear forces on the stitches. Thus, if stitch plates are already in place, it is recommended to add more plates and/or strengthen existing stitch connections. Welded stitches are recommended; bolted ones may in fact cause premature fractures due to the formation of plastic hinges in the post-buckling range (Aslani and Goel, 1991).

Damage to braces is generally concentrated on their connections with adjoining beams and or columns (Nakashima *et al.*, 1998); retrofitting strategies for such types of damage are provided in the next section. Table 3.9 outlines common deficiencies for braces due to the resistance, e.g., low axial, flexural and shear capacity, and/or stability, either local or global. Retrofitting strategies are proposed for each case; some are similar to beam-column counterparts therefore, the observations on the enhancement of strength and stiffness as in Section 3.3.3 should be considered.

Table 3.9. Retrofitting strategies for steel braces.

	Deficiency			
	Axial Capacity	Flexural Capacity	Shear Capacity	Stability
Retrofitting Strategy	• Add steel plates parallel to flanges or the web. • Add plates parallel to the wall thickness. • Reduce unsupported length through stiffeners. • Encase bare steel brace in RC and use welded transverse stiffening bars between flanges • Reduce the level of axial load to 0.80 of the squash load.	• Add steel plates to both flanges. • Encase bare steel brace in RC.	• Add steel plates parallel to the web. • Increase the wall thickness. • Encase bare steel brace in RC. • Provide additional transverse reinforcement of RC encasement.	• Reduce flange and/or web slenderness ratios adding steel plates. • Reduce flange and/or web slenderness ratios via RC encasement with welded transverse stiffening bars between flanges. • Increase stiffness of end connections. • Provide lateral support for both flanges.

The energy absorption characteristics of steel braces may be improved by using stiffened braces (Inoue *et al*., 2001). For example, a viable arrangement is the composite system comprising of unbounded steel flat-bar braces embedded in a pre-cast RC panel (Figure 3.29). The brace is coated with debonding material in order to reduce the bond stress between the steel component and the RC panel. The latter is used to inhibit the buckling of the steel brace and stabilize its cyclic behavior. Stiffening forces between the brace and the panel (stiffening member) are perpendicular to the longitudinal axis of the brace. As a result, the hysteretic response of composite systems is elasto-plastic, thus giving rise to high energy dissipation. However, such systems exhibit two typical failure modes:: (i) overall buckling of the stiffened brace and (ii) local failure at the edge of the panel. Thus, design rules have been formulated to prevent these types of collapse (Inoue *et al*., 2001). By solving the equilibrium equations for the panel and accounting for its stiffening effects, the following adimensionalized relationship is derived:

$$\left(1-\frac{1}{n_E^B}\right)\cdot m_y^B > \frac{a}{l} \tag{3.35}$$

where a and l are the initial imperfection and the length of the steel brace; and non-dimensional parameters m_y^B and n_E^B express the non-dimensional strength and stiffness of the RC panel. They are given as follows:

$$m_y^B = \frac{M_y^B}{N_y \cdot l} \tag{3.36.1}$$

$$n_E^B = \frac{N_E^B}{N_y} \tag{3.36.2}$$

where M_y^B is the yield moment of the stiffening panel while N_E^B and N_y are the Euler load of the panel and the yield strength of the brace, respectively. It is advised to model the RC panel as a flexural member with effective uniform cross section (B_{EF}) of five times the width (B_S) of the steel flat-bar brace, i.e., $B_{EF} = 5 \cdot B_S$ (Inoue *et al*., 2001). Thus, the yield moment is given by:

$$M_y^B = \frac{5 \cdot B_S \cdot T_C^2 \cdot f_t}{6} \tag{3.37.1}$$

where T_C is the thickness of the panel and f_t the tensile strength of the pre-cast concrete.

The Euler load of the panel is as follows:

$$N_E^B = \frac{5 \cdot p^2 \cdot B_S \cdot E_B \cdot T_C^3}{12 \cdot l^2} \tag{3.37.2}$$

where E_B is the elastic modulus of the RC panel.

Equation (3.35) implies that stiffness and strength combinations of the RC panel in the safe region (Figure 3.29) correspond to plastic axial deformations in the compressed brace without buckling. However, a safety factor should be used in Equation (3.35) to account for the expected strength of the brace; its overstrength due to the strain hardening and the nonlinearity of the panel. Moreover, initial imperfections (a) of the brace, expressed as a function of the length (l), affect the stiffening requirement. Therefore, a safety factor between 1.2 and 1.4 is recommended.

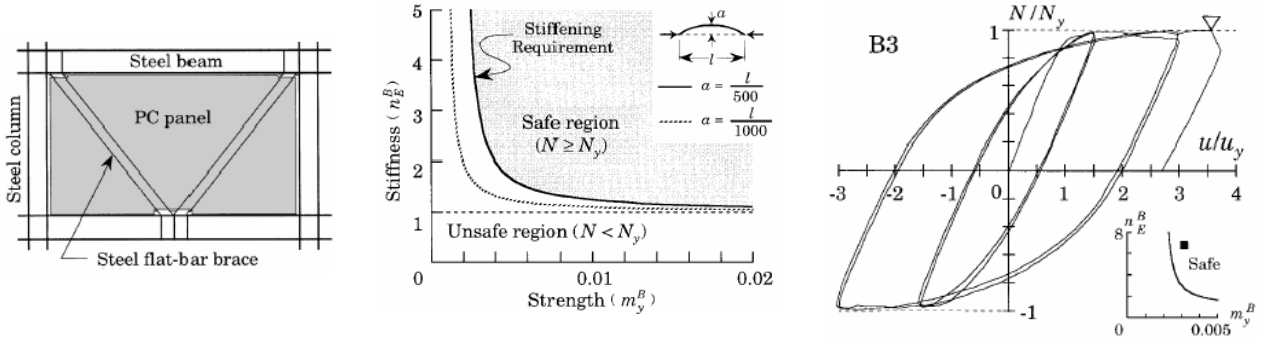

Figure 3.29. Composite system with RC pre-cast panel: layout (*left*), stiffness requirements (*middle*) and test response (*right*) (*after* Inoue *et al*., 2001).

It is worth mentioning that both ends of the brace are welded to the beam flanges, thus the edges of steel bars may be assumed fixed. By contrast, the panel edges are free. As a consequence, when the steel brace is loaded and tends to displace the panel out-of-plane, the latter reacts with forces concentrated at edges (Figure 3.30). These forces produce reactive moments restraining the rotations at panel edges. However, the intensity of stiffening forces is high, about 3-5% of the brace yield (N_y), hence, they give rise to punching shear.

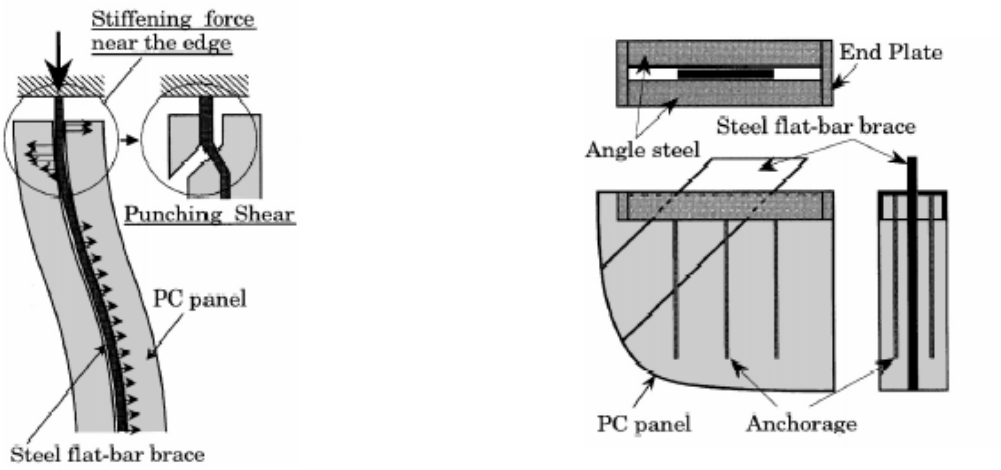

Figure 3.30. Edge of RC pre-cast panel: failure mode (*left*) and reinforcement (*right*).

Recent experimental tests (Inoue *et al*., 2001) have shown that edge reinforcement of the RC panel, adequately anchored (Figure 3.30), is effective to prevent the punching shear.

The use of stiffened braces, either in RC pre-cast walls or concrete-filled tube, e.g., unbounded braces (Figure 3.31), has become very common in Japan in the last decade (Watanabe *et al*., 1988). Advantages of this system are the elasto-plastic response and equal strengths in tension and compression; the brace is embedded (with unbounding material) and hence, is prevented from buckling.

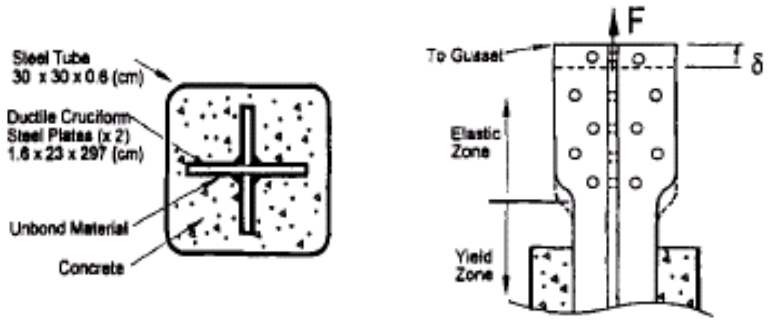

Figure 3.31. Unbounded brace: cross section (*left*) and end detail (*right*).

Design rules for unbounded braces are available in literature (Fu and Kasai, 1998; Kasai *et al*., 1998); they are generally based on simplified models, e.g., SDOFs; hence, equivalent periods and dampings are given as a function of the mechanical properties of frame, braces and added devices (dampers). For example, the equivalent stiffness (K_{eq}), period (T_{eq}) and damping (ξ_{eq}) for elasto-plastic dampers (EPDs) (e.g., unbounded braces) are as follows (Figure 3.32):

$$K_{eq} = \frac{1 + p \cdot (m_{eq} - 1)}{m_{eq} \cdot \left[\left(1 / K_s \right) + \left(1 / K_{fb} \right) \right]} \tag{3.38.1}$$

$$\frac{T_{eq}}{T_f} = \sqrt{\frac{K_f}{K_{eq}}} = \sqrt{\frac{p \cdot m_{eq}}{1 + p \cdot (m_{eq} - 1)}} \tag{3.38.2}$$

$$x_{eq} = x_f + \frac{2}{p \cdot p \cdot m_{eq}} \cdot \ln \left[1 + \frac{p \cdot (m_{eq} - 1)}{m_{eq}} \right] \tag{3.38.3}$$

in which the peak ductility demand μ_{eq} is:

$$m_{eq} = \frac{1 + \left(1 + \frac{K_{fs}}{K_{fb}} \right) \cdot \left(\frac{m_d - 1}{1 + K_d / K_b} \right)}{1 + K_s / K_{fb}} \tag{3.39.1}$$

and the post-yield-to-elastic stiffness ratio (p) of the SDOF is given by:

$$p = \frac{1 + K_{fs} / K_s}{1 + K_{fb} / K_{fs}} \tag{3.39.2}$$

with

$$K_s = K_{fs} + \frac{1}{\left(1/K_b\right) + \left(1/K_d\right)} \tag{3.39.3}$$

where T_f and ξ_f are the period and the damping of the frame (without dampers), respectively; and μ_d is the peak ductility demand of the damper; K_b and K_d are the stiffness of the brace and the damper; and K_f is the lateral stiffness of the DOF, expressed as a function of the shear K_{fs} and bending stiffness K_{fb}:

$$K_f = \frac{1}{\left(1/K_{fb}\right) + \left(1/K_{fs}\right)} \tag{3.40}$$

It is worth noting that the shear stiffness (K_{fs}) is provided by the flexural stiffness of beams and columns, while the bending stiffness (K_{fb}) depends upon the axial deformations of the columns.

Similarly, formulae for the equivalent stiffness (K_{eq}), period (T_{eq}) and damping (ξ_{eq}) for visco-elastic dampers (VEDs) are (Figure 3.32):

$$K_{eq} = \frac{1}{\left(1/K_{fb}\right) + \Gamma_s/K_s} \tag{3.41.1}$$

$$\frac{T_{eq}}{T_f} = \sqrt{\frac{K_f}{K_{eq}}} = \sqrt{\frac{1 + K_{fs} \cdot \Gamma_s / K_s}{1 + K_{fb}/K_{fs}}} \tag{3.41.2}$$

$$x_{eq} = x_f + \frac{h_s/2}{1 + \left(1 + h_d^2\right) \cdot \frac{K_s}{K_{fb}}} \tag{3.41.3}$$

with:

$$\Gamma_s = 1 + \frac{h_d^2}{\left[1 + \left(1 + h_d^2\right) \cdot \frac{K_d}{K_b}\right]^2 \left(1 + \frac{K_{fb}}{K_{fs}}\right) \cdot \left[1 + K_{fs} \cdot \left(\frac{1}{K_b} + \frac{1}{K_d} + \frac{h_d^2}{K_b + K_d}\right)\right]} \tag{3.42.1}$$

$$K_s = K_{fs} + \frac{1}{\frac{1}{K_d} + \frac{h_d^2}{K_b + K_d}} \tag{3.42.2}$$

$$h_s = \frac{h_d}{\left[1 + \left(1 + h_d^2\right) \cdot \frac{K_d}{K_b}\right]^2 \cdot \left[1 + K_{fs} \cdot \left(\frac{1}{K_d} + \frac{h_d^2}{K_b + K_d}\right)\right]} \tag{3.42.3}$$

The equivalent loss factor (η_{eq}) is given by:

$$h_{eq} = \frac{h_s}{1 + \left(1 + h_s^2\right) \cdot \frac{K_s}{K_{fb}}} \tag{3.43}$$

It is worth noting that large values of η_{eq} indicate high energy dissipation; thus, the damper loss factor η_d should be as high as possible (close to 1); the loss factor of the damper is the ratio of the peak viscous force to the peak elastic force of the damper.

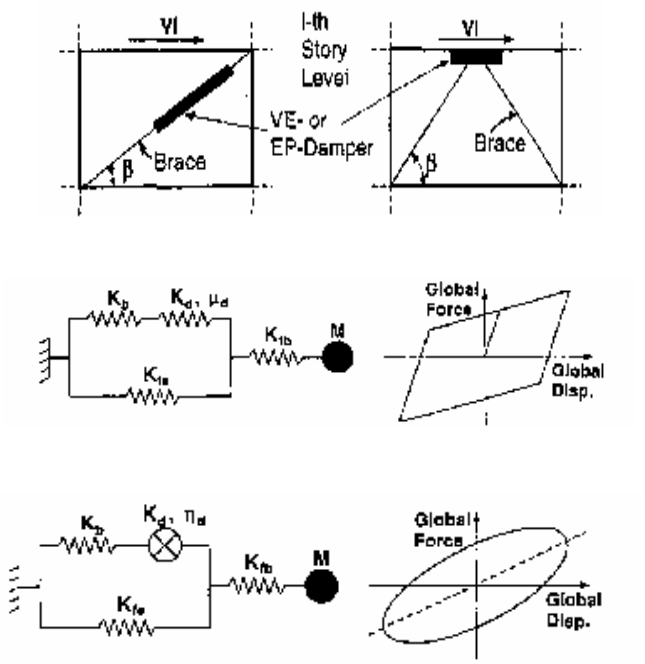

Figure 3.32. Braces with passive dampers: typical layout (*top*) model for EPDs (*middle*) and for VEDs (*bottom*).

Conversions from SDOFs to MDOFs have been suggested along with optimum values for the damper characteristics. By assuming negligible deformations in the columns and braces, the conversion rule from the required stiffness ratio K_d/K_{fs} in the SDOF to that at the *i-th* story of the MRF $K_{d,i}/K_{fs,i}$ is as follows:

$$\frac{1 + \frac{K_{d,i}}{K_{fs,i}}}{1 + \frac{K_d}{K_{fs}}} = \frac{\frac{V_i}{K_{fs,i}}}{\frac{\sum_{i=1}^{N} V_i}{\sum_{i=1}^{N} K_{fs,i}}} \tag{3.44}$$

where $K_{d,i}$ is the total stiffness of the dampers located at the *i-th* floor of the MDOF; $K_{fs,i}$ is the total shear stiffness at the same location; V_i denotes the corresponding total story shear; and N is the number of story.

Extensive analytical work on passive dampers showed that optimized EPDs or VEDs may have 0.4 to 0.5 times the roof story drift and 0.7 times the base shear of an original elastic frame (Kasai *et al*., 1998). Assuming equal dampers at each story, optimum damper stiffnesses (K_d) are one (VEDs) to three (EPDs) times the frame story shear stiffness. Dampers stiffer than optimum do not reduce the drift but increase the seismic forces. On the other hand, dampers less stiff than optimum are not

effective to limit the story drift. Recommended values for the loss factor (η_d) of VEDs should be close to 1.0; while the peak ductility demand (μ_d) for EPDs should range between 3.0 and 4.0.

The formulae in Equations (3.38) through (3.43) may be used to design dampers for seismic retrofitting of either steel or composite buildings. In fact, the analogy with SDOF systems and the conversion rules for MDOFs enable the designer to select appropriate EPDs or VEDs to reduce story drifts. The procedure as outlined below should be followed:

1. Compute the fundamental period (T_f) of the frame (MDOF) without dampers. Eigenvalue analysis is recommended and stiffening effects due to in-fills, if any, should be accounted for.
2. Estimate the damping of the frame ξ_f without dampers.
3. Evaluate the story shear V_i on the basis of code-compliant seismic force distributions.
4. Evaluate the shear $K_{fs,i}$ and bending $K_{fb,i}$ component of the lateral stiffness of the frame at each story.
5. Check that the axial deformability of columns is low, thus the bending $K_{fb,i}$ component may be neglected.
6. Compute the mechanical properties of the SDOF equivalent, i.e., stiffness, period and damping.
7. Select the peak ductility demand μ_d (EPDs) or loss factor η_d (VEDs). Initial values may be assumed on the basis of previous studies; e.g., μ_d=3 and η_d=1.
8. Choose the optimum stiffness ratio K_d/K_{fs} for a target roof drift and/or base shear. Design charts are available in literature (Kasai *et al*., 1998); alternatively, they can be derived on the basis of Equations (3.38) through (3.40).
9. Convert the value for SDOF to MDOF through Equation (3.41).
10. Assess the frame with the dampers and check if the performance is satisfactory. Alternatively, choose different stiffness ratio K_d/K_{fs} for the SDOF and repeat steps (6) through (9).

Further details regarding design parameters of braces with dampers may be found in Section 2.5.3. The use of these devices for seismic retrofitting is aimed at protecting frame components, i.e., beams, columns and connections, in the event of moderate-to-severe earthquakes. Reduced story drifts are guaranteed by the supplemental damping provided by the devices. Moreover, dampers are effective to mitigate the vibrations due ordinary environmental actions, e.g., wind and small earthquakes. However, hysteretic (yield) dampers, friction dampers and VEDs are advised because their design rules are mature and their enhanced seismic performances have been validated in several successful applications worldwide.

3.4. CONNECTION RETROFITTING

3.4.1. GENERAL

Surveys carried out in the aftermath of relatively recent earthquakes, e.g., the 1994 Northridge (California) and the 1995 Hyogoken-Nanbu (Japan) quakes, showed that extensive damage occurred in steel framed structures (AIJ, 1995; Youssef *et al*., 1995). It was observed that unexpected brittle fracture was localized at connections, particularly welded flange-bolted web beam-to-columns. As a result, several research projects were undertaken worldwide to acquire a more thorough understanding of the inelastic response of joints (Malley, 1998; Watanabe *et al*., 1998; Plumier, 2000; Kunnath and Malley, 2002). Many aspects have been investigated through

analytical and experimental tests. The results of such research work have led to several design guidelines particularly in the US where many FEMA documents were issued. Some of them are aimed at providing either pre-qualified connections for new buildings (FEMA 350, 2000) or strategies to repair connections in existing buildings (FEMA 351, 2000). Proprietary connections are also discussed in these documents. Figure 3.33 shows the standardized connections along the relevant references.

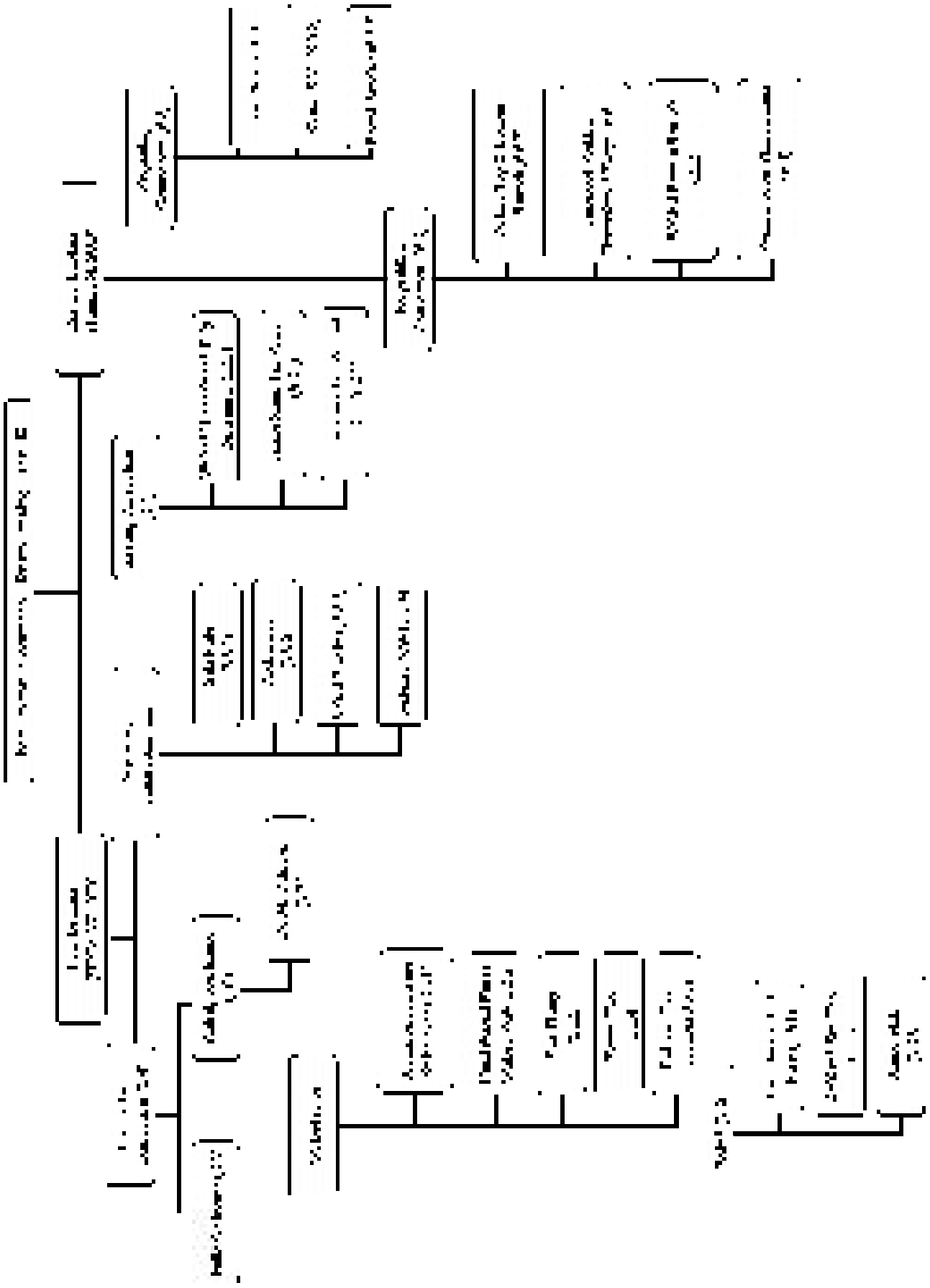

Figure 3.33. Standardized connections in the US.

These connection details primarily refer to buildings with MRF as a seismic lateral resisting system. In the present section, recommendations are provided for the seismic retrofitting of connections of steel and composite framed and braced buildings in Europe. Measures to rehabilitate beam-to-column connections are first addressed and some remedies for brace and link connections are then provided.

3.4.2. BEAM-TO-COLUMN CONNECTIONS

The widespread damage experienced by the traditional steel connections during the last earthquakes has generated a great deal of research aimed at addressing remedies for immediate and long-term needs to solving problems of beam-to-column joints (FEMA 274, 1997). Consequently, several new layouts have been suggested to improve the seismic performance of existing and new steel and composite buildings (Kunnath and Malley, 2002). In all cases, the proposed connection details shift the beam plastic hinge away from the face column (Figure 3.34). Such details may be grouped in two categories as a function of the rehabilitation measure adopted: weakening of the beam section at a certain distance from the column flange and strengthening of the beam section at the column face (Engelhardt and Sabol, 1997).

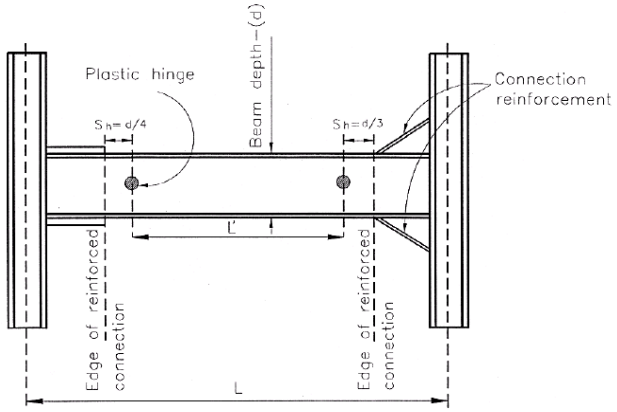

Figure 3.34. Plastic hinge location for reinforced moment connections.

Common examples of the connection details proposed in the US are provided in Figure 3.35 (FEMA 355D, 2000); these includes welded cover plated flange connections (WCPFCs), welded triangular rib plated connections (WTRPCs), welded haunch connections (either bottom (WBHCs) or top and bottom (WTBHCs) haunch), and reduced beam section connections (RBSCs). WCPFCs, WTRPCs, WBHCs and WTBHCs (Figures 3.35(a) to 3.35(c)) are strengthened (or reinforced) connections, while RBSCs (Figure 3.35(d)) are weakened connections. These connections, which are mainly welded, are discussed hereafter; however, bolted and remedies for other connection details more common in Europe are also addressed.

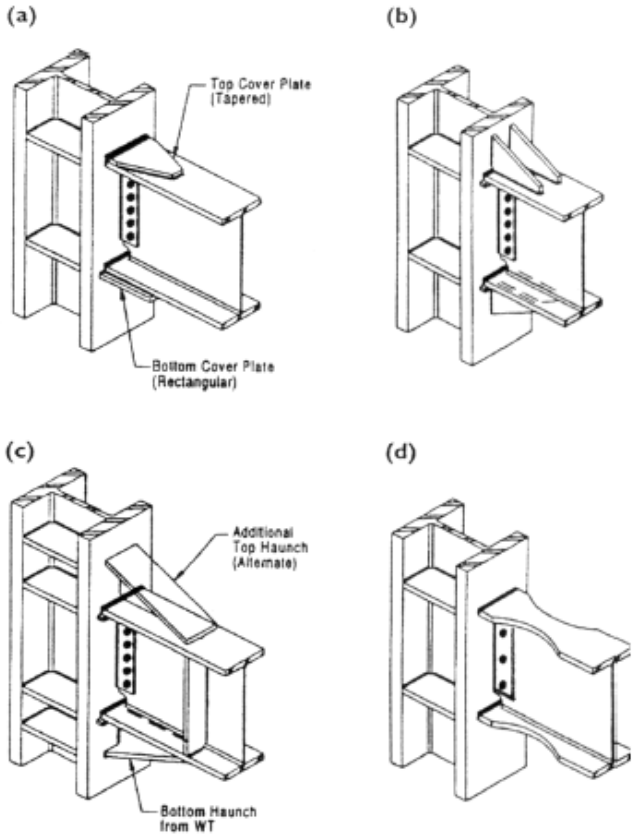

Figure 3.35. Retrofitting measures for beam-to-columns (post-Northridge): (*a*) cover plates, (*b*) triangular rib plates, (*c*) haunches and (*d*) RBS (*after* Engelhardt and Sabol, 1997).

3.4.2.1. IMPROVED UNREINFORCED CONNECTIONS

The simplest way to upgrade welded beam-to-column connections consists of replacing the filler metal at the joined parts. Indeed, the welds may have significant root defects or employ materials with low notch toughness. Therefore, it suffices to gouge out the existing filler material and replace it with a sound one, i.e., minimum CVN toughness of 27.1 J at –28.8 °C (Ricles *et al*., 2002). It is strongly recommended to remove any backing bar after welding because they may cause initiation of cracks. Moreover, continuity plates at the top and bottom of the panel zone and web plates should be used to strengthen and stiffen the column panel. As a rule of thumb, their thicknesses should not be less than those of beam flanges (continuity plates) and column web (web plate). If the beam(s) entering the connections has (have) flanges with different thicknesses, it is required to use continuity plates whose thickness is equal to the thicker flange.

On the other hand, the use of excessively thick plates should be avoided due to the large residual stresses induced. It is also required that such plates should be welded to column flanges and web via complete joint penetration welds. These welds should be stopped short of the *k*-area, thus preventing the likelihood of fracture (FEMA 355B, 2000). The *k*-area is defined as the region extending from about the midpoint of the radius of the filler into the web, approximately 25 to 30 mm beyond the point of tangency between the fillet and web (AISC, 1997).

The panel zone of the column should be checked to remain elastic and avoid premature local buckling. This local failure may be prevented by satisfying the slenderness limitations given in the empirical Equation (3.33) in Section 3.3.3. The shear ($V_{Rd,cp}$) strength of the panel may be evaluated conservatively as:

$$V_{Rd,cp} = d_c \cdot t_p \frac{f_{y,cw}}{\sqrt{3}} \tag{3.45}$$

where d_c is the depth of the column; t_p is the total thickness of the panel zone including doubler plates, if any; and $f_{y,cw}$ is the yield strength of the column web. The thickness of the web doubler plates may be considered to compute t_p, but plug welds between the column web and the added plates are required. Four plug welds arranged symmetrically is the minimum requirement.

The requirement in Equation (3.45) complies with design rules for new steel and composite buildings in Europe (EC8, 1998) and is more stringent than counterparts in other standards. For example, American seismic codes (IBC, 2000) and guidelines allow the shear yielding of the panel zone, which should initiate at the same time as flexural yielding of the beam elements (AISC, 1997; FEMA 351, 2000). Based on early experimental and analytical work on shear in beam-column joints, the US design shear strength of a panel zone is as follows (Krawinkler *et al.*, 1975):

$$V_{Rd,cp} = d_c \cdot t_p \frac{f_{y,cw}}{\sqrt{3}} \left[1 + \frac{3 \cdot b_{cf} \cdot t_{cf}^2}{d_b \cdot d_c \cdot t_p} \right] \tag{3.46}$$

where b_{cf} and t_{cf} are the width and the thickness of the column flange, respectively. The second term in brackets accounts for the contribution of column flanges to the shear strength of the panel beyond yielding; the flanges are assumed to remain elastic. This benign effect is neglected in Equation (3.45).

In addition, it is worth noting that in the US practice, the use of continuity plates at the top and bottom of the panel zone may be omitted in some cases. They are compulsory when the column flange thickness (t_{cf}) does not meet the following requirements (FEMA 351, 2000):

$$t_{cf} > \max \begin{cases} b_f / 6 \\ \dfrac{0.01}{\sqrt{b_f \cdot t_f \cdot \left(f_{yb} / f_{yc} \right)}} \end{cases} \tag{3.47}$$

where b_f (in mm) is the beam flange width; and f_{yb} and f_{yc} are the yield strength of beam and column flange, respectively. By contrast, continuity plates are advised for the retrofitting of beam-to-column connections in Europe in all cases because they are effective to prevent column flange distortion and column web yielding and crippling (Naeim, 2001).

The rehabilitation measure illustrated above is similar to the improved welded unreinforced flange connection (IWUFC) classified as pre-qualified connection in the US guidelines for upgrading of existing steel buildings (FEMA 351, 2000). However, this retrofitting technique assumes that the damage is concentrated solely at the joining parts, i.e., in the welds. Furthermore, it ensures that the repaired connections may sustain inelastic deformations due low-to-moderate earthquakes. Whenever high dissipation capacities are required, it is recommended to either weaken or strengthen the connection with more effective strategies, as described hereunder.

3.4.2.2. RBS CONNECTIONS

The weakening of existing beam-to-column connections may be performed by using RBS beams (Figure 3.36) designed according to the rules in Section 3.3.2. Plastic hinges are forced to occur within the reduced sections, thus reducing the likelihood of fracture occurring at the beam flange welds and surrounding heat affected zones (HAZs). The inelastic deformation of the plastic hinge is ultimately limited by beam instability or by fracture of the flange; thus, more stringent web slenderness limits should be used for beams with reduced sections (Uang and Fan, 1999), as specified by Equation (3.23) of Section 3.3.2. On the other hand, optimizing the shape of the RBS cut minimizes the likelihood of fracture in the flange of the RBS (Jones *et al*., 2002); details for adequate radius-cutting are provided in Section 3.3.2. The presence of a composite slab has a benign effect on the connection performance. This effect is two-fold, i.e., enhancement of beam instability and delaying of strength degradation. However, a gap of about 30 mm between the column flange and the slab face is recommended. Shear studs within the RBS zones may give rise to flange fractures initiating at the stud welds and/or local stress risers; therefore, it is strongly advised to avoid studs in such regions. Moreover, shallower column sections should be preferred to deep ones because the latter could give rise to the twisting. Two factors generally contribute to the column twisting, i.e., LTB and stress in the column due to warping torsion. Requirements to prevent LTB of beams with RBSs are provided in Section 3.3.2. On the other hand, warping in rolled sections is a function of the following ratio (Naeim, 2001):

$$WR = \frac{d_c - t_{cf}}{t_{cf}^3} \tag{3.48}$$

where d_c and t_{cf} are the column depth and flange thickness, respectively. Thus, H-sections, either rolled or built-up, with low WR, around 1.0×10^{-3} mm^{-2}, should be chosen for RBS beam-to-column connections. For example, this requirement is for example useful when selecting sections with similar inertia; the ones with lower WR should be chosen to prevent column twisting.

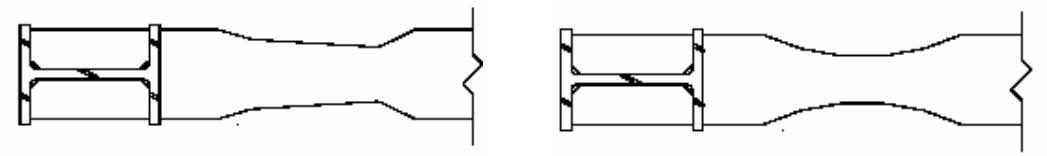

Figure 3.36. RBS beam-to-column connection: tapered (*left*) and circular (*right*) flange profile.

Welded webs should be used to joint the beam to the column flange, because they reduce the stress concentrations at the beam flanges and beam flange groove welds, thus exhibiting lower incidence of fractures than bolted webs (Jones *et al*., 2002). Alternatively, shear tabs may be welded to the column flange face and beam web. The tab length should be equal to the distance between the weld access holes with an offset of 5 mm; its minimum thickness is 10 mm. They may either be cut square or tapered edges (tapering corner about 15°) and should be placed on both sides of the beam web. The welds should be groove welds or fillet for the column face and fillet welds for the beam web. Bolting of the shear tab to the beam web may be used if more convenient economically.

The design procedure for RBS connections is outlined below:

1. Use RBS beams designed in compliance with the procedure in Section 3.3.2. However, it is advised to compute the expected beam probable plastic moment ($M_{pb,e}$) as follows:

$$M_{p,be} = \left(\frac{f_{ye} + f_{te}}{2 \cdot f_{ye}} \right) \cdot Z_{RBS} \cdot f_{ye} \cdot \left(\frac{L - d_c}{L - d_c - 2 \cdot b} \right) \tag{3.49.1}$$

where L is the distance between column centerlines; d_c is the column depth; and b is the length of RBS. Hence, the beam expected shear ($V_{pb,e}$) is given by:

$$V_{p,b_e} = \frac{2 \cdot M_{p,be}}{L'} + \frac{w \cdot L'}{2} \tag{3.49.2}$$

where w is the uniform load along the beam span (L`) between plastic hinges:

$$L' = L - d_c - 2 \cdot b \tag{3.49.3}$$

Additional point vertical loads, if any, should be included in Equation (3.49.2).

2. Check the web connection, e.g., welded shear tab, by using the expected shear $V_{pb,e}$ as given in Equation (3.49.2).

3. Check the strong column-weak beam requirement via the CBMRs, defined as:

$$CBMR = \frac{\sum Z_c \left(f_{yc} - f_a\right)}{\sum Z_b \cdot f_{yb,e} \cdot \left(\frac{L - d_c}{L - d_c - 2 \cdot b}\right) \cdot \left(\frac{f_{ub,e} + f_{yb,e}}{2 \cdot f_{yb,e}}\right)} \geq 1.20 \tag{3.50}$$

where Z_b and Z_c are the plastic moduli of the beams and columns, respectively; the yield stresses are minimum values for the columns (f_{yc}) and expected for beams ($f_{yb,e}$); $f_{tb,e}$ is the expected tensile strength; and f_a is the design stress in the columns.

4. Compute the thickness of the continuity plates to stiffen the column web at top and bottom beam flange. Such thickness should be equal to that of the beam flange.

5. Check the strength and stiffness of the panel zone. It should be assumed that the panel remains elastic, thus:

$$d_c \cdot t_{wc} \cdot \frac{f_{y,cw}}{\sqrt{3}} \geq \frac{\sum Z_b \cdot f_{y,be} \cdot \left(\frac{f_{ub,e} + f_{yb,e}}{2 \cdot f_{yb,e}}\right)}{d_b} \cdot \left(\frac{L - d_c}{L - d_c - 2 \cdot b}\right) \cdot \left(\frac{H - d_b}{H}\right) \tag{3.51}$$

where d_c and t_{wc} are the depth and the thickness of the column web; $f_{y,cw}$ is the minimum specified yield strength; and *H* is the frame story height. The column web thickness t_{wc} should include the doubler plates, if any. Adequate stiffness is guaranteed with width-to-thickness ratios (d_c/t_{wc}) less than 50.

6. Compute and detail the welds between joined parts. It is required minimum CVN toughness equal to 27.1 J at -28.8^{o}C.

3.4.2.3. HAUNCH CONNECTIONS

Beam-to-column connections may be strengthened by placing haunches either at bottom (Figure 3.37) or at top and bottom of the beam flanges (Figure 3.38), thus the flexural yielding of the beam (plastic hinge) is forced to occur at the end of the haunch. However, the former details are more convenient because bottom flanges are generally far more accessible than top ones and the composite slab does not have to be removed. On the other hand, when the damaged connection is strengthened with a bottom haunch, it is highly desirable to either reinforce the existing top flange with steel plates or replace the welds by ones with high notch toughness, if the existing are not sound (Uang and Bondad, 1998). Furthermore, extensive experimental and analytical work has shown that the triangular T-shaped haunches are the most effective among the different types of haunch details (Yu *et al.*, 2000). However, it is recommended to choose triangular haunches with slope equal to 2:1 (Figure 3.38) (2 horizontal and 1 vertical). Their depth should be one-fourth of

the beam depth for bottom haunches (Figure 3.37) (FEMA 267, 1995). Deeper haunches, i.e. one-third of the beam height, are advised for connections with top and bottom haunches (Figure 3.38).

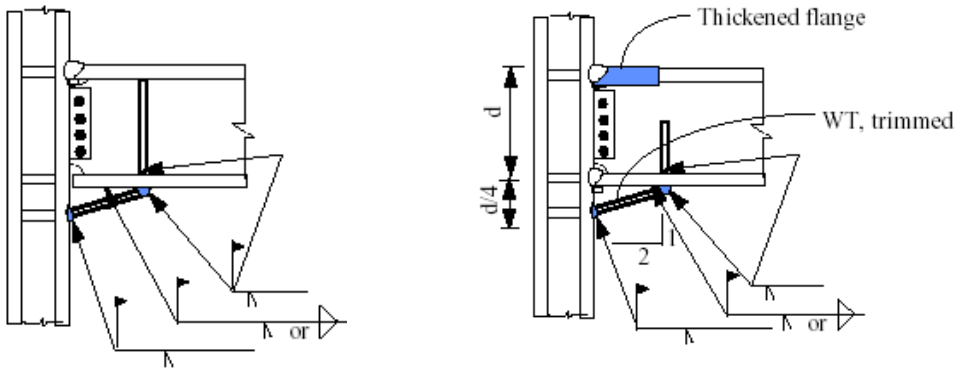

Figure 3.37. Welded bottom haunch connections: unreinforced top flange and bottom flange not welded (*left*), reinforced top flange and welded bottom flange (*right*).

Furthermore, continuity plates should be used to strengthen the column panel and should be placed at top and bottom beam flanges. Their design should be performed in compliance with the requirements described above in Section 3.4.1.1 for the improved unreinforced connections. Moreover, additional plates are required at the haunch edges to stiffen the column web and beam web, respectively. The vertical stiffeners for the beam web should be full depth and welded on both sides of the web. Indeed, full-depth stiffeners tend to shift the local buckling of the beam top flange outside the haunch region (Yu *et al*., 2000). As a result, the welds along the column face are protected from large inelastic demand. The thickness of such stiffeners should be proportioned to withstand the vertical component of the force at that location. However, it should not be less than beam flanges thickness. It is required to perform local checks for flange bending, web yielding and web crippling; formulae and slenderness limitations are provided in the design standards (EC3, 1992; EC8, 1998).

Haunches should be welded via complete joint penetration welds to both column and beam flanges (Figure 3.38). Scrupulous control is required to ascertain that adequate filler material is used, e.g., notch tough electrodes. Welds with low toughness (e.g., less than 27.1 J at –28.8 °C) are likely to cause fracture at beam flanges (Figure 3.39). On the other hand, bolted shear tabs do not undermine the inelastic performance of the connection; thus, they may be left in place, if they exist. Alternatively, shear tabs may be used if required for either structural or erection purposes.

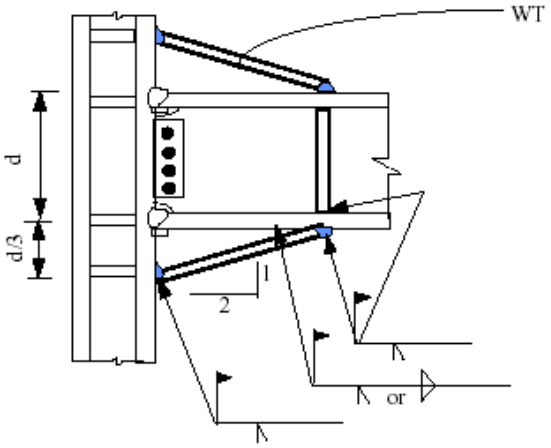

Figure 3.38. - Welded top and bottom haunch connections.

Local buckling of the connected members (Figure 3.39) should be prevented by checking the limitation provided by the interaction formula in Section 3.3.2. Similarly, LTB should be prevented by employing member slendernesses (L/r) not greater than 50. This figure is compliant with recent US guidelines, which recommend $L_b/r_y \le 17500/f_y$ (lengths in mm and stress in N/mm^2) (FEMA 355D, 2000. The American requirement leads to values between 49 (S355) and 74 (S235) for European grades of steel.

Yield mechanisms and failure modes of haunch connections are similar to those of unreinforced connections described in Section 3.4.1.1, as illustrated in Figure 3.39; however, in the former the geometry of the connection is crucial to balance theses modes of response. For example, the average panel zone shear is reduced by considering the haunch effective depth (d_{eff}) (*enlarged or dual panel zone*) which is related to the beam depth (d_b) and haunch depth (h_h) as follows:

(*top and bottom haunch*) $$d_{eff} = d_b + 2 \cdot h_h \qquad (3.52.1)$$

(*bottom only haunch*) $$d_{eff} = d_b + h_h \qquad (3.52.2)$$

Therefore, the panel zone should satisfy the following strength requirement:

$$d_c \cdot t_{wc} \cdot \frac{f_{y,cw}}{\sqrt{3}} \ge \frac{\sum M_f}{d_{eff}} \cdot \left(\frac{L}{L - d_c} \right) \cdot \left(\frac{H - d_{eff}}{H} \right) \qquad (3.53)$$

where d_c and t_{wc} are the depth and the thickness of the column web; $f_{y,cw}$ is the column web yield strength. L and H are the distance between column centerlines and the frame story height, respectively; and M_f is the moment at the column face. The column web thickness t_{wc} should include the doubler plates, if any.

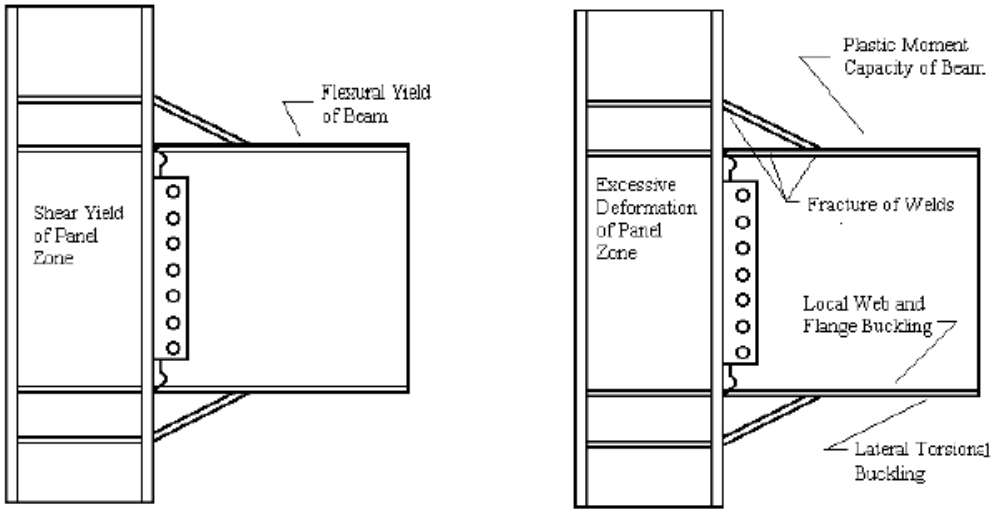

Figure 3.39. Behavior of welded top and bottom haunch connections: yield mechanisms (*left*) and failure modes (*right*) (*after* FEMA 355D, 2000).

Retrofitting steel beam-to-column connections with welded haunches is a viable solution to enhance the rotation capacities. However, the improved inelastic performance depends on several parameters. For example, it varies as a function of the type of haunch used, i.e., bottom only or top and bottom, the details at the beam top flange, repaired or unrepaired welds and the composite action. Haunch connections though, are not significantly influenced by the beam depth. Indeed, the presence of the haunch alters the beam depth at the connection along with the beam depth-to-span ratio. The values computed in recent experimental and numerical tests performed in the US are summarized in Table 3.10 (FEMA 355D, 2000). It is worth noting that connections with bottom haunches exhibit larger plastic rotations (28 μrad as opposed to 18 μrad) than top and bottom counterparts. Similarly, their COVs are much lower (3.57 *vs.* 6.30). However, the results become more disperse when the composite action (e.g., composite slab) is accounted for. The mean plastic rotations listed in Table 3.10 ensure that haunch connections can undergo large plastic rotations and can be used to satisfy the performance requirements of MRFs; e.g., story drift equal to 3% (EC8, 1998). Nevertheless, such upgrading remedies are generally expensive because of the details and the workmanship required. Furthermore, the design of haunches is lengthy and not straightforward. In fact, the stress distribution is not well defined in tapered sections and the normal rules to check shear and flexural stresses in beams are no longer valid for such sections.

Table 3.10. Rotation capacities of haunch connections.

	Plastic rotations without resistance loss			Plastic rotations to resist gravity loads		
Connection Details	Mean Values (rads)	Standard Deviations (rads)	COVs (%)	Mean Values (rads)	Standard Deviations (rads)	COVs (%)
Top and bottom haunch	0.027	0.0017	6.30	0.047	0.0017	6.30
Bottom haunch and top pre-qualified details*	0.028	0.001	3.57	0.048	0.001	3.57
Bottom haunch and nonpre-qualified top details with composite slab	0.026	0.003	11.54	0.036	0.003	11.54
Bottom haunch and pre-qualified top details without composite slab	0.018	0.002	11.11	0.023	0.002	11.11

Keys: *Top pre-qualified details are cover plates and/or reinforced welds.

Design procedures for haunch connections have recently been proposed in the US guidelines (FEMA 267, 1995; FEMA 351, 2000); these procedures have been validated by experimental and

numerical tests (FEMA 355D, 2000). They generally employ force equilibrium and deformation compatibility between the beam and the haunch to size the haunch. This is the case, e.g., of the step-by-step design procedure summarized below (Yu *et al*., 2000). It is based on a simplified model in which the haunch flange is idealized as a spring. The contribution of the haunch web to the stiffness in the haunch flange direction is ignored; thus, the beam shear transmitted to the haunch flange at the haunch tip is as a function of the axial stiffness of the haunch flange:

1. Select preliminary haunch dimensions (Figure 3.40) on the basis of slenderness limitation for the haunch web. The following relationship may be used (Gross *et al*., 1999) as a first trial for the haunch length (a) and its slope (θ):

$$a = 0.55 \cdot d_b \tag{3.54.1}$$

$$q = 30° \tag{3.54.2}$$

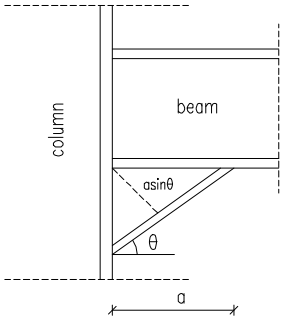

Figure 3.40. Haunch geometry.

where d_b is the beam depth. However, the haunch depth b should be compatible with architectural restraints, e.g., ceilings and nonstructural elements. The haunch depth is given by $b = a \cdot \tan\theta$.

2. Compute the beam probable plastic moment ($M_{p,de}$) at the haunch tip:

$$M_{p,de} = \left(\frac{f_{ye} + f_{te}}{2 \cdot f_{ye}} \right) \cdot Z_b \cdot f_{ye} \tag{3.55}$$

where Z_b is the plastic modulus of the beam; f_{te} and f_{ye} are the expected ultimate and yield strengths, respectively, as specified in Section 3.1. For the rehabilitation of existing connections, it is advised to use the actual dimensions of the beam to evaluate the plastic modulus Z_b.

3. Compute the beam probable plastic shear ($V_{p,de}$) from force equilibrium of the beam span (L`) between plastic hinges (Figure 3.41). Thus, the following relationship may be used:

$$V_{p,de} = \frac{2 \cdot M_{p,de}}{L'} + \frac{w \cdot L'}{2} \tag{3.56}$$

where w is the uniform load between L`. Additional point vertical loads, if any, should be included in Equation (3.56).

4. Check the strong column-weak beam requirement via the CBMRs, defined as:

$$CBMR = \frac{\sum Z_c \cdot \left(f_{y,c} - f_a \right)}{\sum M_c} \geq 1.20 \tag{3.57.1}$$

where Z_c is the plastic section modulus of the columns; f_{yc} is the minimum specified yield strength; f_a is the axial stress in the columns due to the design loads; and M_c is the sum of column moments at the top and bottom ends of the enlarged panel zone resulting from the

development of the beam moment M_{pd} within each beam of the connection. It is given as follows:

$$\sum M_c = \left[2M_{p,de} + V_{p,de} \cdot (L - L')\right] \cdot \left(\frac{H_c - \overline{d_b}}{H_c}\right) \tag{3.57.2}$$

where L is the distance between the column centerlines (Figure 3.41); $\overline{d_b}$ is the depth of the beam including the haunch; and H_c is the story height of the frame.

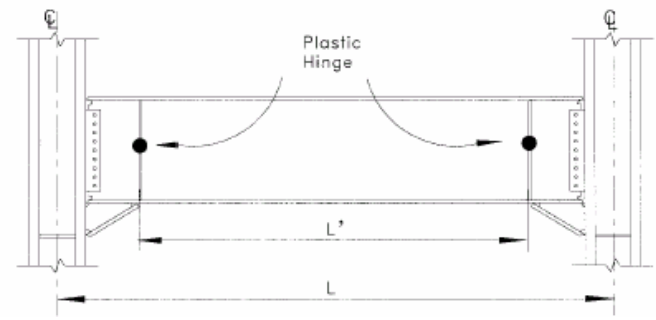

Figure 3.41. Plastic hinge location for welded haunch connection.

It is worth noting that the expression of CBMR given in Equation (3.57.1) is different from the counterpart proposed in the recent FEMA State of Art Report (FEMA 355D, 2000) where:

$$CBMR = \frac{\sum Z_c (f_{yc} - f_a)}{\sum Z_b \cdot \left(\frac{L - d_c}{L - d_c - 2 \cdot a}\right) \cdot \left(\frac{f_{ub,e} + f_{yb,e}}{2}\right)} \geq 1.10 \tag{3.57.3}$$

where Z_b and Z_c are the plastic moduli of the beams and columns, respectively; the yield stresses are minimum values for the columns (f_{yc}) and expected values for beams ($f_{yb,e}$); d_c is the column depth; and *a* the haunch length. It is advised to use both formulae to check the strong-column-weak-beam requirements and hence, refer to the more stringent limit.

5. Compute the actual value of the adimensionalized parameter β given by:

$$b = \frac{b}{a} \cdot \left(\frac{3 \cdot L' \cdot d + 3 \cdot a \cdot d + 3 \cdot b \cdot L' + 4 \cdot a \cdot b}{3 \cdot d^2 + 6 \cdot b \cdot d + 4 \cdot b^2 + \frac{12 \cdot I_b}{A_b} + \frac{12 \cdot I_b}{A_{hf} \cos^3 q}} \right) \tag{3.58}$$

where A_{hf} is the area of the haunch flange. It is instructive to note that the value of β in Equation (3.58) represents the interface force coefficient between the beam and the haunch flange (Figure 3.42).

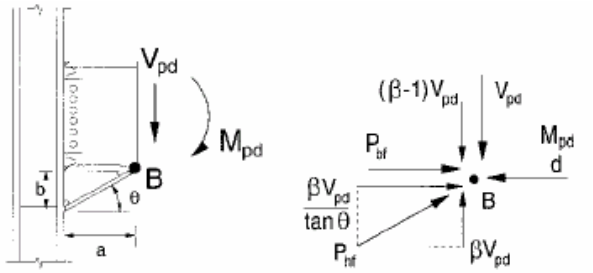

Figure 3.42. Force equilibrium at the haunch tip.

6. Compute the value of the adimensionalized parameter β_{min} given by:

$$b_{\min} = \frac{\frac{\left(M_{p,d} + V_{p,d} \cdot a\right)}{S_x} - 0.80 \cdot f_{wt}}{\frac{V_{p,d} \cdot a}{S_x} + \frac{V_{p,d}}{I_b \cdot \tan q} \cdot \left(\frac{d^2}{4} - \frac{I_b}{A_b}\right)} \tag{3.59}$$

where f_{wt} is the tensile strength of the welds, S_x is the beam elastic (major) modulus; d is the beam depth; and A_b and I_b are the area and moment of inertia of the beam, respectively.
This expression for β_{min} has been derived via equilibrium and compatibility equations, assuming that the allowable tensile stress in the beam flange welds at the column face is 0.80 times the tensile strength of the filler material.

7. Compare the adimensionalized β-values, as calculated above. If $\beta \geq \beta_{min,}$ the haunch dimensions are adequate and further local checks should be performed. By contrast, $\beta < \beta_{min}$ requires an increase of the haunch flange stiffness. Stiffer flanges may be obtained by either increasing the area A_{hf} or modifying the haunch geometry.

8. Perform strength and stability checks for the haunch flange:

(*strength*) $$A_{hf} \geq \frac{b \cdot V_{p,de}}{f_{ye,hf} \cdot \sin q} \tag{3.60.1}$$

(*stability*) $$\frac{b_{hf}}{t_{hf}} \leq 10 \cdot \sqrt{\frac{235}{f_y}} \tag{3.60.2}$$

where $f_{ye,hf}$ is the expected yield strength of the haunch flange; b_{hf} and t_{hw} are the flange outstanding and flange thickness of the haunch, respectively. It is worth noting that the stability in Equation (3.60.2) check has been adapted to the European standards (EC3, 1992).

9. Perform strength and stability checks for the haunch web:

(*strength*) $$t_{hw} = \frac{a \cdot V_{p,de}}{2 \cdot (1+u) \cdot I_b} \left[\frac{L`}{2} - \frac{b}{\tan q}\left(\frac{d}{2}\right) + \frac{(1-b) \cdot a}{3}\right] \leq \frac{f_{ye,hw}}{\sqrt{3}} \tag{3.61.1}$$

(*stability*) $$\frac{2 \cdot a \cdot \sin q}{t_{hw}} \leq 33 \cdot \sqrt{\frac{235}{f_y}} \tag{3.61.2}$$

where $f_{ye,hw}$ is the expected yield strength of the haunch web; t_{hw} is the web thickness; and ν is the Poisson`s ratio of steel, i.e., 0.30. The limitation for stability check in Equation (3.61.2) has been adapted to the European standards and considers the haunch as half of a wide-flange beam section whose depth is equal to $2 \cdot a \cdot \sin\theta$ (EC3, 1992). Equation (3.60.2) and (3.61.2) express width-to-thickness ratios independently for the haunch flange and web; however, it is recommended to check the interaction formula for local buckling as provided in Section 3.2; the web depth (d) in the interaction formula should be replaced with $2 \cdot a \cdot \sin\theta$.

10. Check the shear capacity of the beam web. The shear in the beam web is given by:

$$V_{bw} = (1-b) \cdot V_{p,de} \tag{3.62}$$

Web yielding and web crippling (EC3, 1992) should also be checked on the basis of the shear in Equation (3.62).

11. Design continuity plates and beam web stiffeners: as a rule of thumb, continuity plates should have thickness equal to the beam flange. However, their dimensions should be adequate to withstand the concentrated force $\beta \cdot V_{p,de}/\tan\theta$ (Figure 3.42). Furthermore, web

stiffeners should possess sufficient strength to resist the concentrated load $\beta \cdot V_{p,de}$ along with the beam web. On the other hand, width-to-thickness ratios for continuity plates and web stiffeners should be limited to 15 to prevent local buckling.

12. Perform weld detailing by using complete joint penetration welds to connect each stiffener to the beam flange. Two-sided 8 mm fillet welds are adequate to connect the stiffeners to the beam web. All welds should possess values of CVN not less than 27.1 J at –28.8 °C.

3.4.2.4. COVER PLATE CONNECTIONS

The use of cover plates has been one of the more common connection reinforcing schemes used since the Northridge earthquake (Kunnath and Malley, 2002). Such scheme is effective to retrofit existing beam-to-column connections because they: (i) reinforce the connection, (ii) reduce the stress at the beam flange welds and (iii) force the yielding in the beam at the end of the cover plates. Moreover, cost data suggest that these connections are more economic than haunch counterparts (Engelhardt and Sabol, 1998); the volume of added material is smaller, the welds are less and the design is straightforward. As for haunch connections, reinforcing plates may be used either at bottom or top and bottom beam flanges. Furthermore, the option with cover plate for the top flange located beneath the flange (Figure 3.43) can be installed without demolishing the existing slab. However, such detail requires overhead welding. Thus, the effectiveness of the intervention relies significantly upon the workmanship and the accuracy of the inspection for welds.

Reinforcing plates may be shaped in different ways; however, the most common and efficient shapes are the rectangular and the trapezoidal (Figure 3.43). Recent analytical and experimental tests showed that rectangular reinforcing plates are superior to trapezoidal shaped plates (Kim *et al*., 2002). Therefore, rectangular plates should be used for retrofitting beam-to-column connections; such plates should be fabricated with rolling directions parallel to the beam.

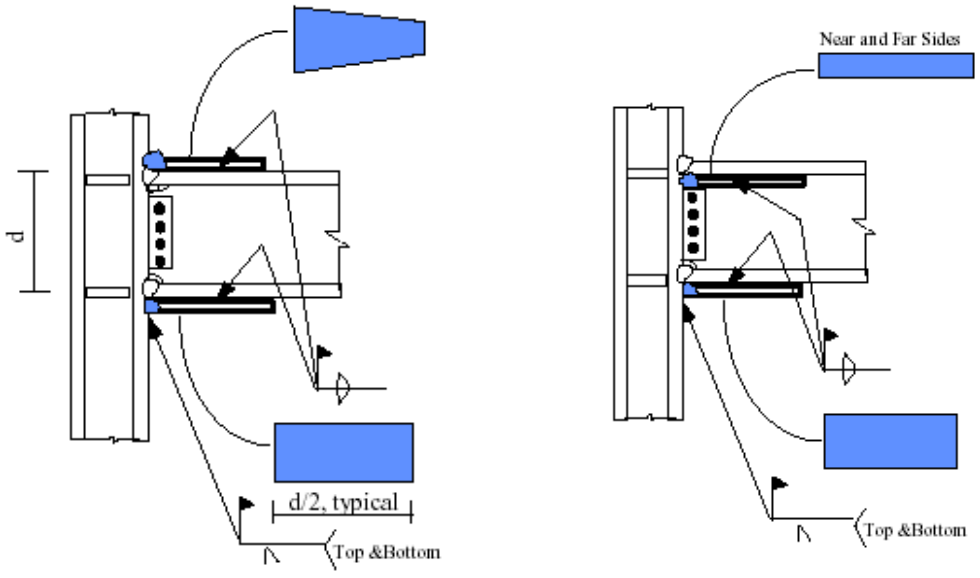

Figure 3.43. Typical welded plate connections.

To achieve high inelastic rotations it is of paramount importance to perform adequate welds between the joined parts, e.g., coverplate, beam and column flanges. Three types of complete penetration weld details (Figure 3.44) have been investigated in the US (FEMA 355D, 2000): two of them (details 1 and 3) refer to the top plate and beam flanges, while detail type 2 is used at the bottom flange of the beam. Detail type 1 should be preferred to type 3; in fact, the latter causes the fracture (through-thickness fracture) of column flanges (Figure 3.44), thus reducing significantly the seismic performance of the connection.

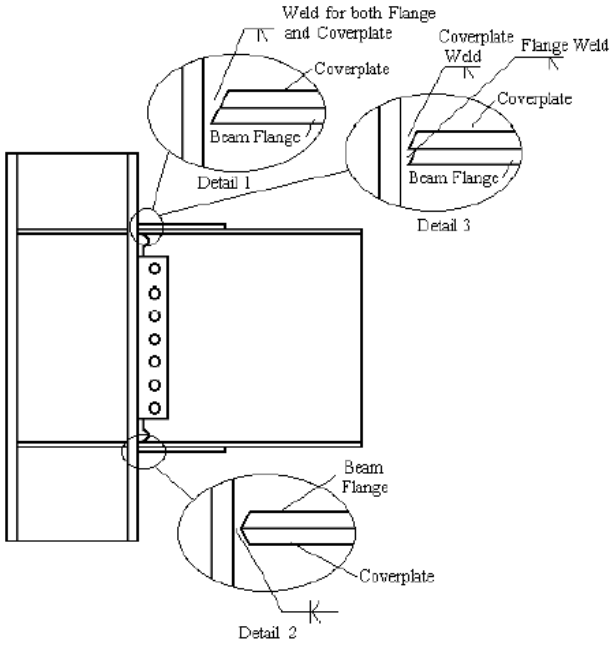

Figure 3.44. Weld details for plate connections (*after* FEMA 355D, 2000).

Similarly, thick welds should be avoided; the thicker the weld the more likely is the occurrence of brittle fracture, e.g., at the joined parts of plates, beam and column (Figure 3.45). Moreover, thick welds give rise to high shrinkage and restraint which may cause distortion of welds and/or surrounding HAZs.

On the other hand, existing welds should be gouged out if they employ low toughness filler materials or have been damaged. A minimum specified CVN toughness should be 27.1 J at -28.8^{o}C and weld overlays should employ the same electrodes or at least with similar mechanical properties.

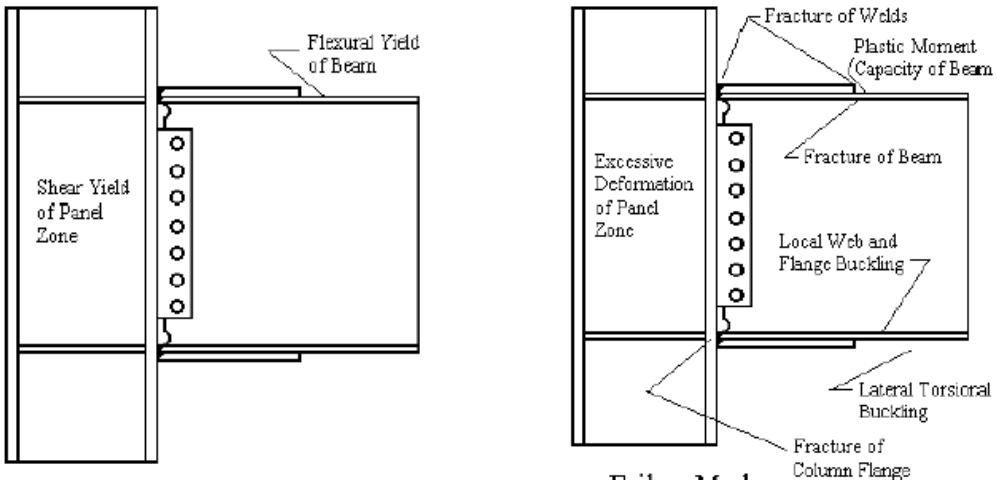

Figure 3.45. Behavior of welded plate connections: yield mechanisms (*left*) and failure modes (*right*) (*after* FEMA 355D, 2000).

Connections with welded beam webs and relatively thin and short cover plates should be preferred to bolted web and heavy and long plates. In fact, large and heavy cover plates may cause high concentrations of tri-axial stresses at column flanges, thus promoting brittle fracture. Such concentrations are due to the large moment amplification generated from the tips of the plates to the face of the column. It is also strongly recommended to avoid long plates for beams with short spans and high moment gradient.

To achieve outstanding rotation capacity, e.g., not less than 3%, the area (A_{cp}) of the cover plates should be limited as follows:

$$A_{cp} \leq 1.20 \cdot A_{bf} \tag{3.63}$$

where A_{bf} is the area of beam flanges.

Rectangular plates as wide as beam flanges are preferable due to their superior performance; hence, the limitation in Equation (3.63) implies that the plate thickness (t_{cp}) should satisfy the following ratio

$$\frac{t_{cp}}{t_{bf}} \leq 1.20 \tag{3.64}$$

which limits t_{cp} as a function of the beam flange thickness (t_{bf}). The length (t_{cp}) of the plates is also related to the beam size; it is typically assumed dependent on the beam depth (d_b) as follows:

$$l_{cp} = \frac{d_b}{2} \tag{3.65}$$

The occurrence of buckling phenomena (Figure 3.45) should be prevented by satisfying the width-to-thickness limitations for beam flanges and webs (local buckling), as in given Section 3.2.2 and providing adequate lateral support (LTB) for beams, as required in relevant standards (EC3, 1992).

Continuity plates should be placed at top and bottom beam flanges thus strengthening and stiffening the panel zone. These plates should be as thick as the flange plate and should be welded to the column flange and web via complete joint penetration welds. Moreover, the deformation of the

column panel zone may be restrained by adding doubler web plates. However, it is required that the panel zone should not yield.

On the other hand, existing shear tabs may be left in place provided they are upgraded in such a way that their thickness (t_{st}) and length (l_{st}) are given by:

$$t_{st} = t_{bw} \tag{3.66.1}$$

$$l_{st} = d_b - 2 \cdot k - 50mm \tag{3.66.2}$$

where d_b is the beam depth, t_{bw} is the beam web thickness; and *k* is the length of the region extending from about the midpoint of the radius of the filler into the web approximately 25 to 30 mm beyond the point of tangency between the fillet and web.

However, shear tabs should have sufficient strength to withstand the following design shear (V_{st}):

$$V_{st} = \frac{2 \cdot M_{cf}}{L - d_c - 2 \cdot l_{cp}} + V_g \tag{3.67}$$

where M_{cf} is the moment at the column face; L the distance between column centerlines; d_c the column depth; and V_g the contribution of the gravity loads on the beam to the shear.

Finally, a step-by-step design procedure is outlined hereafter for cover plate connections; it refers to all-welded beam webs and relatively thin and short cover plates:

1. Select a preliminary cover plate dimensions on the basis of the beam size:

$$b_{cp} = b_{bf} \tag{3.68.1}$$

$$t_{cp} = 1.20 \cdot t_{bf} \tag{3.68.2}$$

$$l_{cp} = \frac{d_b}{2} \tag{3.68.3}$$

2. Compute the beam probable plastic moment ($M_{p,be}$) at the end of the cover plates:

$$M_{p,be} = \left(\frac{f_{ye} + f_{te}}{2 \cdot f_{ye}} \right) \cdot Z_b \cdot f_{ye} \tag{3.69}$$

where Z_b is the plastic modulus of the beam; and f_{ye} and f_{te} are expected yield and tensile strength, respectively, as specified in Section 3.1. For rehabilitation of existing connections, it is advised to use the actual dimensions of the beam to evaluate the plastic modulus Z_b.

3. Compute the beam probable plastic shear ($V_{p,be}$) from force equilibrium of the beam span (L') between plastic hinges:

$$V_{p,be} = \frac{2 \cdot M_{p,be}}{L'} + \frac{w \cdot L'}{2} \tag{3.70.1}$$

where *w* is the uniform load between *L'*. Additional point vertical loads, if any, should be included in Equation (3.70.1). The distance L` between the plastic hinges in the beam is as follows:

$$L` = L - d_c - 2 \cdot l_{cp} \tag{3.70.2}$$

4. Compute the moment at the column flange (M_f):

$$M_f = M_{p,be} + V_{p,be} \cdot l_{cp} \tag{3.71}$$

5. Check that the area of cover plates (A_{cp}) satisfies the following requirement:

$$\left[Z_b + A_{cp} \cdot \left(d_b + t_{cp}\right)\right] \cdot f_y \geq M_f \tag{3.72}$$

6. Check the strong column-weak beam requirement via the CBMRs, defined as:

$$CBMR = \frac{\sum Z_c \left(f_{yc} - f_a\right)}{\sum Z_b \cdot f_{yb,e} \cdot \left(\frac{L - d_c}{L - d_c - 2 \cdot L_{cp}}\right) \cdot \left(\frac{f_{ub,e} + f_{yb,e}}{2 \cdot f_{yb,e}}\right)} \geq 1.20 \tag{3.73}$$

where Z_b and Z_c are the plastic moduli of the beams and columns, respectively. The yield stresses are minimum values for the columns (f_{yc}) and expected values for beams ($f_{yb,e}$).

7. Compute the thickness of the continuity plates to stiffen the column web at top and bottom beam flange. Such thickness should be equal to that of the beam flange.

8. Check the strength and stiffness of the panel zone. It should be assumed that the panel remains elastic, thus:

$$d_c \cdot t_{wc} \cdot \frac{f_{y,cw}}{\sqrt{3}} \geq \frac{\sum M_f}{d_b} \cdot \left(\frac{L}{L - d_c}\right) \cdot \left(\frac{H - d_b}{H}\right) \tag{3.74}$$

where d_c and t_{wc} are the depth and the thickness of the column web, $f_{y,cw}$ is the minimum specified yield strength; and *H* is the frame story height. The column web thickness t_{wc} should include the doubler plates, if any. Adequate stiffness is guaranteed with width-to-thickness ratios (d_c/t_{wc}) less than 50.

9. Compute and detail the welds between joined parts, i.e., beam-to-cover plates, column-to-cover plates and beam-to-column. A minimum CVN toughness of 27.1 J is required at -28.8 ^oC. Moreover, weld overlays should be of the same electrodes or at least with similar mechanical properties.

The main properties of cover plate connections have been compared with those of the configurations discussed in Sections 3.4.1.1 through 3.4.1.3 in Table 3.11.

Table 3.11. Properties of repaired connections.

	IWUFCs	WBHCs	WTBHCs	WCPFCs	RBSCs
Hinge location (from column centerline)	$(d_c/2)+(d_b/2)$	$(d_c/2)+l_h$	$(d_c/2)+l_h$	$(d_c/2)+l_{cp}$	$(d_c/2)+(b/2)+a$
Beam depth (mm)	≤ 1000	≤ 1000	≤ 1000	≤ 1000	≤ 1000
Beam span-to-depth ratio	≥ 7	≥ 7	≥ 7	≥ 7	≥ 7
Beam flange thickness (mm)	≤ 25	≤ 25	≤ 25	≤ 25	≤ 44
Column depth (mm)	any	≤ 570	≤ 570	≤ 570	≤ 570
Rotation @ DL (radians)	0.013	0.018	0.018	0.018	0.020
Rotation @ SD (radians)	0.030	0.038	0.038	0.060	0.030
Rotation @ CP (radians)	0.050	0.054	0.052	0.060	0.045

Keys:

IWUFCs = Improved welded unreinforced flange connections.
WBHCs = Welded bottom haunch connections.
WTBHCs = Welded top and bottom haunch connections.
WCPFCs = Welded cover plate flange connections.

RBSCs = Reduced beam section connections.
DL = LS of damage limitation.
SD = LS of severe damage.
CP = LS of collapse prevention.
d_c = Column depth.
d_b = Beam depth.
l_h = Haunch length.
l_{cp} = Cover plate length.
a = Distance of the radius cut from the beam edge.
b = Length of the radius-cut.

It is instructive to note that the location of the plastic hinges in the beam is, in all cases, shifted away from the column face; however, such location is as a function of the reinforcing detail. Moreover, the rotations derived in experimental and analytical tests at different LSs (i.e., damage limitation, severe damage and collapse prevention) are sufficient to enhance the seismic performance of steel frames. Recommended member sizes have also been included in Table 3.11; they may be used as rough guides in the design of the rehabilitation measure.

3.4.2.5. OTHER STEEL BEAM-TO-COLUMN CONNECTIONS

Several other repairing strategies have been proposed for beam-to-column connections; further details may be found, e.g., in the recent FEMA State of Art Report (FEMA 355D, 2000). Some of these configurations are aimed at solving common drawbacks of the types of connections discussed above in Sections 3.4.1.1 through 3.4.1.4. For example, strengthening with upstanding ribs is a viable alternative to cover plate connections (Figure 3.46). Indeed, it does not require large groove welds; hence, minimizes the detrimental effects due to the high shrinkage. Moreover, through thickness, brittle facture of the column flange is prevented by minimizing the stress concentration (triaxiality) at the column face. Nevertheless, this solution, as for haunch connections, is more expensive than cover plate.

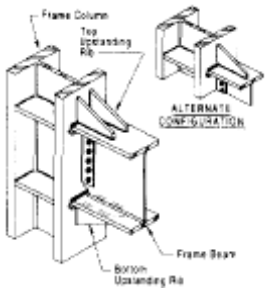

Figure 3.46. Reinforced connection with upstanding ribs (*after* Engelhardt and Sabol, 1998).

Similarly, proprietary connections have been included in recent guidelines for the rehabilitation of existing steel buildings (FEMA 351, 2000). These configurations (Figure 3.47) employ the basic concepts of strengthening (side plate and bolted brackets) or weakening (slotted beam web) the connection. Their main advantages of the most common schemes are provided in Figure 3.47.

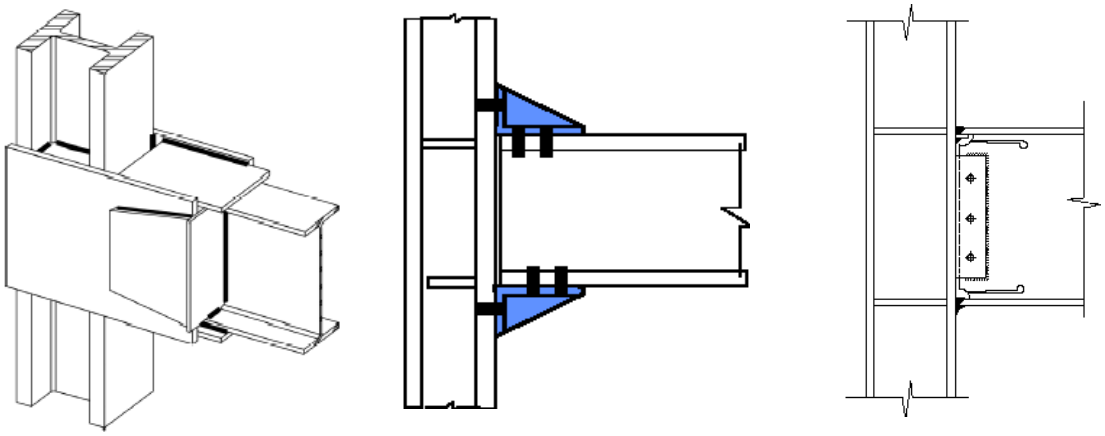

- Physical separation between beam and column.
- Through-thickness fracture is eliminated.
- Triaxial stress concentration is eliminated.
- Stiffness and strength of panel zone is increased.

- Connection rigidity is increased.
- Through-thickness fracture is eliminated.
- Triaxial stress concentration is eliminated.

- Physical separation between beam flanges and web, without changing the flexural stiffness of the beam.
- Stress concentration at flange-to-web intersection is eliminated.
- Beam full plastic moment is achieved.
- LTB of the beam is limited.
- Fatigue life is enhanced.

Figure 3.47. Proprietary connections for existing buildings and relevant advantages: side plate (*left*), bolted bracket (*middle*) and slotted beam web (*right*) (*after* FEMA 351, 2000).

In addition, to achieve web yielding and preventing stress concentrations at the column flange, an alternative option is the reduced web connection (Figure 3.48) in which weakening of the beam web is carried out in the proximity of the connection. In some cases, the openings may be spread along the beam span, thus allowing services to be fitted in them. This type of scheme has been suggested in recent US guidelines for new steel building (FEMA 350, 2000).

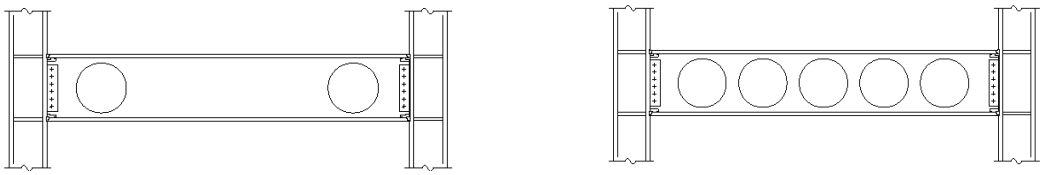

Figure 3.48. Web reduced connections (*after* FEMA 350, 2000).

On the other hand, existing framed buildings may employ simple shear tab connections (Figure 3.49) or other web connections, which were originally designed to sustain only vertical loads. These connections may either be with composite slab or bare steel beam and columns. It has been found that web connections, generally considered pinned in the design, have substantial rotational capacity and may provide supplemental stiffness and resistance to the frame (Liu and Astaneh, 2000). As a result, the cost of seismic retrofitting of existing steel and/or composite structures may be reduced by considering these additional mechanical properties in the performance assessment.

Figure 3.49. - Typical shear tab connections: with (*left*) and without slab (*right*).

The properties of the typical shear tab connections (Figure 3.49) are summarized in Table 3.12; the rotations have been expressed as a function of the LSs proposed for structural retrofitting in Europe. It is worth noting that the rotations depend significantly on the bolt group depth (d_{bg}), i.e., distance from the center of top bolts to the centre of bottom bolts. The higher d_{bg}, the lower the rotation because deeper connections exhibit more significant binding effects. The binding between beam and column flanges, at the top and/or bottom, is more likely to occur as the beam depth and hence, the bolt group depth is increased.

Brittle facture with limited rotational capacity are caused by thick shear tabs and/or beam webs and inadequate tab welds. Therefore, it is essential to ascertain that the thicknesses of the joined components are not excessive and the welds are sound.

For shear tab connections with slabs, the composite action is generally lost when plastic rotations exceed 2.85 to 3.0% (Liu and Astaneh, 2000); however, the rotational capacity to sustain vertical loads is significantly larger.

Table 3.12. - Properties of shear tab connections.

	With Slab	Without Slab
Hinge location	Centerline of bolts	Column centerline
Beam depth	any	any
Column depth	any	any
Rotation @ DL (radians)	0.022	0.027
Rotation @ SD (radians)	0.039	0.128
Rotation @ CP (radians)	0.128	0.128

Keys: DL = LS of damage limitation; SD = LS of severe damage; CP = LS of collapse prevention.

The strength of shear tab connections may be assumed equal to the moment resistance of the bolt group (M_{bg}):

$$M_{bg} = \sum_{i=1}^{N} F_{b,p}^{i} \cdot d_i \tag{3.75}$$

where d_i is the distance between the *i-th* bolt and the centerline of the bolt depth d_{bg}; $F_{b,p}^{i}$ is the plastic shear resistance of each bolt; and N the number of bolts. The shear resistance of bolts refers to the resistance of the bolts with threads.

As a rule of thumb, the connection resistance is generally between 10 to 25% of the plastic beam capacity. However, when composite slab is present (Figure 3.50) the compressive stress of the concrete should be properly accounted for in the evaluation of the positive moment capacity of the connection, while the evaluation of the negative moment should include the reinforcement bars of the slab. Shear tab connections with slabs have non-symmetric behavior under positive and negative moments due to the cracking of the concrete of the slab. Concrete slabs shift the PNA upwards hence, they may provoke detrimental effects at the beam bottom flange; guidelines for the PNA provided in Section 3.2.1. By contrast, composite slabs enhance the stability of simple connections

and reduce the strength deterioration at large rotations. However, the composite action is considered effective if adequate shear connectors are placed between the steel beam and the slab and the reinforcement steel is adequate. Such requirements should be checked in existing buildings because they may not be satisfied in old framed buildings. Nevertheless, studs should not be placed in the region of potential plastic hinges in the beam for a distance equal to the beam depth from the location of the maximum strain hardening moment.

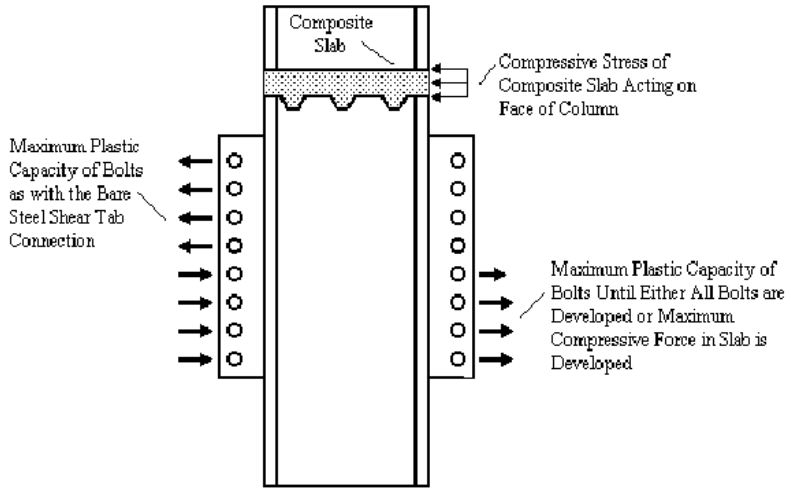

Figure 3.50. Actions for the evaluation of moment capacity in a composite shear tab connection.

Moreover, the secant stiffness of shear tab connections K_s may be assumed as follows:

$$K_s \cong 3160 \cdot (d_{bg} - 140) \tag{3.76}$$

with K_s in kNm and d_{bg} expressed in mm; as a rule of thumb, it ranges between 30% and 150% of the beam flexural stiffness EI/L. The secant stiffness corresponds to rotations at which 50% to 70% of the maximum connection resistance is achieved.

On the other hand, shear tab connections, if inadequate, may be retrofitted by adding top and/or seat cleats; thus, upgrading the simple shear connections in semi-rigid (Figure 3.51). In fact, it has been found that bolted semi-rigid connections (e.g., top, seat and web angles (TSWAs)), provide substantial ductility and stable hysteretic behavior (Nader and Astaneh, 1992; Elnashai *et al.*, 1998). This eliminates the need for imposing column-to-beam overstrength factors in the presence of partial strength connections. As a consequence, relaxations of beam cross section slenderness limitations are possible and thus, significant economies are achieved for the frame upgrade. Moreover, frames with semi-rigid connections may attract lower loads and possess higher damping than welded MRFs. The benign effect of semi-rigid connections is two-fold: period elongation of the frame, as well as the higher energy absorption in the connection.

TSWAs are generally partial strength connections, allowing 40% to 70% of the beam plastic capacity to be achieved. Their secant stiffness K_s may be assumed equal to:

$$K_s \cong 100 \cdot M_{fail,con} \tag{3.77}$$

where $M_{fail,con}$ is the moment associated to the connection failure mode.

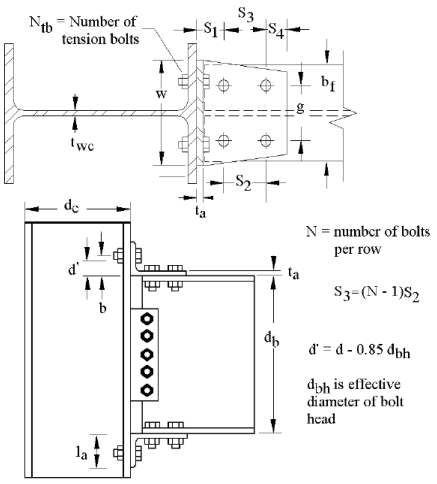

Figure 3.51. Typical layout for connection with top, seat and web angles.

Typical failure modes for beam-to-column connections with top, seat and web angles are as follows (Figure 3.52):

- Plastic bending capacity of upstanding leg of the angle.
- Shear fracture of bolts between outstanding leg of angle and beam flange.
- Fracture of tensile bolts.
- Net section fracture of outstanding leg of angle.

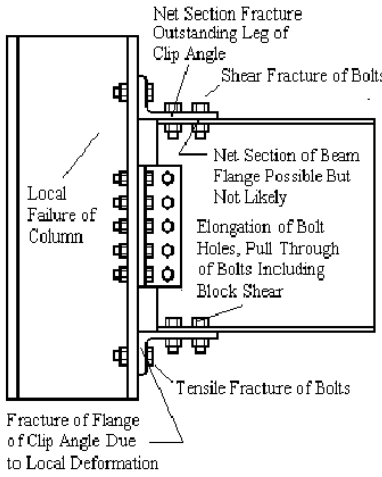

Figure 3.52. Typical failure modes for connections with top, seat and web angles (*after* FEMA 355D, 2000).

Bending moments associated to each of the above failure modes may be evaluated through equilibrium equations (FEMA 355D, 2000). However, because both legs of the angle generally have the same thickness, it is likely that the net section fracture of the outstanding leg of the angle controls the connection capacity. In such a case, the connection moment $M_{fail,con}$ is given by:

$$M_{fail,con} = f_{ta} \cdot [W - 2 \cdot (d_{bt} + 0.125)] \cdot t_a \cdot (d_b + t_a) \cdot \frac{L - d_c}{L - d_c - 2 \cdot S_1} \tag{3.78}$$

where d_b is the bolt diameter; L the distance between column centerlines; f_{ta} is the tensile strength of the angle; and W is equal to:

$$W = g + S_3 \cdot \tan(60 \cdot t_a) \tag{3.79}$$

All of the other dimensions are provided in Figure 3.51.

It is worth noting that whenever simple web connections are strengthened and/or upgraded, e.g., as semi-rigid, additional moments are transmitted to column members. Therefore, it is necessary to check the stability of such members under the gravity loads as well as the new loading condition.

Alternative schemes have recently been proposed for partially restrained connections (PRCs); e.g., an innovative steel PRC with NiTi-SMA tendons has been recently assessed (Des Roches *et al*., 2001). Such scheme relies upon the mechanical properties of SMAs, i.e., shape memory effects and superelastic effects (Section 2.5.3). In the pseudoelastic temperature range, NiTi components not only dissipate energy but also provide the connection with restoring forces. SMA tendons, e.g., 20 to 40 mm diameter rods, may be connected to the column from the top and bottom flanges of the beam (Figure 3.53). Experimental tests showed that the connection behavior is stable and with significant energy dissipation. Moreover, the tendons may recover by heating the original shape even after large deformations and the connection dissipative capacities are preserved. Butan torches are very effective to provide high level of heat at a rapid rate. By contrast, heat tape has the ability to wrap around the tendon, thus uniformly heating it. However, the rate of heat is slow and the maximum temperature more limited, i.e., 140 ^{o}C (heat tape) *vs*. 288 ^{o}C (butan torches).

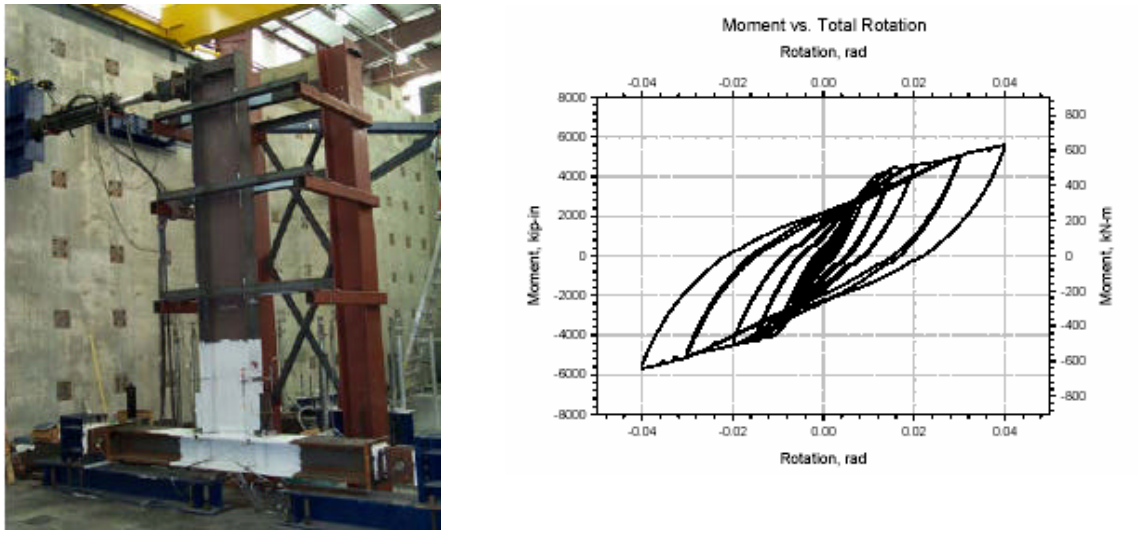

Figure 3.53. Partially restrained connection with SMA tendons: experimental sub-assemblage (*left*) and moment-rotation diagram (*right*) (*after* Des Roches *et al*., 2001).

Supplemental damping may be provided to PR connections via bolt slippage and/or additional friction plates placed at the steel interface (Figure 3.54). However, high number of bolts and long flange plates are required to enhance the moment capacity of such connections, particularly if the friction acts in single shear. Moreover, long slotted holes along with beam gaps are necessary to achieve rotations as high as 3%e.g., slot lengths should be not less than the bolt diameter plus 40 mm while the gap is as a function of the beam depth.

Due to the connection costs, the installation costs (e.g., opening and closing of the floor slab) and likely deterioration of long term friction, these connections have not become very popular; though, design rules are given in literature (Astaneh, 1995; Astaneh, 1997). Brass and bronze have been used as friction plates at the steel interfaces. However, stainless steel is a viable alternative for such applications due to the excellent material properties, as discussed in Section 2.5.2.2.

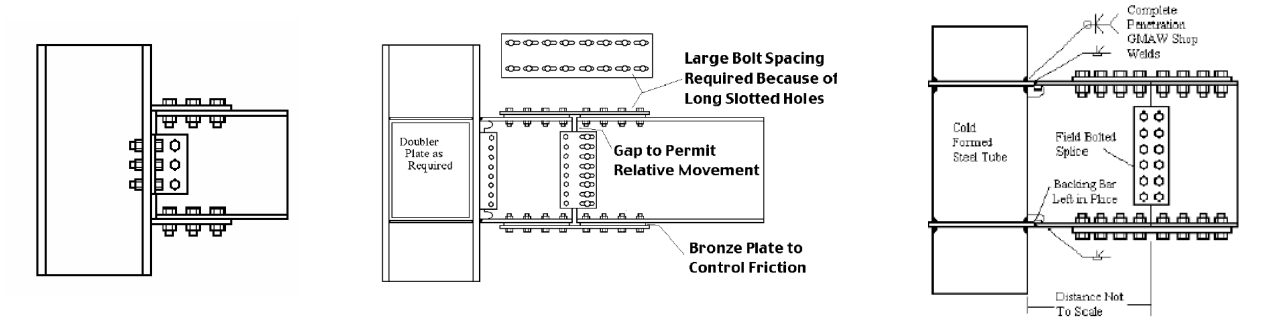

Figure 3.54 Partially restrained connection with additional damping: simple bolted flange plate (*left*), bolted flange plates with friction plates (*middle*) and typical Christmas tree connection (*right*).

Figure 3.54 also shows a typical configuration of a new Japanese connection (*Christmas tree*) with column box section. It is worth mentioning that box column connections exhibit generally outstanding rotation capacities (Nakashima *et al*., 1998). Moreover, they provide effective lateral support to beams and beam-to-column connections, thus preventing their LTB. Due to their large torsional stiffness, box columns are unlikely to buckle laterally; by contrast, they are very efficient for weak-axis bending. Biaxial bending and can be used to minimize the depth for deep columns. Therefore, box sections for column represent a viable solution for seismic upgrading of steel and/or composite structures. However, to ensure good seismic performance it is required to check that (FEMA 355D, 2000):

- Continuity plates are welded internally to all sides of the column box; such plates should be as thick as the beam flange.
- Web connection should not be the weakest link of the joined part because it can reduce the rotation ductility.
- The panel zone should not contribute significantly to the rotation of the connection.

3.4.2.6. COMPOSITE BEAM-TO-COLUMN CONNECTIONS

Several alternative schemes may be used to upgrade beam-to-column connections by relying upon the composite action. For example, typical configurations for fully restrained connections are given in Figure 3.55; they consist of steel beams framing in RC, encased or filled column, respectively. Encasement of steel components is very effective to prevent local buckling provided that the concrete is adequately confined. However, transverse steel plates (*face bearing plates*) should be used to stiffen the flanges of the beams framing into either RC or encased columns. Experimental tests showed that such plates are very effective for the concrete confinement in the joint and represent a viable solution to avoid the congestion of reinforcement at the joint (Sheikh *et al*., 1989). Moreover, it should be ascertained that transverse reinforcement bars in the slab around columns are compliant with the requirements for composite new buildings (EC8, 1998). Transverse bars are essential to provide confinement to the concrete and resist internal tensile forces; bars with small diameters are advised to control the slippage within the joint. Transverse reinforcement is also effective to reduce the cracking of concrete. Further details on composite member confinement may be found in Sections 3.2 and 3.3 and relevant European standards for concrete (EC2, 1992), composite (EC4, 1994) and seismic design (EC8, 1998).

It is worth noting that connection configurations with steel beams through joint (Figure 3.55) avoid the typical undesirable failure mode of welded connections, i.e., brittle fracture of the welds. Moreover, they are highly cost-effective because of the ease of construction, e.g., neither field

welds nor bolting is required. By contrast, connections between steel beams and encased columns, which are very common in Japan, require welding of beam flanges to the steel column (AIJ, 1991).

However, FR composite connections, provided in Figure 3.56, exhibit (AISC, 1997) rotations not less that 3%; thus, they may be used to achieve adequate performance for existing steel and composite buildings.

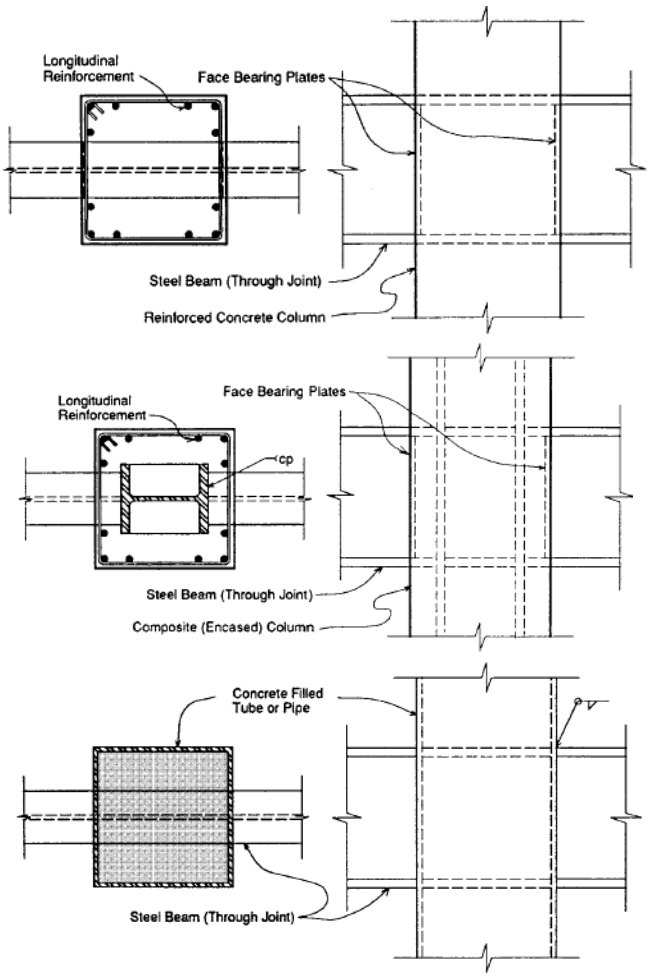

Figure 3.55. Composite beam-to-column connections: RC (*top*), encased (*middle*) and hollow section (*bottom*) column (*after* AISC, 1997).

On the other hand, PR composite connections may be used to achieve large plastic deformations without fracturing (Leon *et al*., 1998). Typical layouts of such connections employ (Figure 3.56) shear tab or double angle web connections and seat angle for the beam bottom flange. Full interaction shear studs are welded to the beam top flange while reinforcing bars are placed around the column, thus activating the composite action. This type of connection exhibits significantly higher moment capacity than a typical top and seat angle connection. Indeed, the reinforcing steel of slab has generally higher strength than structural steel and the lever arm of tensile and compressive forces is increased because of the slab. Similarly, the rotational stiffness is higher due to the slab and fully tensioned high strength bolts, if any.

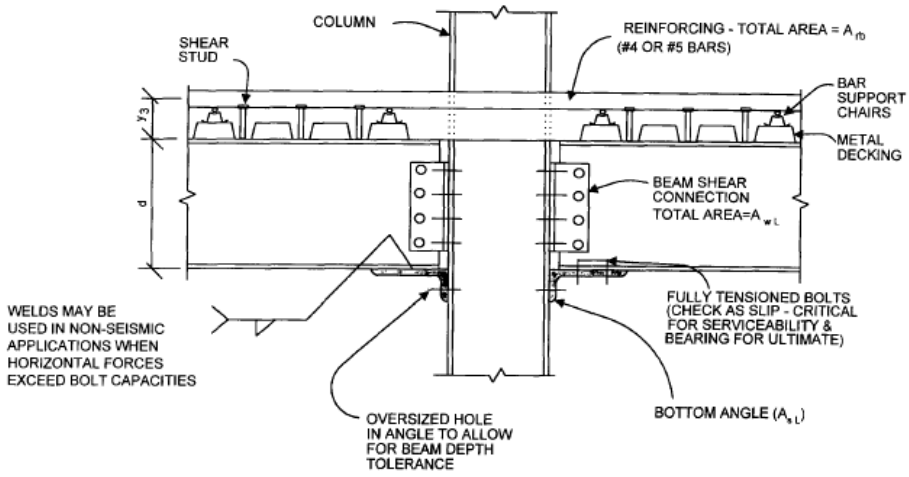

Figure 3.56. Typical partially restrained composite connection: seat angle and double angle web connection (*after* ASCE, 1998).

The design of PR composite connections requires the selection of the connection strength and stiffness. It was found that the most efficient designs require connection strength equal to 75% of the bare steel beam plastic moment (Leon, 1994). The US seismic guidelines for composite buildings (AISC, 1997) require that PR composite connections should have minimum strength equal to 0.50, the nominal plastic capacity of connected bare steel beam ignoring composite action. However, a set of limit states (LSs) should be checked when designing PR connections; these LSs are provided hereafter:

- Shear strength for bolts attaching the seat angle to the beam.
- Bearing strength at the bolt holes.
- Tension yield and rupture of the seat angle.
- Tension strength, including prying action, for the bolts connection the beam to the column.
- Shear capacity of the web angles and seat angle.
- Block shear capacity of the web angles.
- Number and distribution of reinforcing bars in the slab, including transverse reinforcement, to ensure proper strut-and-tie action at ultimate.
- Number and distribution of shear studs to provide adequate composite action.
- Column stiffener requirements.

Analytical and experimental tests have shown that the controlling design parameters are the thickness of the seat angle and the shear capacity of the bolts between the seat angle and the bottom beam flange (ASCE, 1998). In particular, the former controls the positive bending (Figure 3.57) and the latter the negative moments. Thus, it is advised to increase the seat angle thickness and the bolt capacity to enhance the connection strength.

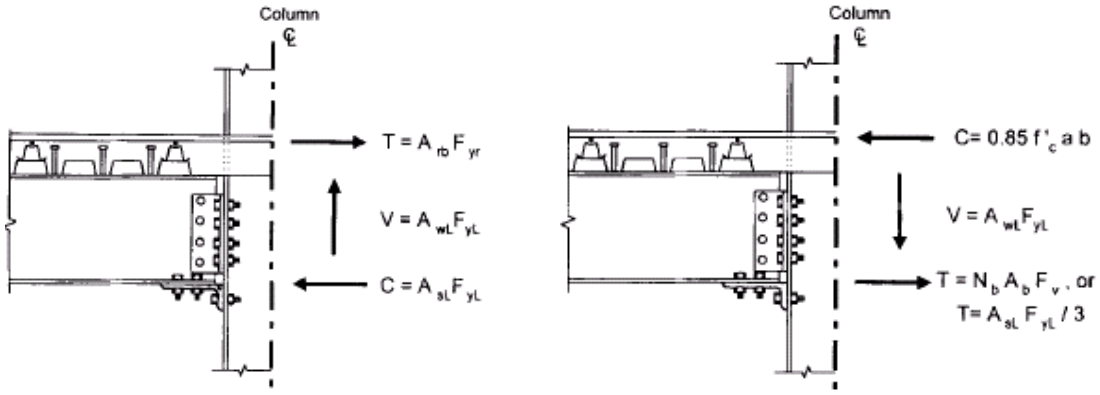

Figure 3.57. Force transfer mechanism in PR seat angle and double angle web composite connection: negative (*left*) and positive (*right*) moment.

The design of PR composite connections may be carried out by assuming that the shear is assigned to the web angles and the bending to the slab reinforcement and beam bottom flange. A step-by-step design procedure is provided hereafter:

1. Consider the plastic moment of the bare steel beam (M_{pb}) and assume that the connection (M_c) will transfer 75% of M_{pb}:
$$M_c = 0.75 \cdot M_{pb} \tag{3.80}$$

2. Compute the slab reinforcement (A_{rb}) necessary to carry the connection moment (M_c):
$$A_{rb} = \frac{M_c}{(d_b + d_1 + d_2) \cdot f_{y,rb}} \tag{3.81}$$
where d_b is the beam depth; d_1 is the right height (metal deck); d_2 should be assumed equal to 10 mm; and $f_{y,rs}$ is the yield strength of the reinforcement bars.

3. Select the seat angle whose leg area (A_{sl}) is capable of transmitting a tensile force equal to 1.33 times that due to the slab reinforcement. This requirement ensures that the angle possesses adequate stiffness when loaded under positive moments.

4. Select the bolts between the beam and the angle. They should be designed for a shear force equal to 1.25 times the shear in the slab in order to avoid that the failure mechanism of the connection is governed by shearing in the bolts. This above figure, i.e., 1.25, accounts for the material overstrength (f_u/f_y) of the reinforcement bars. However, if higher values of the f_u/f_y ratio are expected, they should be replaced by 1.25 in the calculations.

5. Select the double web angles which may withstand the design shear.

Finally, it should be pointed that check CBMRs allowance should be made for all components of the members that may increase the nominal strength of the connection.

3.4.3. BRACING CONNECTIONS

Surveys carried out during past earthquakes showed that braced frames, particularly concentric braced frames (CBFs), exhibit extensive damage at bracing connections if they are not properly designed (AIJ, 1995; Tremblay *et al*., 1996). For example, typical damage to non-ductile CBFs are: (i) net section fracture at bolt holes, (ii) weld fracture, (iii) fracture of welded connections and web tear-out in brace, (iv) local buckling and (v) distortion of the beam without lateral support at location of chevron braces. To achieve adequate strength and ductility and hence, to enhance the seismic performance, design requirements for bracings have been provided in Section 3.3.4. However, recommendations for the bracing connections in steel and composite framed buildings are also required; some of them are thus discussed herein.

During a severe earthquake, bracing members are subjected to large deformations in cyclic tension and compression in the post-buckling range. Therefore, brace connection design should be based upon axial loads and account for the effect of the brace member cyclic post-buckling behavior (Goel, 1992-a; Goel, 1992-b). The required strength of the bracing connection should be adequate to prevent brittle fractures of the connection and failure by out-plane gusset buckling. Net section fractures and block shear rupture at the end of the brace should be avoided by referring to expected rather than nominal strengths in the capacity design checks. Thus, bracing connections should resist axial forces equal to $f_{ye,b} \cdot A_{gb}$, with $A_{g,b}$ the gross area of the brace. Moreover, to avoid yielding in bending; the flexural strength of the connection should be not less than $1.10 \cdot M_{pe,b}$ with $M_{pe,b}$ the expected moment of the brace about the critical buckling axis.

On the other hand, fixed end connections should be preferred to those that are pinned (Goel, 1992-b). The former increase the number of plastic hinges that can occur in the brace, three (fixed) *vs.* one (pinned) and hence, improve the dissipation capacity of the braced system. Notwithstanding, adequate detailing may be used to provide pinned end connections with adequate seismic performance. For example, to permit ductile out-of-plane brace buckling where a single gusset plate connection is used, it is recommended to provide a clear distance of twice the plate thickness (*t*) between the end of the brace and the assumed line of restraint for the gusset plate (Figure 3.58) (AISC, 1997). This restraint corresponds to the line about which the gusset plate may bend unrestrained by the beam, column or other brace joints. Adequate plastic rotations can be accommodated and buckling of the gusset plate prevented; the result of the ductile out-of-plane buckling is the hysteretic response provided in Figure 3.58. Alternatively, connections with stiffness in two directions, e.g., crossed gusset plates, may be used.

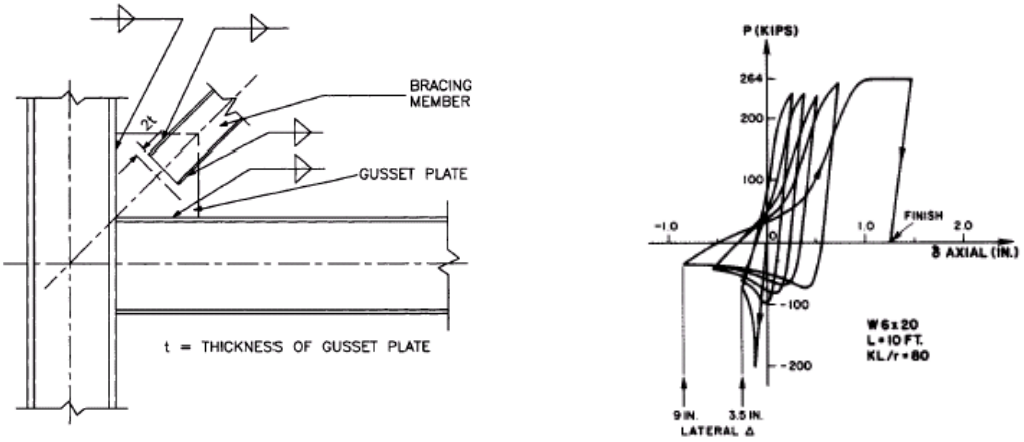

Figure 3.58. Improved brace-to-gusset connection: configuration (*left*) and hysteretic response (*right*) (*after* AISC, 1997).

To improve out-of-plane stability of the bracing connection it is not recommended to interrupt the continuity between beams and columns. Furthermore, the lateral supports of both beam flanges should be designed for a force not less than 2% of the expected beam flange strength, i.e., $0.02 \cdot f_{ye,b} \cdot b_f \cdot t_f$. It is worth noting that this requirement is more stringent than counterparts in the US guidelines, which refer to the nominal strength of the beam flange rather than the expected value (AISC, 1997).

In eccentric braced frames (EBFs) it is required to avoid that the intersection of the brace and the beam centerlines is located outside the link. Indeed, in such detail the eccentricity and the brace axial force produce additional moment in the beam and the brace. Thus, connections between the diagonal brace and the beam should have centerlines intersecting either within the length of the link or at its end (Figure 3.59). Connections at the end of the link should be designed to develop the expected strength of the brace, including overstrength due to composite action, if any. No parts of the connection should be extended over the link length; thus the detrimental effect of shortening the link is avoided. Short (shear) links exhibit higher dissipation capacities than longer (bending) links. For brace and beam centerlines intersecting within the link, an eccentricity advantageously reduces the bending moment at the end of the link. As a consequence beams and braces with lower flexural capacities are required.

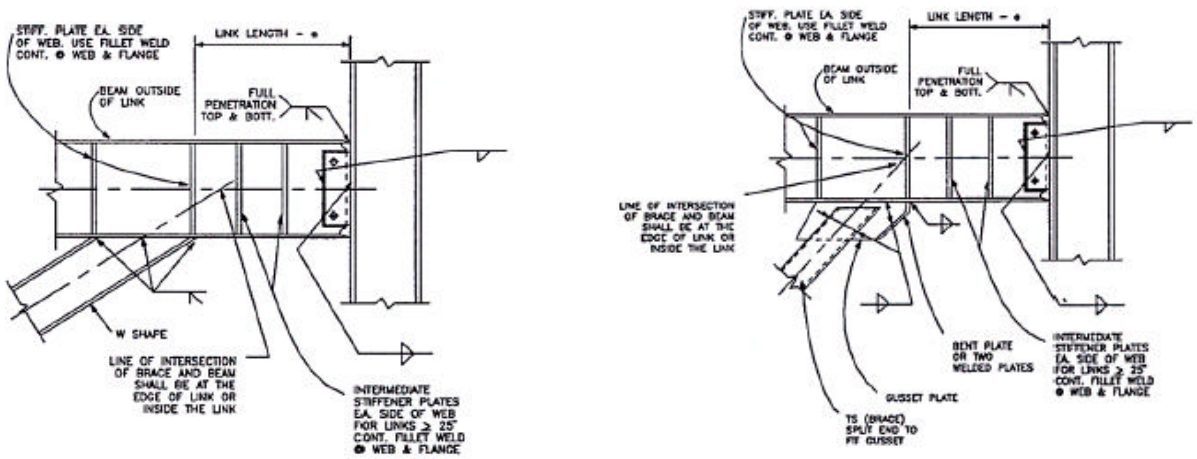

Figure 3.59. Brace-to-beam connection: intersection within (*left*) and at the end of the link (*right*). (*after* Naeim, 2001).

Braces may be either fully restrained or pin-connected to the link. Pinned connections, which are very common for EBFs with short links, should employ gusset plates with stiffeners at the free edges; this requirement prevents local buckling (Roeder and Popov, 1978). Moreover, the beam should resist the entire link moment.

Finally, careful detailing is required for composite bracing connections, either in CBFs or EBFs. They should withstand the full tensile/compressive strength capacity of the brace. The contribution of the concrete for composite braces should be considered when the capacity design of the connection is carried out. Typical configurations for composite connections in CBFs are shown in Figure 3.60: they employ encased and concrete filled columns, while the steel braces are double angles and H-sections, respectively. However, encased columns connected to H-shape steel braced are also used.

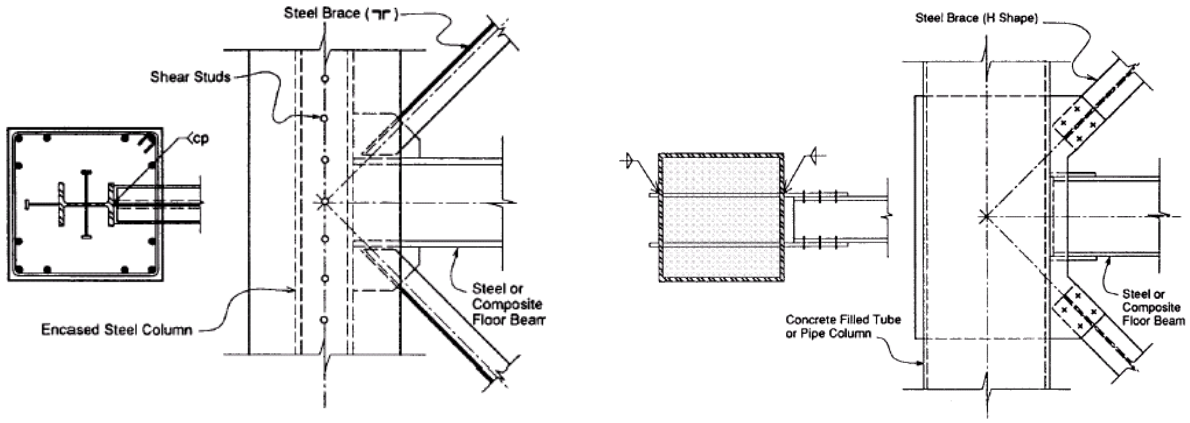

Figure 3.60. Brace-to-beam connection for CBFs: encased (*left*) and concrete filled column (*right*). (*after* AISC, 1997).

Composite connections for EBFs should conform to the requirements for CBFs where the link is not adjacent to the column face. For link-to-column connections at column flange instead, it is advised to employ face bearing plates between the beam flange plates as for composite MRFs. Further details on the link connections are provided in the next section.

3.4.4. LINK CONNECTIONS

Links in EBFs act as a structural fuse to dissipate the energy due to the earthquake ground motions. Adequate strength and stable energy dissipation in such links is significantly influenced by the detailing, particularly at the connection with diagonal members and beam-columns.

Link connections should be capacity designed considering the expected resistance of the links; reference should be made to relevant steel strengths as in Section 3.1. Expected values should include the overstrength due to the presence of the composite slab, if any. It is advised to amplify the link expected shear strength ($V_{pe,l}$) as follows:

$$\overline{V_{pe,l}} = 1.25 \cdot V_{pe,l} \tag{3.82}$$

where the amplification factor (1.25) accounts for the overstrength. It is instructive to note that the US guidelines (AISC, 1997) recommend the value as given in Equation (3.82) to design only diagonal braces; a lower value for the strain-hardening, i.e., 1.10 *vs.* 1.25, is advised to design beams and columns. Nevertheless, Equation (3.82) is suggested for European practice where, for example, shallower I-sections are used for beams along with fully restrained shear studs; the contribution of the composite slab is thus generally more significant.

Link-to-column connections in EBFs are subjected to plastic demands similar to those for beam-to-column connections in MRFs. Recent surveys showed that brittle fracture is a typical failure mode of welded link-to-column connections, particularly for long (bending) links (AIJ, 1995; Youssef *et al*., 1995). Therefore, reinforced connections (e.g., coverplates, ribbed or haunched [Section 3.3.1]), should be used to repair damaged connections; they prevent large inelastic strains in the transition zone between links and columns. Such reinforcements should be designed to behave linearly. Their strength should account for the fully yield and strain hardening of the link strength; the shear strength of the link as in Equation (3.82) should be used for design checks. Moreover, it should be considered that the strengthening of link-to-column connections may modify the link length. Links connected to the column should be short. However, it is advised that shear link should not exceed the following limit (e_{lim})

$$e_{\lim} = \frac{1.6 \cdot M_p}{V_p} \tag{3.83}$$

where M_p and V_p are the plastic bending and shear capacity of the steel bare link. The limit in Equation (3.83) ensures that low-cycle failure of the link flanges due to large strains is prevented (Engelhardt and Popov, 1989). Similarly, welded connections of the link to the column weak-axis should be avoided because they are prone to brittle fracture. Alternatively, bolted partially restrained connections may be used provided that the links yield in shear (short link). The latter design choice is advantageous, particularly for seismic retrofitting (Lu *et al*., 1994):

- Yielding capacity and stiffeners of partially restrained EBFs are the same as those of fully restrained EBFs.
- Failure mode (eventual) of the partially restrained connection is more gradual than those fully restrained.
- Adequacy for retrofitting of weak MRFs as gravity frames employing partially restrained connections.

Furthermore, end lateral supports should be provided at both top and bottom flanges of the link. Such supports should be designed for a force not less than 6% of the expected link flange strength, i.e., $0.06 \cdot f_{ye,f,l} \cdot b_{f,l} \cdot t_{f,l}$.

On the other hand, the diagonal brace-to-beam connection at the end of the link should be fully restrained if the brace resists to the link end moment. However, such connections should not extend along the link length.

3.5. SYSTEM RETROFITTING

3.5.1. GENERAL

Several rehabilitation strategies may be adopted for steel and composite structures (FEMA 273, 1997; FEMA 351, 2000; FEMA 356, 2000). These strategies are generally aimed at strengthening and/or weakening the as-built structural system or modifying physical and mechanical characteristics which influence the dynamic response, e.g., strength, stiffness and damping. They are grouped in two fundamental approaches:

- Local modification of structural components.
- Global modification of the structural system.

Local modification of structural components, e.g., enhancement of stiffness and/or strength and/or ductility of members and connections, may improve the seismic performance of existing buildings damaged by earthquakes. The global seismic response of steel and composite structures depends on the behavior of their components (Elnashai, 1994); e.g., Figure 3.61 shows the conceptual relationship between local and global seismic response characteristics. Furthermore, a significant erosion of the local ductility is typically found in steel structures (Gioncu, 2000); thus, it is important to ascertain that the system components possess adequate reserve to give rise to acceptable seismic performance of the frame as a whole.

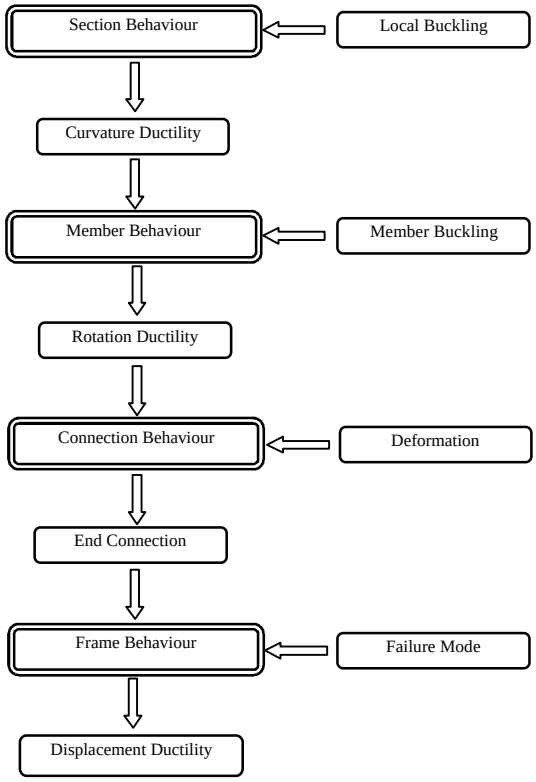

Figure 3.61. Conceptual relationship between local and global seismic response characteristics (*after* Elnashai, 1994).

The modification of vulnerable structural components, e.g., connections, is benign because it increases the allowable drift angles and the roof drifts, thus enhancing the global ductility of framed structures. The total deformation of MRFs, either steel or composite, is the aggregate of member and connection deformations. Moreover, the rotation and deflection ductility of members are related to the overall ductility of frames. At the onset of plastic hinging, curvatures are concentrated at the plastic hinge and the remaining part of the member is near straight. To achieve target deflection ductility, appreciably higher curvature ductility will be required at the plastic hinge. For example, based on plastic analysis, the plastic roof drift (d_p) is related to the plastic rotation ($?_p$) through the following equation:

$$d_p = d_u - d_y = \frac{q_p}{H_0} \tag{3.84}$$

where H_0 is the sum of the interstory height of stories involved in the collapse mechanism as shown in Figure 3.62. Global mechanisms with plastic hinges at column base and within beams should be preferred due to the higher energy dissipation capacity.

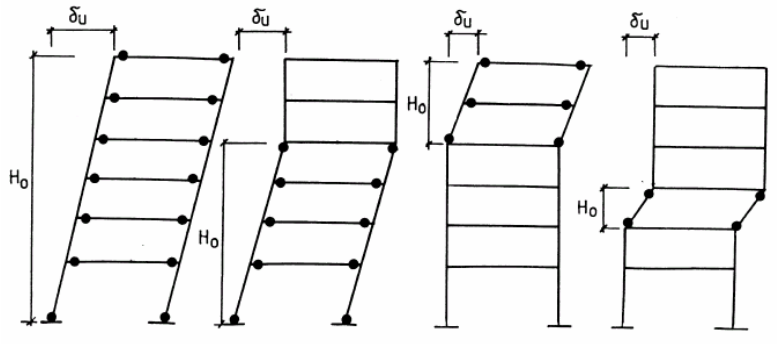

Figure 3.62. Typical plastic mechanisms for MRFs (*after* Gioncu, 2000).

An experimentally-derived expression for the deflection ductility (μ_d) of MRFs, taking into account the level of axial load (N/N_y), is as follows (Sakamoto and Miyamura, 1966):

$$m_d = 0.7 + \frac{0.3 \cdot \sqrt{E/f_y}}{\sqrt{\left(N/N_y\right) \cdot \left(\frac{K \cdot l}{r}\right)}} \tag{3.85}$$

thus showing that the frame ductility is also a function of the member slendernesses (kl/r).

In Japanese practice, the member (μ_m) and frame (μ_f) ductility ratios are related through (Kato, 1994),:

$$m_f = \frac{2}{3} m_m + 2 \tag{3.86}$$

This relation is derived by a semi-empirical procedure assuming that plastic deformation occurs in one member only, then making an allowance for neglected deformations (Kato and Akiyama, 1982).

Local remedies, such as retrofitting of connections, are not sufficient to significantly improve the global response of buildings with inadequate stiffness, strength and ductility. Moreover, repairing all beam-to-column connections may be uneconomical because the number of connections is high and the intervention is not cost-effective. Repairing the connections, either by strengthening or weakening, though is important to avoid brittle fracture in the most vulnerable parts of the frame. Similarly, columns and braces should be retrofitted in such a way they do not fail prematurely, thus ensuring the stability of the building.

It is worth noting that the objective of local retrofitting approaches is to increase the deformation capacity of deficient components so that they will not reach their specified limit state as the building responds at the design level (Figure 3.63). Further details on the requirements for retrofitting structural components and their connections have been provided in the previous sections, i.e., Sections 3.2 through 3.4. This section deals primarily with strategies for global modifications of existing structures with structural deficiencies.

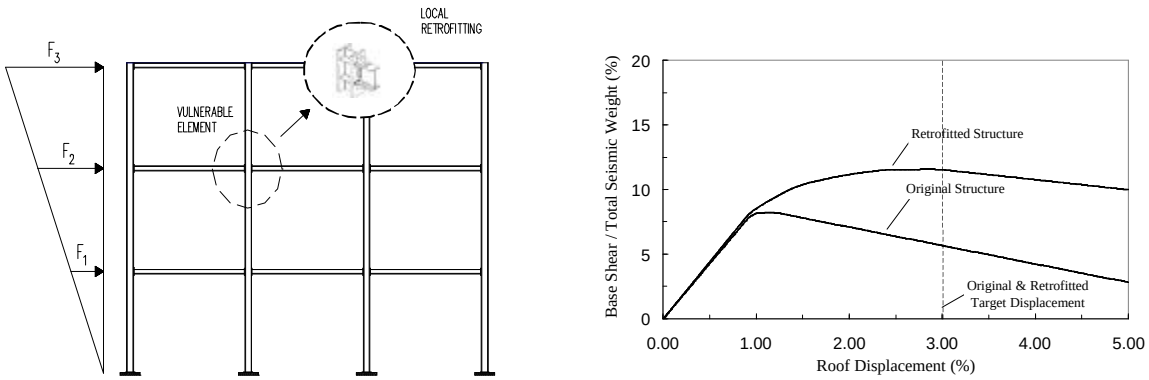

Figure 3.63. Characteristics of local intervention approaches.

Effective global upgrading strategies should be able to increase the capacity of the structure and/or decrease the demand imposed by earthquake loads. In fact, structures with enhanced capacities may safely resist the forces and deformations induced by earthquake response. Generally, global modifications to the structural system are designed so that the design demands, often denoted by target displacement, on the existing structural and nonstructural components are less than their capacities (Figure 3.64). Lower demands may reduce the risk of brittle failures in the structure and/or avoid the interruption of its functionality.

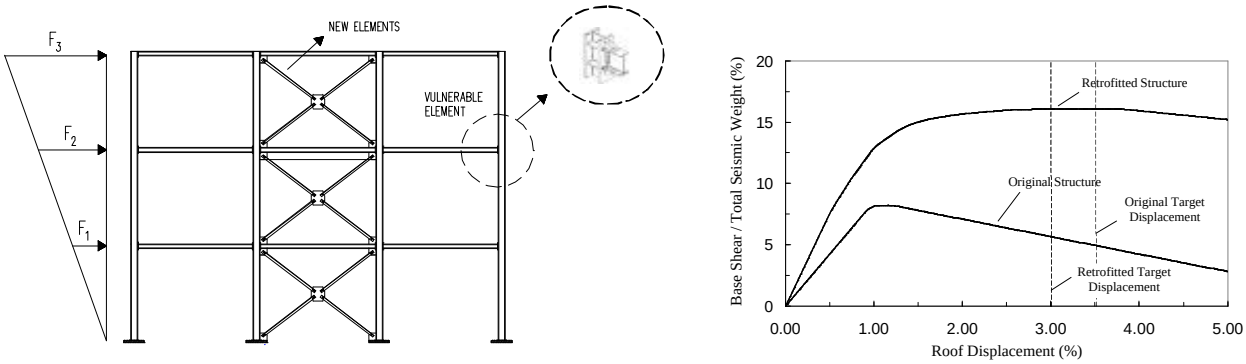

Figure 3.64. Characteristics of global intervention approaches.

The attainment of global structural ductility is achieved within the design capacity by forcing the inelasticity within dissipative zones and ensuring that all other members and connections behave linearly. Such design philosophy may be used in the seismic retrofitting of existing structures. In addition, it is of paramount importance to ensure:

- Continuity and redundancy between members, so as to ensure a clear and uniform load path for horizontal loads and prevent brittle failures.
- Regularity of mass, stiffness and strength distribution, to avoid detrimental torsional effects and/or soft-story mechanisms.
- Reduced masses and sufficient stiffness, to avoid highly flexible structures which may give rise to extensive non-structural damage and significant P-? effects.

Therefore, effective global rehabilitation approaches for steel and composite structures may include strategies to provide regular and ductile systems; supplemental energy dissipation devices are also desirable. Common intervention schemes are summarized hereafter:

- Removal or lessening of existing irregularities and discontinuities.
- Global structural stiffening.
- Global structural strengthening.
- Mass reduction.
- Seismic isolation.
- Supplemental damping.

Concentrations of high inelastic demands within irregular zones should be avoided. Thus, structural irregularities, such as soft and/or weak stories, torsional irregularities, discontinuity of the structural system in plan and/or elevation, should be modified in the existing structures and avoided in the re-design. To do so, introduction of new structural systems, e.g., new lateral resisting system (wall or braced frame), and strengthening or weakening of existing elements, are viable intervention schemes. On the other hand, the removal of structural and nonstructural components reduces also the global seismic weight thus attracting lower inertial forces.

The damage of structural and nonstructural elements is prevented by limiting the amount of deformation. Therefore, the seismic performance of the structure may be enhanced by stiffening its frame. The most effective way to provide global stiffening is to use braced frames and/or shear walls; dual systems are stiffer than ordinary MRFs. Alternatively, the augmentation of the composite action between steel beams and concrete slabs through shear studs, the encasement or beams and columns in RC and/or the upgrading of the pinned connections in gravity-load systems may be used to increase the global stiffness.

The enhancement of global stiffness is generally associated with an increase in the global strength. For example, concrete encasement substantially modifies the frame rigidity and increases the frame strength. It is worth noting, though, that resistance is not a very common deficiency for steel structures, particularly for welded MRFs (FEMA 351, 2000). However, additional global strengthening may be, however, achieved through via cover plates of members in lateral-force resisting systems and more significantly, by using bracings and shear walls.

On the other hand, the seismic performance of existing steel and composite structures may be improved by modifying physical and mechanical characteristics which influence their dynamic response, e.g., mass and damping. The advantage of reducing the mass is two-fold. First, lighter structures possess lower fundamental periods. Short-period structures do not generally exhibit damage, particularly at nonstructural components; in fact, spectral displacements are low for short periods. Second, seismic forces are inertial forces and hence, they are proportional to the mass; the seismic demand of lighter structures is lower than that of heavy ones. Mass reductions may be achieved by: (i) replacement of heavy cladding systems with lighter systems, (ii) removal of unused equipment and storage loads, (iii) replacement of masonry partitional walls with lighter systems and (iv) removal of one or more stories. The latter is a very invasive strategy which is necessary when substantial mass reductions are required. However, it is instructive to note that the relationship between mass and period is for a SDOF:

$$T = 2p\sqrt{\frac{m}{k}} \tag{3.87}$$

therefore, to effectively reduce the lateral displacement demand is required a substantial mass reduction. Alternatively, the dynamic response of steel and composite structures may be controlled

through nonconventional strategies, e.g., base isolation and/or dampers. The latter are very effective retrofitting strategies to enhance earthquake performances in building structures and/or whenever owners can afford the costs of design, fabrication, and installation of these special devices. However, it is essential to note that such costs are offset by the reduced need for stiffening and strengthening otherwise required for rehabilitation objectives.

The effectiveness of base isolation relies upon the elongation of the fundamental period and the introduction of supplemental damping in the original structure, i.e., fixed base (Figure 3.65). Large deformations can be accommodated within the isolators which generally possess high energy dissipation (high damping). As a result, such devices filter the input transmitted to the super-structure: lower forces and deformations give rise to low damage, if any. In fact, the super-structure experiences limited inelastic excursions. In the US seismic design (IBC, 2000), the response modification factor used to design the superstructure is two-thirds of the counterpart for fixed-base. However, seismic isolation is not a panacea; indeed, it is effective for relatively heavy and stiff superstructures. Moreover, if the strength of the existing structure is extremely low, e.g., less than 5% of the weight of the building, then additional strengthening should be considered (Naeim, 2001). Base-fixed structures with periods not greater than 1.0 sec can be upgraded with base isolators. The fundamental period is thus shifted to 2.0 or 3.0 seconds, as a function of the device used. Similarly, the damping rises from 1.0 to 5.0% for the base-fixed structure to 15.0 or 30.0% for the isolated system.

Dampers are energy dissipation devices which can be installed in steel and/or composite structures to reduce the amount of deformation and hence, limiting the damage. In fact, such devices provide in fact supplemental damping which enormously increases the structural damping: visco-elastic and viscous dampers may enhance the structural damping from 1.0 to 5.0%, to 40.0-50.0%; relatively lower values, around 10.0 to 20.0%, characterize hysteretic, friction and SMA dampers. Moreover, it is worth noting that steel structures are ideal candidates for damper devices because of their lateral flexibility. The energy dissipated by dampers depends upon the force transmitted by the structure and the distance through which this force acts. As a result, typical story drifts of steel structures enable the damper devices to dissipate energy at low forces. Furthermore, dampers avoid large concentrated forces to be applied to the structure. Passive seismic protection via dampers may be considered a mature technique today, particularly in the US and Japan where devices with different dissipative capacities are used. Further details on supplemental damping devices and base isolation may be found in Section 2.5.3.2.

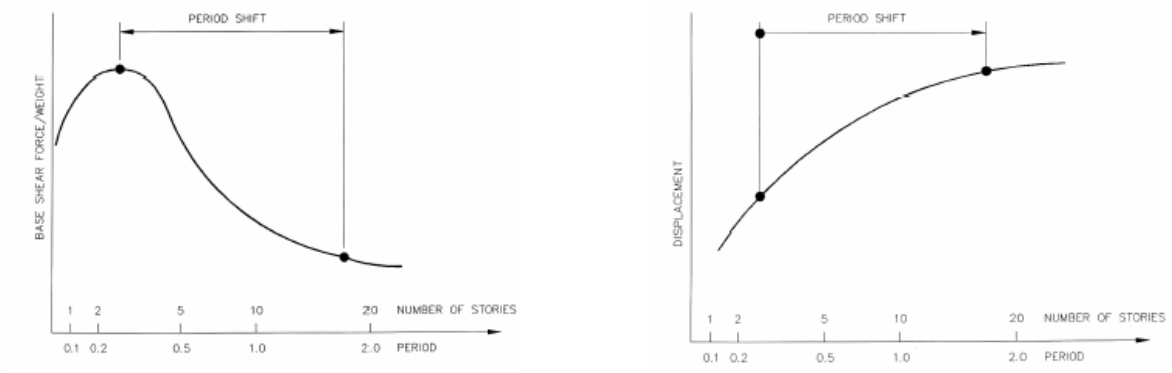

Figure 3.65. Effects of period shift due to base isolation (*after* Naeim, 2001).

Examples of significant seismic retrofitting of steel and composite frames as a whole are presented hereafter; however, the most common strategies have been summarized in Table 3.13, as a function of the structural typology, i.e., MRFs, CBFs and EBFs.

Table 3.13. Retrofitting strategies for steel framed structures.

	MRFs	CBFs	EBFs*
Retrofitting Strategy	• Encase columns and/or beams in RC. • Strengthen/weaken beam-to-column and column-base connections. • Augment composite slab participation. • Add braces to one or more bays at each story. • Add concrete or masonry infills to one or more bays at each story. • Add concrete shear wall. • Add new MRFs to the exterior of the building. • Use base isolation systems. • Add supplemental damping devices.	• Replace or modify braces with insufficient strength/ductility. • Replace tension only systems with tension/compression braces. • Encase columns and/or beams in RC. • Change the brace configuration. • Add concrete or masonry infills to one or more bays at each story. • Add concrete shear wall. • Reinforce inadequate connections. • Use base isolation systems. • Add supplemental damping devices.	• Add cover plates to beam flanges at link location. • Add doubler plates and/or web stiffeners to the link web. • Change the brace configuration.

Keys: Remedies similar to MRFs and CBFs may be used for EBFs.

It is instructive to note that some of the interventions modify the original configuration of the frame. For example, adding bracings may transform a MRF into CBF or EBF; similarly, adding concrete shear walls modify MRFs or simple CBFs and EBFs in dual systems. MRFs exhibit adequately ductile behavior under earthquake loading but their low transverse stiffness in particular situations may result in high story drifts, thus leading to unacceptable damage to non-structural components and appendages. This is the primary justification for using braced frames. However, the latter structural configuration often suffers from lack of ductility once compression braces buckle. EBFs may be then used to safeguard against this undesirable mode of failure. In this structural configuration, bending or shear link beams are provided between bracing points such that plastic hinges are developed there. This protects bracing members from buckling and increases energy absorption capacity through plastic yielding of the carefully-designed link member. Shear RC may also be used to stiffen and strength steel and composite frames. The seismic performance of the rehabilitated structures is discussed in the next section.

3.5.2. FRAMES WITH INFILLS

It has long been recognized that frame panel infilling has a profound effect on stiffness, strength and ductility of steel structures (Saneinejad and Hobbs, 1995). Extensive experimental and analytical studies carried out at Imperial College in the 1980s indicated that the increase of stiffness, strength and ductility due to the infill increases is a function of the bare frame stiffness (Moghaddam *et al*., 1988). An increase in stiffness of 15 to 40 times was observed over that of the bare steel frame. The strength enhancement was less and ranged between 2.75 and 9 times the corresponding bare frame strength. However, early work to address the strength and stiffness of steel frames with masonry infills was carried out in the 1960s (Holmes, 1961). The behavior of 13

small scale tests of different sizes, structural configurations and support conditions specimens was studied; the solid infills had an aspect ratio between $0.7 \leq h/l \leq 1.4$, where *h* is the height and *l* the length of the frame. As a result, a linear equivalent strut with a width equal to one-third of the panel diagonal length was proposed for computing the ultimate stiffness and strength of the infilled frames. The analytical model was suggested because of the large scatter of the experimental results. Moreover, it has been proved that the strut properties vary as a function of the applied load, e.g., the area of the strut is not linear. Thus, to analyze the infilled frame stiffness, it is advised to assume the strut width at one-half the peak load equal to three-fourths of the strut width for the initial stiffness (Flanagan and Bennett, 1999-b). At the peak load the strut width should be approximately one-half the strut width for initial stiffness, i.e., the secant stiffness at peak load should be one-half the initial stiffness of the infilled frame (Saneinejad and Hobbs, 1995). The strut area (A_d) and length (L_d) may be assumed as follows (Figure 3.66):

$$A_d = (1 - a_c) \cdot a_c + h' \cdot \frac{s_c}{f_c} + a_b \cdot t \cdot l' \cdot \frac{t_b}{f_c} \leq \frac{0.5 \cdot t \cdot h'}{\cos q} \cdot \frac{f_a}{f_c} \qquad (3.88.1)$$

$$L_d = \sqrt{(1 - a_c) \cdot h'^2 + l'^2} \qquad (3.88.2)$$

where h` and l` are the panel height and length, respectively; t is the infill thickness; θ the sloping angle of the diagonal of the infill; f_c is the compressive strength of the infill; and f_a is the permissible compressive stress at the infill in the central region, e.g., $f_a \approx 0.30 \cdot f_c$. The stresses σ_c and τ_b are the normal contact stress at the column top section and the shear contact stress at the beam edge, respectively. The maximum normal contact stresses in the beam ($\sigma_{b,max}$) and the column ($\sigma_{c,max}$) are:

$$s_{b,\max} = \frac{f_c}{\sqrt{1 + 3 \cdot m^2 \cdot r^4}} \qquad (3.89.1)$$

$$s_{c,\max} = \frac{f_c}{\sqrt{1 + 3 \cdot m^2}} \qquad (3.89.2)$$

where μ the coefficient of friction for infill-frame interface, e.g., μ =0.45 for masonry; and r is the aspect ratio of the infill, i.e., r =h/l. Note that either σ_c and σ_b should not exceed the values in Equations (3.89.1) and (3.89.2).

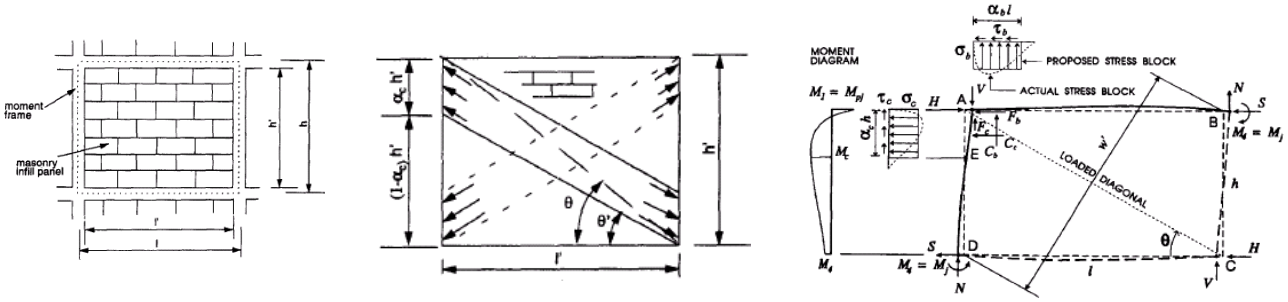

Figure 3.66. Equivalent strut model for masonry infill panels in steel frames: masonry infill sub-assemblage *(left)*, masonry infill panel (*middle*) and frame force equilibrium (*right*) (*after* Saneinejad and Hobbs, 1995).

The contact shear stresses in the beams (τ_b) and in the columns (τ_c) are as follows:

$$t_b = m \cdot s_b \qquad (3.90.1)$$

$$t_b = m \cdot r^2 \cdot s_c \tag{3.90.2}$$

The normalized contact length for the beams ($\alpha_b l$) and columns ($\alpha_c h$) are given by:

$$a_b = \sqrt{\frac{2.4 \cdot M_{pl,b}}{s_{b,\max} \cdot t}} \le 0.4 \cdot l' \tag{3.91.1}$$

$$a_c = \sqrt{\frac{2 \cdot M_{pl,b} + 0.4 \cdot M_{pl,c}}{s_{c,\max} \cdot t}} \le 0.4 \cdot h' \tag{3.91.2}$$

with $M_{b,pl}$ and $M_{c,pl}$ the plastic bending moments of the beam and column, respectively. Note that the expressions in Equations (3.91.1) and (3.91.2) for α_b and α_c have been adapted to account for the capacity design requirements.

As a result, the initial stiffness (K_0) of infilled frames is:

$$K_0 = \frac{2 \cdot H}{\Delta} \tag{3.92.1}$$

and the secant stiffness (K_s) (at the peak load) is:

$$K_s = \frac{H}{\Delta} \tag{3.92.2}$$

where the collapse horizontal load of the infilled frame (H) may be computed as follows:

$$H = s_c \cdot t \cdot (1 - a_c) \cdot a_c \cdot h + t_b \cdot t \cdot a_b \cdot l + \frac{M_{pl,b} + M_j}{h} \tag{3.92.3}$$

M_j is the bending moment at the unloaded corner (Figure 3.66). An empirical expression to evaluate the lateral deflection at peak load is also provided:

$$\Delta = 5.8 \cdot e_c \cdot h \cdot \cos q \cdot \left(a_b^2 + a_c^2\right)^{0.333} \tag{3.92.4}$$

where ε_c is the infill strain at the peak uniaxial (unconfined) compression.

Today, other analytical models are available in literature to estimate the response of steel frames with masonry infills under monotonic and cyclic loads (Madan *et al.*, 1997). However, all of them recognize the difficulty in analyzing brick-clad steel frames due to the uncertainty of the interaction masonry wall-steel frame. Nevertheless, for small deformations (e.g., less than 0.2%) the steel and the masonry behave as a composite flexural system. Increasing the lateral displacements beyond the ultimate tensile strength of the infill, cracks initiate within the masonry. As cracks spread in the panel, the wall lateral resistance degrades and the loads are then carried primarily by the steel frame. Further experimental and numerical studies may be found in the literature for either solid infill panels (Mander *et al.*, 1993; Flanagan and Bennett, 1999-b) or panels with openings (Schneider *et al.*, 1998). For ordinary design situations, e.g., buildings with large window and/or door openings, it was found that the shear resistance is also dependent on the imposed deformation; the resistance degrades significantly between 1.25% and 1.5% of the drift. Moreover, the flexural cracks significantly reduce the initial supplemental stiffness due to the masonry. Tests on five large-scale steel frames with unreinforced masonry infills (window opening height to the pier width ratio between 1.44 and 2.88) showed that nearly 70% of the initial masonry stiffness was lost at low drift (0.20%) while the remaining stiffness was deteriorated completely by 2.0% drift. By contrast,

stocky solid infills made of unreinforced masonry are capable of handling large drift displacements (1% to 2%) because of the arching and the development of membrane forces (Flanagan and Bennett, 1999-a). Out-of-plane anchors and ties, e.g., dovetail anchors, are not recommended because they may lead to premature localized failures, which decrease both the in-plane and out-of-plane strength of the infill. On the other hand, very slender panels, i.e., high aspect ratios, are generally unable to develop arching and are hence, vulnerable to loss of stability under seismic loads; therefore, their use is not recommended. Moreover, ductility of masonry infills with openings depends on the pier width and the number of wythes. Narrow piers tended to be more ductile than wide piers. Similarly, the double wythe infills tended to be more ductile than single wythe infills. Experimental studies carried out at the University of Illinois also highlighted the necessity to consider the additional shear produced by the strut action of the infill on the beam-to-column connections (Schneider *et al*., 1998). The latter may indeed produce fracture of the connection if it has inadequate shear capacity.

3.5.3. FRAMES WITH SHEAR WALLS

Recently, novel panel systems have been proposed for seismic rehabilitation of steel and composite structures (Driver *et al*., 1998; Astaneh, 2001; Bruneau and Bhagwagar, 2002); these systems employ steel plate walls. The response of steel shear panel under horizontal loads is similar to a vertical plate girder (Figure 3.67) in which the columns act as flanges, the steel plate is the girder web and the floor beams act as transverse stiffeners. They provide additional stiffness, strength and enhance the energy dissipation capacity of frame to which they are connected. The story drifts are significantly reduced without increasing floor accelerations. The lightness of steel panels reduces the inertial loads on the retrofitted structure and gives rise to lower additional loads to existing columns and foundations if compared with traditional concrete or masonry shear walls. Panel with thinner plates are advised to achieve ductile behavior and to prevent column instability.

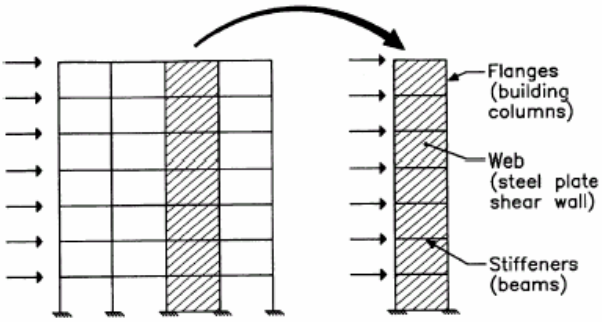

Figure 3.67. Steel shear walls and plate girder analogy (*after* Bruneau and Bhagwagar, 2002).

Moreover, thicknesses of steel panels is much smaller than those of concrete or masonry walls, i.e., 5 to 15 mm (steel wall) *vs*. 250 to 400 mm (concrete and masonry walls), hence, the former results are less invasive from an architectural point of view. In medium-to-high-rise buildings, if RC shear walls are used, the walls in the lower floors become very thick and occupy large area of the floor plan. Furthermore, steel plate systems can be constructed with shop welded-field bolted elements, giving much more efficient and faster systems than conventional solutions. The amount of steel required for steel panels is about one-third of equivalent MRFs. Therefore, such panels have been used as effective lateral resisting systems in several medium-to-high-rise buildings located in areas with low-to-high seismicity and high wind speed (Table 3.14). Some of these buildings sustained recent large earthquakes, namely Northridge and Kobe ground motions, with minor or no damage.

Table 3.14. Buildings with steel shear walls (Astaneh, 2001).

Location	Year of construction	No. of story	Lateral resisting system	Steel wall characteristics
Tokyo (Japan)	1978	*n.a.*	MRFs & steel walls (long.) & steel walls (transv.)	2743 mm (width) x 3719 mm (height) 4.76 mm to 12.70 mm (thickness)
Tokyo (Japan)	1978	53	Perimeter MRFs & steel walls	3048 mm (width) x 5029 mm (height)
Kobe (Japan)	1988	35	Dual system (MRFs & walls): RC walls at basement, composite walls at 1st & 2nd floor and steel walls elsewhere.	*n.a.*
Dallas (USA)	1988	30	Braced frames (long.) & steel walls (transv.)	*n.a.*
Los Angeles (USA)	1988	6	Spatial MRFs and walls: RC wall at 1st & 2nd floor and steel walls elsewhere.	7620 mm (width) x 4724 mm (height) 9.53 mm to 19.05 mm (thickness)
Seattle (USA)	2001	21	Concrete field steel tubes & steel walls with coupling beams.	*n.a.*
San Francisco (USA)	2002	52	Concrete field steel tubes & steel walls with coupling beams.	*n.a.*

Keys: *n.a.* = not available; long. = longitudinal direction; transv. = transverse direction.

In early applications in Japan and the US the steel panels were generally stiffened (Astaneh, 2001). In fact, the stiffeners increase the shear yield strength; welding stiffeners though, is an expensive and time-consuming process. On the other hand, recent experimental tests (e.g., Table 3.15) have shown that the seismic performance of bare steel plates is not significantly lower than that of stiffened plates; plate buckling is not detrimental because of the high post-buckling strength and stiffness. Therefore, unstiffened plates may be used for retrofitting of existing steel and composite buildings. The width-to-thickness ratio (h/t_w) between 70 and 100 (*semi-compact*) is advised, thus buckling is expected while some shear yielding has already occurred. Nevertheless, if openings exist, the continuity of tension field action should be ascertained. As a rule of thumb, the windows and/or doors should be placed in the areas between the mid-height of the columns and the mid-span of the beams. Alternatively, coupling beams rigidly connected to the columns (Figure 3.68) may be used.

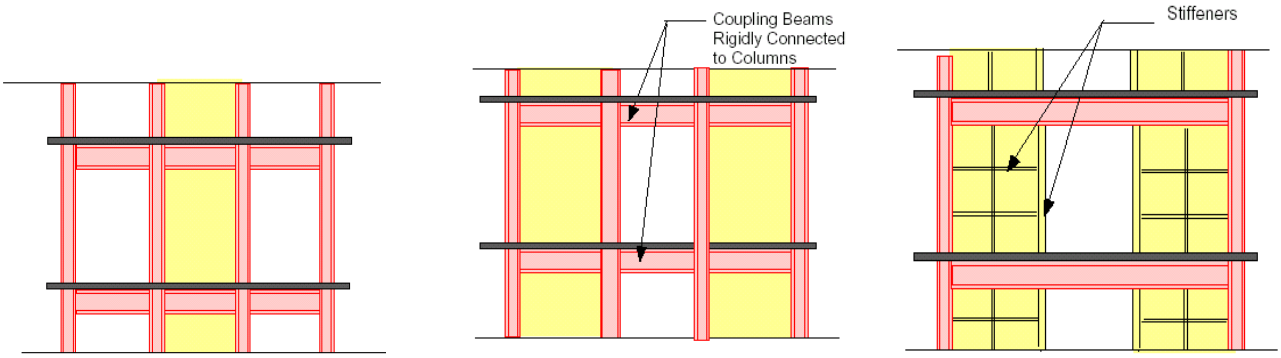

Figure 3.68. Steel shear walls with openings: single unstiffened panel with coupling beams on both sides *(left)*, two unstiffened panels with coupling beams (*middle*) and stiffened panel (*right*) (*after* Astaneh, 2001).

Table 3.15. Experimental tests on steel shear walls.

Researcher	Overstrength	Translation ductility	Specimen	Load type
Timler and Kulak (1983)	2.0	3.5	2 story-1 bay	Cyclic
Rezai *et al.* (1988)	1.5	6.0	1 story-1 bay	Cyclic
Roberts (1992)	*n.a.*	7.0	Small square panel	Cyclic
Lubell (1997)	1.2	1.5*	4 story-1 bay	Shaking table
Driver *et al.* (1998)	1.3	6.0	4 story-1 bay	Cyclic

Keys: * Ductility of the single panel. *n.a.* = not available.

Experimental tests carried out worldwide have shown that steel shear walls exhibit overstrength ranging between 1.2 and 2 (Astaneh, 2001); while the (translation) ductility varies between 3.5 and 7.0. The panel response is linear, up to 0.6% to 0.7% of the story drifts; ultimate values of 3% may

be achieved with adequate detailing of the wall-to-frame connections, e.g., Figure 3.69. Moreover, story shears are primarily resisted by shear walls, thus the demand on frame component and connections is much lower. As a consequence, special strengthening requirements are not needed for such members; thus, steel panels are very cost-effective for seismic upgrading. The results of the most significant experimental tests are summarized in Table 3.15.

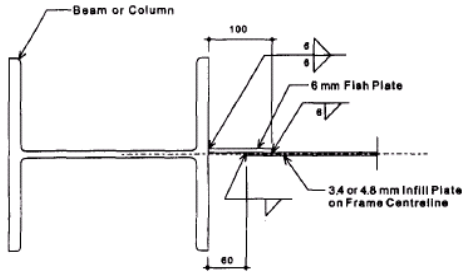

Figure 3.69. Wall steel plate-to-column welded connection (*after* Driver *et al*., 1998).

The effects of steel panels with different mechanical properties were studied through nonlinear numerical analyses carried out on flexible and rigid steel frames located in zones with low (New York) and high seismicity (Memphis) (Bruneau and Bhagwagar, 2002). The assessed structure is a typical three-bay frame with 20 stories. The frame was retrofitted with infills made of the standard A572 Grade 50 steel, low yield steel and Shearfill fabric membranes. LYP100 and LYP235 are low yield steels with yield strengths of 100 and 235 MPa, respectively. These steels are suitable for seismic retrofitting because of their enhanced energy dissipation, high ultimate strain (72% for LYP 100 and 60% for LYP235), lower strain rate dependency, longer low-cycle fatigue life and improved weldability.

The seismic response of multi-story frame retrofitted with steel panels was analyzed through a series of inclined strip members capable of transmitting tension forces only. The area of such strips is equal to the product of the strip width and the plate thickness (Figure 3.70); they are oriented along the principal stresses in the panel (Figure 3.70). As a rough guide the angle α between columns and tension strips may be assumed equal to 45°. However, the analytical expression based on experimental and numerical tests is as follows:

$$\tan\, g^{4}a \;=\; \frac{1 + L \cdot w \cdot \left(\dfrac{1}{2 \cdot A_c} + \dfrac{L^3}{120 \cdot I_b \cdot h} \right)}{1 + h \cdot w \cdot \left(\dfrac{1}{2 \cdot A_b} + \dfrac{L^3}{320 \cdot I_c \cdot L} \right)} \tag{3.93}$$

where w is the wall thickness; L the width of the panel; h is the height of the panel; A_c (A_b) and I_c (I_b) are the cross section area and moment of inertia of the columns (beams), respectively.

Adequate beam and column member stiffness to provide effective tension field distribution should be equal to the flexibility coefficient (φ):

$$j \;=\; 0.7 \cdot h \cdot \left(\frac{w}{2 \cdot L \cdot I_c} \right)^{0.25} \tag{3.94}$$

while low panel aspect ratio (l/h), e.g., l/h$\leq$ 3, are essential to ensure development of yielding of the plate; hence, providing enhanced energy dissipation capacity of the retrofitted frame.

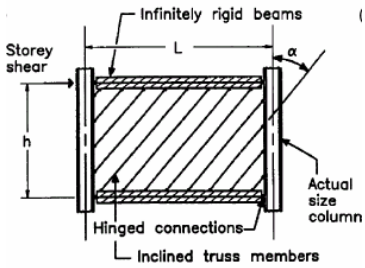

Figure 3.70. Strip model for steel plates (*after* Bruneau and Bhagwagar, 2002).

Based on more than 40 time history analyses performed with synthetic records for M=6.3 (New York) and M=8 (Memphis) earthquakes, it was shown that steel plate infills reduce the fundamental periods to less than half that of the bare frame in most cases (Table 3.16).

Table 3.16. Stiffening effects of shear steel plates: fundamental periods of 20 story MRFs.

	New York		Memphis	
Panel type	Rigid connections	Pinned connections	Rigid connections	Pinned connections
Bare frame	3.13*	8	3.14*	8
Gr.50 infills	1.90 (-65%)	2.53**	1.49 (-111%)	1.79**
LYS 100 infills	1.52 (-106%)	1.84 (-38%)	1.32 (-138%)	1.54 (-16%)

Keys: * and ** Value assumed as a benchmark for rigid and pinned frames, respectively; bracketed values correspond to variations.

Furthermore, since ticker LYS100 infills are required to provide the same resistance of Grade 50 steel (Figure 3.71), frames retrofitted with LYS are stiffer and hence, exhibit lower periods. However, the extra material for LYS improves the seismic performance. For example, reduction of story drifts equal to 200% and ductility ratios of 6 (three times higher than the grade 50 ones) were found in some cases. The values of the wall thicknesses and strip areas used for the assessed frames are provided in Figure 3.71, as a function of the height. These diagrams may be useful in the design of seismic retrofitting because they provide a simple guide on the stiffness distribution along the building height.

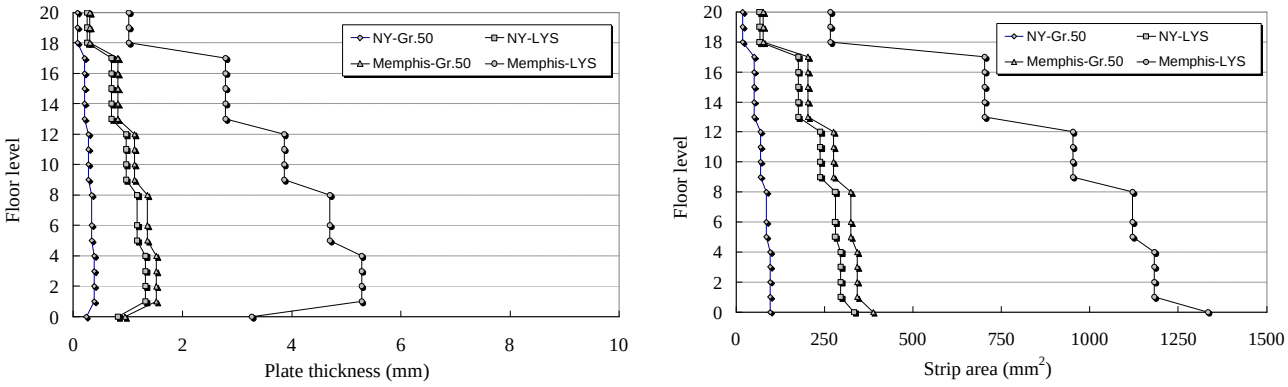

Figure 3.71. Steel plate physical properties: thickness (*left*) and strip area (*right*) (*after* Bruneau and Bhagwagar, 2002).

Design rules for steel walls are not still well codified; guidelines may be found, e.g., in Canada (CSA, 1994) and the US (IBC, 2000). However, it is advised to use force reduction factors equal to 6.5 for stiffened and unstiffened steel plate shear walls to retrofit a gravity carrying steel frames with simple beam-to-column connections. Dual systems, i.e., MRFs and steel walls, have as much

high ductility as bare MRFs; thus reduction factors equal to 8.0 may be used. Similar response factors may be conservatively used for stiffened and unstiffened walls. It is worth noting that the combination of MRFs with steel panels is very effective because the former act as back up systems to the primary lateral-force resisting system (steel walls).

The expected yielding shear resistance of noncompact steel panels should be evaluated as follows (Astaneh, 2001):

$$V_{y,e} = \frac{f_{u,w} + f_{y,w}}{2 \cdot f_{y,w}} \cdot \frac{A_w \cdot f_{y,w,e}}{\sqrt{3}} \cdot 0.17 \cdot (1 - C_v) \tag{3.95.1}$$

where the coefficient C_v is given by:

$$C_v = \frac{2.46 \cdot \sqrt{E / f_{yw,e}}}{h / t_w} \tag{3.95.2}$$

where $f_{y,w}$ and $f_{u,w}$ are the yield and ultimate strength; $f_{y,w,e}$ is the expected yield strength (Section 3.1); and A_w is the panel shear area. Note, that if heavy stiffeners are used, e.g., heavy vertical and/or horizontal channels, Equations (3.95.1) and (3.95.2) should be modified accordingly. Width-to-thickness (h/t_w) ratios that correspond to compact and slender walls are given in Table 3.17, as a function of the steel grades used in Europe, i.e., S235, S275 and S355.

Table 3.17. Width-to-thickness ratios for steel shear walls.

	Panel Slenderness*	
Steel grade	Compact	Slender
S235	≤ 73	≥ 92
S275	≤ 68	≤ 85
S355	≤ 60	≤ 75

Keys: * Conservative values of plate buckling coefficient k_v, i.e., 5, are used.

The use of semi-compact walls, i.e., with h/t_w between those in Table 3.17, is recommended for seismic retrofitting of steel and composite framed buildings. Moreover, steel grades with lower yield strengths are advised to achieve ductile failure modes in steel walls, e.g., shear yielding; thus, S235 should be preferred to either S275 or S355.

It is instructive to note that other metals, e.g., stainless steels and aluminum, are ideal candidates for steel walls. Indeed, they have low yield points (proof stress), elevated ductility and excellent low-fatigue resistance, as discussed in Sections 2.5.2.1 and 2.5.2.3. Nonetheless, their viability for seismic design of new and existing structures has not been yet assessed; thus, further research is needed.

Alternatively, steel walls may be encased in RC (composite steel plate shear walls). In such a case, the concrete stiffening may be placed on one or both sides of the plate; infilled panels may also be used (Figure 3.72).

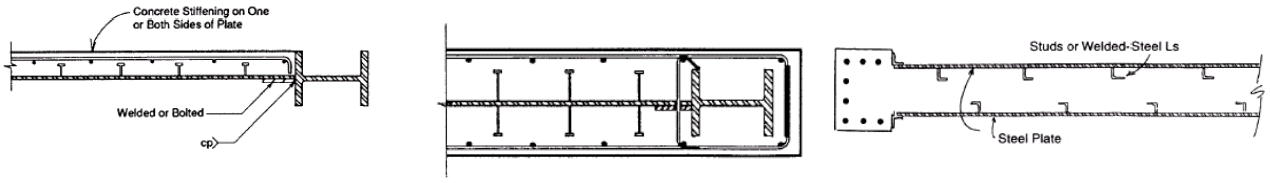

Figure 3.72. Composite steel wall: RC on single side (*left*), typical RC encasement (*middle*) and infilled with two plates (*right*) (*after* AISC, 1997).

Due to the limited data available, the design of these systems should be performed ignoring the composite action. Moreover, it is worth noting that the strength of the steel wall is generally much higher than the RC encasement, hence, the composite action has no practical impact. As a result, the shear strength of the system may be assumed to be equal to that of the steel panel.

The thickness of the concrete and the shear studs should be designed to allow the yielding of the plate and preventing elastic local and global buckling. A minimum thickness of 100 mm (concrete on both sides) or 200 mm (concrete on single side only) should be used for encasement. Reinforcement bars should be placed in vertical and horizontal directions; the spacing should not be less than 400 mm. The connections between the plate and boundary members may be either welded or bolted; complete penetration welds and high strength bolts are advised.

Traditional systems to upgrade steel frames consist of RC concrete shear walls, thus efficient dual systems are obtained (Figure 3.73). In such hybrid systems the RC core provides strength and stiffness for resisting earthquake loads, while the steel frame provides ductility (Roeder, 1998). The enhanced stiffness, particularly for structures designed originally only for gravity and wind loads, allows floor drifts to be controlled. Preliminary estimates of the lateral displacements of frame-shear wall systems may be obtained using design charts available in literature (Khan and Sbarounis, 1964). However, the added mass is significant, hence, higher seismic forces are attracted and significant upgrading of the foundations is required. For example, it may be required to modify superficial foundations of existing frames into deep foundations on piles; the walls present high overturning moments when loaded horizontally.

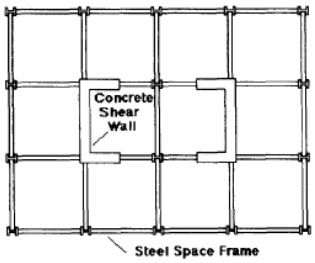

Figure 3.73 Hybrid system with steel frame and RC core (*after* Roeder, 1998).

Typically, RC walls are connected to partially or fully encased structural steel members, as shown in Figure 3.74 (*columns*) and Figure 3.75 (*beams*). Adequate steel reinforcement and connectors are required at the connection of the wall with the steel members. For example, cross ties should be placed in the wall for a length equal to the section width (*embedment details*). This requirement avoids undesirable splitting along vertical planes inside the wall near the columns. Moreover, shear studs provide a uniform transfer of forces between the RC wall and the boundary members. Detailing should comply with the requirements for the design of new buildings (EC8, 1998).

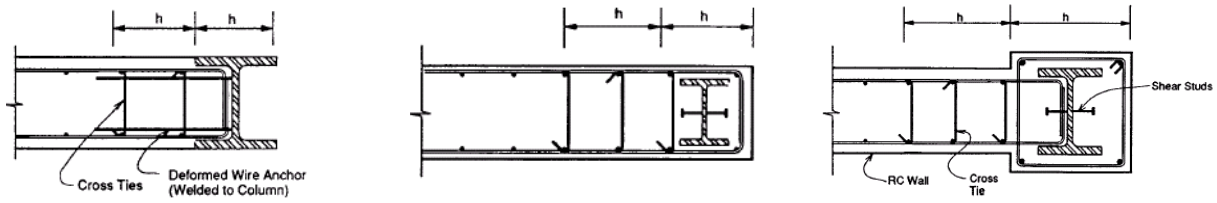

Figure 3.74. RC shear wall with steel columns: partially encased (*left*) and fully encased (*middle and right*) (*after* AISC, 1997).

The strength, stiffness and the dissipative capacities of dual systems are comparable to those of pure RC walls. The in-plane strength of the columns is enhanced by the composite action with the wall (Figure 3.74). These boundary members are also effective to delay the flexural hinges in slender walls.

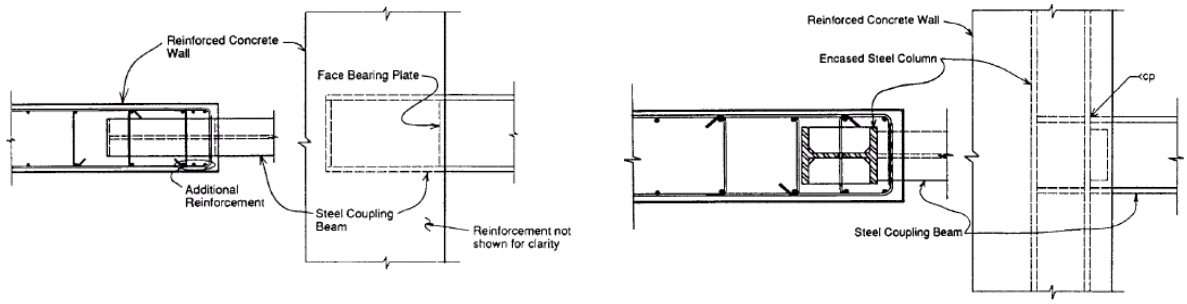

Figure 3.75. RC shear wall with steel beams: partially encased (*left*) and fully encased (*right*) (*after* AISC, 1997).

On the other hand, coupling beams may undergo high inelastic flexural and shear deformations if connected rigidly to the wall (Figure 3.75) (Harries *et al*., 1993; Shahrooz *et al*., 1993). As a result, they significantly improve the strength and stiffness, as well as ductility for the structural system. Moreover, the concrete encasement at the joints, particularly beam-to-column connections, increases the strength and stiffness of the connections by as much as 30 to 50% (for partially restrained) to several hundred percent (flexible) (Roeder, 1998). The ductility of such connections is not less than the bare steel counterparts. Further details on the effects of composite action and the influence of retrofitted connections are provided in the next sections.

3.5.4. FRAMES WITH COMPOSITE ACTION

It is well recognized that the composite action enhance stiffness, strength and ductility of existing steel frames, either MRFs or braced. The improvement of the seismic performance depends upon the deficiencies of the existing buildings and usually on the composite system adopted (Roeder 1998). Several types of composite systems are available nowadays; e.g., concrete encasement (CE), concrete filled (CF) and hybrid RC and structural steel (RCSS). All of them are technologies suitable for the seismic retrofitting of steel and composite structures due to the compatibility between the joined materials, the availability of design rules and the ease of construction. Requirements for upgrading members and connections accounting for composite actions have been provided in Sections 3.3 and 3.4; nevertheless, the influence of the rehabilitation strategies on the global response was not addressed. This section assesses the seismic performance of frames with composite actions, particularly CE and CF, in order to quantify the improvement with respect to

bare steel frames. The latter, in fact, generally violate story drift limitations under earthquake loads and hence, they may be conveniently upgraded as composite.

Analytical work carried out on a set of 20 low-to-medium rise buildings showed that by encasing columns of the bare steel frames, the fundamental period elongates marginally (Elnashai and Broderick, 1996); this effect is in fact, less than 5%. By contrast, frames with encased columns exhibit higher overstrength than those in bare steel; the increase is a function of the height: the higher the frame the higher is the overstrength. The results of the analyses are summarized in Table 3.18: the overstrength of systems with encased columns increases from 1.65% (2-story) to 9.24% (6-story) with respect to bare steel. In addition, the computed column rotation ductilities for encased members are generally 10% higher than those of bare beam-columns.

Table 3.18. Composite MRFs: geometrical and response properties (*after* Elnashai and Broderick, 1996).

Frame	No. Bays	No. Story	Beam type	Column type	Period (sec)	Ovestrength*
S2S2B-A	2	2	Steel	Steel	0.66	1.14
C2S2B-A	2	2	Steel	Composite	0.72	1.20
S2S2B-B	2	2	Steel	Steel	0.60	1.29
C2S2B-B	2	2	Steel	Composite	0.59	1.27
S3S3B-A	3	3	Steel	Steel	0.67	1.18
C3S3B-A	3	3	Steel	Composite	0.70	1.19
S3S3B-B	3	3	Steel	Steel	0.74	1.33
C3S3B-B	3	3	Steel	Composite	0.76	1.41
S3S5B-A	5	3	Steel	Steel	0.73	1.35
C3S5B-A	5	3	Steel	Composite	0.77	1.41
S3S5B-B	5	3	Steel	Steel	0.79	1.36
C3S5B-B	5	3	Steel	Composite	0.81	1.36
S6S3B-A	3	6	Steel	Steel	1.11	1.29
C6S3B-A	3	6	Steel	Composite	1.18	1.40
S6S3B-B	3	6	Steel	Steel	1.13	1.11
C6S3B-B	3	6	Steel	Composite	1.16	1.24
S6S5B	5	6	Steel	Steel	1.12	1.18
C6S5B	5	6	Steel	Composite	1.16	1.25
S10S5B	5	10	Steel	Steel	1.25	1.25
C10S5B	5	10	Steel	Composite	1.28	1.33

Keys: * Ratio of the shear corresponding to 3.0% drift and the shear corresponding to the column yielding.

On the other hand, the encasement of steel beams is more effective than that of columns. Composite beams display large variations in stiffness and strength between regions of positive moments (60 to 70% of the beam span) and negative moments (30 to 40% of the beam, at the edges); however, their behavior is controlled by positive moments. Significant benefit in terms of energy dissipation is derived from the highly stable response available in the positive moment regions for properly designed composite beams (Section 3.3). Combined with the influence of tensile strain-hardening in the steel joist and the consequent increase of the compression in concrete flange, this leads to greater post-yield increases in bending resistance and residual stiffness being provided by composite beams in positive bending, than is the case of their bare steel equivalents. Thus, the slab increases the bending stiffness between 1.6 to 1.9 times in the positive zone (Leon, 1998). As a result, the lateral resistance of composite frames increases monotonically even under large lateral drifts.

The extensive analyses performed in this research quantified the enhanced energy dissipation capacity of composite frames through behavior factors; they are as 40% higher than steel counterparts. Thus, assuming the overstrength ranging between 1.20 and 1.30, the enhanced global ductility is about 10 to 20% than that of steel frames.

Further studies ongoing at Imperial College on a set of 48 composite frames, consisting of 2-bay-2-story, 2-bay-4-story and 4-bay-6-story, have shown that encasing only steel beams may shorten the period (Elnashai and Tsujii 1999). However, the stiffening effect is r around 5%. All the other combinations, i.e., encased beams-encased columns and encased-columns, increase the period; such lengthening effect is about 5%. Experimental tests carried out in this research have also shown, in agreement with other studies, that reductions to 30% of shear connection do not reduce the energy dissipation capacity of the frames (Bursi and Zandonini, 1998). Such reduction is thus advised for seismic retrofitting to achieve a great economy in the design.

Nevertheless, more significant benefits of encased beams have been found in recent numerical studies (Liew *et al*., 2001): the composite action enhances the global stiffness and strength of about 30%; however, the stiffening is generally higher than the strengthening. Based on experimental evidence, it has also been suggested to compute the deflections using the averaged inertia (I_c):

$$I_c = 0.4 \cdot I^+ + 0.6 \cdot I^- \tag{3.96.1}$$

and hence, replacing:

$$I_c = 0.6 \cdot I^+ + 0.4 \cdot I^- \tag{3.96.2}$$

where I^+ and I^- are respectively the moment of inertia of the composite section under positive and negative moments.

Based on the above findings and other experimental tests carried out in Europe (Plumier, 2000) and North America (Roeder, 1998; Hajjar, 2002) CE is a suitable strategy to increase the strength and stiffness of existing steel and/or partially composite structures between 10 and 20%. Similarly, the global ductility, referred e.g., to the roof drift, is improved on average of 20%.

On the other hand, CF systems are very convenient because they confine the concrete and improve the strength and ductility of the concrete acting alone. Recent experimental tests showed that CF structures possess high damping, enhanced ductility and toughness compared to traditional steel frames (Hajjar, 2002). Moreover, CF systems used jointly with steel MRFs show high strength-to-weight ratio due to the continuous bracing of the steel tube to delay local buckling, other than the concrete confinement. Furthermore, multiple continuous bays of infilled members provide adequate system redundancy. To achieve adequate performance it is essential to satisfy section and member requirements given in Sections 3.2 and 3.3. As a result, CF is suitable for seismic retrofitting and may be more cost-effective than CE and RCSS. The economic benefits of CF are two-fold. First, CF members require a minimum amount of reinforcement steel because the external structural tube is able to resist bending moments, uni- and bi-axial, and axial loads. Second, the hollow sections act as form work thus reducing construction cost and time.

Further details on the effects of composite actions are provided in the next section, e.g., composite connections.

3.5.5. FRAMES WITH STRENGTHENED AND WEAKENED CONNECTIONS

Steel and composite buildings retrofitted with the connection details, as in Section 3.4, are able to withstand low-to-moderate earthquakes with no or minor damage and prevent collapse under major events.

The reinforced or weakened connections exhibit plastic rotations, e.g., greater then 30 millirads, thus allowing at least 3% drifts to be achieved (FEMA 350, 2000). However, it could be argued that some repairing details influence the stiffness and/or strength of the frame as a whole. Extensive experimental tests and numerical simulations have been performed in Europe, Japan and America to address this issue (Mele, 2002). Some of the results obtained so far are summarized hereafter; they should serve as design guidelines for seismic retrofitting of existing steel and composite buildings. For example, it has been shown that cutting the beam flanges of RBSs (Section 3.3.2) may significantly reduce the frame stiffness and the yield resistance (Shen *et al*., 2000). The larger the cutting the higher the reduction. If the cut is less than 40% of the flange, the stiffness reduction) in the elastic and inelastic range) is negligible for practical applications, i.e., less than 5%. Similar drop is observed for the frame yield strength. By contrast, 10 to 20% increase of the drift and reduction of the yield strength are found when 60% of the flange is cut. Both these effects are predictable. By trimming more material from the flanges; the contribution of the beams to the frame deformability increases; the weaker the reduced section is, the earlier the frame yields because capacity designed frames the beams are the weakest links. Earlier yielding of beams is beneficial; however, if drift limitations are critical, it is strongly recommended to comply the requirements in §3.3.2 to design the RBS. Alternatively, steel beams with reduced sections may be encased in RC; fully hysteresis loops beyond 3.5% plastic rotations are achieved with little mechanical degradation (Hajjar, 2002). Moreover, shear studs should not be placed within the RBSs in order to control the failure mode, i.e., beam plastic hinges. On the other hand, the benefit of composite action is significant, particularly for flexible (Liu and Astaneh, 2000) and semi-rigid connections (Leon *et al*., 1998); the increase of strength and stiffness is due to the concrete slab. However, such increase depends on the connection layout, beam type and slab thickness. PR or pinned steel frames may be conveniently upgraded as PR composite frames (PR-CFs), since they only represent a small, incremental change in the construction of steel frames and can provide good energy dissipation and drift control. PR-CFs are suitable for low-rise buildings where the relatively small stiffness and strength provided by each PR connection is balanced by the large number of frames and connections available to resist lateral loads (Leon, 1998). Moreover, the economy of semi-rigid connections in structural weight with respect to the pinned solution is about 10% for multi-story frames (Faella *et al*., 1997). Furthermore, the augmentation of composite slabs increases the strength, rigidity and redundancy of the structural system. PR-CFs are susceptible to stability problems; nevertheless, their drifts under seismic loads, are generally lower than traditional MRFs. The latter has been proven analytically and experimentally for steel (Nader and Astaneh, 1992; Elnashai *et al*., 1998) and composite (Leon, 1998) PR-frames. In both systems the lower drift ratios are due to: (i) longer periods, (ii) higher damping and (iii) more frames and connections resist the lateral loads. Therefore, the PR frames possess a self-isolation thus attracting less inertial forces. As a consequence, PR frames may be used efficiently for seismic retrofitting by weakening or strengthening existing connections. However, the design should be based on slip capacity design and adequate effective lengths for the column stability checks (Elnashai *et al*., 1998). Several studies have analytically quantified the mechanical properties of PR frames. For example, the period may be evaluated as a function of the connection relative rigidity (m) defined as follows (Nader and Astaneh, 1992):

$$m = \frac{\left(K_j\right)_{con}}{\left(EI/L\right)_b} \tag{3.97}$$

where K_ϕ is the connection rotation stiffness; I and L are the moment of inertia and the beam span, respectively; and E is Young's modulus of the beam.

Based on shaking table tests for a single-story steel frame with flexible (double web angle), semi-rigid (top and seat angle with double web angle) and rigid (welded top and bottom flange with double web angle) connections, it was suggested to compute the fundamental period as follows:

$$T = 0.085 \cdot H^{\left(0.85 - m/120\right)} \qquad 5 < m < 18 \qquad (semi\text{-}rigid) \qquad (3.98.1)$$

$$T = 0.085 \cdot H^{3/4} \qquad m \geq 18 \qquad (rigid) \qquad (3.98.2)$$

where H is the frame height in meters.

Experimental tests on a two-story steel frame with semi-rigid and fully rigid connections have shown that a reduction of the connection stiffness by 50% and 60% leads to a reduction in the frame stiffness by 20% and 30%, respectively (Elnashai *et al.*, 1998). This in turn influences the natural period of the frame; the same reduction of connection stiffness lengthens the period of about 15%. On the other hand, the connection capacity influences the load bearing capacity of the frame. For example, a 60% decrease in connection capacity results in 30% reduction of the overall capacity of the structure; while an increase in connection capacity of 80 and 150% leads to an increase in frame yield of an estimated 30% and 40%, respectively. Global overstrengths may vary between 1.4 and 1.6, thus leading to enhanced plastic redistribution and energy dissipation.

The ductility of PR frames is also influenced by the connection behavior; the stiffness and capacity of connections affect the number, location and extent of plastic hinges developing in frame members. This in turn determines the distribution of local ductility within the frame and influences the overall ductility of the structure. The displacement ductility of the frame increases with the increase in connection stiffness and strength. For interstory drifts corresponding to LS of collapse prevention, e.g., 3%, the ductility varies between 2.7 and 3.4; however, values of 4 to 5 are exhibited for larger drifts.

To efficiently design PR-frames a modified distribution of seismic forces for static analyses has been proposed (Nader and Astaneh, 1992) as follows:

$$F_{xi} = \frac{W_{xi} \cdot h_{xi}^{d}}{\sum W_{xj} \cdot h_{xj}^{d}} \cdot F_{tot} \qquad (3.98.1)$$

with the power exponent ***d*** given by:

$$d = \begin{cases} 1.0 & \mathrm{T} \leq 0.50\,\mathrm{s} \\ 0.50 \cdot T + 0.75 & 0.50 < \mathrm{T} < 2.50\,\mathrm{s} \\ 2.0 & \mathrm{T} > 2.50\,\mathrm{s} \end{cases} \qquad (3.98.2)$$

Equations (3.98) and (3.99) are very useful for the seismic upgrading of steel and composite frames as PR.

However, an economic design should require yield overstrengths equal to 40% for the beams, thus preventing their yielding (Elnashai *et al.*, 1998). The need for imposing column-to-beam overstrength factors is eliminated; in fact, the connection overstrengths are in range 1.3 to 1.4.

3.5.6. BRACED FRAMES

Bracing is a very effective method to enhance the global stiffening and strengthening of steel and composite frames. The use of bracing systems is generally advantageous because of: (i) the ability to accommodate openings, (ii) minimal added weight to the structure and (iii) minimum disruption to the function of the buildings and its occupants during retrofitting. However, this technique may be inefficient if the braces are not adequately capacity designed. In addition, braces result in some

cases being aesthetically unpleasant because they change the original architectural features of the building.

Several configurations of braced frames may be used for seismic rehabilitation; however, the most common are concentric braced frames (CBFs), eccentric braced frames (EBFs) and the novel knee-brace frames (KBFs), recently proposed for low-to-high earthquake loads (Sam *et al*., 1995; Balendra *et al*.,2001). The existence of tension/compression braces in CBFs results in a lateral stiffness well above that of MRFs. However, due to buckling of the compression strut and softening due to the Bauschinger effect, the hysteretic behavior of CBFs is unreliable. It follows that the key to improved behavior is the scrupulous design of the bracing members. Common configurations for CBFs are provided in Figure 3.76; they include V and inverted-V bracings, K, X and diagonal bracings. Nevertheless, both types of V bracing are not advised as retrofitting strategy because of the likelihood of the damage in the beam mid-span. Under horizontal forces the compressed braces may buckle, thus their load bearing capacity drops abruptly. By contrast, the force in the tension braces increases monotonically reaching the yield strength and eventually strain-hardening. The net result is an unbalanced force concentrated at the brace-to-beam connection. The effects in the beam, e.g., additional bending and shear, should be added to those due to gravity loads (Goel, 1992-b). Experimental tests have shown that typical bracing members possess a residual post-buckling compressive strength of about 30% of the initial compressive strength. Therefore, if existing frames with V bracings needs to be upgraded, it is advised to check the beam capacity at mid-span for the design load combinations and additional effects due to the point load (F_b) given as follows:

$$F_b = 1.30 \cdot f_{ye} \cdot \left(\frac{f_u + f_y}{2 \cdot f_y} \right) \cdot A_b \tag{3.99}$$

where f_{ye} is the expected yield strength of the brace, as specified Section3.1; f_u and f_y are the nominal ultimate and yield strengths of the brace; and the A_b is the area of the brace.

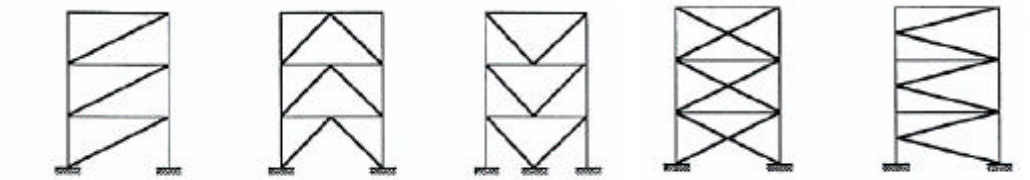

Figure 3.76. Common configurations for CBFs (*after* AISC, 1997).

Alternatively, the unbalanced force in the beams may be eliminated through ad hoc bracing configurations (Figure 3.77) such as macro-bracings (Taranath, 1997); e.g., two, three story X-bracings or V-bracings with a zipper column (Khatib *et al*., 1988).

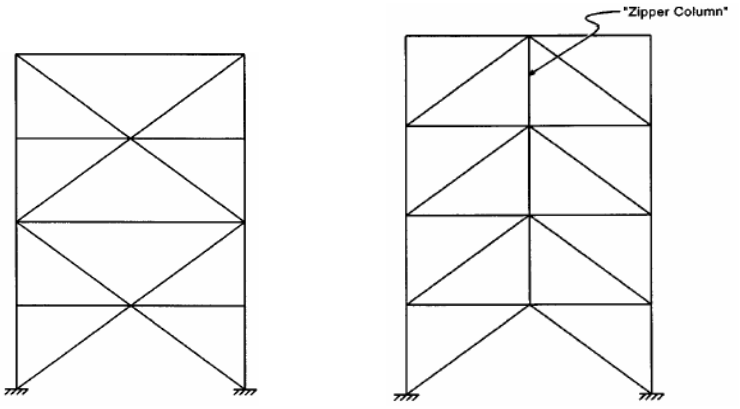

Figure 3.77. Configurations for CBFs without unbalanced forces in the beams (*after* AISC, 1997).

The design of bracings in CBFs should conform to the standards for new steel or composite structures (EC8, 1998). However, it is recommended to provide at least 50% of the tensile capacity in compression; experimental tests showed that this requirement gives rise to satisfactory hysteretic behavior (Goel, 1992-b). Moreover, to control the global ductility, the brace slenderness (λ_b):

$$l_b = \frac{K \cdot l_b}{r} \cdot \sqrt{\frac{f_y}{235}} \tag{3.100}$$

should comply with the limits in Table 3.19, as a function of the brace slenderness ratio, bracing layout and the number of stories (Walpole, 1985).

On the other hand, several experimental tests have shown that EBFs exhibit excellent performance under earthquake excitation because of the high ductility and energy dissipation capacity (Nishiyama *et al*., 1988; Yang, 1982; Whittaker *et al*., 1987). In such frames, the bracing members intersect the girder at an eccentricity *e* and hence, forces are transferred to the brace members through bending and steel forces developed in the ductile steel link. The link beam, i.e., the length of the girder defined by *e*, may behave predominantly in either shear or bending. The link acts as a fuse by yielding and dissipating energy and prevents buckling of the brace members. While retaining the advantages of CBFs in terms of drift control, eccentrically braced frames also represent the best available configuration for failure mode control. Another important advantage is that by providing an eccentricity, a higher degree of flexibility in locating doors and windows in the structure is achieved (Figure 3.78).

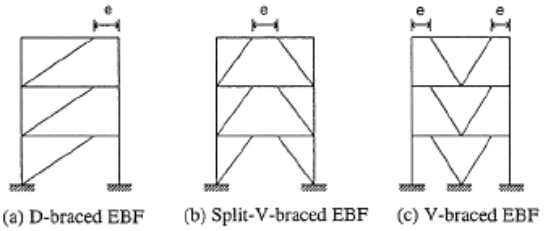

Figure 3.78. Typical configurations for EBFs (*after* Naeim, 2001).

By careful design of the link beam, sustained energy dissipation capacity can be achieved. Moreover, zones of excessive plastic deformations are shifted away from beam-column connections, thus improving the overall integrity of the frame. The relation between eccentricity ratio (e/L) and the lateral stiffness is shown in Figure 3.79 (Hjelmstad and Popov, 1984). As e/L tends to unity, the stiffness of the MRF is given, while the zero eccentricity ratio corresponds to the CBF stiffness. The lateral stiffness of EBFs may be calibrated by varying the length of the link beam; reductions of the interstory drifts more than 50% may be achieved with short (shear) links. Design rules for the detailing of link beams should conform to the standards for new buildings (EC8, 1998). However, expected rather than nominal yield strengths should be used for capacity checks as discussed in Sections 3.1 and 3.4.

Table 3.19. Ductility values for CBFs (*after* Walpole, 1985).

Frame Type	Story No.	$l_b \leq 40$	$41 \leq l_b < 80$	$81 \leq l_b < 135$
	1	5.0	3.9	3.0

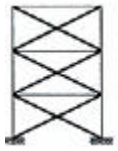	1	5.0	3.9	3.0
	2	4.5	3.5	2.4
	3	4.0	3.0	1.8
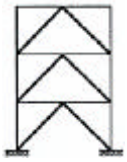	1	3.7	2.4	1.5
	2	3.0	1.8	1.2
	3	2.7	1.5	1.0

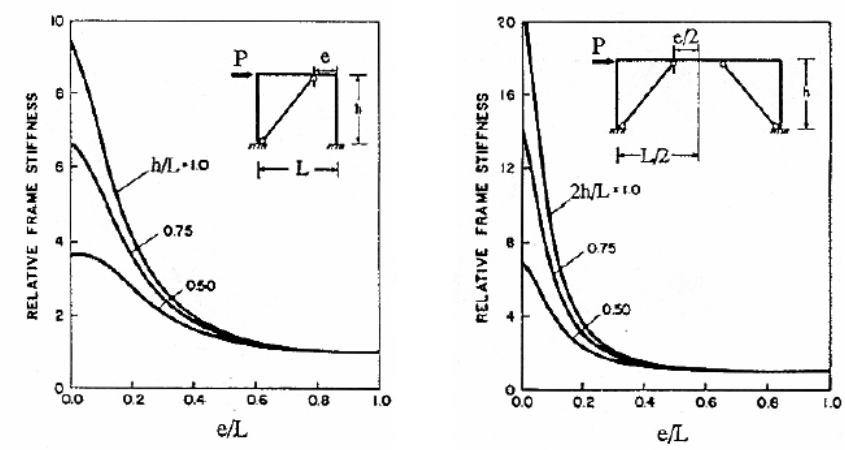

Figure 3.79. Configurations for CBFs without unbalanced forces in the beams (*after* Hjelmstad and Popov, 1984).

Simplified analysis of plastic collapse mechanisms of a single link EBF (Figure 3.80) gives the relationship between frame (θ_p) and link deformations (γ_p) as follows (Kasai and Popov, 1985):

$$g_p = \frac{L}{e} \cdot q_p \tag{3.101}$$

Since the span of the frame is significantly larger than the eccentricity *e*, it follows that the ductility demand in the link is higher than that for the frame. From the above equation, it is also apparent that increasing the length of the link, while decreasing shear yielding energy dissipation, reduces link ductility demand. The variation in ductility demand, as a function of e/L, is shown in Figure 3.81. The choice of link length and location is governed by the balance between available ductility (favoring a long link) and required energy dissipation capacity (favoring a short link).

Recently, aluminum alloys (i.e., 3003 and 6061) have been used to enhance the energy dissipation of shear links in EBFs. Such alloys are very attractive for shear links because of (Section 2.5.2.1): (i) low yield strengths, (ii) high metallic damping, (iii) high strain hardening and (iv) low strain-rate effects (Rai and Wallace, 1998). The low yield strength allows the use of thicker webs which, in turn prevents the web buckling; while strain hardening in shear modes is favorable for plastic redistribution within the dissipative zones of the frame. Moreover, soft alloys undergo many large plastic deformation cycles without tearing. Figure 3.81 illustrates aluminum specimen after large shear deformations and a typical hysteresis loop. Therefore, hybrid braced frames with aluminum shear links represent a viable alternative to traditional EBFs. However, to enhance the energy dissipation, it is advised to use softer alloys (e.g., 3003) for the link webs and stronger alloys (e.g., 6061) for the flanges.

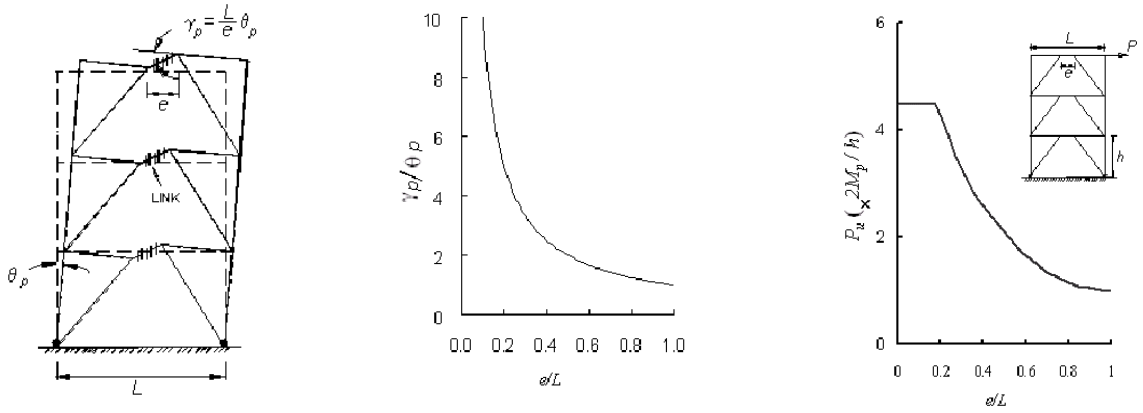

Figure 3.80. Response of EBFs as a function of the eccentricity ratio (*e*/*L*): plastic mechanism (*left*), rotation ductility demand (*middle*) and ultimate strength (*right*) (*after* Kasai and Popov, 1985).

The shear resistance (V_w) of the aluminum link to be used for capacity checks is given by:

$$V_l = 1.9 \cdot f_{0,2} \cdot g^{0.2} \cdot A_w \tag{3.102.1}$$

$f_{0.2}$ is the proof stress, A_w is the horizontal web area:

$$A_w = l \cdot t_w \tag{3.102.2}$$

where l is the link length; and t_w is the web thickness. The size of shear links may be determined by calculating the area A_w to resist the design story shear ($V_{d.i}$):

$$A_w = \frac{V_{d,i}}{1.64 \cdot f_{0.2}} \tag{3.102.3}$$

in which the shear stress ($1.64 \cdot f_{0.2}$) corresponding to the strains equal to 0.10 is assumed.

Transverse stiffeners are required to avoid web buckling and to ensure ductile shear failure; their design should be based on stability and strength checks. Minimum thickness should be 10 mm and should be placed on both sides of the link.

Adequate stiffness is ensured by assuming the moment of inertia of stiffeners (I_{st}) about the centroidal axis parallel to the web as:

$$I_{st} \geq 4 \cdot j \cdot a \cdot (t_w)^3 \tag{3.103.1}$$

where the coefficient j is given by:

$$j = \left[2.5 \cdot \left(\frac{a}{t_w} \right)^2 - 2 \right] \geq 0.50 \tag{3.103.2}$$

The minimum strength of the stiffeners may be evaluated assuming that each stiffener behaves like a strut with an axial force equal to one-third of the expected shear in Equation (3.102.1).

The spacing (a) of transverse stiffeners to avoid web buckling and to ensure ductile shear failure should satisfy the following equation:

$$\frac{9.37 \cdot k_s}{b^2} = 0.20 \tag{3.104.1}$$

where the plate buckling coefficient k_s, assuming clamped end conditions for the web panel, is given by:

$$k_s = \begin{cases} 5.6 + 9.0/a^2 & a \le 1 \\ 9.0 + 5.6/a^2 & a > 1 \end{cases} \tag{3.104.2}$$

where β is the web panel depth-to-thickness ratio; and α the panel aspect ratio, defined as:

$$a = \frac{a}{d - 2 \cdot t_f} \tag{3.104.3}$$

where d the total depth of the link; and t_f the thickness of the flanges. Intermediate stiffeners may be omitted when web depth-to-thickness ratio is not greater than 20, while end stiffeners are necessary for the ductile response of the link.

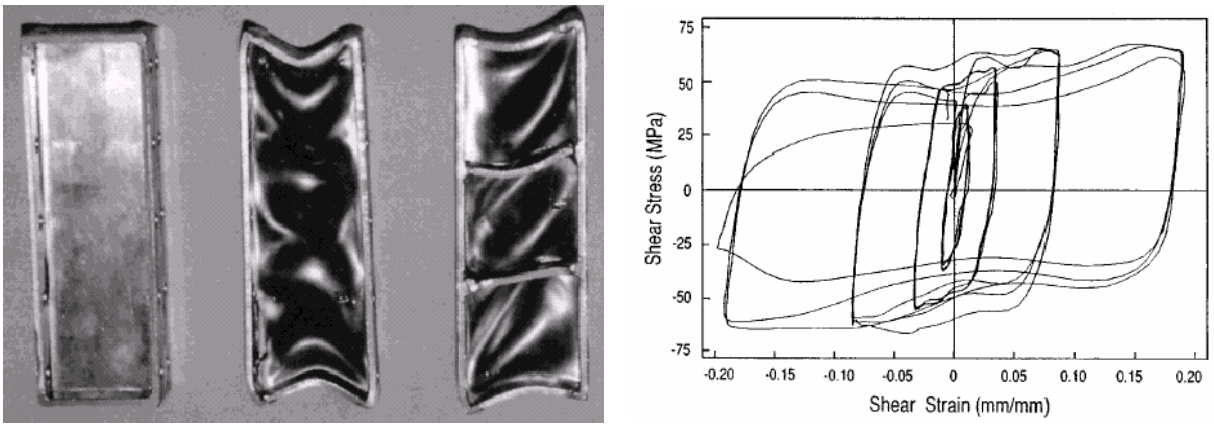

Figure 3.81. - Aluminum shear links: tested specimen (*left*) and typical hysteretic loop (*right*) (*after* Rai and Wallace, 1998).

In EBFs with short links, a sufficient amount of stiffness from the brace is retained while ductility is achieved through shear yielding of the link. However, shear links are an integral part of the beams, which are the main structural members; hence, extensive damage may occur at the floor level during moderate-to-strong earthquakes. Therefore, the concentration of structural damage in secondary elements is a cost-effective strategy for new and existing steel and composite frames. In such cases the dissipative zones may be replaced at minimum cost during the intervention of retrofitting, if necessary.

KBFs are framed systems (Figure 3.82) in which the diagonal braces are connected to a dissipative zone (*knee element*) which is a secondary member, instead of the beam-to-column connection. It has been shown that knee elements dissipate a significant amount of energy through shear yielding (*short knee*) (Sam *et al*., 1995; Balendra *et al*., 1997). Thus the damage is confined in such elements which makes retrofitting more economical and relatively easier. Moreover, the non-buckling brace

provide the stiffness to the system; thus, KBFs combine the advantages of the MRFs and CBFs, similar to EBFs.

Hot rolled sections are suitable for knee elements; however, to prevent LTB it is advisable to use rectangular hollow sections. Bolted connections are preferable because replacement of the damaged knee on site is easier.

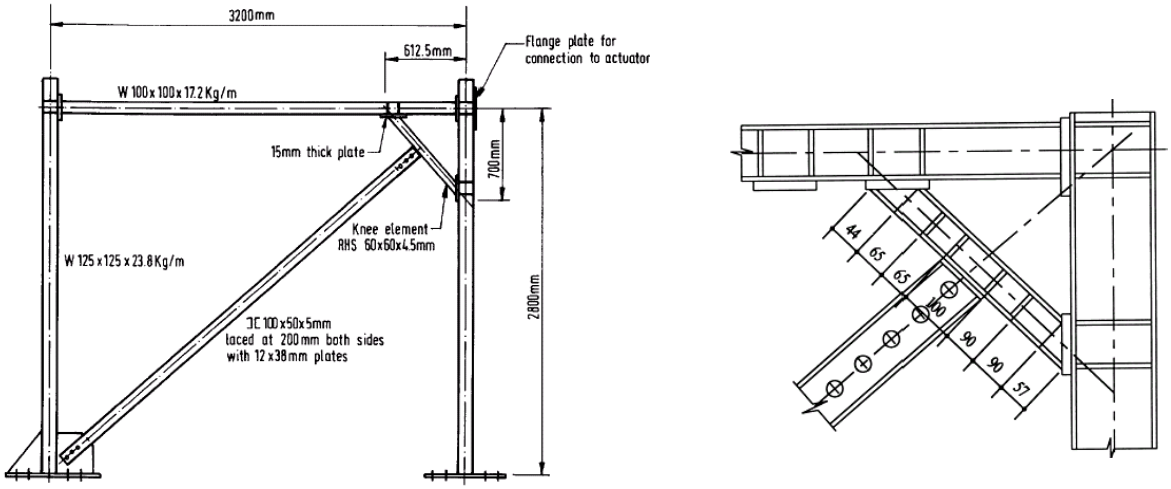

Figure 3.82. KBFs: layout for a single story frame (*left*) and knee detail (*right*) (*after* Sam *et al.*, 1995).

The size and length of knee elements can be easily adjusted to provide the required level of stiffness and ductility. If the knee is very short, then it yields in shear; alternatively flexible knees dissipate energy in bending. However, for short links in EBFs, short knees exhibit higher dissipation capacity and hence, are advisable for seismic retrofitting. Shear knees are those with the maximum length (l_{max}) of the two parts of the element (Figure 3.82) satisfying the following:

$$l_{\max} \le \frac{2 \cdot M_p`}{V_p`} \tag{3.105.1}$$

where the moments $M_p`$ and $V_p`$ are as follows:

$$M_p` = t_f \cdot b \cdot (d - t_f) \cdot f_y \tag{3.105.2}$$

$$V_p` = t_w \cdot (d - t_f) \cdot \frac{f_y}{\sqrt{3}} \tag{3.105.3}$$

where f_y is the yield strength; and d, t_f, b and t_w are the depth, flange, thickness width and web thickness of the knee member, respectively. KBFs with knees designed according to Equation (3.105) exhibit displacement ductilities between 4 and 6. Moreover, floor displacements and interstory drifts for KBFs are very small, e.g., about two-thirds of those exhibited by EBFs with same fundamental periods. In addition, the distribution of lateral deformability is more uniform and much less floor distortions may be found in KBFs.

Based on plastic mechanisms (Figure 3.83), the floor distortions (γ_s) for KBFs are given as follows:

$$g_s = \frac{d_c + d_k}{b} + \frac{2 \cdot d_k}{L - 2 \cdot b} \tag{3.106.1}$$

where δ_c and δ_u are the vertical displacements of the floor at the column; L the length of the beam; δ_k is the vertical displacement of the floor at the knee beam connection; and b is the length from the column to the knee-beam connection.

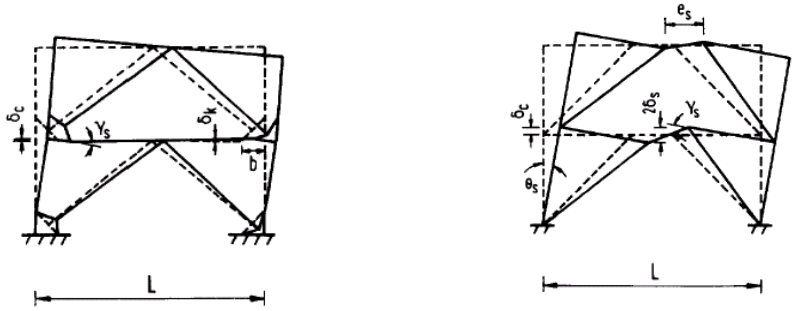

Figure 3.83. Plastic mechanisms for KBF (*left*) and EBF (*right*) (*after* Sam *et al*., 1995).

Similarly, for EBFs (Figure 3.83) the distortion γ_s are as follows:

$$g_s = \frac{2 \cdot (d_c + d_s)}{L - e_s} \tag{3.106.2}$$

where δ_c is the vertical displacements of the floor at the brace ends; and e_s is the length of the beam link. It is instructive to note that in EBFs, either with short (shear) or long (moment) links, large floor distortions are inevitable due to the frame configuration. By contrast, in KBFs with short knee the floor distortion is minimized to an extent that is generally hardly noticeable; this renders the KBFs very economically convenient for seismic retrofitting.

Further improvements of the seismic performance for KBFs may be achieved by employing slotted bolted connections (SBCs) as described in Section 2.5.3. Such connections require only a slight modification of the standard construction practice and are made of materials that are widely e commercially available. It is advised that SBCs are activated at frame drift equal to 1/1500 and can stop at 1/560 corresponding to the serviceability (Balendra *et al*., 2001). The resulting frame hysteretic loops are unpinched with no deterioration in strength and stiffness, thus adequate for structural rehabilitation.

Retrofitting of existing braces and/or use of new braced frames is a very common strategy for steel buildings. For example, more than 240 medium rise residential steel buildings damaged during the 1990 earthquake (M=7.3) in Iran were upgraded by strengthening the existing braces and adding new MRFs (Nateghi, 1995; Nateghi, 1997). The structural deficiencies of such systems built in the 1980s were:: (i) excessive slenderness for cross bars in X-braces (in some cases kL/r>300), (ii) weak columns with likelihood to buckle and (iii) inadequate foundations with possibility of uplifting. New steel plates 5 mm thick were welded to existing braces to stiffen the weak axis; thus, original channel sections designed for tension only were transformed in compact box sections. Long braces were divided into sections and two new braces installed; members with reduced lengths with a belt in between were thus obtained. New braces increase the stiffness and give rise to more uniform distribution of forces. The global intervention cost was less than 25% of replacement value and required 33 tons added; which is around 2.4% of the total weight, i.e., 1,415 tons (final) *vs*. 1,382 tons (original). The frame stiffness increased about 25% along the longitudinal direction and

about 40% along the transverse. The fundamental periods were 0.63s (longitudinal) and 0.85s (transverse) before the intervention and 0.51s (longitudinal) and 0.61s (transverse) after the strengthening. The significant reduction of displacements along the principal directions of the structure (Figure 3.84) was the result of new braces and modification of existing connections in fully rigid. Displacements at the first floor reduced from 2.5 cm to 0.1 cm and from 11 cm to 0.1 cm along the principal directions *x* and *y*. Thus, confirming the effectiveness of the bracing system added.

Strengthening and stiffening of steel buildings with additional braces may also employ stiff macro-braced frames (MBFs). This strategy was adopted to retrofit a 10 story office steel building damaged by the 1985 Michoacan earthquake in Mexico City (Tena-Colunga and Vergara, 1997). The mid-rise structure, built in the 1950s, experienced severe damage during the quake because of the resonant response with the site. To increase the lateral stiffness and hence, to avoid resonance with the soil, concentric diagonal steel bracings were used for the retrofitting. An appendage of three stories was also removed, thus reducing the seismic weight and shortening the period.

The stiffening and strengthening consisted of MBFs (Figure 3.85): 2 MBFs (frames A* and D*) were used in the longitudinal direction and 4 MBFs (frames 1*, 2*, 8* and 12*) in the transverse direction. Each MBF has a story height equivalent to 4 stories of the original frames (*macro-braced*). The other frames resisting to lateral forces were ordinary MRFs.

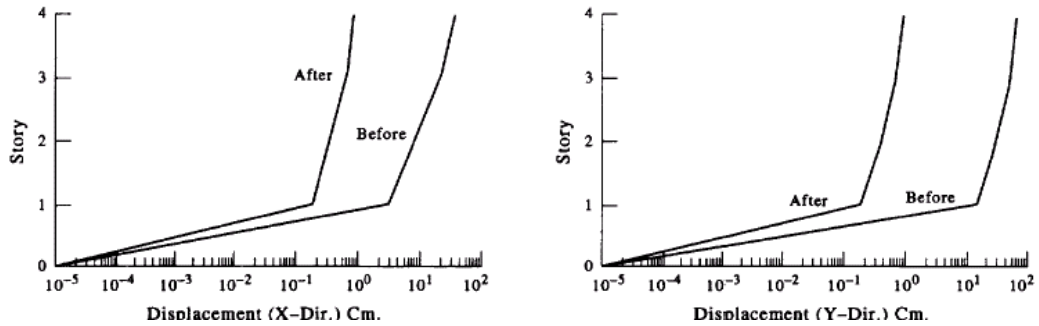

Figure 3.84. - Floor displacements for original and retrofitted framed buildings (*after* Nateghi, 1995).

The columns of MBFs are square box sections, 350x350 mm with plate thicknesses of 19.1 mm for the first story and 9.5 mm for the remaining stories; other exterior columns are 300x300 mm with plate 9.5 mm thick. MBFs along employ beam sections 400 mm high for the transverse frames and 250 mm for longitudinal frames. The diagonal braces are box section 350x350 mm with wall thicknesses equal to 9.5 mm for frames A* and D* and 15.9 mm for frames 1*, 5*, 8* and 12*. Further details may be found in literature (Tena-Colunga and Vergara, 1997). However, the retrofitting with MBF required 285ton of structural steel, including 15% waste because of the complexity of the connection layouts; thus, the added weight is 2.6% of the original.

A recent study has compared the enhancement of seismic performance and cost-effectiveness of MBFs with an alternative retrofitting using added damping and added stiffness (ADAS) devices (Tena-Colunga and Vergara, 1997). These devices (Section 2.5.3.3) were placed in chevron braces (Figure 3.86) along the same locations of MBFs; the design required 162 ADAS to be mounted at the joint between the diagonals and the beams. However, the braces with passive devices were designed to sustain 60% of the seismic base shear, while MBFs carried 100% of the shear.

It is worth mentioning that the cost of the retrofitting with ADAS is nearly twice the cost for MBFs. The added steel is 145 tons including 10% waste for the connections; thus, the initial relative cost

due to structural steel is only one-half of MBF counterpart. Nevertheless, the devices cost about 1.40 times the structural steels; therefore, there is no cost-effectiveness for the alternative intervention of retrofitting. By contrast, energy dissipation with ADAS devices is high and more stable than MBFs; translation ductilities as high as 10 are easily achieved.

Time history analyses showed that maximum drifts are higher for the building with ADAS, while the maximum story shears for the ADAS retrofitting are less than half. However, the initial stiffness of MBFs is much higher (Table 3.20) than the original frames and the one with ADAS. Eigenvalue analysis showed that the fundamental periods for MBFs are about 110% less than the original structure, while the reduction due to the ADAS is about 50%. However, both retrofitting options are effective to provide adequate stiffness to eliminate torsional coupling, i.e., the translational modes are almost pure (Table 3.20).

MBFs are effective to provide much more strength than ADAS at a lower cost, e.g., 0.352W *vs.* 0.191W along one direction or 0.299W *vs.* 0.275W along the orthogonal one. Moreover, the yield strength of ADAS retrofit is lower because the devices yield at smaller shear forces; thus, the energy dissipation is enhanced. Braces with passive devices also cause damping of the forces transmitted to the foundations; the axial forces transferred are half of those relative to MBFs. As a consequence, retrofitting of steel buildings with ADAS is particularly suitable to avoid foundation strengthening.

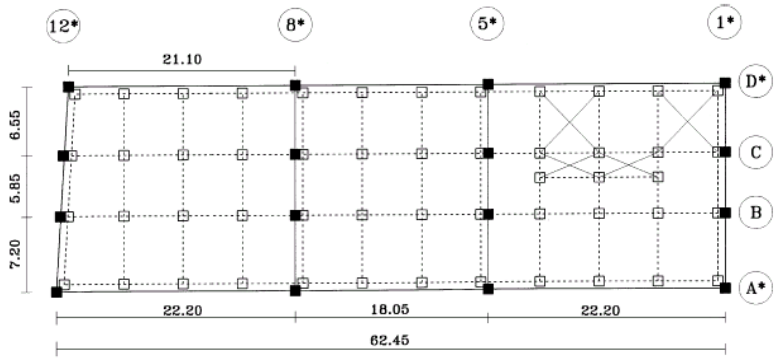

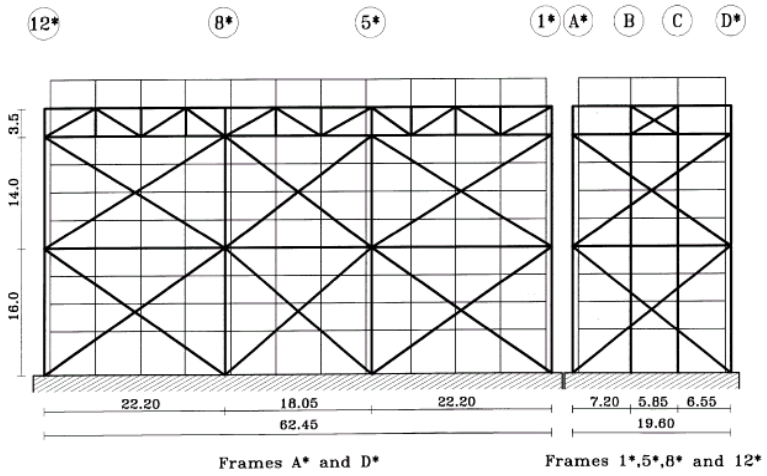

Figure 3.85. Plan view (*top*) and elevation (*bottom*) of the building retrofitted with MBFs (*after* Tena-Colunga and Vergara, 1997).

Table 3.20. Comparisons between alternative retrofitting for a mid-rise steel building.

Structure	Weight (*ton*)	Mode of vibration (*type*)	Period (*sec*)	Maximum base shear (*% W* [*])
Original	8784	1st : Coupled 2nd : Coupled 3rd : Coupled	1st : 1.96 2nd : 1.83 3rd : 1.17	0.108 (N-S) 0.092 (E-W)
Retrofitted with MBFs	9015	1st : Translation (N-S) 2nd : Translation (E-W) 3rd : Torsion	1st : 0.90 2nd : 0.81 3rd : 0.54	0.352 (N-S) 0.299 (E-W)
Retrofitted with ADAS	8907	1st : Translation (N-S) 2nd : Translation (E-W) 3rd : Torsion	1st : 1.12 2nd : 1.24 3rd : 0.86	0.191 (N-S) 0.275 (E-W)

Keys: * W is the total seismic weight.

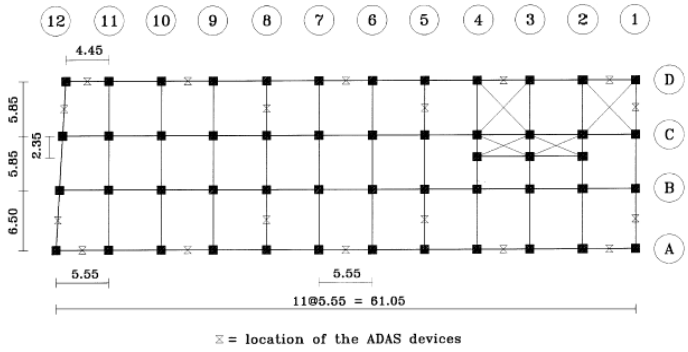

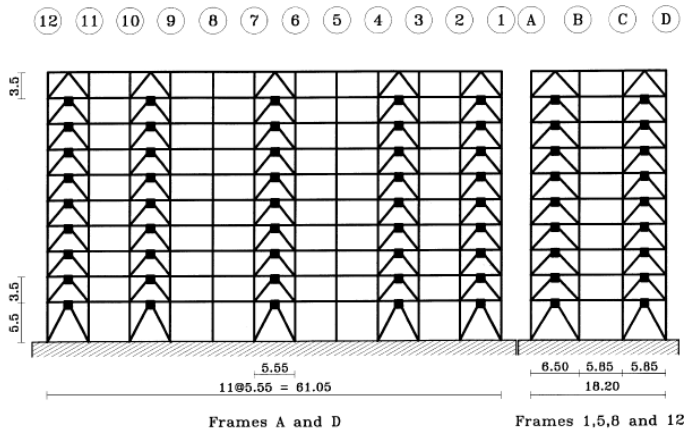

Figure 3.86. Plan view (*top*) and elevation (*bottom*) of the building retrofitted with ADAS devices (*after* Tena-Colunga and Vergara, 1997).

The retrofitting of the medium-rise steel building in Mexico City shows that passive energy dissipation devices, e.g., ADAS, may also be used in conjunction with the bracing to efficiently increase dynamic damping. However, if the bracing system increases the stiffness of the frame considerably, the efficiency of the damping mechanism is compromised since these normally require large levels of displacement to be cost-effective. The basic principles of nonconventional strategies for seismic retrofitting have been discussed in Section 2.5.3. Some examples of the application of passive devices for retrofitting of existing steel and/or composite buildings are outlined in the next section.

3.5.7. FRAMES WITH PASSIVE ENERGY DISSIPATION DEVICES

Passive energy encompasses a wide range of materials and devices to enhance the damping, stiffness and strength of structural systems. Passive energy dissipation devices rely upon: (i) metal yielding, (ii) friction, (iii) phase transformation in metals and (iv) deformations of viscoelastic solid or fluids. Extensive experimental and numerical tests have shown that such devices are very effective for damping vibrations in new and existing buildings. The basic principles and the main design parameters have been discussed in Section2.5.3; the results of some recent applications are summarized hereafter. The significance of the improved performance is assessed in terms of story drifts, enhanced damping and story shears.

Experimental tests and numerical simulations on a one-half scale model of 4-story steel frame, showed that the retrofitting with chevron braces and ADAS devices halves (reduces by 50%) the interstory drifts of the original frame (Tehranizadeh, 2001). Similarly, the natural period of the retrofitted structure is shortened of about 50%. Higher reductions, i.e., on average 80-90%, were found for the story shears. Maximum interstory drifts and story shears relative to the assessed frame are given in Table 3.21 for three earthquakes, namely El Centro (1940), Naghan (1977) and Tabas (1978); the quakes have PGA equal to 0.35g. The trend of the numerical results was confirmed by shaking table tests on the one-half scale model.

Table 3.21. Maximum interstory drifts and story shears for a 4-story steel frame without and with ADAS.

	Interstory drift (mm)						Story shear (kN)					
	Without ADAS			With ADAS			Without ADAS			With ADAS		
Floor	El Centro	Naghan	Tabas	El Centro	Naghan	Tabas	El Centro	Naghan	Tabas	El Centro	Naghan	Tabas

1	20	10	21	13	6	11	541	496	493	198	164	197
2	17	14	10	6	8	2	480	473	545	162	125	154
3	49	4	11	3	8	2	392	383	412	135	127	124
4	24	5	10	3	3	4	310	301	320	112	104	105

However, to achieve such structural benefits, e.g., reduction of story displacements and shears, device-structure interactive parameters should be chosen adequately. Bracing-to-device stiffness ratio (K_b/K_d) should be not less than 2; similarly, the recommended brace/device-to-frame stiffness (K_t/K_{fs}) should be greater than 2. Moreover, device-to-structure force ratios between 0.20 and 0.60 are advised. It is instructive to note that the brace/device stiffness K_t is as follows:

$$K_t = \frac{K_d \cdot K_b}{K_d + K_b} \tag{3.107}$$

Analytical expressions for the plastic capacity (V_{pl}) and the yielding displacement (Δ_y) of the ADAS devices may be derived on the basis of plastic analysis; these relationships are as follows:

$$V_{pl} = \frac{f_y \cdot b_{l_{eq}} \cdot t^2}{2 \cdot l} \tag{3.108.1}$$

$$\Delta_y = \frac{3 \cdot f_y \cdot l^2}{4 \cdot E \cdot t} \tag{3.108.2}$$

where f_y is the steel yield strength; b_{leq} is the width of the edge of the ADAS (Figure 3.87); t is the thickness of the single steel plate, L the height of the damper; and E is the Young's modulus. Thus, the elastic shear stiffness (K_a) is given by:

$$K_a = \frac{V_{pl}}{\Delta_y} \tag{3.108.3}$$

The shape of the ADAS device may be idealized with an hourglass (Figure 3.87), while the variable width b(z) is expressed by the following exponential function:

$$b(z) = \begin{cases} b_1 \cdot e^{-a \cdot z} & 0 \le z \le l/2 \\ b_2 \cdot e^{a \cdot (z - l/2)} & l/2 \le z \le l \end{cases} \tag{3.109.1}$$

with the power exponent α given as:

$$a = \frac{2}{l} \cdot \ln\left(\frac{b_1}{b_2}\right) \tag{3.109.2}$$

where b_1 and b_2 are derived from regression analysis:

$$b_1 = 0.60 \cdot l \tag{3.109.3}$$

$$b_2 = 0.10 \cdot l \tag{3.109.4}$$

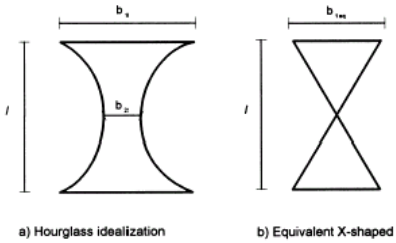

Figure 3.87. Geometry of ADAS devices (*after* Tehranizadeh, 2001).

The application of viscoelastic (VE) dampers for retrofitting of existing steel buildings has also been found very effective due to their high seismic energy dissipation capacity. Early studies aimed at investigating the applicability of such devices started in the late 1980s (Lin *et al*., 1988). A three-storey model frame using 18 different dampers showed that with the most favorable damper configuration, the average reductions in structural response are 80% for relative displacement, 70% for story drifts and about 50% for absolute accelerations. Moreover, the study highlighted that: (i) the VE properties are temperature-dependent, (ii) diagonal placement of the dampers gives rise to the maximum energy dissipation and (iii) the effectiveness of VE dampers in structural response modification diminishes as damping increases beyond a certain limit. Similarly, the assessment of the seismic response of a 2/5-scale steel structure showed that at 25^{o}C the dampers were able to achieve a reduction of about 80% of the maximum response quantities, e.g., maximum floor displacement, maximum story drift and maximum floor acceleration (Chang *et al*., 1995). However, the VE material softens as the ambient temperature increases and hence, the effectiveness of the dampers diminishes (Section 2.5.3.6). Nevertheless, at about 40^{o}C the dampers were still able to achieve more than 40% reduction in response. Based on regression analysis, two empirical formulae were proposed for the damper stiffness (K_d) and the loss factor (η_v) as a function of the frequency (f) of vibration (in Hertz) and the ambient temperature (T in Celsius) (Chang *et al*., 1991):

$$K_d = e^{26.85} f^{0.69} T^{-2.26} \tag{3.110.1}$$

$$h_v = e^{0.85} f^{-0.27} T^{-0.12} \tag{3.110.2}$$

The loss factor is related to the damping ratio, i.e. $h_v = 0.5 \cdot x$, hence, the contribution of N visco-elastic dampers to the global damping of the structure is as follows:

$$x = N \cdot \frac{g_0 \cdot G`` \cdot A \cdot t}{2 \cdot I_m \cdot (b \cdot h_v \cdot f)^2} \tag{3.110.3}$$

where G`` is the loss shear modulus; $\gamma_0$is the design shear strain; A and t the contact area and the thickness of the VE material (Section 2.5.3.6); I_m is the mass moment of inertia of the structure; and β is the deflection slope of the structure. Equation (3.110.3) is very useful to design VE dampers; additional damping ξ required to achieve a given structural performance may be provided via N dampers.

VE dampers were used for the seismic retrofitting of the 13-story Santa Clara County steel building in San Jose (California, USA) in 1993 (Soong and Spenser, 2002). This framed structure was built in 1976; its plan layout is nearly square, 51m wide with a frame height of about 64m. Two sides of the exterior cladding are full-height glazing, while the other two consist of metal siding; such a cladding system does not restrain the story drifts. The equivalent viscous damping in the fundamental mode was 1% of critical; it was determined on site because the building was instrumented. To mitigate the effects of large and long-duration response, including torsional

coupling, the 13-story frame was retrofitted with two VE dampers per building face per floor level. It is, however, interesting to note that initially, three different types of devices were considered, i.e., a steel-yielding damping device, a friction-slip energy dissipation restraint and a VE (Figure 3.88). The VE dampers were chosen primarily because they provide the structure with significantly increased damping for frequent low-to-high intensity earthquakes. In fact, the equivalent damping in the fundamental mode was increased from 1% to about 17% of critical.

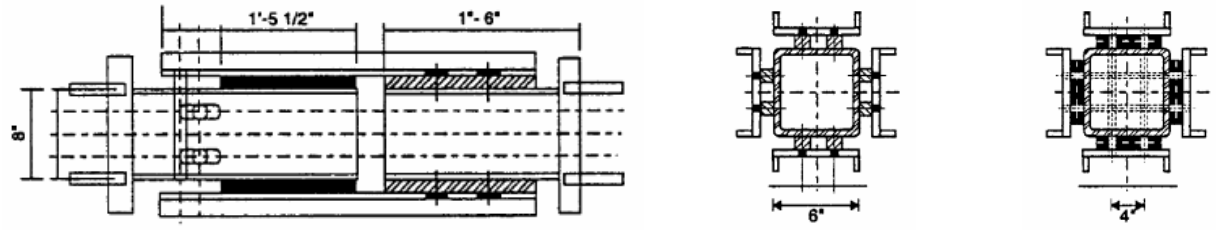

Figure 3.88. VE dampers used in Santa Clara County building: longitudinal view (*left*) and cross sections (*middle and left*) (*after* Soong and Spencer , 2002).

Recent studies have contrasted the efficacy of VE dampers for seismic retrofitting to alternative strategies for passive energy dissipation, e.g., devices with hysteretic damping (or elasto-plastic, EP) (Fu and Kasai, 1997; Kasai *et al*., 1998). The lateral flexibility of a 14-story steel MRF has been reduced by introducing chevron brace with either EP or VE devices. The multistory building is (Figure 3.89) 39x48m in plan and 56.31 m high. The columns are built-up hollow sections, square and rectangular in shape and 450-550 mm wide. The wall thickness varies from 190 mm at the top level to 320 mm at the ground. Beams are wide flanges profiles, 600 to 800 mm deep with flanges 200-300 mm wide. The MRF has periods of 2.32 seconds along the x-direction and 2.12 seconds along the y-direction (Figure 3.89); the initial global damping is about 2 to 4%. The retrofitting with dampers along the x-direction reduces the fundamental period of about 40%; 2.32 sec (MRF) vs. 1.40 sec (EP) and 1.70 (VE). However, the stiffening effect due to the application of VE dampers diminishes as the temperature increases: the period is 1.45, 1.70 and 1.87 seconds respectively at 10, 20 and 30°C. Nevertheless, at 30°C the reduction of the MRF period is still 20%. Similarly, the global damping increases from the initial value of 2 to 4% to 12 to 15% for VE at 20 to 25°C, but the higher the temperature the lower the added damping; at 35°C the damping is still 5%.

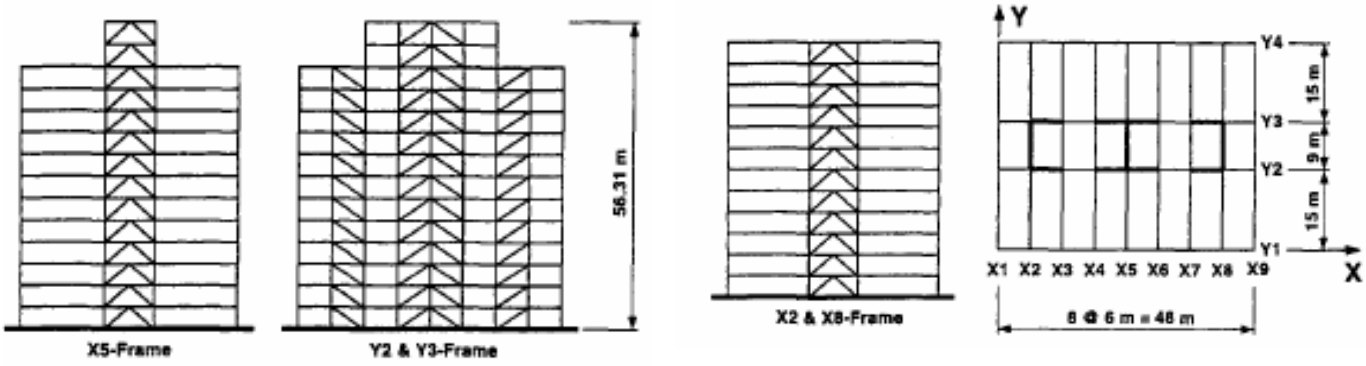

Figure 3.89. Steel frames retrofitted with hysteretic and viscoelastic dampers (*after* Kasai *et al*., 1998).

EP and VE are able to reduce at least 0.4 to 0.5 times the roof story drift and 0.7 times the base shear of the original elastic MRF. Moreover, they give rise to uniform distributions of drifts and

story shear along the building height, thus eliminating concentrations of deformation and strength demands. However, it is worth noting that VE devices exhibit neither residual deformations nor forces, while EP dampers give rise to residual deformations and forces, up to 12% of the yield strength. Nevertheless, it has been shown that hysteretic dampers, e.g., unbounded braces (Figure 3.90), are able to reduce interstory drifts and story shears to less than three-fourths the level of the conventional braced structure (Soong and Spencer, 2002). Unbounded braces are very economical and efficient for seismic retrofitting (Section 2.5.3.3); they employ low yield steel plates in unbonding material, e.g., steel-fiber reinforced concrete.

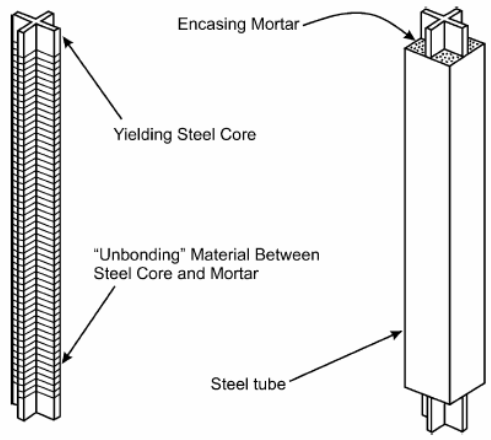

Figure 3.90. Typical unbounded brace (*after* Soong and Spencer , 2002).

The optimal design of EP and VE requires that the bracing-to-story stiffness ratio (K_b/K_{fs}) should be about 10, while the device should be as stiff (K_d) as the story stiffness (K_{fs}); K_d = 2-3 K_{fs} is advisable. The shear stiffness (K_{fs}) of the frames should be much higher than the bending counterpart (K_{fb}); e.g., K_{fs} equal to 10 times $K_{fb.}$ This requirement may be achieved by reducing the axial deformability of the columns, if any. Moreover, EP should have design ductility (μ_d) equal to 3 to 4 and peak coefficient (p) of about 0.3. For VE, it is advised to assume loss ?$_d$ is between 1.0 and 1.5 (Lai *et al*., 1995; Fu and Kasai, 1997).

3.6. GUIDELINES FOR QUALITY CONTROL

The enhancement of the seismic performance of existing structures via retrofitting is strictly dependent upon the quality of the procedures, materials and workmanship used during construction. Therefore, it is of paramount importance to ascertain the fulfillment of quality requirements as appropriate for the various components of the structure at all construction stages.

Base and parent materials should be sound and compatible with the existing ones. Structural steel should exhibit: (i) consistent strength, (ii) high yield-to-tensile strength ratio, (iii) large inelastic strains, (iv) metallurgical soundness, (v) adequate toughness, i.e., 27J measured at 20^{o}C via Charpy test (CVN) and (vi) good weldability. For in-place materials, these properties should be ascertained preferably by testing (Section 3.1.6); alternatively, original drawings and testing records, if any, can be referred to. The coupons should be cut from webs (higher strength) or flanges (lower strength) as appropriate. Furthermore, welds should be performed by qualified workmanship either *in situ* or in workshops and should employ parent materials with adequate toughness, e.g., CVN equal to 27J at 20^{o}C. Base metal thicker than 40 mm when subjected to through thickness weld shrinkage strains should be inspected carefully to avoid discontinuities behind and adjacent to such welds after joint

completion. Visual inspection is a rapid and economic method which should always be performed; nevertheless it is limited to superficial screening. Destructive (sampling) and/or nondestructive testing, e.g., (liquid penetrant, magnetic particle, acoustic emission), ultrasonic or tomographic methods,` should be used for critical regions of the structure. Moreover, bolting, especially in slip-critical connections and/or subjected to net tension, requires thorough controls during installation and tightening. Built-up sections should be assembled in such a way to minimize the effects of geometrical and mechanical imperfections. Geometrical tolerances should conform to those used in the design.

On the other hand, regular inspection is required during and upon completion of RC components and/or connections. Concrete classes should range between C20/25 and C40/50, while bars, stirrups and welded meshes should be ribbed. Checks on the quality and size of aggregates are essential to ensure adequate bond between the concrete and reinforcement bars. Detailing, e.g., anchorages and overlaps, should be carefully inspected; indeed, poor details may undermine the ductile response under earthquake loads. Reinforcement bars should be protected by adequate concrete covers; it is required to ascertain that the thickness of such covers corresponds to the value assumed in the design. Spacing of stirrups, particularly in dissipative zones, should be ascertained before casting. All the other testing procedures and structural observations should comply with the requirements for new constructions.

Special devices, such as base isolators and/or dampers, should be qualified by the manufactures. However, the connections with the structure should be inspected during and after installation. Additional controls should be performed on such devices as specified by local authorities.

Special inspections, testing and structural observations should be specified by the designer in a quality control document (QCD). The QCD should contain: (i) the required contractor quality control procedures, (ii) the significant construction stages during which the checks should be performed and (iii) the requirements for tests on sub-assemblages to obtain design information not included in the guidelines.

4. REFERENCES

Abbas, H. and Kelly, J.M. (1993). A methodology for design of visco-elastic dampers in earthquake-resistant structures. *Report No. UCB/EERC-93/09,* University of California at Berkeley, California, USA.

Achenbach, M., Atanochovic, T. and Muler, I. (1986). A model for memory alloys in plane strain. *International Journal of Solid and Structures*, 22(2), 171-193.

AIJ (1991). Standards for structural calculation of steel reinforced concrete structures. Architectural Institute of Japan, Tokyo, Japan.

AIJ (1995). Performance of steel buildings during the 1995 Hyogoken-Nanbu earthquake. Architectural Institute of Japan, Tokyo, Japan.

Aiken, I. D. and Kelly, J.M. (1990). Earthquake simulator testing and analytical studies of two energy-absorbing systems for multistory structures. *Report No. UCB/EERC-90/03,* University of California at Berkeley, California, USA.

Aiken, I., Nims, D., Whittaker, A. and Kelly, J.M. (1993). Testing of passive energy dissipation systems. *Earthquake Spectra*, 9(2), 335-370.

American Institute of Steel Construction (1993). Load and Resistance Factor Design Specification for Structural Steel Buildings. AISC, Chicago, Illinois, USA.

American Institute of Steel Construction (1997). Seismic provisions for structural steel buildings. AISC, Chicago, Illinois, USA.

Aoki, H. (2000). Establishment of design standards and current practice for stainless steel structural design in Japan. *Journal of Constructional Steel Research*, 54 (1), 191-210.

Arima, F., Miyazaki, M., Tanaka, H. and Yamazaki, Y. (1988). A study on buildings with large damping using viscous damping walls. *Proceedings of the 9th World Conference on Earthquake Engineering*, Tokyo (Japan), August 2-9, V, 821-826.

ASCE (1998). Design guide for partially restrained composite connections. ASCE Task Committee on Design Criteria for Composite Structures in Steel and Concrete. *Journal of Structural Engineering*, ASCE, 128(10), 1099-1114.

Aslani, F. and Goel, S.C. (1991). Stitch spacing and local buckling in seismic resistant double angle bracing members. *Journal of Structural Engineering*, ASCE, 177(8), 2442-2463.

Astaneh, A.A. (1995). Seismic design of bolted steel moment resisting frames. *Steel Tips*, Structural Steel Education Council, Technical Information and Product Service, Alamo, California, USA.

Astaneh, A.A. (1997). Seismic design of steel column-tree moment resisting frames. *Steel Tips*, Structural Steel Education Council, Technical Information and Product Service, Alamo, California, USA.

Astaneh, A.A. (2001). Seismic behavior and design of steel shear walls. *Structural Tips*, Structural Steel Eduaction Council, Technical Information and Product Service, July, Berkeley, California, USA.

Austin, M.A. and Pister, K.S. (1985). Design of seismic-resistant friction-braced frames. *Journal of Structural Engineering*, ASCE, 111(12), 2751-2769.

Avent, R.R., Mukai, D.J. and Heymsfield, E. (2001). Repair of localized damage in steel by heat straightening. *Journal of Structural Engineering*, ASCE, 127(10), 1121-1128.

Azizinamini, A. and Ghosh, S.K. (1996). Steel reinforced concrete structures in 1995 Hyogoken-Nanbu Earthquake. *Journal of Structural Engineering*, ASCE, 123(8), 986-990.

Bachmann, H., Ammann, W.J., Deischl, F., Eisenmann, J., Floegl, I., Hirsch, G.H., Klein, G.K., Lande, G.J., Mahrenholtz, O., Natke, H.G., Nussbaumer, H., Pretlove, A.J., Rainer, J.H., Saemann, E.U. and Steinbeisser, L. (1995). Vibration problems in structures. Practical guidelines. Birkhauser Verlag, Basel.

Balendra, T., Lin, E.L. and Liaw, C.Y. (1997). Large-scale seismic testing of knee-brace-frame. *Journal of Structural Engineering*, 123(1), 11-19.

Balendra, T., Yu, C.H. and Lee, F.L. (2001). An economical structural system for wind and earthquake loads. *Engineering Structures*, 23(5), 491-501.

Barsom, J.M. and Korvink, S.A. (1998). Through-thickness properties of structural steels. *Journal of Structural Engineering*, ASCE, 124(7), 727-735.

Barsom, J.M. and Rolfe, S.T. (1999). Fracture and fatigue control in structures, applications of fracture mechanics. American Society for Testing and Materials.

Bertero, V.V. (1988). Ductility-based structural design: a state-of-the-art report. *Ninth World Conference on Earthquake Engineering*, Tokyo/Kyoto, Japan, Vol. 8, 673-86.

Boyd, P.F., Cofer, W.F. and McLean, D.I. (1995). Seismic performance of steel-encased concrete columns under flexural loading. *ACI Structural Journal*, 92(3), 355-364.

Broderick, B.M. and Elnashai, A.S. (1996). Seismic response of composite frames, I: Response criteria and input motion. *Engineering Structures*, 18(9), 696-706.

Bruneau, M. and Mahin, S.A. (1990). Ultimate behavior of heavy steel section welded splices and design implications. *Journal of Structural Engineering*, ASCE, 116(8), 2214-2235.

Bruneau, M., Uang, C.M. and Whittaker, C.M. (1997). Ductile design of steel structures. McGraw Hill, New York, New York, USA.

Bruneau, M. and Bhagwagar, T. (2002). Seismic retrofit of flexible steel frames using thin infill panels. *Engineering Structures*, 24(4), 443-453.

Burgan, B.A., Baddoo, N.R. and Gilsenan, K.A. (2000). Structural design of stainless steel members: Comparison between Eurocode 3, Part 1.4 and tests results. *Journal of Constructional Steel Research*, 54(1), 51-73.

Bursi, O.S. and Gramola, G. (1999). Behaviour of headed stud shear connectors under low-cycle high amplitude displacements. *Materials and Structures*, 32(5), 290-297.

Bursi, O.S. and Zandonini, R. (1998). Quasi-static cyclic and pseudo-dynamic tests on composite substructures with softening behaviour. Stability and Ductility of Steel Structures, Usami T. and Itoh Y. Eds., Elsevier, 119-130.

Byfield, M.P. (1996). Steel design and reliability using Eurocode 3. *PhD Thesis*, University of Nottingham, Department of Civil Engineering, Nottingham, UK.

Byfield, M.P. and Nethercot, D.A. (1997). Material and geometric properties of structural steel for use in design. *The Structural Engineer*, *Journal of the Institution of Structural Engineers*, 75(21), 363-367, London, UK.

Cecconi, A., Croce, P. and Salvatore, W. (1997). Statistical properties of the European production of structural steels. *Proceedings of ESREL `97* in "Advances in Safety and Reliability", Vol.2, Lisbon, June 17-20 1997, 1567-1574.

Chang, K.C., Lin, Y.Y. and Lai, M.L. (1996). Seismic design of structures with added viscoelastic dampers. *Proceedings of the 11th World Conference on Earthquake Engineering*, Acapulco (Mexico), June 23-28.

Chang, K.C., Soong, T.T., Oh, S.T. and Lai, M.L. (1991). Seismic response of a 2/5 scale steel structure with added visco-elastic dampers. *Technical Report No. NCEER-91-0012*, National Center for Earthquake Engineering Research, Buffalo, New York, USA.

Chang, K.C., Soong, T.T., Oh, S.T. and Lai, M.L. (1992). Effect of ambient temperature on viscoelastically damped structure. *Journal of Structural Engineering*, ASCE, 118(7), 1955-1973.

Chang, K.C., Soong, T.T., Lai, M.L. and Nielsen, E.J. (1993). Development of a design procedure for structures with added viscoelastic dampers. *Proceedings ATC 17-1 on Seismic Isolation, Energy Dissipation and Active Control*, 2, 473-484.

Chang, K.C., Soong, T.T., Oh, S.T. and Lai, M.L. (1995). Seismic behavior of steel frame with added viscoelastic dampers. *Journal of Structural Engineering*, ASCE, 121(10), 1418-1426.

Chen, S.J. (1996). A simple and effective retrofit method for steel beam-to-column connections. *Seventh US-Japan Workshop on the improvement of structural design and construction practices*, ATC, Redwood City, California, USA.

Ciampi, V. (1993). Development of passive energy dissipation techniques for buildings. *Proceedings International Post-SMIRT Conference Seminar on Isolation, Energy Dissipation and Control of Vibrations of Structures*, Capri (Italy), 495-510.

Ciampi, V., De Angelis, M. and Paolacci, F. (1997). Una metodologia di progetto su base energetica per controventi dissipativi viscoelastici. *Proceedings of the 8th National Conference on Earthquake Engineering*, Taormina (Italy), September 21-24, 1, 653-660 (*in Italian*).

Colajanni, P. and Papia, M. (1997). Hysteretic characterization of friction-damped braced frames. *Journal of Structural Engineering*, ASCE, 123(8), 1020-1028.

Constantinou, M.C., Symans, M.D., Tsopelas, P. and Taylor, D.P. (1993). Fluid viscous dampers in applications of seismic energy dissipation and seismic isolation. *Proceedings ATC 17-1* on *Seismic Isolation, Passive and Active Control*, 2, 581-592.

CSA. (1994). CAN/CSA-S16.1-94. Limit states design of steel structures, 6th Edition. *Canadian Standard Association*, Willowdale, Ontario, Canada.

Daali, M., L. and Korol, R.M. (1995). Prediction of local buckling and rotation capacity at maximum moment. *Journal of Constructional Steel Research*, 32(1), 1-13.

De Matteis, G., Moen, L.A., Langseth, M., Landolfo, R., Hopperstad, O.S. and Mazzolani, F.M. (2001). Cross sectional classification for aluminum beams. Parametric study. *Journal of Structural Engineering*, ASCE, 127(3), 271-279.

Des Roches and R., Delemont, M. (2002). Seismic retrofit of simply supported bridges using shape memory alloys. *Engineering Structures*, 24(3), 325-332.

Des Roches, R., Leon, R., Hess, G. and Ocel, J. (2001). Innovative Beam-Column Joint Connections Using Shape Memory Alloy Components. *Proceeding of the SPIE Smart Systems for Bridges, Structures and Highways*, New Port Beach, California, USA.

Dexter, R.J. and Melendrez, M.I. (2000). Through-thickness properties of column flanges in welded moment connections. *Journal of Structural Engineering*, ASCE, 126(1), 24-31.

Di Sarno, L. (2000). Seismic performance assessment of stainless steel frames. MSc Dissertation, Imperial College, London, UK.

Di Sarno, L., Elnashai, A.S. and Nethercot, D.A. (2002). Comparison between seismic response characteristics of carbon steel and stainless steel. *Proceedings of the 12th European Conference on Earthquake Engineering*, London, UK.

Dolce, M., Cardone, D. and Marnetto, R. (2000). Implementation and testing of passive control devices based on shape memory alloys. *Earthquake Engineering and Structural Dynamics*, 29 (7), 945-968.

Driver, R.G., Kulak, G.L., Kennedy, D.J.L. and Elwi, A.E. (1998). Cyclic test of four-story steel plate shear wall. *Journal of Structural Engineering*, ASCE, 124(2), 112-120.

Duerig, T.W., Melton, K.N., Stockel, D. and Wayman, C.M. (1990). Engineering aspects of shape memory alloys. Butterworth-Heinemann, London, UK.

Elnashai, A.S. (1994). Local ductility in steel structures subjected to earthquake loading. *Behaviour of Steel Structures in Seismic Areas*, F.M. Mazzolani and V. Gioncu Eds., STESSA `94, E&FN Spon, 133-148.

Elnashai, A.S., (2000). Modern seismic design of steel structures and EC8 developments. *Proceedings of the 12th World Conference of Earthquake Engineering*, Auckland, New Zealand.

Elnashai, A.S. and Broderick, B.M. (1994). Seismic resistance of composite beam-columns in multi-storey structures, Part I: experimental studies. *Journal of Constructional Steel Research*, 30(3), 201-230.

Elnashai, A.S. and Broderick, B.M. (1996). Seismic response of composite frames-II. Calculation of behaviour factors. *Engineering Structures*, 18(9), 707-723.

Elnashai, A.S. and Chryssanthopoulos, M. (1991). Effect of random material variability on seismic design parameters of steel frames. *Earthquake Engineering and Structural Dynamics*, 20 (2), 101-114.

Elnashai, A.S., Elghazouli, A.Y. and Danesh, Ashtiani, F.A. (1998). Response of semirigid steel frames to cyclic and earthquake loads. *Journal of Structural Engineering*, ASCE, 124(8), 857-867.

Elnashai, A.S. and Izzuddin, B.A. (1993). Modelling of material nonlinearities in steel structures subjected to transient dynamic loading. *Earthquake Engineering and Structural Dynamics*, 22(6), 509-532.

Elnashai A.S. and Tsujii M. (1999). Shaking table tests and analysis of steel and composite frames. ICONS Topic 4 report, Ispra, Italy.

El-Tawil, S., Mikesell, T. and Kunnath, S.K. (2000). Effect of local details and yield ratio on behaviour of FR steel connections. *Journal of Structural Engineering*, ASCE, 126(1), 79-87.

EN 10025 (1990). Hot rolled products of nonalloy structural steels. Technical Delivery Condition. European Communities for Standardisation, Brussels, Belgium.

Engelhardt, M.D. and Popov, E.V. (1989). On the design of eccentrically braced frames. *Earthquake Spectra*, EERI, 5(3), 495-511.

Engelhardt, M.D. and Sabol, T.A. (1997). Seismic-resistant steel moment connections: development since the 1994 Northridge earthquake. *Progress in Structural Engineering and Materials*, 1(1), 68-77.

Engelhardt, M.D. and Sabol, T.A. (1998). Reinforcing of steel moment connections with cover plates: benefits and limitations. *Engineering Structures*, 20(4-6). 510-520.

Engelhardt, M.D., Winnerberg, T., Zekany, A.J. and Potyraj, T.J. (1998). Experimental investigation of dog-bone moment connections. *Engineering Journal*, AISC, 35(4), 22-27.
Eurocode 2. (1992). Design of concrete structures. Part 1.1: General rules and rules for buildings. European Communities for Standardisation, Brussels, Belgium.

Eurocode 3. (1992). Design of steel structures. Part 1.1: General rules and rules for buildings. European Communities for Standardisation, Brussels, Belgium.

Eurocode 3. (1996). Design of steel structures. Part 1.4: General rules - Supplementary rules for stainless Steel. European Communities for Standardisation, Brussels, Belgium.

Eurocode 4. (1994). Design of composite steel and concrete structures. Part 1.1: General rules and rules for buildings. European Communities for Standardisation, Brussels, Belgium.

Eurocode 8. (1998). Design provisions for earthquake resistance of structures. Part 1.3: General rules. Specific rules for various materials and elements. European Communities for Standardisation, Brussels, Belgium.

Eurocode 9. (1999). Design of aluminum alloy structures. Part 1.1. : General rules and rules for buildings. European Communities for Standardisation, Brussels, Belgium.

Euro Inox. (1994). Design manual for structural stainless steel. European Stainless Steel Development & Information Group, Nickel Development Institute, Toronto, Canada.

Fabbrocino, G., Manfredi, G. and Cosenza, E. (2001). Ductility of composite under negative bending: an equivalence index for reinforcing steel classification. *Journal of Constructional Steel Research*, 57(2), 185-202.

Faella, C., Piluso, V. and Rizzano, G. (1997). A new method to design extended end plate connections and semirigid braced frames. *Journal of Constructional Steel Research*, 41(1), 61-91.

Federal Emergency Management Agency (1995). Interim Guidelines: Evaluation, repair, modification and design of welded steel moment frames. *Report No. FEMA 267/SAC-95-02*, SAC Joint Venture, Sacramento, California, USA.

Federal Emergency Management Agency (1997). NEHRP guidelines for the seismic rehabilitation of buildings. *Report No. FEMA 273*, Washington, D.C., USA.

Federal Emergency Management Agency (1997). NEHRP Commentary on the guidelines for the seismic rehabilitation of buildings. *Report No. FEMA 274*. Washington, D.C., USA.

Federal Emergency Management Agency (1998). Handbook for the seismic evaluation of buildings- A prestandard. *Report No. FEMA 310*. Washington, D.C., USA.

Federal Emergency Management Agency (2000). Recommended seismic design criteria for new steel moment-frame buildings. *Report No. FEMA 350*. Washington, D.C., USA.

Federal Emergency Management Agency (2000). Recommended seismic evaluation and upgrade criteria for existing welded steel moment-frame buildings. *Report No. FEMA 351*. Washington, D.C., USA.

Federal Emergency Management Agency (2000). Recommended postearthquake evaluation and repair criteria for welded steel moment-frame buildings. *Report No. FEMA 352*. Washington, D.C., USA.

D.C.Federal Emergency Management Agency (2000). NEHRP guidelines for the seismic rehabilitation of buildings. State of the art Report on base metals and fracture. *Report No. FEMA 355A*. Washington, D.C., USA.

Federal Emergency Management Agency (2000). State of the art Report on welding and inspection. *Report No. FEMA 355B*. Washington, D.C., USA.

Federal Emergency Management Agency (2000). NEHRP guidelines for the seismic rehabilitation of buildings. State of the art Report connection performance. *Report No. FEMA 355D*. Washington, D.C., USA.

Federal Emergency Management Agency (2000). State of Art Report on past performance of steel moment frame buildings in earthquakes. *Report No. FEMA 355E*. Washington, D.C., USA.

Federal Emergency Management Agency (2000). Pre-standard and commentary for the seismic rehabilitation of buildings. *Report No. FEMA 356*. Washington, D.C., USA.

Federal Emergency Management Agency (2000). Global topics report on the pre-standard and commentary for the seismic rehabilitation of buildings. *Report No. FEMA 357*, Washington, D.C., USA.

Federal Emergency Management Agency (2001). NEHRP recommended provisions for seismic regulations for new buildings and other structures, Part 1 - Provisions. *Report No. FEMA 368*, Washington, D.C., USA.

Federal Emergency Management Agency (2001). NEHRP recommended provisions for seismic regulations for new buildings and other structures, Part 2 - Commentary. *Report No. FEMA 369*, Washington, D.C., USA.

Filiatrault, A. and Cherry, S. (1987). Performance evaluation of friction damped braced frames under simulated earthquake loads. *Earthquake Spectra,* 3(1), 57-78.

Filiatrault, A. and Cherry, S. (1989). Parameters influencing the design of friction-damped braced frames. *Canadian Journal of Civil Engineering*, 16, 753-766.

Filiatrault, A. and Cherry, S. (1990). Seismic design spectra for friction-damped structures. *Journal of Structural Engineering,* ASCE, 116(5), 1334-1355.

Flanagan, R.D. and Bennett, R.M. (1999-a). Bidirection behavior of structural tile infilled frames. *Journal of Structural Engineering,* ASCE, 125(3), 236-244.

Flanagan, R.D. and Bennett, R.M. (1999-b). Plane behavior of structural clay tile infilled frames. *Journal of Structural Engineering,* ASCE, 125(6), 590-599.

Foutch, D.A., Wood, S.L. and Brady, P.A. (1993). Seismic retrofit of nonductile reinforced concrete frames using viscoelastic dampers. *Proceedings ATC 17-1 on Seismic Isolation, Passive and Active Control*, 2, 605-616.

Fu, Y. and Kasai, K. (1998). Comparative study of frames using viscoelastic and viscous dampers. *Journal of Structural Engineering,* ASCE, 124(5), 513-522.

Fukumoto, Y. (1996). New constructional steels and structural stability. *Engineering Structures*, 18(10), 786-791.

Fukumoto, Y. (2000). Reduction of structural ductility factor due to the variability of steel properties. *Engineering Structures*, 22 (2), 123-127.

Galambos, T.V. (1998). Guide to stability design criteria for metal structures. Fifth Edition, John Wiley and Son, New York.

Galambos, T.V. and Ravindra, M.K. (1978). Properties of steel for use in LRFD. *Journal of Structural Division*, ASCE, 104 (ST9), 1459-68.

Gioncu, V. (2000). Ductility and seismic response. General Report. *Journal of Constructional Steel Research*, 55(1-3), 125-154.

Gioncu, V. and Mazzolani, F.M. (1994). Alternative methods for assessing local ductility. *Behaviour of Steel Structures in Seismic Areas*, STESSA 1994, F.M. Mazzolani and V. Gioncu Eds., E&FN Spon, London, 182-190.

Gioncu, V. and Petcu, D. (1997). Available rotation capacity of wide-flange beams and beam-columns., Part.1. Theoretical approaches. *Journal of Steel Constructional Steel Research*, 43, (1-3), 161-217.

Goel, S.C. (1992-a). Cyclic post-buckling behaviour of steel bracing members. *Stability and Ductility of Steel Structures Under Cyclic Loading*, Y. Fukumoto and G.C. Lee Eds., CRC Press, 75-104.

Goel, S.C. (1992-b). Earthquake resistant design of ductile braced structures. *Stability and Ductility of Steel Structures Under Cyclic Loading*, Y. Fukumoto and G.C. Lee Eds., CRC Press, 297-308.

Graesser, E.J. and Cozzarelli, F.A. (1991). Shape memory alloys as new materials for seismic isolation. *Journal of Engineering Mechanics*, ASCE, 117(11), 2590-2608.

Grigorian, C.E., Yang, T.S. and Popov, E.V. (1993). Slotted bolted connection energy dissipators. *Earthquake Spectra*, 9(3), 491-504.

Gross, J.L., Engelhardt, M.D., Uang, C.M., Kasai, K. and Iwankiw, N. (1999). Modification of existing welded moment frame connections for seismic resistance. *Steel Design Guide Series 12*, AISC, Chicago, Illinois, USA.

Hajjar. J.F. (2002). Composite steel and concrete structural systems for seismic engineering. *Journal of Constructional Steel Research*, 58(5-8), 703-723.

Harries, K., Mitchell, D., Cook, W.D. and Redwood, R.G. (1993). Seismic response of steel beams coupling concrete walls. *Journal of Structural Engineering*, ASCE, 119(12), 3611-3629.

Hjelmstad, K.D. and Popov, E.P. (1984). Characteristics of eccentrically braced frames. *Journal of Structural Engineering*, ASCE, 110(2), 340-353.

Holmes, M. (1961). Steel frames with brickwork and concrete infillings. *Proceedings of the Institution of Civil Engineers*, London, UK, August 19, 473-478.

Holmes, W. T. (2000). Risk assessment and retrofit of existing buildings. *Bulletin of the New Zealand National Society for Earthquake Engineering*, 33(3), 222-247.

Housner, G.W., Bergman, L.A., Caughey, T.K., Chassiakos, A.G., Claus, R.O., Masri, S.F., Skelton, R.E., Soong, T.T., Spenser, B.F.,Jr. and Yao, T.P. (1997). Structural control: past, present and future. *Journal of Engineering Mechanics*, ASCE, 123(9), 897-971.

Inoue, K., Sawaizumi, S. and Higashibata, Y. (2001). Stiffening requirements for unbonded braces encased in concrete panels. *Journal of Structural Engineering*, ASCE, 127(6), 712-719.

International Code Council (2000). International Building Code. Whittier, California, USA.

International Conference of Building Officials (1997). Uniform Building Code. Whittier, California, USA.

Iwankiw, N.R. and Carter, C.J. (1996). The dog-bone: A new idea to chew on. *Modern Steel Construction*, AISC, 36(4), 18-23.

Jennings, P.C. (1971). Engineering features of the San Fernando earthquake of February 9, 1971. *EERL Report No.71-02*, Earthquake Engineering Research Laboratory, California Institute of Technology.

Jirsa, O. (1994). Divergent issues in rehabilitation of existing buildings. *Earthquake Spectra*, 10(1), 95-112.

Johansson, B. and Olsson, A. (2000). Current design practice and research on stainless steel structures in Sweden. *Journal of Constructional Steel Research*, 54(1), 3-29.

Jones, N. and Birch, R.S. (1998). Dynamic and static tensile tests on stainless steel for The Steel Construction Institute. Confidential Report, Ascot, Berkshire, UK.

Jones, S.L., Fry, G.T. and Engelhard, M.D. (2002). Experimental evaluation of cyclically loaded reduced beam section moment connections. *Journal of Structural Engineering*, ASCE, 128(4), 441-451.

Kasai, K., Fu, Y. and Watanabe, A. (1998). Passive control systems for seismic damage mitigation. *Journal of Structural Engineering*, ASCE, 124(5), 501-512.

Kasai, K. and Popov, E.P. (1985). On seismic design of eccentrically braced frames. *Proceedings of the 8th World Conference on Earthquake Engineering*, Vol. V, 387-394, IAEE, San Francisco, California, USA.

Kato, B. (1989). Rotation capacity of H-section members as determined by local buckling. *Journal of Constructional Steel Research*, 13(2-3), 95-109.

Kato, B. (1994). Development and design of seismic resistant steel structures in Japan. *Behaviour of Steel Structures in Seismic Areas*, STESSA 1994, F.M. Mazzolani and V. Gioncu Eds., E&FN Spon, London, UK 28-42.

Kato, B. and Akiyama, H. (1982). *Seismic design of steel buildings. Journal* of Structural Division, ASCE, 108 (ST8), 1705-1721.

Kelly, J.M. (1996). Earthquake-resistant design with rubber. 2nd Edition, Springer-Verlag, Inc., New York, New York, USA.

Kelly, T.E. (2001). In-structure damping and energy dissipation. Design guidelines. Holmes Consulting Group.

Kemp, A.R. and Nethercot, D.A. (2001). Required and available rotations in continuous composite beams with semi-rigid connections. *Journal of Constructional Steel Research*, 57(4), 375-400.

Khan, F.R. and Sbarounis, J.A. (1964). Interaction of shear walls and frames. *Journal of the Structural Division*, ASCE, 90(ST3), 285-335.

Khatib, I., Mahin, S.A. and Pister, K.S. (1988). Seismic behavior of concentrically braced steel frames. *Report No.UCB/EERC-88-01*, Earthquake Engineering Research Center, Berkeley, California, USA.

Kim, T., Whittaker, A.S., Gilani, A.S.J. and Bertero, V.V. and Takhirov, S.M. (2002). Cover-plate and flange-plate steel moment resisting connections. *Journal of Structural Engineering*, ASCE, 128(4), 474-482.

Krawinkler, H., Bertero, V.V. and Popov, E.P. (1975). Shear behavior of steel frame joints. *Journal of Structural Division*, ASCE, 101(ST11), 2317-2338.

Kunnath, S.K. and Malley, J.O. (2002). Advances in seismic design and evaluation of steel moment frames: recent findings from FEMA/SAC Phase II Project. *Journal of Structural Engineering*, ASCE, 128(4), 415-419.

Kuwamura, H. (1988). Effect of the yield ratio on the ductility of high strength steels under seismic loading. *Proceedings of the Structural Stability Research Council*, 201-210.

Kuwamura, H. and Kato, B. (1989). Effect of randomness in structural members. *Journal of Constructional Steel Research*, 13(6), 79-93.

Lai, M.L., Chang, K.C., Soong, T.T., Hao, D.S. and Yeh, Y.C. (1995). Full-scale visco-elastically damped steel frame. *Journal of Structural Engineering*, ASCE, 121(1), 1443-447.

Lay, M.G. and Galambos, T.V. (1965). Inelastic steel beams under uniform moment. *Journal of Structural Engineering*, ASCE, 91(6), 67-93.

Lee, G.C., Chang, K.C. and Sugiura, K. (1992). The experimental basis of material constitutive laws of structural steel under cyclic and nonproportional loading. *Stability and Ductility of Steel Structures Under Cyclic Loading*, Y. Fukumoto and G.C. Lee Eds., CRC Press, 3-15.

Liew, J.Y.R., Chen, H. and Shanmugam, N.E. (2001). Inelastic analysis of steel frames with composite beams. *Journal of Structural Engineering*, ASCE, 127(2), 194-202.

Leon, R.T. (1994). Composite semi-rigid construction. *Engineering Journal*, AISC, 31(2), 57-60.

Leon, R.T (1998). Analysis and design problems for PR composite frames subjected to seismic loads. *Engineering Structures*, 20(4-6), 364-371.

Leon, R.T., Hajjar, J., Gustafson, M.A. and Shield, C.M. (1998). Seismic response of composite moment-resisting connections, I: Performance. *Journal of Structural Engineering*, ASCE, 124(8), 868-876.

Levy, R., Marianchik, E., Rutenberg, A. and Segal, F. (2000). Seismic design methodology for friction damped braced frames. *Earthquake Engineering and Structural Dynamics*, 29(11), 1569-1585.

Lin, R.C., Liang, Z., Soong, T.T. and Zhang, R.H. (1988). An experimental study of seismic structural response with added visco-elastic dampers. *Technical Report No. NCEER-88-0018*, National Center for Earthquake Engineering Research, Buffalo, New York, USA.

Liu, J. and Astaneh, A.A. (2000). Cyclic testing of simple connections including effects of slab. *Journal of Structural Engineering*, ASCE, 126(1), 32-39.

Lu, L.W., Ricles, J.M. and Kasai, K. (1994). Research on seismic behaviour of steel and composite structures at Lehigh University. *Proceedings of the International Workshop on Behaviour of Steel Structures in Seismic Area* (Stessa '94), F.M. Mazzolani and V. Gioncu Eds., Timisoara, Romania.

Madan, A., Reinhorn, A.M., Mander, J.B. and Valles, R.E. (1997). Modeling of masonry infill panels for structural analysis. *Journal of Structural Engineering*, ASCE, 123(10), 1295-1302.

Mahin, S.A. (1998). Lessons from damage to steel buildings during the Northridge earthquake. *Engineering Structures*, 20(4-6), 261-270.

Makris, N., Dargush, G.F. and Constantinou, M.C. (1993). Dynamic analysis of generalized viscoelastic fluids. *Journal of Engineering Mechanics*, ASCE, 119, 1663-1679.

Malley, J.O. (1998). SAC Steel Project: Summary of Phase 1 testing investigating results. *Engineering Structures*, 20(4-6), 300-309.

Mander, J.B., Nair, B., Wojtkowski, K. and Ma, J. (1993). An experimental study on the seismic performance of brick-infilled steel frames with and without retrofit. *Technical Report No. NCEER-93-0001*, National Center for Earthquake Engineering Research, Buffalo, New York, USA.

Manzocchi, G.M.E., Chryssanthopoulos, M. and Elnashai, A.S. (1992). Statistical analysis of steel tensile test data and implications on seismic design criteria. *ESEE Research Report No. 92-7*, Imperial College, London, UK.

Matos, C.G. and Dodds, R.H. (2002). Probabilistic modelling of weld fracture in steel frame connections. Part II: Seismic loadings. *Engineering Structures*, 24(6), 687-705.

Mazzolani, F.M. (1995). Aluminum alloy structures. 2nd Edition, E&FN Spon, London, UK.

Mazzolani, F. M. and Mandara, A. (2002). Modern trends in the use of special metals for the improvement of historical and monumental structures. *Engineering Structures*, 24(7), 834-856.

Mele, E. (2002). Moment resisting welded connections: an extensive review of design practice and experimental research in USA, Japan and Europe. *Journal of Earthquake Engineering*, 6(1), 111-145.

Miller, D. K. (1998). Lessons learned from the Northridge earthquake. Engineering Structures, 20(4-6), 249-260.

Mirambell, E. and Real, E. (2000). On the calculation of deflections in structural stainless beams: An experimental and numerical investigation. *Journal of Constructional Steel Research*, 54(1), 109-133.

Miyazaki, M. and Mitsusaka, Y. (1992). Design of a building with 20% or greater damping. *Proceedings of the 10th World Conference on Earthquake Engineering*, Madrid (Spain), July 19-24, 8, 4143-4148.

Mizuno, E., Kato, M. and Fukumoto, Y. (1987). Multi-surface model application to beam-columns subjected to cyclic loads. *Journal of Constructional Steel Research*, 7(4), 253-277.

Moen, L. Hopperstad, O.S. and Langseth, M. (1999). Rotational capacity of aluminum beams under moment gradient. I: Experiments. *Journal of Structural Engineering*, ASCE, 125(8), 910-920.

Moghaddam, H., Dowling, P.J. and Ambraseys, N.N. (1988). Shaking table study of brick masonry infilled frames subjected to seismic excitation. *Proceedings of the Ninth World Conference on Earthquake Engineering*, Tokyo/Kyoto, Japan, Vol. 8, 913-18.

Morino, S. (1998). Recent developments in hybrid structures in Japan - research design and construction. *Engineering Structures*, 20(4-6), 336-346

Mualla, I.Y. and Belev, B. (2002). Performance of steel frames with a new friction damper device under earthquake excitation. *Engineering Structures*, 24 (3), 365-371

Nader, M.N. and Astaneh, A.A. (1992). Seismic behaviour and design of semi-rigid steel frames. Report No. UCB/EERC-92/06, University of California, Berkeley, California, USA.

Naeim, F. (2001). The seismic design handbook, 2nd Edition. Kluwer Academic Publisher.

Naeim, F. and Kelly, J.M. (1999). Design of seismic isolated structures: from theory to practice. John Wiley & Sons Inc., New York, New York, USA.

Naeim, F., Lew, M., Huang, C.H., Lam, H.K. and Carpenter, L.D. (2000). The performance of tall buildings during the 21 September 1999 Chi-Chi earthquake Taiwan. *The Structural Design of Tall Buildings*, 9(2), 137-160.

Nakashima, M., Inoue, K. and Tada, M. (1998). Classification of damage to steel buildings observed in the 1995 Hyogoken-Nanbu earthquake. *Engineering Structures*, 20(4-6), 271-281.

Nakashima, M. and Sawaizumi, Y. (2000). Column-to-beam strength ratio required for ensuring beam-collapse mechanism in earthquake responses of steel frames. *Proceedings of the 12th World Conference on Earthquake Engineering*, Auckland, New Zealand.

Nateghi, F.A. (1995). Retrofitting of earthquake damaged steel buildings. *Engineering Structures*, 17(10), 749-755.

Nateghi, F.A.(1997). Seismic upgrade design of a low-rise steel buildings. *Engineering Structures*, 19(11), 954-963.

Nethercot, D.A., Li, T.Q. and Choo, B.S. (1995). Required rotations and moment redistributions for composite frames and continuous beams. *Journal of Constructional Steel Research*, 35(2), 121-164.

National Information Service for Earthquake Engineering (2000). NISEE on line resources @ http://nisee.berkeley.edu.

Nishitani, A. and Inoue, Y. (2001). Overview of the application of active/semiactive control to building structures in Japan. *Earthquake Engineering and Structural Dynamics*, 30(11), 1565-1574.

Nishiyama, I. Midorikawa, M. and Yamanouchi, H. (1988). Inelastic behaviour of full scale eccentrically k-braced steel building. *Proceedings of the 9th World Conference on Earthquake Engineering*, Tokyo/Kyoto, Japan, Vol. 4, 261-266.

Pall, A.S. and Marsh, C. (1982). Response of friction damped braced frames. *Journal of Structural Division*, ASCE, 108(9), 1313-1323.

Pekcan, G., Mander, J.B. and Chen, S.S. (1995). The seismic response of a 1:3 scale model RC structure with elastomeric spring dampers. *Earthquake Spectra*, 11(2), 249-267.

Petersson, H. and Popov, E.P. (1977). Constitutive relations for generalized loadings. *Journal of the Engineering Mechanics Division*, Proceedings of the American Society of Civil Engineers, 103(EM4), 611-627.

Plumier, A. (1990). New idea for safe structure in seismic zones. *Proceedings of the IABSE Symposium* of mixed structures including new materials, Brussels, Belgium, 431-436.

Plumier, A. (2000). General report on local ductility. *Journal of Constructional Steel Research*, 55 (1-3), 91-107.

Popov, E.P. and Petersson, H. (1978). Cyclic metal plasticity: experiments and theory. *Journal of the Engineering Mechanics Division*, Proceedings of the American Society of Civil Engineers, 104(EM6), 1371-1388.

Popov, E.V., Yang, T.S. and Grigorian, C.E. (1993). New directions in structural seismic design. *Earthquake Spectra*, 9(4), 845-875.

Rai, D.C. and Wallace, B.J. (1998). Aluminum shear-links for enhanced seismic resistance. *Earthquake Engineering and Structural Dynamics*, 27 (4), 315-342.

Richard-Yen, J.Y., Lin Y. and Lai, M.T. (1997). Composite beams subjected to static and fatigue loads, *Journal of Structural Engineering*, ASCE, 123(6), 765-771.

Ricles, J.M., Changshi, M., LU, L.W. and Fisher, J.W. (2002). Inelastic cyclic testing of welded unreinforced moment connections. *Journal of Structural Engineering*, ASCE, 128(4), 429-440.

Ricles, J.M. and Paboojian, S.D. (1994). Seismic performance of steel-encased composite columns. *Journal of Structural Engineering*, ASCE, 120(8), 2474-2494.

Roeder, C.W. (1998). Overview of hybrid and composite systems for seismic design in the United States. *Engineering Structures*, 20(4-6), 355-363.

Roeder, C.W. and Popov, E.P. (1978). Eccentrically braced steel frames for earthquakes. *Journal of Structural Division*, ASCE, 104(ST3), 391-411.

SAC (1997). Interim guidelines: Advisory No.1. Supplement to FEMA 267. *Report No. FEMA 267A/SAC-96-03*, SAC Joint Venture, Sacramento, California.

SAC Joint Venture (1999). Seismic design criteria for new moment resisting steel frame construction (50% Draft). Report No. FEMAXXX, January.

Sakamoto, J. and Miyamura, A. (1966). Critical strength of elastoplastic steel frames under vertical and horizontal loading. *Transaction Architectural Institute of Japan*,124, 1-7.

Sam, M.T., Balendra, T. and Liaw, C.Y. (1995). Earthquake resistant steel frames with energy dissipating knee. *Engineering Structures*, 17(5), 334-343.

Saneinejad, A. and Hobbs, B. (1995). Inelastic design of infilled frames. *Journal of Structural Engineering*, ASCE, 121(4), 634-650.

Schneider, S.P. (1998). Axially loaded concrete-filled steel tubes. *Journal of Structural Engineering*, ASCE, 124(10), 1125-1138.

Schneider, S.P., Roeder, C.W. and Carpenter, J.E. (1993). Seismic behavior of moment resisting steel frames: experimental studies. *Journal of Structural Engineering*, ASCE, 119(ST6), 1885-1902.

Schneider, S.P., Zagers, B.R. and Abrams, D.P. (1998). Lateral strength of steel frames with masonry infills having large openings. *Journal of Structural Engineering, ASCE*, 124(8), 896-904.

Shahrooz, B.M., Remmetter, M.E. and Quin, F. (1993). Seismic design and performance of composite coupled walls. *Journal of Structural Engineering*, ASCE, 119(11), 3291-3309.

Sheikh, T.M., Deierlein, G.G., Yura, J.A. and Jirsa, J.O. (1989). Part I: Beam column moment connections for composite frames. *Journal of Structural Engineering*, ASCE, 115(11), 2859-2876.

Shen, J., Kitjasateanphun, T. and Srivanich, W. (2000). Seismic performance of steel frames with reduced beam sections. *Engineering Structures*, 22(8), 968-983.

Shen, K.L. and Soong, T.T. (1995). Modeling of viscoelastic dampers for structural applications. *Journal of Engineering Mechanics*, ASCE, 121(6), 694-701.

Shen, K.L., Soong, T.T., Chang, K.C. and Lai, M.L. (1995). Seismic behavior of reinforced concrete frame with added visco-elastic dampers. *Engineering Structures*, 17(5), 372-380.

Shukla, A.K. and Datta, T.K. (1999). Optimal use of viscoelastic dampers in building frames for seismic forces. *Journal of Structural Engineering*, ASCE, 125(4), 401-409.

Skinner, R.I., Robison, W.H. and McVerry, G.H. (1993). An introduction to seismic isolation. John Wiley & Sons, Inc., New York, New York, USA.

Soong, T.T. and Costantinou, M.C. (1994). Passive and active structural vibration control in civil engineering. Springer-Verlag, Wien.

Soong, T.T. and Dargush, G.F. (1997). Passive energy dissipation systems in structural engineering. John Wiley & Sons, Inc., New York, New York, USA.

Soong, T.T. and Spenser, B.F. Jr. (2002). Supplemental energy dissipation: state-of-the-art and state-of-practice. *Engineering Structures*, 24(3), 243-259.

Soroushian, P. and Choi, K.B. (1987). Steel mechanical properties at different strain rates. *Journal of Structural Engineering*, ASCE; 113(4), 663-672.

Steel Construction Institute (2000). Development of the use of stainless steel in construction. Workpage No. 7 "Fatigue", *Final Report to European Coal and Steel Community*, Ascot, Berkshire, UK.

Stojadinovic, B., Goel, S.C., Lee, K.H., Margarian, A.G. and Choi, J.H. (2000). Parametric tests on unreinforced steel moment connections. *Journal of Structural Engineering*, ASCE, 126(1), 40-49.

Structural Engineers Association of California (1995). Performance-based seismic engineering of buildings - Part 2: Conceptual framework. SEAOC, Vision 2000 Committee, California, USA.

Structural Shape Producers Council (1994). Statistical analysis of tensile data for wide-flange structural shapes. Chaparral Steel Company, Midlothian, Texas, USA.

Tang, X. and Goel, S.C. (1989). Brace fractures and analysis of Phase I Structure. *Journal of Structural Engineering*, ASCE, 115(8), 1960-1976.

Taranath, B.S. (1997). Steel, concrete and composite design of tall buildings. McGraw-Hill, New York, New York, USA.

Tehranizadeh, M. (2001). Passive energy dissipation device for typical steel frame building in Iran. *Engineering Structures*, 23(6), 643-655.

Tena-Colunga, A. and Vergara, A. (1997). Comparative study on the seismic retrofit of a mid-rise steel building: steel bracing vs. energy dissipation. *Earthquake Engineering and Structural Dynamics*, 26(6), 637-655.

Tide, R.H.R. (2000). Evaluation of steel properties and cracking in "k"-area of W shapes. *Engineering Structures*, 22 (2), 128-134.

Tsai, C.S., Chen, H.W., Hong, C.P. and Su, Y.F. (1993). Design of steel triangular plate energy absorbers for seismic-resistant construction. *Earthquake Spectra*, 9(3), 505-528.

Tsopelas, P. and Constantinou, M.C. (1994). Experimental and analytical study of a system consisting of sliding bearings and fluid restoring forces/damping devices. *Technical Report NCEER-94-0014*, National Center for Earthquake Engineering Research, Buffalo, New York, USA.

Tremblay, R., Bruneau, M., Nakashima, M., Prion, H.G.L., Filiatrault, A. and De Vall, R. (1996). Seismic design of steel buildings : lessons from the 1995 Hyogoken Nanbu Earthquake. *Canadian Journal of Civil Engineering*, 23(3), 757-770.

Tremblay, R., Timler, P., Bruneau, M. and Filiatrault, A. (1995). Performance of steel structures during the January 17, 1994 Northridge Earthquake. *Canadian Journal of Civil Engineering*, 22(2), 338-360.

Tryland, T. Clausen, A.H. and Remseth, S. (2001). Effect of material and geometry variations on beam under patch loading. *Journal of Structural Engineering*, ASCE, 127(8), 930-939.

Uang, C.M. and Bondad, D. (1998). Cyclic performance of haunch repaired steel moment connections: Experimental testing and analytical modelling. *Engineering Structures*, 20(4-6), 552-561.

Uang, C.M. and Fan, C.C. (1999). Cyclic stability with moment connections with Reduced Beam Section. *Report No.SSRP-99/21*, Department of Structural Engineering, University of California, San Diego, La Jolla, California, USA.

Van Humbeeck, J. (2001). Shape memory alloys: a material and a technology. *Advanced Engineering Materials*, 3(11), 837-850.

Vann, W.P., Thompson, L.E., Walley, L.E. and Ozier, L.D. (1973). Cyclic behaviour of rolled steel members. *Proceedings of the 5th World Conference on Earthquake Engineering, Rome,* Vol. 1, International Association for Earthquake Engineering, 1187-93.

Vulcano, A. (1991). Uso di controventi metallici con dispositivi dissipativi nell'adeguamento antisismico di strutture intelaiate. *Costruzioni Metall*iche, 4, 244-261 (*in Italian*).

Wakabayashi, M., Nakamura, T., Yoshida, N. and Iwai, S. (1978). Effect of strain rate on the stress-strain relationships of concrete and steel. *Proceedings of the Fifth Japan Earthquake Engineering Symposium*, Tokyo, Japan, 1313-1320.

Walpole, W.R (1985). Concentrically braced frames. *Bulletin of NZ National Society for Earthquake Engineering,* 18(4), Section E, 351-5.

Watanabe, A., Hitomi, Y., Saeki, E., Wada, A. and Fujimoto, M. (1988). Properties of braced encased in buckling-restraint concrete and steel tube. *Proceedings of the 9th World Conference on Earthquake Engineering*, Tokyo-Kyoto, Japan.

Watanabe, E., Sugiura, K., Nagata, K. and Kitane, Y. (1998). Performances and damages to steel structures during 1995 Hyogoken-Nanbu earthquake. *Engineering Structures*, 20(4-6), 282-290.

Weng, C.C., Yen, S.I. and Chen, C.C. (2001). Shear strength of concrete-encased composite structural members. *Journal of Structural Engineering*, ASCE, 127(10), 1190-1197.

Whittaker, A.S., Bertero, V.V., Thompson, C.L. and Alonso, L.J. (1991). Seismic testing of steel plate energy dissipation devices. *Earthquake Spectra*, 7(4), 563-604.

Whittaker, A.S., Uang, C., M. and Bertero, V.V. (1987). Earthquake simulation tests and associated studies of a 0.3 scale model of a six storey eccentrically braced steel structure. EERC *Report No. UBC/EERC-87/02*, University of California, Berkeley, California, USA.

Wilde, K. Gardoni, P., Fujino, Y. (2000). Base isolation system with shape memory alloy devices for elevated highway bridges. *Engineering Structures*, 22(3), 222-229.

Xia, C. and Hanson, R.D. (1992), Influence of ADAS element parameters n building seismic response. *Journal of Structural Engineering*, ASCE, 118(7), 1903-1918.

Yang, M. (1982). Seismic behaviour of an eccentrically X-braced steel structure. EERC Report *No. UBC/EERC-82/14*, University of California, Berkeley, California, USA.

Youssef, N.F.G., Bonowitz, D. and Gross, J.L. (1995). A survey of steel moment-resisting frame buildings affected by the 1994 Northridge earthquake. *Report No. NISTR 56254*, National Institute for Science and Technology, Gaithersburg, Maryland, USA.

Yu, Q.S., Uang, C.M. and Gross, J. (2000). Seismic rehabilitation design of steel moment connection with welded haunch. *Journal of Structural Engineering*, ASCE, 126(1), 67-78.

Zhang, R.-H. and Soong, T.T. (1992). Seismic design of viscoelastic dampers for structural applications. *Journal of Structural Engineering*, ASCE, 118(5), 1375-1392.